Dynamic Interplay between Varicelloviruses and their Primate Hosts

Werner J.D. Ouwendijk

The research described in this thesis was conducted at the department of Viroscience, Erasmus Medical Center, Rotterdam, the Netherlands, and supported in part by Public Health Service grant AG032958 from the National Institutes of Health. Furthermore, the research for this thesis was performed within the framework of the Erasmus Postgraduate School Molecular Medicine.

Financial support for printing of this thesis by the following companies is gratefully acknowledged: **Advanced Cell Diagnostics Inc.**, **GlaxoSmithKline**, **Greiner Bio-One B.V.**, **GR Instruments B.V., Preprotech and Star-Oddi.**

Cover: Back (gray): characteristic varicella skin lesion obtained at 9 days after primary SVV infection, immunohistochemically stained for SVV antigens. Front (color): Confocal microscopy image of human retinal pigment epithelium cells infected with VZV.ORF66-EGFP (green), immunefluorescently stained for VZV glycoprotein E (red) and counterstained with DAPI to visualize nuclei (blue). A multinucleated giant cell is shown.

Lay-out: Werner J.D. Ouwendijk
Printed by: Proefschriftmaken.nl || Uitgeverij BOXpress

ISBN: 978-90-8891-726-4

Copyright © 2013, Werner J.D. Ouwendijk.
All rights reserved. No part of this publication may be reproduced, stored in a retrievaldatabase or published in any form or by any means, electronic, mechanical or photocopying, recording or otherwise, without the prior written permission of the author.

Dynamic Interplay between Varicelloviruses and their Primate Hosts

Dynamische Wisselwerking tussen Varicellovirussen en hun Primaten Gastheer

Proefschrift

ter verkrijging van de graad van doctor aan de
Erasmus Universiteit Rotterdam
op gezag van de
rector magnificus

Prof.dr. H.A.P. Pols

en volgens besluit van het College voor Promoties.

De openbare verdediging zal plaatsvinden op

woensdag 4 december 2013 om 11.30 uur

door
Werner Jan Dieter Ouwendijk
geboren te Maassluis

Promotiecommissie

Promotor:	Prof.dr. A.D.M.E. Osterhaus
Overige leden:	Prof.dr. R.Q. Hintzen Prof.dr. W.N.M. Dinjens Prof.dr. R.W. Hendriks
Copromotor:	Dr. G.M.G.M. Verjans

Contents

Chapter 1

General Introduction

Partially based on:

T-cell Immunity to Human Alphaherpesviruses

Werner J.D. Ouwendijk,[1] Kerry J. Laing,[2] Georges M.G.M. Verjans,[1] and David M. Koelle[2,3,4,5,6]

[1]Department of Viroscience, Erasmus Medical Center, Rotterdam, the Netherlands; [2]Department of Medicine, University of Washington, Seattle, Washington, USA; [3]Department of Laboratory Medicine, University of Washington, Seattle, Washington, USA; [4]Department of Global Health, University of Washington, Seattle, Washington, USA; [5]Vaccine and Infectious Diseases Division, Fred Hutchinson Cancer Research Center, Seattle, Washington, USA; [6]Benaroya Research Institute, Seattle, Washington, USA

Curr Opin Virol. 2013;3(4):452-60

1. Human Herpesviruses

Classification

The order of *Herpesvirales* consists of evolutionary highly successful viruses that are widely disseminated throughout nature [1]. To date, over 138 distinct herpesviruses (HVs) have been identified that can be categorized into three remotely related families [1-3]. The largest and most well studied is the family of *Herpesviridae*, which comprises HVs of mammals, birds and reptiles [1]. HVs of fish and amphibians belong to the family of *Alloherpesviridae* and those of bivalves to the family of *Malacoherpesviridae* [1]. Molecular phylogenetic studies suggest that HVs originated from an ancestral virus that dated close to the emergence of vertebrates in the Cambrian period (570 – 500 million years ago) [1]. HVs coevolved with their hosts for extended periods of time and have adapted extremely well to their host [1]. Consequently, these viruses have a restricted host range and a single HV typically infects a single species in nature. HVs are among the largest and most complex viruses and share several distinctive biological features: (1) HVs express enzymes involved in nucleic acid metabolism, DNA synthesis and processing of proteins; (2) Viral DNA replication and synthesis of the capsid take place in the nucleus and complete assembly of the virion occurs in the cytoplasm; (3) Production of infectious progeny is invariably accompanied by destruction of the infected cell; and (4) HVs are able to establish a lifelong latent infection in their natural host, allowing the virus to reactivate intermittingly [4]. Viral latency can be defined as the presence of the viral genome in host cells without production of infectious progeny, provided that the virus retains the capacity to reactivate.

Table 1. The Human Herpesviruses.

Designation	Common Name	Subfamily[a]	Disease[b]
Human herpesvirus 1	Herpes simplex virus type 1	α	Herpes labialis (cold sores)[c]
Human herpesvirus 2	Herpes simplex virus type 2	α	Herpes genitalis[c]
Human herpesvirus 3	Varicella-zoster virus	α	Varicella (chickenpox) and herpes zoster (shingles)
Human herpesvirus 4	Epstein-Barr virus	γ	Infectious mononucleosis and cancer (e.g. Burkitt's lymphoma and nasopharyngeal carcinoma)
Human herpesvirus 5	Human cytomegalovirus	β	Cytomegalovirus mononucleosis, birth defects, pneumonia, retinitis
Human herpesvirus 6		β	Roseola infantum
Human herpesvirus 7		β	Roseola infantum
Human herpesvirus 8	Kaposi's sarcoma virus	γ	Cancer (e.g. Kaposi's sarcoma, primary effusion lymphoma and Castleman's disease)

[a] α: *alphaherpesvirinae*; β: *betaherpesvirinae* and γ: *gammaherpesvirinae*.
[b] Most common diseases caused by the respective herpesvirus.
[c] Herpes simplex virus type 1 (HSV-1) and HSV-2 can cause both labial and genital herpes, although classically HSV-1 is associated with oral lesions and HSV-2 with genital lesions [4]

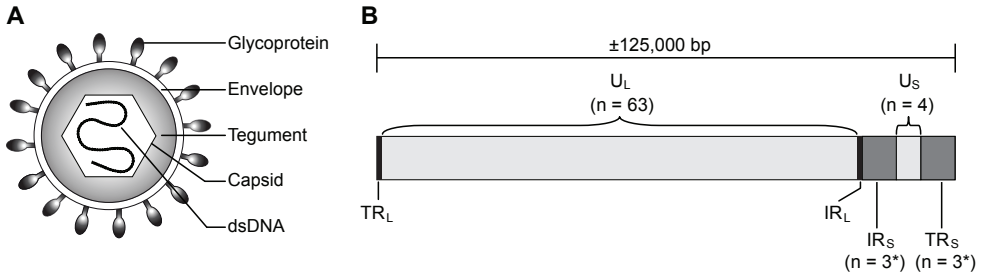

Figure 1. *Schematic representation of the VZV virion and genome. (A) VZV virions are composed of a double-stranded (ds) DNA core located within the capsid, which is surrounded by the protein rich tegument layer and the complex is packaged by a lipid envelope carrying the viral glycoproteins. (B) The VZV genome is about 125,000 base pairs (bp) in length and most genes are located in the unique long (U_L; n = 63 genes) and unique short (U_S; n = 4 genes) regions. Three VZV genes (ORFs 62/71, 63/70, 64/69) are present in duplicate within the internal and terminal repeat regions flanking the U_S region (IR_S and TR_S, respectively). No genes are encoded by small repeat regions flanking the U_L region (TR_L and IR_L).*

The family of *Herpesviridae* can be categorized into three subfamilies designated as *Alphaherpesvirinae* (αHV), *Betaherpesvirinae* (βHV) and *Gammaherpesvirinae* (γHV), based on the genomic and biological properties of the virus [4]. The αHV have a short reproductive cycle, rapid spread in cell culture and establish latent infections primarily in sensory ganglion neurons [4]. The βHV have a restricted host range, replicate slowly in cell culture and establish latency in secretory glands, lymphoreticular cells and kidneys [4]. The γHV establish latency in B- and T-cells [4]. Humans form the natural host for eight distinct HVs comprising all three subfamilies, each causing characteristic disease(s) (Table 1). The αHVs comprise the genera *Simplexviruses* and *Varicelloviruses* [4]. Varicella-zoster virus (VZV) is the only human *Varicellovirus* and, among humans, is most similar to the *Simplexviruses* herpes simplex virus type 1 (HSV-1) and HSV-2 [4].

Structure and Genomic Organization of VZV

Like all other HVs the VZV virion is composed of four elements: a DNA core located within a nucleocapsid that is surrounded by a layer of tegument and this complex is packaged within a lipid envelope (Figure 1A). VZV particles are pleomorphic to spherical and 180 – 200 nm in diameter [5]. The VZV genome is the smallest of human HVs and consists of approximately 125,000 base pairs (bp) of linear double-stranded DNA [6]. The VZV genome is composed of two main coding regions termed unique long (U_L) and unique short (U_S) (Figure 1B) [6]. The U_L region is approximately 105,000 bp in length and flanked by two small inverted repeats TR_L and IR_L (each 88 bp) [5-6]. The U_S region is approximately 5,232 bp long and flanked by two large inverted repeats TR_S and IR_S (each 7,319 bp) [5-6]. VZV encodes for at least 74 open reading frames (ORFs) that constitute 70 unique genes, since transcripts of ORF42 and ORF45 form a single protein product and three genes are present in two copies in the TR_S and IR_S regions: ORFs 62/71, 63/70 and 64/69 [5-6]. By analogy to HSV-1, it is assumed that the VZV genome is arranged as regularly spaced

concentric layers within the nucleocapsid [5]. The VZV icosahedral nucleocapsid is composed of 162 capsomers containing 12 pentameric and 150 hexameric capsomers [7]. VZV ORF33.5 and ORF40 encode the nucleocapsid assembly protein and major nucleocapsid protein, respectively [8-9]. In the absence of experimental data, VZV proteins encoded by ORFs 20, 23, 33 and 41 have been postulated to be components of the nucleocapsid by analogy to homologous HSV proteins [5]. The capsid is surrounded by a proteinaceous structure, termed tegument, that allows the virus to release a collection of already synthesized proteins into newly infected cells and immediately alter the host environment to inhibit antiviral defenses and support viral replication [5]. The VZV tegument carries viral transcriptional activators encoded by ORFs 4, 10, 62 and 63, protein kinases ORF47 and ORF66, and the protein products of ORFs 1, 9, 11 and 12 [5, 10-12], as well as host proteins [13]. The VZV envelope contains at least 9 different glycoproteins (glycoprotein B (gB), gC, gE, gH, gI, gL, gK, gM and gN) that are involved in viral attachment and entry into the host cell, envelopment of the virus, viral egress and cell-to-cell spread [5, 14].

VZV Infection in Cell Culture

VZV enters the host cell by fusion of the viral envelope with the cell membrane or by endocytosis (Figure 2) [5]. Initial attachment of VZV particles to cells occurs nonspecifically via gB, and possibly gC, that bind cell surface heparan sulfate [15-16]. Three VZV entry receptors have been identified so far, although none of these appear to be uniquely expressed on the viral target cells *in vivo*. The cation-independent mannose 6-phosphate receptor (MPR^{ci}), insulin degrading enzyme (IDE) and myelin-associated glycoprotein (MAG) function as entry receptors for VZV [15, 17-18]. Multiple viral glycoproteins contain mannose 6-phosphate groups and may bind to MPR^{ci} [15-16]. VZV gE and gB engage with IDE and MAG, respectively [17-18]. Both MPR^{ci} and IDE are expressed at low levels on the cell surface and within endosomes on various cell types [15, 17]. MAG is predominantly expressed on the cell surface of glial cells in nervous tissue and is absent on both neurons and epithelial cells [18]. Following binding of VZV to its entry receptor(s), penetration of the host cell occurs by fusion of the viral envelope with the plasma membrane or endosomal membrane, most likely mediated by the conserved herpesvirus fusion machinery composed of gB, gH and gL [18-21]. Fusion releases viral tegument proteins and the nucleocapsid into the cytoplasm, after which the nucleocapsid is transported to the nuclear membrane to release the viral genome into the nucleus [5]. The VZV DNA circularizes and viral genes are transcribed by host cell RNA polymerase II in combination with viral proteins [5]. VZV transcription is presumed to occur in a temporal cascaded fashion analogous to HSV [5]. The inability to culture high-titer cell-free virus has hampered definitive identification of the temporal classes of individual VZV genes, although recent studies have identified that VZV genes are also coordinately expressed [22-23]. Initially, immediate early (IE) genes are expressed that encode transcriptional regulatory proteins [5]. IE proteins enter the nucleus and initiate expression of early (E) genes. The E proteins include enzymes involved in DNA and nucleotide metabolism that enter the nucleus and form the viral DNA replication machinery [5]. Late (L) genes are only expressed after DNA replication has commenced and encode structural proteins involved in viral genome packaging and formation of the virion,

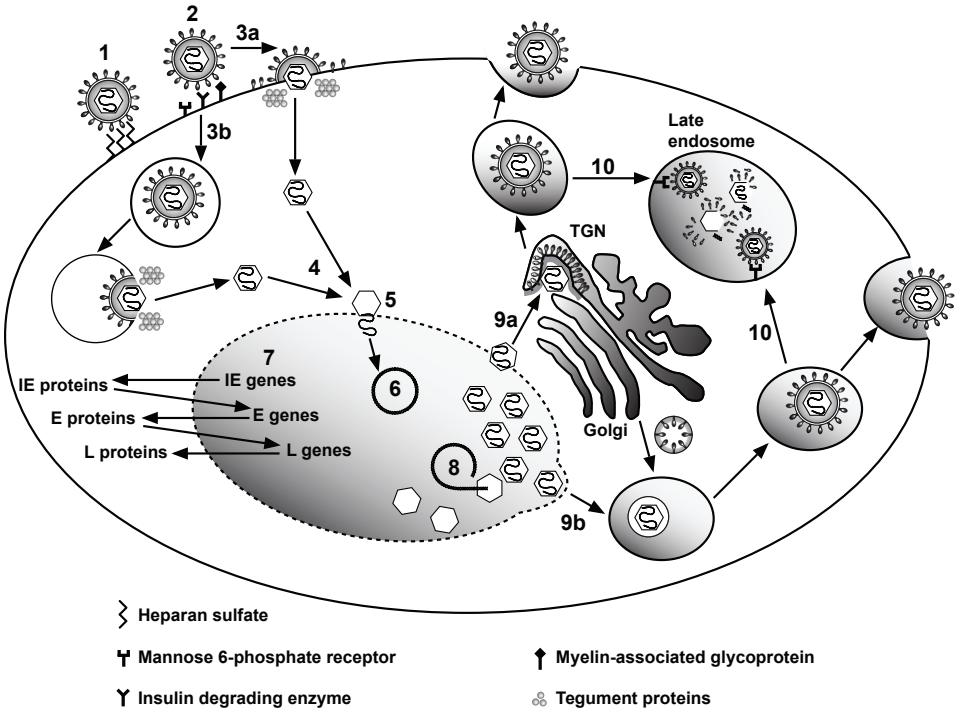

Figure 2. *Schematic representation of lytic VZV infection of the host cell. Initial attachment of VZV particles to the cell occurs via surface heparan sulfates (1), after which the virus engages with one or more of its three currently known entry receptors (mannose 6-phosphate receptor (MPR^{ci}), insulin degrading enzyme and myelin-associated glycoprotein) (2). The virus may enter the cells by direct fusion to the plasma membrane (3a) or via endocytosis (3b) followed by fusion and release of tegument proteins and capsids into the cytoplasm. Capsids are transported to the nuclear membrane (4), where viral DNA is released into the nucleus (5). The viral genome circularizes (6) and gene expression is believed to occur in a coordinated temporal fashion: first immediate early (IE) are expressed, then early (E) genes and subsequently late (L) viral genes (7). Following DNA replication nascent viral DNA is packaged within newly assembled capsids in the nucleus (8). Assembly and egress may occur by one of two possible routes: Naked nucleocapsids may be released in the cytoplasm and acquire their tegument proteins, envelope and glycoproteins in the trans-Golgi network (TGN) (9a). Alternatively, capsids gain their envelope from the nucleus and acquire their tegument proteins and glycoproteins by fusion with Golgi-derived vesicles (9b). Virus particles egress by exocytosis, although most particles are degraded in late endosomes through their association with MPR^{ci} (10).*

such as capsomers and glycoproteins [5]. Assembly and release of progeny VZV may occur by two pathways *in vitro* [5, 24-26]. First, VZV acquires its envelope from the nuclear membrane and associates with its tegument and glycoproteins in large cytoplasmatic vesicles, which migrate to the cell surface to release progeny virus by exocytosis [24]. Second, virions are assembled in the trans-Golgi network (TGN) by association of nucleocapsids with aggregates of tegument and viral glycoproteins on TGN membranes. Viral particles are released or are diverted to and degraded in

MPR^{ci}-expressing late endosomes [26]. The high titers of intact infectious progeny VZV particles in aerosols and vesicle fluids of varicella and zoster patients suggest that virion assembly and release is markedly different *in vivo* compared to *in vitro* infection [5]. The absence of MPR^{ci} from superficial, but not basal, epidermal cells may in part explain the *in vivo-in vitro* paradox [15].

Clinical Features of VZV Infection

VZV causes two distinct diseases: primary infection causes varicella (chickenpox) and reactivation of latent virus produces herpes zoster (shingles). Primary VZV infection is usually acquired during childhood and results from inhalation of infectious virus. The incubation period of primary infection is approximately 14 days (range 10 – 21 days) [5, 27-28]. Clinical illness is characterized by fever, malaise, headache and loss of appetite concurrent with the appearance of a generalized characteristic cutaneous rash referred to as chickenpox [5, 27-28]. The rash starts as pruritic erythematous macules and rapidly evolves to papules and vesicles, which crust after 24 – 72 hours [5, 27-28]. First lesions usually appear on the face and scalp, after which additional "crops" of vesicles continue to form on the trunk and, to a lesser extent, the limbs [5, 27-28]. New lesion are produced for 3 – 5 days, eventually leveling off at about 250 – 500 lesions in immunocompetent individuals [5, 27-28]. Additional lesions may be present on mucous membranes of oropharynx and conjunctivae [5, 27-28]. Varicella patients have a transient lymphopenia and granulocytopenia and frequently develop a mild hepatitis [5, 27-28]. Whereas primary VZV infections are commonly benign, some individuals may suffer from serious complications. The most common complications of varicella include secondary bacterial infections, mainly caused by group A β-haemolytic streptococci, pneumonia and central nervous system (CNS) disease [5, 27-28]. CNS complications range from relatively mild cerebellar ataxia to life-threatening meningoencephalitis, meningitis or large- and small-vessel vasculitis [29]. Older age at onset of infection and a compromised immune system are associated with increased severity of primary VZV infection [5, 27-28]. Immunocompromised children have prolonged lesion formation, many cutaneous lesions and are at increased risk of visceral VZV dissemination and associated complications (e.g. pneumonia, hepatitis and CNS disease) [5, 27-28]. Varicella during pregnancy is associated with morbidity and mortality in both mother and infant [5, 27-28]. Note that not all individuals develop skin rash following primary VZV infection, as evidenced by the detection of virus-specific humoral immunity in individuals without a history of varicella [30]. This issue was studied in **Chapter 2**.

Herpes zoster, also referred to as shingles, occurs most frequently in elderly individuals. Herpes zoster is a localized vesicular skin rash in the dermatomal distribution of one or more adjacent sensory nerves [5]. Zoster rash progresses from pruritic erythematous lesions (often missed) through papular and vesicular stages [31]. New lesions are produced for 3 – 7 days, but complete healing may take up to 6 weeks [5, 27, 31]. Most frequently involved are dermatomes innervated by thoracic, cervical or the ophthalmic branch of the trigeminal ganglia, the latter results in zoster ophthalmicus [32]. Zoster skin rash is preceded or accompanied by acute neuritis with severe local pain and hyperesthesia [5, 27, 31]. Pain may persist beyond 4 – 6 weeks fol-

lowing herpes zoster, termed post-herpetic neuralgia (PHN), and is highly resistant to treatment [5, 27, 29, 31]. Patients may develop PHN in the absence of skin rash, which is referred to as zoster sine herpete [5, 27, 29, 31]. Zoster ophthalmicus is associated with ocular complications, such as keratitis and uveitis, in 50% – 72% of patients [33-34]. The virus-host interactions involved in VZV uveitis were studied in **Chapter 8**. Herpes zoster is more severe in immunocompromised individuals, posing the risk of visceral dissemination (10% – 40% of patients) and consequent development of pneumonia, hepatitis or CNS disease [5, 27, 29, 31].

Epidemiology of VZV Infection

The majority of the world population is infected with VZV. Annual epidemics of varicella are observed in temperate climates, with peak incidence in late winter and early spring [5, 27-28]. VZV is highly contagious and transmission rates exceed 90% in daycare centers or secondary household contacts [5, 27]. Lower transmission rates (10% – 35%) are observed following less intense exposures (e.g. classroom contacts) [5, 27]. Consequently, over 93% of children in developed countries become infected with VZV prior to the age of 5 years and more than 97% of adults are latently infected with VZV [35]. Most individuals develop only one episode of varicella, suggesting that symptomatic VZV superinfection is rare [5, 27-28]. Herpes zoster results from reactivation of endogenous latent VZV in about 20% – 30% of infected individuals [36-37]. The overall incidence of herpes zoster in developed countries is estimated at about 3.2 – 3.4 cases per 1,000 persons/year [5, 27, 31-32]. However, the risk of developing herpes zoster is strongly correlated with age and immune status of the host. The incidence of herpes zoster increases with advancing age to over 7.8 cases per 1,000 persons/year in individuals >60 years old [5, 27, 31-32]. Incidence rates are particularly high in immunocompromised individuals, e.g. transplant recipients and HIV patients [5, 27, 31]. Most individuals develop zoster only once in a lifetime, but second or third episodes may occur [5, 27, 31].

2. Pathogenesis of VZV Infection

Primary Infection

VZV is spread from varicella or herpes zoster patients to susceptible individuals by aerosols or by direct contact with vesicular fluid [38]. Airborne transmission of VZV, suggested by epidemiological data and case reports, is unique among human herpesviruses [5, 39]. The initial target cells of VZV are unknown, but most likely the virus enters the body by infecting mucosal epithelial cells of the upper respiratory tract [5, 38]. Depending on the size of the aerosols virus may also reach the lower respiratory tract [40]. Following primary infection, VZV requires an incubation period of about 2 weeks (range 10 – 21 days) to cause varicella and establish neuronal latency in sensory ganglia [5]. Infectious virus and VZV DNA can be detected in peripheral blood mononuclear cells (PBMC) just prior to and immediately after the onset of varicella [41-44], suggesting viremic spread of VZV to the skin. In the absence of experimental data, VZV pathogenesis was initially thought to resemble

that of mousepox [38]. Virus replication would take place in regional lymph nodes, after which virus spreads to reticuloendothelial organs such as liver and spleen via a primary viremia. Just prior to the onset of varicella a secondary more prominent viremia was assumed to transport virus to skin. This scenario is supported by the detection of VZV in various tissues, including lymphoid organs and liver, in immunocompromised patients that died during acute varicella [45]. However, more recent studies on VZV infections in the SCID-hu mouse model argue for a different route of virus dissemination of VZV after primary infection [46-47]. The SCID-hu mouse model studies VZV infection of human fetal tissues that have been transplanted into severe combined immunodeficient (SCID) mice, which lack an adaptive immune system [46-47]. In this model, VZV has a tropism for T-cells within thymus and liver xenografts [48]. These studies argue that VZV initially replicates in respiratory epithelial cells and is transferred to T-cells within tonsilar lymphoid tissue contacting the upper respiratory tract [38, 48]. Transfer of virus from the airways to the draining lymph nodes may be mediated by dendritic cells (DC) as VZV productively infects human DCs in cell culture and VZV-infected DC can transmit virus to fibroblasts and T-cells [49]. VZV productively infects activated human memory T-cells *in vitro*, including T-cells expressing the skin-homing markers C-C type chemokine receptor type 4 and cutaneous lymphocyte antigen (CLA) [50]. Direct intravenous injection of cell culture-derived VZV-infected human T-cells into SCID-hu mice resulted in virus delivery to and infection of human fetal skin or sensory ganglion xenografts [51-52]. Although inoculated VZV-infected T-cells reached the transplanted skin of SCID-hu mice within 24 hours, skin rash did not develop until 10 – 21 days after inoculation suggesting that local innate immune responses inhibit VZV replication in the skin at early time points [51]. However, the VZV SCID-hu mouse model does not reproduce the complex and dynamic virus-host interactions involved in the dissemination of VZV to its target organs during primary infection. Therefore, we have used simian varicella virus (SVV), the nonhuman primate homologue of VZV, infection of African green monkeys to study the phenotype of SVV-infected cells during primary infection in **Chapter 3**.

During primary infection, VZV establishes a persistent latent infection of sensory neurons within the dorsal root ganglia (DRG) and trigeminal ganglia (TG) (Figure 3) [53-54]. Two non-mutually exclusive routes have been proposed by which VZV infects sensory ganglion neurons [5]. First, VZV has been hypothesized to enter nerve endings in the epidermis of cutaneous lesions and gain access to ganglia by retrograde axonal transport. Indirect evidence comes from the detection of viral antigens in nerve endings of skin biopsies and observations that herpes zoster occurs at the site of varicella vaccine inoculation or sites most severely affected by varicella [32, 55]. More recently, VZV infection of axons and retrograde axonal transport to neuronal cell bodies was demonstrated in cell culture [56-57]. Second, detection of VZV DNA in ganglia obtained at autopsy from patients in the prodromal stage of varicella suggests that VZV may also reach ganglia by hematogenous spread [5]. Similarly, SVV reaches ganglia of infected monkeys prior to the onset of skin rash [58]. The data are supported by the T-cell-mediated transfer of VZV to ganglia in the SCID-hu mouse model [59].

Latent Infection

The mechanisms by which VZV latency is established and maintained are largely unknown. In the SCID-hu mouse model VZV establishes latency in human fetal ganglia in the absence of a functional adaptive immune system, suggesting that local host innate immunity is sufficient to control VZV replication in ganglia and to force VZV into latency [52]. In the absence of an *in vitro* model for VZV latency and given the limitations of the SCID-hu mouse model, the vast majority of studies on VZV latency analyzed human ganglia obtained at autopsy. VZV establishes latency in neurons of sensory and autonomic ganglia along the entire neuraxis [60-64]. The dominant sites of VZV latency are the DRG and TG [63], but viral DNA can also be detected in other sensory (e.g. geniculate and vestibular ganglia) [61, 64] and autonomic ganglia (e.g. nodose and enteric ganglia) [60, 62]. Sensory ganglia are composed of neuronal cell bodies that are enwrapped by a sheath of neuron-interacting satellite glial cells (SGC) [65]. Each neuron and its surrounding SGC form a distinct morphological and functional unit [65]. VZV establishes latency in 0.8% – 6.9% of TG neurons, but not in SGC [53-54, 66]. The latent viral genome is maintained in a circular configuration [67] and is associated with histones of the host cell [68]. Individual latently infected neurons contain approximately 5 – 7 copies of viral DNA [54, 66]. VZV latency is not associated with morphological changes of neurons in human DRG and TG. VZV latency differs markedly from that of the much better studied and closely related human *Simplexviruses*. Neuronal HSV latency is associated with the abundant expression of the non-coding latency-associated transcripts (LAT) and microRNAs [69-70]. The LAT-encoding region is not present in the VZV genome and no VZV-specific microRNAs have been detected in latently infected human ganglia [5, 71]. Instead, VZV latency has been associated with the detection of a restricted set of viral transcripts and even proteins [53, 72-77]. The number and abundance of individual VZV transcripts varies per study, but a restricted set of transcripts corresponding to VZV putative immediate early, early and even late genes have been detected consistently in latently infected human ganglia [53, 72-77]. VZV ORF63 is the most frequent and abundant gene transcribed in latently infected human TG [53, 72-77]. Regulation of VZV gene expression during latency may involve epigenetic modifications of the viral genome [68]. The major confounding factor in these studies is the long postmortem interval (PMI), frequently >24 hours, at which human DRG and TG were available for VZV transcript analyses. In **Chapter 5** we analyzed the potential role of PMI on the breadth and extent of VZV transcripts in latently infected human TG specimens. Expression of VZV proteins in latently infected human ganglia is even more unclear. Some groups reported on high frequencies of VZV protein expressing neurons in ganglia [78-80], whereas others showed that viral protein expression in human ganglia is rare [76, 81-83]. The latter is also supported by the lack of chronic immune infiltrates in VZV latently infected ganglia, whereas HSV-1 latency is associated with lymphocytic infiltrates [80, 84]. The majority of the studies report on expression of IE62 and IE63, but not late VZV proteins, in the cytoplasm of neurons [78-80]. The staining patterns obtained are unusual and suggest deposition of VZV proteins in autophagomes or TGN-associated vesicles in neurons during-latent infection. In **Chapter 4** we have analyzed if the immunohistochemical staining patterns obtained with IE62- and IE63-specific monoclonal antibodies (mAb) on

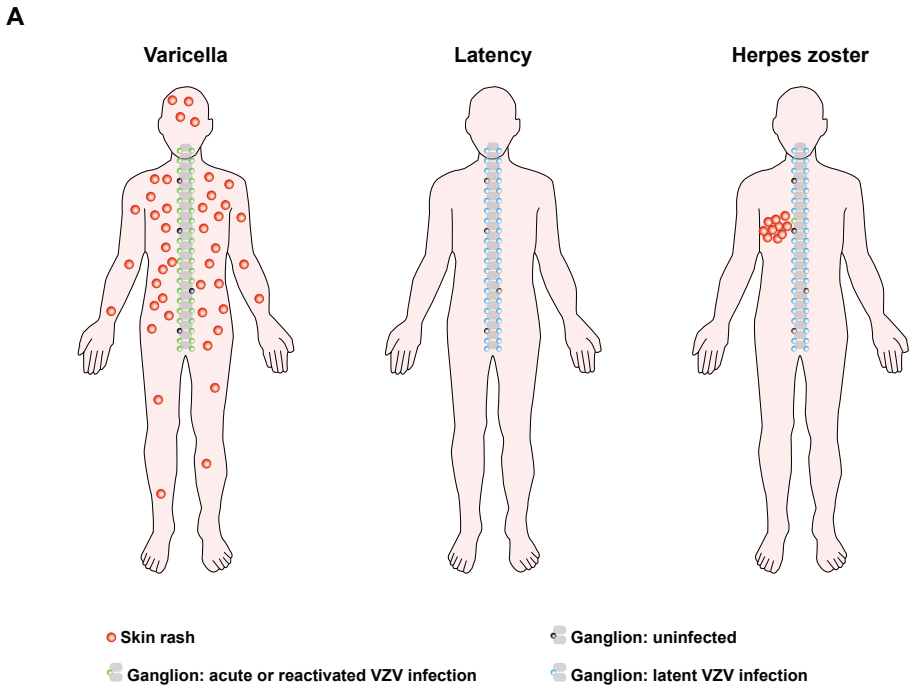
A
Varicella
Latency
Herpes zoster
Skin rash
Ganglion: acute or reactivated VZV infection
Ganglion: uninfected
Ganglion: latent VZV infection
B
Primary infection
Latency
Reactivation
Skin
Blood
1
2
Axon
3
A(n)
???
IE genes
E genes
L genes
IE proteins
E proteins
L proteins
4
VZV transcripts
VZV proteins

Figure 3. *Schematic representation of primary, latent and reactivated VZV infection. (A) Primary VZV infection results in generalized vesicular skin rash (chickenpox) and ganglionic infection, after which the virus establishes neuronal latency in ganglia along the entire neuraxis. Later in life, the virus may reactivate to cause recrudescent skin rash (herpes zoster) in the dermatomal distribution of one or more adjacent sensory nerves. (B) Left panel: during primary infection, the virus gains access to ganglionic neurons via retrograde axonal transport from skin lesions (1) and/or by hematogenous transport (2). Upon release into the nucleus the VZV genome is maintained in a circular configuration (3). Middle panel: during latency expression of several VZV transcripts and, possibly, their corresponding proteins have been described. Right panel: upon reactivation, VZV genes of all kinetic classes are expressed (possibly involving the temporal gene expression associated with lytic infection in vitro; 1) resulting in DNA replication and assembly of nascent VZV particles (2). VZV is believed to spread within the ganglion and replicate in satellite glial cells, both neuron-surrounding and neighboring, and neurons (3). VZV reaches the skin by anterograde axonal transport (4).*

human ganglia reflect local expression of the corresponding VZV protein or are the result of nonspecific mAb-binding.

Virus Reactivation

The virus and host factors that underlie VZV reactivation are largely unknown. However, it is clear that virus-specific T-cell immunity is essential to prevent clinical VZV reactivation, as demonstrated by the increased risk of developing herpes zoster in the elderly and in immunocompromised individuals [85-86]. Upon VZV reactivation the virus replicates and spreads within ganglia before descending down the sensory nerve axons to the nerve endings at the dermal-epidermal junction (Figure 3). This scenario is supported by the detection of nuclear inclusion bodies, VZV proteins and viral nucleic acids in neurons, their surrounding SGC and resident fibroblasts in ganglia of herpes zoster patients [87-88]. Furthermore, these ganglia contain mature VZV virions in both neurons and SGC [87-88] and infectious virus [89]. As a result of VZV replication, ganglia of herpes zoster patients demonstrate profound hemorrhagic necrosis and inflammation [87-88, 90]. Additional virus-induced pathology may include degeneration of motor and sensory nerve roots, distal peripheral nerves and spinal cord [5, 87-88, 90]. Ganglia obtained at variable intervals after herpes zoster may show permanent damage, cells loss and fibrin deposition [90], or demonstrate complete recovery with intact neurons and SGC [90-91]. Following herpes zoster immune infiltrates mostly composed of $CD8^+$ T-cells are retained in ganglia [91]. In **Chapter 7** we analyzed infiltration of T-cells into ganglia of cynomolgus macaques at variable times after herpes zoster.

VZV reaches the skin by anterograde axonal transport. This is evidenced by the characteristic herpes zoster skin rash that is restricted to the dermatomal distribution of usually one sensory nerve [32, 90]. Also, herpes zoster skin biopsies showed viral proteins in Schwann cells and dermal sensory nerve fibers [55]. VZV is released at the dermal-epidermal junction, where nerve endings of sensory nerve axons are located. It is conceivable that, like during primary infection, the virus needs to overcome local innate immune responses to produce vesicular skin rash [51]. The prodromal pain and itching in the dermatome where skin lesions will appear

therefore most likely reflects virus replication and spread within the ganglion and possibly skin. In addition, VZV DNA is detected in PBMC of zoster patients [92], suggesting that lymphocytes trafficking through ganglia can become infected and disseminate the virus to the virus' target organs (e.g. lung, liver and spleen). VZV reactivation is a significant cause of neurological disease, most frequently PHN [29]. The mechanisms underlying PHN are poorly understood, but may involve damage to neuronal cell bodies and axons [90, 93] or persistent ganglionic virus replication and ganglionitis [94-95]. VZV-induced large- and small-vessel encephalitis may involve direct transfer of virus from ganglia to cerebral arteries [96]. Although most individuals develop only one episode of herpes zoster [31], the presence of VZV DNA in PBMC [97-98] and saliva [99-101] of healthy adults without clinical signs of VZV infection suggests that asymptomatic VZV reactivation may occur more frequently. Notably, neurological complications of VZV reactivation frequently occur in the absence of rash (e.g. zoster sine herpete) [102]. These findings suggest that the host immune system may contain VZV replication and spread in ganglia or skin prior to development of rash. In **Chapter 6** we compared the incidence and extent of asymptomatic HSV-1 and VZV shedding in the saliva of HIV-infected individuals.

3. Immune Response to VZV Infection

Innate Immunity

The fist encounter between pathogen and host involves the local innate immune response of the infected tissue, which is generally rapid and recognizes pathogen-associated molecular patterns (PAMPs) shared by many pathogens [103]. PAMPs interact with pattern recognition receptors (PRRs) expressed by cells of the innate immune system such as neutrophils, macrophages, natural killer (NK) cells and dendritic cells (DCs) [103]. PRRs include the prototypic membrane-associated Toll-like receptors (TLRs) and cytosolic non-TLRs such as retinoic acid-inducible gene (RIG-I)-like receptors and nucleotide-binding oligomerization domain (NOD)-like receptors (NLRs) [103]. PAMP recognition by PRRs activates transcription factors such as nuclear factor kappa-light-chain-enhancer of activated B-cells (NF-κB), interferon regulatory factor 3 (IRF3) and IRF7, which induce the expression of IFN-α, IFN-β and pro-inflammatory cytokines that inhibit viral replication and recruit effector cells of the immune system [103]. VZV particles or virion proteins may interact with TLR-2 located on the cell surface, resulting in secretion of pro-inflammatory cytokines including interleukin-6 (IL-6), IL-8 and tumour necrosis factor alpha (TNF-α) [104]. Genomic VZV double-stranded DNA is recognized by TLR-9 in endosomes and induces the production of type 1 interferons like interferon alpha (IFN-α) [105]. By unknown mechanisms VZV is sensed by NLRP3 resulting in inflammasome formation and IL-1β production [106]. In addition, PRR-independent intrinsic responses limit viral replication and spread. Promyelocytic leukemia protein nuclear bodies (PML-NBs) sense and sequester nuclear aggregates of aberrant proteins, including newly synthesized VZV proteins and/or virions [107]. Further, VZV replication induces cellular stress responses, endoplasmatic reticulum stress and unfolded protein re-

sponse, leading to autophagy and degradation of virus particles in autophagosomes [108-109]. The contribution of innate immune cells inhibition of VZV replication is unknown, but children with deficiencies in NK and NKT cells commonly develop more severe varicella [110-113]. NK cells have potent antiviral activity *in vitro* by production of IFN-γ and granulysin or direct lysis of VZV-infected fibroblasts [114-115]. VZV has developed multiple mechanisms to block the induction and perpetuation of innate antiviral responses. VZV encodes three proteins (ORF47, ORF61 and ORF62) that prevent phosphorylation of IRF3 and the virus inhibits the NF-κB pathway [116-120]. VZV interferes with IFN-α/β signalling by inhibiting phosphorylation and nuclear translocation of signal transducers and activators of transcription 1 (STAT1) [51]. IFN-α activates protein kinase R (PKR) that phosphorylates the α-subunit of eukaryotic initiation factor 2 (eIF-2α), thereby preventing initiation of transcription, and this process can be inhibited by VZV ORF63 [121]. VZV-induced phosphorylation of STAT3 results in expression of the anti-apoptotic protein survivin, which promotes virus replication and spread [122]. Nevertheless, IFN-α is detected in serum of healthy children with varicella and reduces the severity of varicella when administered to immunocompromised children [123-124]. Furthermore, IFN-α/β receptor blockage enhances VZV replication and lesion formation in human fetal skin xenografts in the SCID-hu model [51]. Thus, clinical and experimental data suggest that innate immunity contributes to the containment of VZV replication during primary infection.

The innate immune response initiates adaptive cellular and humoral immune responses. In contrast to innate immunity, the adaptive immune response is pathogen-specific and provides long-term immunological memory. Humoral, or antibody-mediated, immunity contributes predominantly to antiviral immunity by virus neutralization and antibody-dependent cell-mediated cytotoxicity. $CD4^+$ and $CD8^+$ T-cells form the cellular arm of adaptive immunity. $CD4^+$ T-cells recognize virus-derived peptides presented by human leukocyte antigen type II (HLA-II) molecules, which are mainly expressed on professional antigen presenting cells (APCs) such as macrophages and DCs. $CD4^+$ T-cells exert direct antiviral activity by secreting anti-viral cytokines like TNF-α and IFN-γ and cytolysis of virus-infected cells. The indirect role of $CD4^+$ T-cells involves the induction of virus-specific B-cell and $CD8^+$ T-cell responses. $CD8^+$ T-cells recognize viral peptides in the context of HLA-I molecules, which are ubiquitously expressed on all nucleated cells, and inhibit virus replication through secretion of cytokines or cytolysis of the virus-infected cells.

B-cell Immunity

The role of humoral immunity in recovery from varicella and for prevention of and resurgence from herpes zoster appears to be limited. Instead, virus-specific humoral immunity most likely prevents or limits VZV superinfection. Patients with antibody deficiency due to agammaglobulinemia have uncomplicated varicella [5]. Maternal antibodies present in infants during the first 6 months of life protect from or modify the severity of varicella [125] and passive immunization with varicella-zoster immune globulin during the early incubation phase (<72 hours after infection) can decrease VZV pathogenicity [5, 126]. Antibodies may limit VZV replication and spread by neutralization of the virus – directly or in the presence of complement –, antibody-

dependent cell-mediated cytotoxicity or by affecting virion production and cell-to-cell fusion [115, 127-128]. During primary infection VZV-specific IgG, IgM and IgA antibodies become detectable 1 – 6 days after the onset of skin rash [42, 123]. The onset and magnitude of the VZV-specific antibody response does not correlate with the severity of varicella or herpes zoster [123, 129]. The initial antibody response is predominantly directed to VZV glycoproteins [130], while antibodies recognizing a large variety of structural and non-structural proteins are detected at later stages after primary infection [130-131]. VZV-specific IgA antibodies, either nasopharyngeal or serum, and serum IgM antibody levels decline within a few months after varicella [132-133]. In contrast, serum VZV-specific IgG antibody levels peak at 4 – 8 weeks after varicella and persist for decades at relatively stable levels [86, 132]. Exogenous re-exposure to VZV and subclinical reactivation induce transient increased virus-specific IgG, IgA and IgM antibody levels [130, 133-134]. VZV-specific humoral immunity does not correlate with the risk of developing herpes zoster [86]. VZV reactivation results in high levels of broadly reactive IgG, IgA and IgM antibodies [130, 133].

T-cell Immunity

VZV-specific T-cells are considered pivotal for the recovery from varicella and for the prevention of and resurgence from herpes zoster. VZV-specific T-cells become detectable 1 – 3 days after appearance of skin rash [123]. The magnitude of the VZV-specific T-cell response initiated during primary infection inversely correlates with the severity of varicella and termination of viremia [123, 135]. Studies on SVV indicate that $CD4^+$ T-cell immunity plays a more critical role than antibody and $CD8^+$ T-cell responses to control varicella [136]. Compared to HSV, studies on local tissue-restricted VZV-specific T-cells are scarce. Yet, both $CD4^+$ and $CD8^+$ T-cells are known to infiltrate the dermis of varicella and HZ patients [137-140], possibly relocating via skin-homing receptors [135]. T-cells infiltrate the eye of VZV uveitis patients and recognize a wide variety of VZV proteins, secrete Th1/Th0-like cytokines, have cytolytic potential, and are able to inhibit virus replication in retinal pigment epithelium cells [141-143]. The combined data suggest a detrimental role of VZV-specific T-cells in the pathology of VZV uveitis. In **Chapter 8** we identified and characterized the functional properties of human ocular derived HSV/VZV cross-reactive $CD4^+$ T-cells.

Memory VZV-specific T-cells are maintained at low frequency [144], likely involving exogenous re-exposure to VZV or endogenous (subclinical) reactivation, and have a mixed central and effector memory phenotype [135, 145-147]. Circulating VZV-specific memory $CD4^+$ T-cells are commonly CLA-negative and preferentially express CD38 and PD-1 [145-146], suggesting recent antigenic stimulation and/or exhaustion. Although similar frequencies of circulating VZV-specific $CD4^+$ and $CD8^+$ cytotoxic T-cells have been reported [148-149], recent studies indicate that VZV-specific $CD8^+$ T-cells are less abundant than $CD4^+$ T-cells [147, 150-151]. T-cell reactivity to VZV antigens include structural proteins including the glycoproteins gB, gC, gE, gH, gI and the IE proteins IE4, IE62 and IE63 [145-146, 148-149, 151-156]. However, the latter studies were restricted to the analysis of only a limited set of virus proteins, which does not allow identification of the immunodominant T-cell antigens involved

in protection and immunopathogenesis.

It is well established that the risk of herpes zoster increases with age [32]. This is largely attributed to the decline of VZV-specific T-cell immunity, but not humoral immunity, with progressing age [85-86, 157]. Notably, the frequency of IL-4 producing VZV-specific T-cells remains unaltered [147, 152, 157-162]. Whether waning of VZV-specific T-cell immunity reflects quantitative or qualitative changes in circulating virus-specific T-cells is unknown. Regardless, herpes zoster induces rapid, profound and sustained T-cell responses [163-164], so that individuals typically develop zoster only once during their life. The magnitude of the VZV-specific T-cell immunity after zoster is inversely correlated with disease severity and the risk of developing PHN [164]. Despite their protective role in preventing reactivation, VZV-specific T-cells have not been detected in latently infected ganglia [84].

VZV developed multiple strategies to evade T-cell immunity. VZV decreases the capacity of DCs to induce specific T-cell responses by reducing surface expression of both the T-cell co-stimulatory molecules (i.e. CD80, CD83 and CD86) and HLA-I and –II molecules [147, 165]. In addition, the virus reduces HLA-I expression and inhibits IFN-γ–induced HLA-II expression on VZV-infected cells to escape $CD8^+$ and $CD4^+$ T-cell recognition, respectively [166-169]. T-cell recognition of VZV is further impaired by reduction of intercellular adhesion molecule 1 (ICAM-1) expression on VZV-infected keratinocytes [139].

VZV Vaccine

The only human herpesvirus vaccine available to date is the live-attenuated VZV vaccine, which induces both B-cell and T-cell mediated immune responses in vaccinated children and the elderly, thereby preventing varicella and herpes zoster, respectively [170-173]. The varicella vaccine is administered using a 2-dose regimen, scheduled for children 12 – 15 months of age and children 4 – 6 years of age [174] and prevents varicella in up to 98% of vaccinated individuals [175]. The zoster vaccine is given to individuals over 60 years of age and effectively prevents the development of zoster in 51% and PHN in 67% of individuals over a 5-year follow-up period [172, 176]. However, the vaccine virus may cause mild varicella and establishes latency posing the risk of reactivation and dissemination in the population [174]. Furthermore, childhood varicella vaccination may result in an increased incidence of herpes zoster and at earlier age as a consequence of decreased exogenous boosting of VZV-specific T-cell immunity [177-179].

4. Animal Models of VZV Infection

VZV Infection in Small Animal Models

VZV is a human-restricted pathogen and does not cause disease in experimental animal models [37], possibly with the exception of Chimpanzees and Gorillas [180-182]. However, certain aspects of VZV pathogenesis have been studied in small

animal models. Infection of guinea pigs with VZV results in a transient viremia, seroconversion and infection of DRG, TG and enteric ganglia [183-184]. The VZV guinea pig model has been used to study the immunogenicity of VZV and, more recently, to investigate VZV infection of enteric ganglia [60, 185]. Inoculation of rats in the footpad or subcutaneously with VZV results in VZV infection of dorsal root ganglia [186-187] and behavioral allodynia and hyperalgesia resembling PHN [188-189]. The VZV rat model has been used to study the role of individual viral genes in establishing latency [190]. However, VZV-infected rat DRG contain virus in both neurons, satellite glial cells and even axons and frequently express late VZV genes – features that are markedly different from VZV latency in humans [186-187, 191-192]. Furthermore, the inability of the virus to reactivate in both the guinea pig and rat model implicate an abortive rather than a latent VZV infection. Nevertheless, the VZV rat model may prove valuable in studying the mechanisms underlying PHN [188-189]. To circumvent the restricted host range of VZV, a mouse model has been developed that studies VZV infection of human fetal tissues which have been transplanted in severe combined immunodeficient (SCID) mice (SCID-hu mouse model) [46, 83]. This model has been successfully used to study the tropism and pathogenesis of VZV in human fetal thymus, liver, skin and ganglion xenografts [48, 52]. In particular, the VZV SCID-hu mouse model has contributed significantly to the identification of virus and host factors involved in VZV pathogenesis in skin and the establishment of latency [46-47]. However, the use of fetal tissues and, especially, the lack of an adaptive immune system are likely to affect VZV pathogenesis. Similar to the other small animal models of VZV infection, the virus is not able to reactivate and cause zoster.

Simian Varicella Virus Infection of Nonhuman Primates

An outbreak of varicella-like disease in nonhuman primates was first reported in 1967 by Clarkson et al. following the introduction of newly acquired African green vervet monkeys (*Cercopithecus aethiops*) into an established colony of vervet monkeys [193]. Subsequent epidemic outbreaks of varicella-like disease were reported in African green monkeys, Patas monkeys (*Erythocebus patas*) and various species of macaque monkeys (*Macaca nemestrina, M. fascicularis, M. fuscata and M. mulatta*) at primate centers [194]. The causative agent was isolated and identified as a herpesvirus, termed SVV, based on both the cytopathic effect observed in affected tissues and cell culture, and the morphology of the virion by electron microscopy [193-194]. SVV and VZV share a high degree of antigenic relatedness [195] and immunization of monkeys with VZV induces protective cross-reactive immunity [181]. Full genome sequencing showed that SVV and VZV genomes are similar in size and structure [196]. The SVV genome contains 71 unique ORFs, 68 of which share extensive homology with the corresponding VZV genes [196-197]. SVV and VZV genomes deviate most in the leftward terminus of the genome [196-197]. SVV does not encode a homologue of VZV ORF2, but contains two additional ORFs not present in the VZV genome (ORF A and ORF LE) [196-197].

SVV causes a natural disease in Old World monkeys with clinical, pathological and immunological features resembling human varicella infection [194, 198]. SVV caus-

es varicella as a primary infection, becomes latent in neurons of ganglia along the entire neuraxis and reactivates after stress or immunosuppression to cause zoster [194, 199]. Both natural and experimental primary SVV infection result in a generalized vesicular cutaneous rash that appears 7 – 14 days after inoculation [194, 199]. Usually the rash first appears in the inguinal area after which the rash becomes generalized with “crops” of lesions appearing predominantly on the face and trunk [194, 199]. Lesions may appear on the mucous membranes of the oropharynx [194, 199]. SVV rash starts as macules and rapidly progresses to papules and vesicles [194, 199]. Additional clinical manifestations include fever, loss of appetite, lethargy and development of a mild hepatitis [194, 199]. Disease severity varies and primary SVV infection can give rise to severe disease, associated with hemorrhagic rash, pneumonia and hepatitis, that may be fatal [194, 199]. Latent SVV infection of neurons in the DRG and TG is established during primary infection and associated with restricted viral gene expression [198-200]. In contrast to VZV latency, latent SVV infections are associated with expression of both sense and anti-sense ORF61 transcripts [198, 201]. Low levels of SVV DNA may persist in peripheral blood and organs for prolonged periods of time in latently infected African green monkeys [19, 202-203] and cynomolgus macaques [199], but possibly not rhesus macaques [198]. SVV reactivation may occur spontaneously in response to stress [194] or can be experimentally induced by immunosuppression and irradiation [204-205]. Similar to VZV reactivation in humans, SVV reactivation results in recrudescent cutaneous rash restricted to a single sensory dermatome [204]. Severe immunosuppression may result in disseminated SVV reactivation [205-206], comparable to the generalized zoster that is occasionally observed in immunocompromised humans. Thus, SVV infection of nonhuman primates provides the first experimental animal model that can be used to study the pathogenesis of varicella, latency and herpes zoster in its natural and immunocompetent host.

5. Aim and Outline of this Thesis

The human-restricted alphaherpesvirus VZV causes varicella as a primary infection, establishes latency in ganglionic neurons and can reactive to cause herpes zoster. The highly cell-associated nature and restricted host range of the virus have seriously hampered the development of *in vitro* and animal models, respectively. Consequently, the pathogenesis of primary and reactivated VZV infections are largely unknown and the VZV latent state remains enigmatic. SVV infection of nonhuman primates mimics VZV in humans and therefore provides a useful model to study the pathogenesis of varicella and herpes zoster in its natural host. The aim of the studies presented in this thesis was to provide novel insights into the virus and host factors involved in the pathogenesis of varicellovirus infections in humans and nonhuman primates.

Primary VZV infection typically results in varicella after a 10 – 21 day incubation period, although some infected individuals may never develop rash. During primary

infection the virus establishes a lifelong latent infection of ganglionic neurons and virus-specific adaptive immune responses are mounted. Most likely, virus is transported to susceptible organs via a cell-associated viremia. However, the cell types involved in dissemination of VZV during primary infection are unknown. The pathogenesis of primary VZV infection cannot be studied in humans and therefore we have used SVV infection of nonhuman primates as a model. In **Chapter 2**, the virus-host interactions involved in asymptomatic primary SVV infection in Chinese rhesus macaques are discussed. **Chapter 3** aimed to characterize the kinetics of virus infection and the cell types involved in the dissemination of SVV to the virus' target organs during primary infection of African green monkeys.

The virus and host factors involved in establishment and maintenance of latency are poorly understood. Studies of VZV latency have been restricted to the analysis of human ganglia obtained at autopsy and have reported discrepant numbers and abundance of VZV transcripts. Moreover, several VZV proteins have been described to be expressed in latently infected human ganglia, demonstrating aberrant cytoplasmatic localization in neurons. VZV protein expression in ganglia is under debate. The study described in **Chapter 4** investigated the possibility that VZV-specific mAbs cross-react with blood group A1-associated antigens in neurons, resulting in false-positive neuronal VZV staining in snap-frozen human TG and DRG. Discrepancies in detected VZV transcripts in latently infected human ganglia may be due to methodological differences and/or variable postmortem intervals. **Chapter 5** describes the study on the breadth and magnitude of VZV transcription in human TG obtained at variable intervals after death.

Symptomatic VZV reactivation, i.e. herpes zoster, due to waning of virus-specific T-cell immunity typically occurs once in a lifetime. Like VZV, the more extensively studied human alphaherpesvirus HSV-1 establishes latency in sensory neurons and both viruses may even establish latency within the same neuron. Symptomatic and asymptomatic HSV-1 reactivation occurs frequently, but the incidence of subclinical VZV reactivation and its relation to HSV-1 shedding in the same individual is less well studied. **Chapter 6** describes the prevalence and kinetics of oral HSV-1 and VZV shedding in HIV patients. The pathogenesis of VZV reactivation is largely unknown and detailed studies on the pathological changes in ganglia upon herpes zoster are scarce. Rare ganglia obtained at autopsy from zoster patients showed profound histopathology and ganglionitis associated with the infiltration of T-cells. However, the stimulus initiating the infiltration and retention of T-cells in ganglia upon reactivation is unknown. In **Chapter 7** ganglia of cynomolgus macaques with herpes zoster were analyzed for the presence of T-cell infiltrates, virus replication and the expression of the T-cell recruiting chemokine CXCL10 at variable times after reactivation. VZV reactivation may cause acute retinal necrosis, a potentially blinding inflammatory eye disease in which virus-specific T-cells are considered to exert a pathogenic role. A common target of ocular-derived VZV-specific T-cells is IE62, which shares extensively sequence homology with the orthologous HSV protein ICP4. **Chapter 8** describes the identification and functional characterization of ocular-derived IE62/ICP4 cross-reactive $CD4^+$ T-cells.

References

1. McGeoch DJ, Rixon FJ and Davison AJ. Topics in herpesvirus genomics and evolution. Virus Res 2006;117:90-104
2. Davison AJ. Herpesvirus systematics. Vet Microbiol 2010;143:52-69
3. Davison AJ, Eberle R, Ehlers B, et al. The order Herpesvirales. Arch Virol 2009;154:171-7
4. Pellett PE and Roizman B. The Family of Herpesviridae: A brief introduction. In: Knipe DM, Howley PM, Griffin DE, et al., eds. Fields Virology. 5th ed. Vol. 2. Philadelphia: Lippincott-Williams and Wilkins, 2007:2479-2499
5. Cohen JI, Straus SE and Arvin AM. Varicella-zoster virus replication, pathogenesis, and management. In: Knipe DM, Howley PM, Griffin DE, et al., eds. Fields Virology. 5th ed. Vol. 2. Philadelphia: Lippincott-Williams and Wilkins, 2007:2773-2818
6. Davison AJ, Scott JE. The complete DNA sequence of varicella-zoster virus. J Gen Virol 1986;67 (Pt 9):1759-816
7. Almeida JD, Howatson AF and Williams MG. Morphology of varicella (chicken pox) virus. Virology 1962;16:353-5
8. McMillan DJ, Kay J and Mills JS. Characterization of the proteinase specified by varicella-zoster virus gene 33. J Gen Virol 1997;78 (Pt 9):2153-7
9. Vafai A, Wroblewska Z and Graf L. Antigenic cross-reaction between a varicella-zoster virus nucleocapsid protein encoded by gene 40 and a herpes simplex virus nucleocapsid protein. Virus Res 1990;15:163-74
10. Che X, Oliver SL, Reichelt M, et al. ORF11 Protein Interacts with the ORF9 Essential Tegument Protein in Varicella-Zoster Virus Infection. J Virol 2013;87:5106-17
11. Koshizuka T, Sadaoka T, Yoshii H, Yamanishi K and Mori Y. Varicella-zoster virus ORF1 gene product is a tail-anchored membrane protein localized to plasma membrane and trans-Golgi network in infected cells. Virology 2008;377:289-95
12. Liu X, Li Q, Dowdell K, Fischer ER and Cohen JI. Varicella-Zoster virus ORF12 protein triggers phosphorylation of ERK1/2 and inhibits apoptosis. J Virol 2012;86:3143-51
13. Leisenfelder SA, Kinchington PR and Moffat JF. Cyclin-dependent kinase 1/cyclin B1 phosphorylates varicella-zoster virus IE62 and is incorporated into virions. J Virol 2008;82:12116-25
14. Storlie J, Maresova L, Jackson W and Grose C. Comparative analyses of the 9 glycoprotein genes found in wild-type and vaccine strains of varicella-zoster virus. J Infect Dis 2008;197 Suppl 2:S49-53
15. Chen JJ, Zhu Z, Gershon AA and Gershon MD. Mannose 6-phosphate receptor dependence of varicella zoster virus infection in vitro and in the epidermis during varicella and zoster. Cell 2004;119:915-26
16. Zhu Z, Gershon MD, Ambron R, Gabel C and Gershon AA. Infection of cells by varicella zoster virus: inhibition of viral entry by mannose 6-phosphate and heparin. Proc Natl Acad Sci U S A 1995;92:3546-50
17. Li Q, Ali MA and Cohen JI. Insulin degrading enzyme is a cellular receptor mediating varicella-zoster virus infection and cell-to-cell spread. Cell 2006;127:305-16
18. Suenaga T, Satoh T, Somboonthum P, Kawaguchi Y, Mori Y and Arase H. Myelin-associated glycoprotein mediates membrane fusion and entry of neurotropic herpesviruses. Proc Natl Acad Sci U S A 2010;107:866-71
19. Connolly SA, Jackson JO, Jardetzky TS and Longnecker R. Fusing structure and function: a structural view of the herpesvirus entry machinery. Nat Rev Microbiol 2011;9:369-81
20. Oliver SL, Brady JJ, Sommer MH, et al. An immunoreceptor tyrosine-based inhibition motif in varicella-zoster virus glycoprotein B regulates cell fusion and skin pathogenesis. Proc Natl Acad Sci U S A 2013;110:1911-6
21. Vleck SE, Oliver SL, Brady JJ, et al. Structure-function analysis of varicella-zoster virus glycoprotein H identifies domain-specific roles for fusion and skin tropism. Proc Natl Acad Sci U S A 2011;108:18412-7
22. Lenac Rovis T, Bailer SM, Pothineni VR, et al. A comprehensive analysis of varicella zoster virus proteins using a new monoclonal antibody collection. J Virol 2013
23. Reichelt M, Brady J and Arvin AM. The replication cycle of varicella-zoster virus: analysis of the

kinetics of viral protein expression, genome synthesis, and virion assembly at the single-cell level. J Virol 2009;83:3904-18
24. Gershon AA, Sherman DL, Zhu Z, Gabel CA, Ambron RT and Gershon MD. Intracellular transport of newly synthesized varicella-zoster virus: final envelopment in the trans-Golgi network. J Virol 1994;68:6372-90
25. Hambleton S, Gershon MD and Gershon AA. The role of the trans-Golgi network in varicella zoster virus biology. Cell Mol Life Sci 2004;61:3047-56
26. Harson R, Grose C. Egress of varicella-zoster virus from the melanoma cell: a tropism for the melanocyte. J Virol 1995;69:4994-5010
27. Arvin AM, Gershon AA. Live attenuated varicella vaccine. Annu Rev Microbiol 1996;50:59-100
28. Heininger U, Seward JF. Varicella. Lancet 2006;368:1365-76
29. Gilden DH, Kleinschmidt-DeMasters BK, LaGuardia JJ, Mahalingam R and Cohrs RJ. Neurologic complications of the reactivation of varicella-zoster virus. N Engl J Med 2000;342:635-45
30. Barak M, Weinberger R. Outcome of IgM- and IgG-seropositive cases of varicella zoster in pregnancy. J Reprod Med 2004;49:38-40
31. Dworkin RH, Johnson RW, Breuer J, et al. Recommendations for the management of herpes zoster. Clin Infect Dis 2007;44 Suppl 1:S1-26
32. Hope-Simpson RE. The Nature of Herpes Zoster: A Long-Term Study and a New Hypothesis. Proc R Soc Med 1965;58:9-20
33. Liesegang TJ. Varicella-zoster virus eye disease. Cornea 1999;18:511-31
34. Remeijer L, Osterhaus A and Verjans G. Human herpes simplex virus keratitis: the pathogenesis revisited. Ocul Immunol Inflamm 2004;12:255-85
35. de Melker H, Berbers G, Hahne S, et al. The epidemiology of varicella and herpes zoster in The Netherlands: implications for varicella zoster virus vaccination. Vaccine 2006;24:3946-52
36. Gershon AA, Chen J, Davis L, et al. Latency of varicella zoster virus in dorsal root, cranial, and enteric ganglia in vaccinated children. Trans Am Clin Climatol Assoc 2012;123:17-33; discussion 33-5
37. Kinchington PR. Latency of varicella zoster virus; a persistently perplexing state. Front Biosci 1999;4:D200-11
38. Grose C. Variation on a theme by Fenner: the pathogenesis of chickenpox. Pediatrics 1981;68:735-7
39. Sawyer MH, Chamberlin CJ, Wu YN, Aintablian N and Wallace MR. Detection of varicella-zoster virus DNA in air samples from hospital rooms. J Infect Dis 1994;169:91-4
40. Lemon K, de Vries RD, Mesman AW, et al. Early target cells of measles virus after aerosol infection of non-human primates. PLoS Pathog 2011;7:e1001263
41. Asano Y, Itakura N, Hiroishi Y, et al. Viremia is present in incubation period in nonimmunocompromised children with varicella. J Pediatr 1985;106:69-71
42. Asano Y, Itakura N, Hiroishi Y, et al. Viral replication and immunologic responses in children naturally infected with varicella-zoster virus and in varicella vaccine recipients. J Infect Dis 1985;152:863-8
43. Koropchak CM, Graham G, Palmer J, et al. Investigation of varicella-zoster virus infection by polymerase chain reaction in the immunocompetent host with acute varicella. J Infect Dis 1991;163:1016-22
44. Ozaki T, Ichikawa T, Matsui Y, et al. Viremic phase in nonimmunocompromised children with varicella. J Pediatr 1984;104:85-7
45. Cheatham WJ, Dolan TF, Jr., Dower JC and Weller TH. Varicella: report of two fatal cases with necropsy, virus isolation, and serologic studies. Am J Pathol 1956;32:1015-35
46. Arvin AM, Moffat JF, Sommer M, et al. Varicella-zoster virus T cell tropism and the pathogenesis of skin infection. Curr Top Microbiol Immunol 2010;342:189-209
47. Zerboni L, Reichelt M and Arvin A. Varicella-zoster virus neurotropism in SCID mouse-human dorsal root ganglia xenografts. Curr Top Microbiol Immunol 2010;342:255-76
48. Moffat JF, Stein MD, Kaneshima H and Arvin AM. Tropism of varicella-zoster virus for human CD4+ and CD8+ T lymphocytes and epidermal cells in SCID-hu mice. J Virol 1995;69:5236-42
49. Abendroth A, Morrow G, Cunningham AL and Slobedman B. Varicella-zoster virus infection of human dendritic cells and transmission to T cells: implications for virus dissemination in the host. J Virol 2001;75:6183-92
50. Ku CC, Padilla JA, Grose C, Butcher EC and Arvin AM. Tropism of varicella-zoster virus for

human tonsillar CD4(+) T lymphocytes that express activation, memory, and skin homing markers. J Virol 2002;76:11425-33
51. Ku CC, Zerboni L, Ito H, Graham BS, Wallace M and Arvin AM. Varicella-zoster virus transfer to skin by T Cells and modulation of viral replication by epidermal cell interferon-alpha. J Exp Med 2004;200:917-25
52. Zerboni L, Ku CC, Jones CD, Zehnder JL and Arvin AM. Varicella-zoster virus infection of human dorsal root ganglia in vivo. Proc Natl Acad Sci U S A 2005;102:6490-5
53. Kennedy PG, Grinfeld E and Gow JW. Latent varicella-zoster virus is located predominantly in neurons in human trigeminal ganglia. Proc Natl Acad Sci U S A 1998;95:4658-62
54. Wang K, Lau TY, Morales M, Mont EK and Straus SE. Laser-capture microdissection: refining estimates of the quantity and distribution of latent herpes simplex virus 1 and varicella-zoster virus DNA in human trigeminal Ganglia at the single-cell level. J Virol 2005;79:14079-87
55. Annunziato PW, Lungu O, Panagiotidis C, et al. Varicella-zoster virus proteins in skin lesions: implications for a novel role of ORF29p in chickenpox. J Virol 2000;74:2005-10
56. Grigoryan S, Kinchington PR, Yang IH, et al. Retrograde axonal transport of VZV: kinetic studies in hESC-derived neurons. J Neurovirol 2012;18:462-70
57. Markus A, Grigoryan S, Sloutskin A, et al. Varicella-zoster virus (VZV) infection of neurons derived from human embryonic stem cells: direct demonstration of axonal infection, transport of VZV, and productive neuronal infection. J Virol 2011;85:6220-33
58. Mahalingam R, Wellish M, Soike K, White T, Kleinschmidt-DeMasters BK and Gilden DH. Simian varicella virus infects ganglia before rash in experimentally infected monkeys. Virology 2001;279:339-42
59. Zerboni L, Reichelt M, Jones CD, Zehnder JL, Ito H and Arvin AM. Aberrant infection and persistence of varicella-zoster virus in human dorsal root ganglia in vivo in the absence of glycoprotein I. Proc Natl Acad Sci U S A 2007;104:14086-91
60. Chen JJ, Gershon AA, Li Z, Cowles RA and Gershon MD. Varicella zoster virus (VZV) infects and establishes latency in enteric neurons. J Neurovirol 2011;17:578-89
61. Furuta Y, Takasu T, Suzuki S, Fukuda S, Inuyama Y and Nagashima K. Detection of latent varicella-zoster virus infection in human vestibular and spiral ganglia. J Med Virol 1997;51:214-6
62. Gilden DH, Gesser R, Smith J, et al. Presence of VZV and HSV-1 DNA in human nodose and celiac ganglia. Virus Genes 2001;23:145-7
63. Mahalingam R, Wellish M, Wolf W, et al. Latent varicella-zoster viral DNA in human trigeminal and thoracic ganglia. N Engl J Med 1990;323:627-31
64. Richter ER, Dias JK, Gilbert JE, 2nd and Atherton SS. Distribution of herpes simplex virus type 1 and varicella zoster virus in ganglia of the human head and neck. J Infect Dis 2009;200:1901-6
65. Hanani M. Satellite glial cells in sensory ganglia: from form to function. Brain Res Brain Res Rev 2005;48:457-76
66. Levin MJ, Cai GY, Manchak MD and Pizer LI. Varicella-zoster virus DNA in cells isolated from human trigeminal ganglia. J Virol 2003;77:6979-87
67. Clarke P, Beer T, Cohrs R and Gilden DH. Configuration of latent varicella-zoster virus DNA. J Virol 1995;69:8151-4
68. Gary L, Gilden DH and Cohrs RJ. Epigenetic regulation of varicella-zoster virus open reading frames 62 and 63 in latently infected human trigeminal ganglia. J Virol 2006;80:4921-6
69. Stevens JG, Haarr L, Porter DD, Cook ML and Wagner EK. Prominence of the herpes simplex virus latency-associated transcript in trigeminal ganglia from seropositive humans. J Infect Dis 1988;158:117-23
70. Umbach JL, Kramer MF, Jurak I, Karnowski HW, Coen DM and Cullen BR. MicroRNAs expressed by herpes simplex virus 1 during latent infection regulate viral mRNAs. Nature 2008;454:780-3
71. Umbach JL, Nagel MA, Cohrs RJ, Gilden DH and Cullen BR. Analysis of human alphaherpesvirus microRNA expression in latently infected human trigeminal ganglia. J Virol 2009;83:10677-83
72. Cohrs RJ, Barbour M and Gilden DH. Varicella-zoster virus (VZV) transcription during latency in human ganglia: detection of transcripts mapping to genes 21, 29, 62, and 63 in a cDNA library enriched for VZV RNA. J Virol 1996;70:2789-96
73. Cohrs RJ, Gilden DH. Varicella zoster virus transcription in latently-infected human ganglia. Anticancer Res 2003;23:2063-9
74. Cohrs RJ, Gilden DH. Prevalence and abundance of latently transcribed varicella-zoster virus genes in human ganglia. J Virol 2007;81:2950-6

75. Cohrs RJ, Srock K, Barbour MB, et al. Varicella-zoster virus (VZV) transcription during latency in human ganglia: construction of a cDNA library from latently infected human trigeminal ganglia and detection of a VZV transcript. J Virol 1994;68:7900-8
76. Kennedy PG, Grinfeld E and Bell JE. Varicella-zoster virus gene expression in latently infected and explanted human ganglia. J Virol 2000;74:11893-8
77. Nagel MA, Choe A, Traktinskiy I, Cordery-Cotter R, Gilden D and Cohrs RJ. Varicella-zoster virus transcriptome in latently infected human ganglia. J Virol 2011;85:2276-87
78. Grinfeld E, Kennedy PG. Translation of varicella-zoster virus genes during human ganglionic latency. Virus Genes 2004;29:317-9
79. Lungu O, Panagiotidis CA, Annunziato PW, Gershon AA and Silverstein SJ. Aberrant intracellular localization of Varicella-Zoster virus regulatory proteins during latency. Proc Natl Acad Sci U S A 1998;95:7080-5
80. Theil D, Derfuss T, Paripovic I, et al. Latent herpesvirus infection in human trigeminal ganglia causes chronic immune response. Am J Pathol 2003;163:2179-84
81. Mahalingam R, Wellish M, Cohrs R, et al. Expression of protein encoded by varicella-zoster virus open reading frame 63 in latently infected human ganglionic neurons. Proc Natl Acad Sci U S A 1996;93:2122-4
82. Zerboni L, Sobel RA, Lai M, et al. Apparent expression of varicella-zoster virus proteins in latency resulting from reactivity of murine and rabbit antibodies with human blood group a determinants in sensory neurons. J Virol 2012;86:578-83
83. Zerboni L, Sobel RA, Ramachandran V, et al. Expression of varicella-zoster virus immediate-early regulatory protein IE63 in neurons of latently infected human sensory ganglia. J Virol 2010;84:3421-30
84. Verjans GM, Hintzen RQ, van Dun JM, et al. Selective retention of herpes simplex virus-specific T cells in latently infected human trigeminal ganglia. Proc Natl Acad Sci U S A 2007;104:3496-501
85. Burke BL, Steele RW, Beard OW, Wood JS, Cain TD and Marmer DJ. Immune responses to varicella-zoster in the aged. Arch Intern Med 1982;142:291-3
86. Miller AE. Selective decline in cellular immune response to varicella-zoster in the elderly. Neurology 1980;30:582-7
87. Esiri MM, Tomlinson AH. Herpes Zoster. Demonstration of virus in trigeminal nerve and ganglion by immunofluorescence and electron microscopy. J Neurol Sci 1972;15:35-48
88. Nagashima K, Nakazawa M and Endo H. Pathology of the human spinal ganglia in varicella-zoster virus infection. Acta Neuropathol 1975;33:105-17
89. Shibuta H, Ishikawa T, Hondo R, Aoyama Y, Kurata K and Matumoto M. Varicella virus isolation from spinal ganglion. Arch Gesamte Virusforsch 1974;45:382-5
90. Head H, Campbell AW. The pathology of herpes zoster and its bearing on sensory localisation. Brain 1900;23:170
91. Gowrishankar K, Steain M, Cunningham AL, et al. Characterization of the host immune response in human Ganglia after herpes zoster. J Virol 2010;84:8861-70
92. Gilden DH, Hayward AR, Krupp J, Hunter-Laszlo M, Huff JC and Vafai A. Varicella-zoster virus infection of human mononuclear cells. Virus Res 1987;7:117-29
93. Oaklander AL. The density of remaining nerve endings in human skin with and without postherpetic neuralgia after shingles. Pain 2001;92:139-45
94. Mahalingam R, Wellish M, Brucklier J and Gilden DH. Persistence of varicella-zoster virus DNA in elderly patients with postherpetic neuralgia. J Neurovirol 1995;1:130-3
95. Watson CP, Deck JH, Morshead C, Van der Kooy D and Evans RJ. Post-herpetic neuralgia: further post-mortem studies of cases with and without pain. Pain 1991;44:105-17
96. Gilden D, Cohrs RJ, Mahalingam R and Nagel MA. Varicella zoster virus vasculopathies: diverse clinical manifestations, laboratory features, pathogenesis, and treatment. Lancet Neurol 2009;8:731-40
97. Devlin ME, Gilden DH, Mahalingam R, Dueland AN and Cohrs R. Peripheral blood mononuclear cells of the elderly contain varicella-zoster virus DNA. J Infect Dis 1992;165:619-22
98. Schunemann S, Mainka C and Wolff MH. Subclinical reactivation of varicella-zoster virus in immunocompromised and immunocompetent individuals. Intervirology 1998;41:98-102
99. Cohrs RJ, Mehta SK, Schmid DS, Gilden DH and Pierson DL. Asymptomatic reactivation and shed of infectious varicella zoster virus in astronauts. J Med Virol 2008;80:1116-22
100. Mehta SK, Cohrs RJ, Forghani B, Zerbe G, Gilden DH and Pierson DL. Stress-induced subclinical

reactivation of varicella zoster virus in astronauts. J Med Virol 2004;72:174-9
101. Nagel MA, Choe A, Cohrs RJ, et al. Persistence of varicella zoster virus DNA in saliva after herpes zoster. J Infect Dis 2011;204:820-4
102. Gilden D, Cohrs RJ, Mahalingam R and Nagel MA. Neurological disease produced by varicella zoster virus reactivation without rash. Curr Top Microbiol Immunol 2010;342:243-53
103. Vandevenne P, Sadzot-Delvaux C and Piette J. Innate immune response and viral interference strategies developed by human herpesviruses. Biochem Pharmacol 2010;80:1955-72
104. Wang JP, Kurt-Jones EA, Shin OS, Manchak MD, Levin MJ and Finberg RW. Varicella-zoster virus activates inflammatory cytokines in human monocytes and macrophages via Toll-like receptor 2. J Virol 2005;79:12658-66
105. Yu HR, Huang HC, Kuo HC, et al. IFN-alpha production by human mononuclear cells infected with varicella-zoster virus through TLR9-dependent and -independent pathways. Cell Mol Immunol 2011;8:181-8
106. Nour AM, Reichelt M, Ku CC, Ho MY, Heineman TC and Arvin AM. Varicella-zoster virus infection triggers formation of an interleukin-1beta (IL-1beta)-processing inflammasome complex. J Biol Chem 2011;286:17921-33
107. Reichelt M, Wang L, Sommer M, et al. Entrapment of viral capsids in nuclear PML cages is an intrinsic antiviral host defense against varicella-zoster virus. PLoS Pathog 2011;7:e1001266
108. Carpenter JE, Jackson W, Benetti L and Grose C. Autophagosome formation during varicella-zoster virus infection following endoplasmic reticulum stress and the unfolded protein response. J Virol 2011;85:9414-24
109. Takahashi MN, Jackson W, Laird DT, et al. Varicella-zoster virus infection induces autophagy in both cultured cells and human skin vesicles. J Virol 2009;83:5466-76
110. Banovic T, Yanilla M, Simmons R, et al. Disseminated varicella infection caused by varicella vaccine strain in a child with low invariant natural killer T cells and diminished CD1d expression. J Infect Dis 2011;204:1893-901
111. Levy O, Orange JS, Hibberd P, et al. Disseminated varicella infection due to the vaccine strain of varicella-zoster virus, in a patient with a novel deficiency in natural killer T cells. J Infect Dis 2003;188:948-53
112. Malavige GN, Jones L, Kamaladasa SD, et al. Natural Killer Cells During Primary Varicella Zoster Virus Infection. J Infect 2010
113. Notarangelo LD, Mazzolari E. Natural killer cell deficiencies and severe varicella infection. J Pediatr 2006;148:563-4; author reply 564
114. Hata A, Zerboni L, Sommer M, et al. Granulysin blocks replication of varicella-zoster virus and triggers apoptosis of infected cells. Viral Immunol 2001;14:125-33
115. Ihara T, Kamiya H, Starr SE, Arbeter AM and Lange B. Natural killing of varicella-zoster virus (VZV)-infected fibroblasts in normal children, children with VZV infections, and children with Hodgkin's disease. Acta Paediatr Jpn 1989;31:523-8
116. Jones JO, Arvin AM. Inhibition of the NF-kappaB pathway by varicella-zoster virus in vitro and in human epidermal cells in vivo. J Virol 2006;80:5113-24
117. El Mjiyad N, Bontems S, Gloire G, et al. Varicella-zoster virus modulates NF-kappaB recruitment on selected cellular promoters. J Virol 2007;81:13092-104
118. Sen N, Sommer M, Che X, White K, Ruyechan WT and Arvin AM. Varicella-zoster virus immediate-early protein 62 blocks interferon regulatory factor 3 (IRF3) phosphorylation at key serine residues: a novel mechanism of IRF3 inhibition among herpesviruses. J Virol 2010;84:9240-53
119. Zhu H, Zheng C, Xing J, et al. Varicella-zoster virus immediate-early protein ORF61 abrogates the IRF3-mediated innate immune response through degradation of activated IRF3. J Virol 2011;85:11079-89
120. Vandevenne P, Lebrun M, El Mjiyad N, et al. The varicella-zoster virus ORF47 kinase interferes with host innate immune response by inhibiting the activation of IRF3. PLoS One 2011;6:e16870
121. Ambagala AP, Cohen JI. Varicella-Zoster virus IE63, a major viral latency protein, is required to inhibit the alpha interferon-induced antiviral response. J Virol 2007;81:7844-51
122. Sen N, Che X, Rajamani J, et al. Signal transducer and activator of transcription 3 (STAT3) and survivin induction by varicella-zoster virus promote replication and skin pathogenesis. Proc Natl Acad Sci U S A 2012;109:600-5
123. Arvin AM, Koropchak CM, Williams BR, Grumet FC and Foung SK. Early immune response in

healthy and immunocompromised subjects with primary varicella-zoster virus infection. J Infect Dis 1986;154:422-9
124. Arvin AM, Kushner JH, Feldman S, Baehner RL, Hammond D and Merigan TC. Human leukocyte interferon for the treatment of varicella in children with cancer. N Engl J Med 1982;306:761-5
125. Brunell PA. Varicella in pregnancy, the fetus, and the newborn: problems in management. J Infect Dis 1992;166 Suppl 1:S42-7
126. Zaia JA, Levin MJ, Preblud SR, et al. Evaluation of varicella-zoster immune globulin: protection of immunosuppressed children after household exposure to varicella. J Infect Dis 1983;147:737-43
127. Grose C, Edmond BJ and Brunell PA. Complement-enhanced neutralizing antibody response to varicella-zoster virus. J Infect Dis 1979;139:432-7
128. Vleck SE, Oliver SL, Reichelt M, et al. Anti-glycoprotein H antibody impairs the pathogenicity of varicella-zoster virus in skin xenografts in the SCID mouse model. J Virol 2010;84:141-52
129. Asada H, Nagayama K, Okazaki A, et al. An inverse correlation of VZV skin-test reaction, but not antibody, with severity of herpes zoster skin symptoms and zoster-associated pain. J Dermatol Sci 2013;69:243-9
130. Weigle KA, Grose C. Molecular dissection of the humoral immune response to individual varicella-zoster viral proteins during chickenpox, quiescence, reinfection, and reactivation. J Infect Dis 1984;149:741-9
131. Vizoso Pinto MG, Pfrepper KI, Janke T, et al. A systematic approach for the identification of novel, serologically reactive recombinant Varicella-Zoster Virus (VZV) antigens. Virol J 2010;7:165
132. Bogger-Goren S, Baba K, Hurley P, Yabuuchi H, Takahashi M and Ogra PL. Antibody response to varicella-zoster virus after natural or vaccine-induced infection. J Infect Dis 1982;146:260-5
133. Brunell PA, Gershon AA, Uduman SA and Steinberg S. Varicella-Zoster Immunoglobulins during Varicella, Latency, and Zoster. J Infect Dis 1975;132:49-54
134. Gershon AA, Steinberg SP, Borkowsky W, Lennette D and Lennette E. IgM to varicella-zoster virus: demonstration in patients with and without clinical zoster. Pediatr Infect Dis 1982;1:164-7
135. Malavige GN, Jones L, Kamaladasa SD, et al. Viral load, clinical disease severity and cellular immune responses in primary varicella zoster virus infection in Sri Lanka. PLoS One 2008;3:e3789
136. Haberthur K, Engelmann F, Park B, et al. CD4 T cell immunity is critical for the control of simian varicella virus infection in a nonhuman primate model of VZV infection. PLoS Pathog 2011;7:e1002367
137. Leinweber B, Kerl H and Cerroni L. Histopathologic features of cutaneous herpes virus infections (herpes simplex, herpes varicella/zoster): a broad spectrum of presentations with common pseudolymphomatous aspects. Am J Surg Pathol 2006;30:50-8
138. Morizane S, Suzuki D, Tsuji K, Oono T and Iwatsuki K. The role of CD4 and CD8 cytotoxic T lymphocytes in the formation of viral vesicles. Br J Dermatol 2005;153:981-6
139. Nikkels AF, Sadzot-Delvaux C and Pierard GE. Absence of intercellular adhesion molecule 1 expression in varicella zoster virus-infected keratinocytes during herpes zoster: another immune evasion strategy? Am J Dermatopathol 2004;26:27-32
140. Zak-Prelich M, McKenzie RC, Sysa-Jedrzejowska A and Norval M. Local immune responses and systemic cytokine responses in zoster: relationship to the development of postherpetic neuralgia. Clin Exp Immunol 2003;131:318-23
141. Milikan JC, Baarsma GS, Kuijpers RW, Osterhaus AD and Verjans GM. Human ocular-derived virus-specific CD4+ T cells control varicella zoster virus replication in human retinal pigment epithelial cells. Invest Ophthalmol Vis Sci 2009;50:743-51
142. Milikan JC, Kinchington PR, Baarsma GS, Kuijpers RW, Osterhaus AD and Verjans GM. Identification of viral antigens recognized by ocular infiltrating T cells from patients with varicella zoster virus-induced uveitis. Invest Ophthalmol Vis Sci 2007;48:3689-97
143. Milikan JC, Kuijpers RW, Baarsma GS, Osterhaus AD and Verjans GM. Characterization of the varicella zoster virus (VZV)-specific intra-ocular T-cell response in patients with VZV-induced uveitis. Exp Eye Res 2006;83:69-75
144. Asanuma H, Sharp M, Maecker HT, Maino VC and Arvin AM. Frequencies of memory T cells specific for varicella-zoster virus, herpes simplex virus, and cytomegalovirus by intracellular detection of cytokine expression. J Infect Dis 2000;181:859-66
145. Jones L, Black AP, Malavige GN and Ogg GS. Phenotypic analysis of human CD4+ T cells specific for immediate-early 63 protein of varicella-zoster virus. Eur J Immunol 2007;37:3393-403

146. Malavige GN, Jones L, Black AP and Ogg GS. Varicella zoster virus glycoprotein E-specific CD4+ T cells show evidence of recent activation and effector differentiation, consistent with frequent exposure to replicative cycle antigens in healthy immune donors. Clin Exp Immunol 2008;152:522-31
147. van Besouw NM, Verjans GM, Zuijderwijk JM, Litjens NH, Osterhaus AD and Weimar W. Systemic varicella zoster virus reactive effector memory T-cells impaired in the elderly and in kidney transplant recipients. J Med Virol 2012;84:2018-25
148. Arvin AM, Sharp M, Smith S, et al. Equivalent recognition of a varicella-zoster virus immediate early protein (IE62) and glycoprotein I by cytotoxic T lymphocytes of either CD4+ or CD8+ phenotype. J Immunol 1991;146:257-64
149. Sadzot-Delvaux C, Arvin AM and Rentier B. Varicella-zoster virus IE63, a virion component expressed during latency and acute infection, elicits humoral and cellular immunity. J Infect Dis 1998;178 Suppl 1:S43-7
150. Frey CR, Sharp MA, Min AS, Schmid DS, Loparev V and Arvin AM. Identification of CD8+ T cell epitopes in the immediate early 62 protein (IE62) of varicella-zoster virus, and evaluation of frequency of CD8+ T cell response to IE62, by use of IE62 peptides after varicella vaccination. J Infect Dis 2003;188:40-52
151. Kleemann P, Distler E, Wagner EM, et al. Varicella-zoster virus glycoproteins B and E are major targets of CD4+ and CD8+ T cells reconstituting during zoster after allogeneic transplantation. Haematologica 2012;97:874-82
152. Arvin AM, Sharp M, Moir M, et al. Memory cytotoxic T cell responses to viral tegument and regulatory proteins encoded by open reading frames 4, 10, 29, and 62 of varicella-zoster virus. Viral Immunol 2002;15:507-16
153. Huang Z, Vafai A, Lee J, Mahalingam R and Hayward AR. Specific lysis of targets expressing varicella-zoster virus gpI or gpIV by CD4+ human T-cell clones. J Virol 1992;66:2664-9
154. Jones L, Black AP, Malavige GN and Ogg GS. Persistent high frequencies of varicella-zoster virus ORF4 protein-specific CD4+ T cells after primary infection. J Virol 2006;80:9772-8
155. Sadzot-Delvaux C, Kinchington PR, Debrus S, Rentier B and Arvin AM. Recognition of the latency-associated immediate early protein IE63 of varicella-zoster virus by human memory T lymphocytes. J Immunol 1997;159:2802-6
156. van der Heiden PL, de Boer R, van der Steen DM, et al. Identification of varicella-zoster virus-specific CD8 T cells in patients after T-cell-depleted allogeneic stem cell transplantation. J Virol 2009;83:7361-4
157. Levin MJ, Smith JG, Kaufhold RM, et al. Decline in varicella-zoster virus (VZV)-specific cell-mediated immunity with increasing age and boosting with a high-dose VZV vaccine. J Infect Dis 2003;188:1336-44
158. Jenkins DE, Redman RL, Lam EM, Liu C, Lin I and Arvin AM. Interleukin (IL)-10, IL-12, and interferon-gamma production in primary and memory immune responses to varicella-zoster virus. J Infect Dis 1998;178:940-8
159. Tyring SK, Stek JE, Smith JG, et al. Varicella-zoster virus-specific enzyme-linked immunospot assay responses and zoster-associated pain in herpes zoster subjects. Clin Vaccine Immunol 2012;19:1411-5
160. Weinberg A, Lazar AA, Zerbe GO, et al. Influence of age and nature of primary infection on varicella-zoster virus-specific cell-mediated immune responses. J Infect Dis 2010;201:1024-30
161. Zhang Y, Cosyns M, Levin MJ and Hayward AR. Cytokine production in varicella zoster virus-stimulated limiting dilution lymphocyte cultures. Clin Exp Immunol 1994;98:128-33
162. Zhang Y, White CJ, Levin M and Hayward A. Cytokine production in varicella-zoster virus-stimulated lymphocyte cultures. Neurology 1995;45:S38-40
163. Hayward A, Levin M, Wolf W, Angelova G and Gilden D. Varicella-zoster virus-specific immunity after herpes zoster. J Infect Dis 1991;163:873-5
164. Weinberg A, Zhang JH, Oxman MN, et al. Varicella-zoster virus-specific immune responses to herpes zoster in elderly participants in a trial of a clinically effective zoster vaccine. J Infect Dis 2009;200:1068-77
165. Morrow G, Slobedman B, Cunningham AL and Abendroth A. Varicella-zoster virus productively infects mature dendritic cells and alters their immune function. J Virol 2003;77:4950-9
166. Abendroth A, Lin I, Slobedman B, Ploegh H and Arvin AM. Varicella-zoster virus retains major histocompatibility complex class I proteins in the Golgi compartment of infected cells. J Virol

2001;75:4878-88
167. Abendroth A, Slobedman B, Lee E, Mellins E, Wallace M and Arvin AM. Modulation of major histocompatibility class II protein expression by varicella-zoster virus. J Virol 2000;74:1900-7
168. Cohen JI. Infection of cells with varicella-zoster virus down-regulates surface expression of class I major histocompatibility complex antigens. J Infect Dis 1998;177:1390-3
169. Eisfeld AJ, Yee MB, Erazo A, Abendroth A and Kinchington PR. Downregulation of class I major histocompatibility complex surface expression by varicella-zoster virus involves open reading frame 66 protein kinase-dependent and -independent mechanisms. J Virol 2007;81:9034-49
170. Asano Y, Nagai T, Miyata T, et al. Long-term protective immunity of recipients of the OKA strain of live varicella vaccine. Pediatrics 1985;75:667-71
171. Levin MJ, Oxman MN, Zhang JH, et al. Varicella-zoster virus-specific immune responses in elderly recipients of a herpes zoster vaccine. J Infect Dis 2008;197:825-35
172. Oxman MN, Levin MJ, Johnson GR, et al. A vaccine to prevent herpes zoster and postherpetic neuralgia in older adults. N Engl J Med 2005;352:2271-84
173. Takahashi M, Otsuka T, Okuno Y, Asano Y and Yazaki T. Live vaccine used to prevent the spread of varicella in children in hospital. Lancet 1974;2:1288-90
174. Gershon AA, Gershon MD. Perspectives on vaccines against varicella-zoster virus infections. Curr Top Microbiol Immunol 2010;342:359-72
175. Shapiro ED, Vazquez M, Esposito D, et al. Effectiveness of 2 doses of varicella vaccine in children. J Infect Dis 2011;203:312-5
176. Weaver BA. Update on the advisory committee on immunization practices' recommendations for use of herpes zoster vaccine. J Am Osteopath Assoc 2011;111:S31-3
177. Goldman GS, King PG. Review of the United States universal varicella vaccination program: Herpes zoster incidence rates, cost-effectiveness, and vaccine efficacy based primarily on the Antelope Valley Varicella Active Surveillance Project data. Vaccine 2013;31:1680-94
178. Grant KA, Carville KS and Kelly HA. Evidence of increasing frequency of herpes zoster management in Australian general practice since the introduction of a varicella vaccine. Med J Aust 2010;193:483
179. Leung J, Harpaz R, Molinari NA, Jumaan A and Zhou F. Herpes zoster incidence among insured persons in the United States, 1993-2006: evaluation of impact of varicella vaccination. Clin Infect Dis 2011;52:332-40
180. Cohen JI, Moskal T, Shapiro M and Purcell RH. Varicella in Chimpanzees. J Med Virol 1996;50:289-92
181. Felsenfeld AD, Schmidt NJ. Varicella-zoster virus immunizes patas monkeys against simian varicella-like disease. J Gen Virol 1979;42:171-8
182. Myers MG, Kramer LW and Stanberry LR. Varicella in a gorilla. J Med Virol 1987;23:317-22
183. Lowry PW, Sabella C, Koropchak CM, et al. Investigation of the pathogenesis of varicella-zoster virus infection in guinea pigs by using polymerase chain reaction. J Infect Dis 1993;167:78-83
184. Myers MG, Connelly BL. Animal models of varicella. J Infect Dis 1992;166 Suppl 1:S48-50
185. Lowry PW, Solem S, Watson BN, et al. Immunity in strain 2 guinea-pigs inoculated with vaccinia virus recombinants expressing varicella-zoster virus glycoproteins I, IV, V or the protein product of the immediate early gene 62. J Gen Virol 1992;73 (Pt 4):811-9
186. Annunziato P, LaRussa P, Lee P, et al. Evidence of latent varicella-zoster virus in rat dorsal root ganglia. J Infect Dis 1998;178 Suppl 1:S48-51
187. Sadzot-Delvaux C, Debrus S, Nikkels A, Piette J and Rentier B. Varicella-zoster virus latency in the adult rat is a useful model for human latent infection. Neurology 1995;45:S18-20
188. Fleetwood-Walker SM, Quinn JP, Wallace C, et al. Behavioural changes in the rat following infection with varicella-zoster virus. J Gen Virol 1999;80 (Pt 9):2433-6
189. Kinchington PR, Goins WF. Varicella zoster virus-induced pain and post-herpetic neuralgia in the human host and in rodent animal models. J Neurovirol 2011;17:590-9
190. Cohen JI. Rodent models of varicella-zoster virus neurotropism. Curr Top Microbiol Immunol 2010;342:277-89
191. Grinfeld E, Goodwin R and Kennedy PG. Varicella-Zoster virus gene expression at variable periods following death in a rat model of ganglionic infection. Virus Genes 2007;35:29-32
192. Kennedy PG, Grinfeld E, Bontems S and Sadzot-Delvaux C. Varicella-Zoster virus gene expression in latently infected rat dorsal root ganglia. Virology 2001;289:218-23
193. Clarkson MJ, Thorpe E and McCarthy K. A virus disease of captive vervet monkeys

(Cercopithecus aethiops) caused by a new herpesvirus. Arch Gesamte Virusforsch 1967;22:219-34
194. Gray WL. Simian varicella: a model for human varicella-zoster virus infections. Rev Med Virol 2004;14:363-81
195. Fletcher TM, 3rd, Gray WL. Simian varicella virus: characterization of virion and infected cell polypeptides and the antigenic cross-reactivity with varicella-zoster virus. J Gen Virol 1992;73 (Pt 5):1209-15
196. Gray WL, Starnes B, White MW and Mahalingam R. The DNA sequence of the simian varicella virus genome. Virology 2001;284:123-30
197. Mahalingam R, Gray WL. The simian varicella virus genome contains an invertible 665 base pair terminal element that is absent in the varicella zoster virus genome. Virology 2007;366:387-93
198. Messaoudi I, Barron A, Wellish M, et al. Simian varicella virus infection of rhesus macaques recapitulates essential features of varicella zoster virus infection in humans. PLoS Pathog 2009;5:e1000657
199. Mahalingam R, Messaoudi I and Gilden D. Simian varicella virus pathogenesis. Curr Top Microbiol Immunol 2010;342:309-21
200. Meyer C, Kerns A, Barron A, Kreklywich C, Streblow DN and Messaoudi I. Simian varicella virus gene expression during acute and latent infection of rhesus macaques. J Neurovirol 2011;17:600-12
201. Ou Y, Davis KA, Traina-Dorge V and Gray WL. Simian varicella virus expresses a latency-associated transcript that is antisense to open reading frame 61 (ICP0) mRNA in neural ganglia of latently infected monkeys. J Virol 2007;81:8149-56
202. White TM, Mahalingam R, Traina-Dorge V and Gilden DH. Persistence of simian varicella virus DNA in CD4(+) and CD8(+) blood mononuclear cells for years after intratracheal inoculation of African green monkeys. Virology 2002;303:192-8
203. White TM, Mahalingam R, Traina-Dorge V and Gilden DH. Simian varicella virus DNA is present and transcribed months after experimental infection of adult African green monkeys. J Neurovirol 2002;8:191-203
204. Mahalingam R, Traina-Dorge V, Wellish M, et al. Latent simian varicella virus reactivates in monkeys treated with tacrolimus with or without exposure to irradiation. J Neurovirol 2010;16:342-54
205. Mahalingam R, Traina-Dorge V, Wellish M, et al. Simian varicella virus reactivation in cynomolgus monkeys. Virology 2007;368:50-9
206. Kolappaswamy K, Mahalingam R, Traina-Dorge V, et al. Disseminated simian varicella virus infection in an irradiated rhesus macaque (Macaca mulatta). J Virol 2007;81:411-5

Chapter 2

Simian Varicella Virus Infection of Chinese Rhesus Macaques produces Ganglionic Infection in the Absence of Rash

Werner J. D. Ouwendijk,[1] Ravi Mahalingam,[2] Vicki Traina-Dorge,[3] Geert van Amerongen,[1] Mary Wellish,[2] Albert D. M. E. Osterhaus,[1] Don Gilden,[2,4] and Georges M. G. M. Verjans[a]

[1]Department of Viroscience, Erasmus Medical Center, Rotterdam, the Netherlands; Departments of [2]Neurology and [4]Microbiology, University of Colorado Denver Medical School, Aurora, Colorado, USA; [3]Division of Microbilogy, Tulane National Primate Research Center, Tulane University, Covington, Louisiana, USA

J. Neurovirol. 2012;18:91-99

Abstract

Varicella-zoster virus (VZV) causes varicella (chickenpox), becomes latent in ganglia along the entire neuraxis and may reactivate to cause herpes zoster (shingles). VZV may infect ganglia via retrograde axonal transport from infected skin or through hematogenous spread. Simian varicella virus (SVV) infection of rhesus macaques provides a useful model system to study the pathogenesis of human varicella zoster virus (VZV) infection. To dissect the virus and host immune factors during acute SVV infection, we analyzed four SVV-seronegative Chinese rhesus macaques infected intratracheally with cell-associated 5 x 10^3 plaque-forming units (pfu) of SVV-expressing green fluorescent protein (n = 2) or 5 x 10^4 pfu of wild-type SVV (n = 2). All monkeys developed viremia and SVV-specific adaptive B- and T-cell immune responses, but none developed skin rash. At necropsy 21 days postinfection, SVV DNA was found in ganglia along the entire neuraxis and in viscera, and SVV RNA was found in ganglia, but not in viscera. The amount of SVV inoculum was associated with the extent of viremia and the immune response to virus. Our findings demonstrate that acute SVV infection of Chinese rhesus macaques leads to ganglionic infection by the hematogenous route and the induction of a virus-specific adaptive memory response in the absence of skin rash.

Introduction

Varicella-zoster virus (VZV) is an exclusively human ubiquitous neurotropic alphaherpesvirus. Primary infection usually causes varicella (chickenpox), after which the virus becomes latent in neurons of sensory ganglia along the entire neuraxis. Primary VZV infection typically results in a generalized maculopapular vesicular rash, although some infected individuals never develop rash [1]. During primary infection, virus is transported from the respiratory mucosa to sites of secondary replication and skin via VZV-infected lymphocytes [2-3]. Virus reaches ganglia either by retrograde axonal transport from infected skin or by hematogenous spread via VZV-infected lymphocytes [4-5]. Reactivation of latent VZV results from a decline in virus-specific cellular immunity [6], mostly in elderly individuals as well as in immunocompromised organ transplant recipients and HIV^+ patients, resulting in zoster and multiple other serious neurological and ocular disorders [7-10].

Simian varicella virus (SVV) causes varicella in non-human primates. Like VZV, SVV becomes latent in ganglionic neurons [11-12] and may reactivate to produce zoster [13]. SVV and VZV antibodies cross-react, and open reading frames (ORFs) of the two viruses share amino acid identity ranging from 27.3% to 75.4% [14]. Intrabronchial inoculation of SVV into seronegative Indian rhesus macaques produces pathological and immunological features like those seen in primary VZV infection in humans [15]. The aim of the present study was to dissect virus and host immune factors after primary SVV infection of Chinese rhesus macaques.

Materials and methods

Cells and viruses

Wild-type SVV (SVV-WT) and SVV expressing green fluorescent protein (SVV-GFP) were used. SVV-WT (Delta herpesvirus strain) was originally isolated from a naturally infected monkey (*Erythrocebus patas*) [16]. SVV-GFP is not attenuated *in vitro* or *in vivo* [17-18]. Low-passage SVV isolates were obtained from peripheral blood mononuclear cells (PBMC) of acutely infected African green monkeys and propagated <5 times either in a fetal rhesus macaque lung fibroblasts (DBS-FRhL-2) to generate cell-associated SVV-GFP and wild-type stocks for intratracheal inoculation or in Vero cells to produce wild-type SVV protein lysates for ELISA and functional T-cell assays [17-18]. Protein lysates were identically prepared from mock-infected DBS-FRhL-2.

Macaque studies

Four juvenile (3 to 4 years old) SVV-seronegative Chinese rhesus macaques were inoculated intratracheally at the bronchial bifurcation with 5×10^3 plaque-forming units (pfu) of cell-associated SVV-GFP (animals 0075 and 2135) or 5×10^4 pfu cell-associated SVV-WT (animals 2207 and 9021) diluted to a volume of 5 ml in phosphate-buffered saline (PBS). While the inoculation titers varied slightly, both virus

titers have been shown to produce viremia and skin rash in Indian rhesus macaques [19]. Animals were housed in negatively pressurized hepa-filtered BSL-3 isolator cages. Before inoculation, the abdomen and back of the animals were shaved to allow careful examination for rash every other day from 1 to 21 days postinfection (dpi). Heparinized blood samples were collected at 0, 2, 5, 7, 9, 11, 13, 15 and 21 dpi. Plasma separated from the blood by centrifugation was heat-inactivated (30 min at 56ºC) and stored at -20ºC. PBMCs were isolated by density-gradient centrifugation for flow cytometry, DNA and RNA isolation and functional B- and T-cell assays (see below). Animals were euthanized at 21 dpi by sedation with ketamine (20 mg/kg body weight) followed by exsanguination. Tissue samples were snap-frozen in liquid nitrogen and stored at -80ºC. The study was approved by the Institutional Animal Welfare Committee and performed according to Dutch guidelines for animal experimentation.

Nucleic acid extraction and real-time PCR

DNA was extracted from PBMC, individual or pooled ganglia, and from portions of liver, lung and spleen using the QIAamp DNA Mini Kit (Qiagen, Valencia, CA, USA). Total RNA was isolated from the same tissues using TRIzol reagent (Invitrogen, Carlsbad, CA, USA) and subsequently with the RNeasy Mini Kit (Qiagen). cDNA synthesis was performed as described [15] using 1 µg total RNA and Superscript III RT (Invitrogen) with random primers. Quantitative real-time PCR (qPCR) was performed in triplicate on DNA and cDNA using Taqman 2X PCR Universal Master Mix (Applied Biosystems, Foster City, CA, USA) with primers and probes specific for SVV DNA open reading frames (ORFs) 21, and ORFs 9, 61 and 63 (cDNA) as described [15]. SVV DNA amplicons were included in each qPCR assay and yielded a consistent inverse relationship between the Ct value and the amount of input template DNA. The detection limit of the SVV DNA qPCR assay, based on the ORF21 primers/probe set, was 1 copy SVV DNA/µg DNA (Figure 1A). Single-copy gene oncostatin-M (OSM) and GAPDH (glyceraldehyde-3-phosphate dehydrogenase) were used as endogenous controls for DNA and RNA integrity, respectively, according to the manufacturer's instructions and as described [20].

SVV-specific ELISA

Plasma SVV-specific IgG titers were determined by ELISA. Briefly, 96-well flat-bottom plates were coated with protein lysates of mock- and SVV-infected Vero cells (2 µg/ml) overnight at 4°C, washed twice with distilled water, and blocked with 3% bovine serum albumin (BSA) diluted in PBS for 1 h at 37°C. Three-fold dilutions of plasma samples were prepared in PBS containing 1% BSA and incubated for 1 h at 37°C. After 10 washes with 0.05% Tween 20 in PBS, the wells were incubated with horseradish peroxidase (HRP)-conjugated rabbit anti-human IgG (DakoCytomation) diluted in 1% BSA in PBS for 1 h. The plates were washed 10 times and incubated with the substrate 3, 3', 5, 5'-etramethylbenzidine (TMB) at room temperature. After 10 min, the reaction was stopped by addition of 2 M sulfuric acid, and optical density (OD) was measured at 405 nm using 620 nm as a reference. End-point titers were obtained by log-log transformation of the linear proportion of the curve using 0.2 OD units as a cut-off.

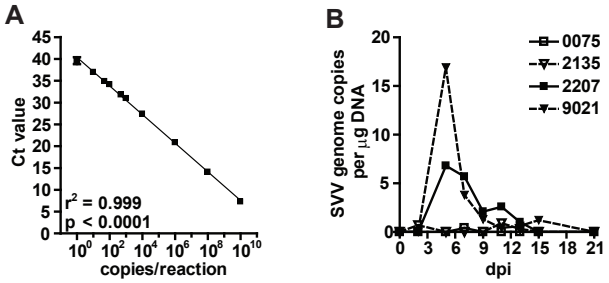

Figure 1. *Detection of SVV DNA in blood leukocytes of SVV-infected Chinese rhesus macaques. (A) The efficiency of SVV DNA quatitation was determined in real-time PCR using 1 to 10x10[10] copies of SVV ORF21 mixed with 100 ng of herring sperm DNA. The SVV ORF21 primer set reliably detected 1 to 10x10[10] copies of SVV DNA (r^2 = 0.999). (B) SVV DNA levels were determined using real-time PCR with primers specific for SVV ORF 21. All monkeys were positive for SVV DNA, with peak viremia occurring at 5 dpi. SVV DNA copy number varied from very low (monkeys 0075 and 2135) to high (monkeys 2207 and 9021).*

Virus neutralization assay

Plasma SVV neutralization IgG titers were determined by plaque reduction assay on Vero cells as described [21]. Briefly, serial 2-fold dilutions of heat-inactivated macaque plasma samples were incubated with ~100 pfu of SVV for 1 h at room temperature. Plasma samples were plated in duplicate on confluent Vero cells in 6-well plates. After 7 days of culture at 37°C, monolayers were fixed in 4% paraformaldehyde and stained with 0.2% crystal violet solution to visualize virus plaques. The SVV neutralizing titer was expressed as the highest dilution showing an 80% reduction in virus plaques compared to control samples cultured in the absence of plasma.

Flow cytometry

PBMCs were stained with monoclonal antibodies (mAbs) directed against human CD20 (clone L27; BD Biosciences, San Diego, CA, USA), IgD (Southern Biotech, Birmingham, AL, USA) and CD27 (O323; BD Biosciences) to discriminate between naïve and memory B-cell subsets [15, 22]. T-cell subsets were identified using mAbs directed against human CD3 (SP34-2), CD4 (L200), CD8 (SK1), CD28 (CD28.2) and CD95 (DX2) (all BD Biosciences) to distinguish between naïve, central memory and effector memory T-cells [15, 23]. Cells were fixed in Cytofix/Cytoperm (BD Biosciences) and stained with antibodies against granzyme B (grB) (GB11; BD Biosciences) to detect cytotoxic T-cells. To detect proliferating B- and T-cells, the nuclear membrane was permeabilized using 10% DMSO in Cytofix/Cytoperm (BD Biosciences), and cells were stained with antibody directed against the cell proliferation marker Ki67 (clone B56; BD Biosciences). Fluorescence was detected on a FACS Canto II and analyzed using FACS Diva sofware (BD Biosciences).

Detection of SVV-specific T-cells

PBMCs were stimulated overnight with predefined optimal concentrations of protein lysates generated from mock and SVV- infected Vero cells, and mock-infected DBS-FRhL-2 cells, followed by incubation with Golgistop (BD Biosciences) for 6 h at 37°C

Table 1. Quantification of SVV-Specific DNA and Transcripts in Ganglia from Chinese Rhesus Macaques at 21 Days Post Infection.

		DNA target[a]		RNA target[b]			
Monkey	**Ganglion**	**ORF 21**	**OSM[c]**	**ORF 9**	**ORF 61**	**ORF 63**	**GAPDH[d]**
0075	Trigeminal	6	positive[e]	nd[f]	nd	nd	nd
	Cervical	0	positive	nd	nd	nd	nd
	Thoracic	0	positive	nd	nd	nd	nd
	Lumbar	trace[g]	positive	und[h]	3	und	positive
	Sacral	4	positive	und	8	und	positive
2135	Trigeminal	28	positive	nd	nd	nd	nd
	Cervical	8	positive	trace	81	trace	positive
	Thoracic	117	positive	trace	372	6	positive
	Lum/Sac[i]	16	positive	trace	138	trace	positive
2207	Trigeminal	60	positive	nd	nd	nd	nd
	Cervical	2	positive	trace	75	7	positive
	Thoracic	73	positive	nd	nd	nd	nd
	Lumbar	99	positive	und	15	trace	positive
	Sacral	38	positive	nd	nd	nd	nd
9021	Trigeminal	860	positive	nd	nd	nd	nd
	Cervical	230	positive	und	582	trace	positive
	Thoracic	687	positive	nd	nd	nd	nd
	Lumbar	698	positive	trace	692	trace	positive
	Sacral	64	positive	9	8089	239	positive

[a] SVV genome copies/ug of total DNA.
[b] SVV transcript copies/µg of total RNA.
[c] Oncostatin-M.
[d] Glyceraldehyde 3-phosphate dehydrogenase.
[e] Specific amplicon detected.
[f] Not done.
[g] >2 copies of SVV DNA or cDNA in 1 or 2 out of 3 reactions.
[h] SVV DNA or transcript undetectable.
[i] Pooled lumbar and sacral ganglia

to block cytokine secretion. After stimulation, cells were stained with mAbs directed against human CD3, CD4, CD8, CD28 and CD95 as described above. Samples were fixed and permeabilized using Cytofix/Cytoperm and incubated with a human interferon (IFN)-γ-specific mAb B27 (BD Biosciences). Fluorescence was measured on a FACS Canto II and analyzed using FACS Diva software.

Table 2. Quantification of SVV-Specific DNA and Transcripts in Non-Ganglionic Tissues from Chinese Rhesus Macaques at 21 Days Post Infection.

		DNA PCR[a]		cDNA PCR[b]			
Monkey	**Tissue**	**ORF 21**	**OSM[c]**	**ORF 9**	**ORF 61**	**ORF 63**	**GAPDH[d]**
0075	Lung	3	positive[e]	und[f]	und	und	positive
	Liver	und	positive	und	und	und	positive
	Spleen	und	positive	und	und	und	positive
2135	Lung	und	positive	und	und	und	positive
	Liver	und	positive	und	und	und	positive
	Spleen	und	positive	und	und	und	positive
2207	Lung	und	positive	und	und	und	positive
	Liver	und	positive	und	und	und	positive
	Spleen	und	positive	und	und	und	positive
9021	Lung	und	positive	und	und	und	positive
	Liver	3	positive	und	und	und	positive
	Spleen	1	positive	und	und	und	positive

[a] SVV genome copies/ug of total DNA.
[b] SVV transcript copies/µg of total RNA.
[c] Oncostatin-M.
[d] Glyceraldehyde 3-phosphate dehydrogenase.
[e] Specific amplicon detected.
[f] SVV DNA or transcript undetectable.

Results

Clinical course of acute SVV infection in Chinese rhesus macaques

To investigate the virus and host immune factors during acute SVV infection, four SVV naïve Chinese rhesus macaques were infected intratracheally with $5x10^4$ pfu cell-associated SVV-WT (n=2) or $5x10^3$ pfu SVV-GFP (n=2). SVV-GFP was used to enable visualization of SVV-infected cells in blood during viremia and in skin lesions. Physical examinations every other day revealed no skin lesions. All animals developed a viremia. SVV DNA levels were higher in monkeys 2207 and 9021 that received the highest SVV dose, compared to animals 0075 and 2135 that received a lower dose of SVV and had trace levels of SVV DNA in peripheral blood mononuclear cells (PBMCs) (Figure 1B). SVV DNA was detected 2 to 15 dpi and peaked at 5 dpi. No infectious SVV was recovered from PBMCs at any time during viremia, and no SVV- or GFP-positive cells were detected by flow cytometry in whole-blood (data not shown).

Detection of SVV DNA and RNA in ganglionic and non-ganglionic tissues of SVV-infected rhesus macaques

To determine if SVV ganglionic infection was inhibited by the absence of overt viral replication in skin, the SVV DNA load in dorsal root ganglia (DRG) and trigeminal ganglia (TG) at 21 dpi was determined by qPCR (Table 1). SVV DNA was detected in most pooled ganglia, indicating hematogenous infection. The SVV DNA load was higher in monkeys infected with higher doses of virus (monkeys 2207 and 9021). SVV DNA load in non-ganglionic tissues (i.e., lung, liver and spleen) was undetectable or lower compared to ganglia of the same monkey (Tables 1 and 2).

Similar to latent VZV infections in humans, SVV latency is associated with the restricted transcription of several immediate early and early transcripts [24-25]. Levels of the SVV latency-associated ORF 61 and ORF 63 transcripts, as well as the late SVV ORF 9 transcript were determined in ganglia and non-ganglionic tissues of all monkeys. No SVV transcripts were detected in lung, liver and spleen (Table 2). SVV ORF 61 was the most prevalent and abundant SVV transcript found in ganglia (Table 1). Lower levels of SVV ORF 63 transcripts were detected in ganglia from all but one monkey (0075) that also had a low SVV DNA load. Trace levels of SVV ORF 9 transcripts were detected in ganglia of 3 of 4 monkeys. The detection of low levels of the late SVV gene ORF 9 transcript, along with higher levels of SVV latency-associated transcripts in monkey 9021 indicated that latency was not completely established at 21 dpi.

B-cell response in SVV-infected rhesus macaques

All monkeys had detectable plasma SVV-specific IgG titers at 7 dpi, which peaked between 9 and 11 dpi and remained high until the end of the 21-day study period

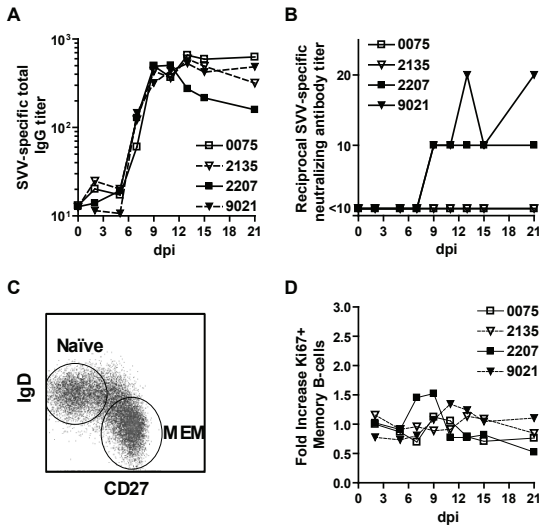

Figure 2. *Induction of SVV-specific B-cell response in infected Chinese rhesus macaques. (A) SVV-infected macaques developed a SVV-specific plasma IgG response starting at 7 dpi, peaking at 9 to 11 dpi and remaining high until 21 dpi as determined by SVV ELISA. (B) SVV neutralizing antibodies were detected in animals 2207 and 9021 starting at 9 dpi. (C) Peripheral blood B-cells identified by flow cytometry based on expression of CD20 were further distinguished as naïve (IgD^+CD27^-) or memory (MEM; IgD^-CD27^+) B-cells. (D) Proliferation of memory B-cells as assessed by flow cytometry based on expression of the cell proliferation marker Ki67 and given as fold-increase in $Ki67^+$ cells compared to the sample obtained at 0 dpi*

(Figure 2A). Comparable levels of SVV-specific plasma IgG titers were found in all monkeys and monkeys 2207 and 9021 developed virus-neutralizing antibody titers ≥1:10 (Figure 2B).

Upon antigen recognition, antigen-specific B-cells proliferate and mature into isotype-switched memory B-cells and plasma cells [26]. To identify proliferating B-cell subsets, $CD20^+$ cells were divided into naïve (IgD^+CD27^-) and memory (IgD^-CD27^+) B-cells using flow cytometry (Figure 2C) and stained for the proliferation marker Ki67 [22, 27]. Compared to 0 dpi, only a marginal increase (1.2- to 1.5-fold) in proliferating memory B-cells was seen in 3 of 4 monkeys from 9 to 11 dpi (Figure 2D).

T-cell response in SVV-infected rhesus macaques

Primary VZV infection in humans induces a profound T-cell mediated immune response, which occurs after the onset of varicella skin rash and is essential in controlling viremia [28]. Upon recognition of the cognate antigen, T-cells proliferate and mature to memory T-cells. To assess T-cell expansion in SVV-infected rhesus macaques, blood-derived T-cells ($CD3^+$ cells) were differentiated into naïve ($CD28^+CD95^-$), central memory ($CD28^+CD95^+$) and effector memory ($CD28^-CD95^+$) [23] and stained for Ki67 (Figure 3Ai and Aii). Intratracheal inoculation with cell-associated SVV induced proliferation of CD4+ and CD8+ T-cells in the central and effector memory compartments of all rhesus macaques at 7 dpi (Figure 3B). More proliferation was induced in $CD8^+$ compared to $CD4^+$ T-cells, and more proliferating $CD8^+$ T-cells were found in monkeys that received the highest virus dose (monkeys 2207 and 9021). VZV infection also induces virus-specific cytotoxic $CD4^+$ and $CD8^+$ T-cells that express granzyme B (grB) and secrete soluble mediators such as IFN-γ [29-30]. Intratracheal inoculation with cell-associated SVV resulted in an increase in grB-expressing $CD4^+$ and $CD8^+$ central but not effector memory T-cells, with the highest numbers seen at 7 dpi; induction of grB^+CD8^+ central memory T-cells was found only in monkeys 2207 and 9021 (Figure 3C).

The Ki67 and grB response shown in Figures 3B and 3C might have been induced by either viral proteins or allogeneic major histocompatibility complex (MHC) proteins expressed by uninfected DBS-FRhL-2 cells used to generate the SVV inoculum. Thus, the frequency of antigen-specific T-cells was determined by intracellular staining for IFN-γ at all time points in all monkeys using various control cell lysates (Figure 3Aiv and 3D). First, we included protein lysates of mock- and SVV-infected Vero cells to differentiate T-cell reactivity directed against SVV antigens. Second, T-cell reactivity directed towards proteins lysates of mock-infected DBS-FRhL-2 cells was assayed to detect the induction of allo-MHC specific T-cell responses after intratracheal inoculation of cell-associated SVV in rhesus macaques. While no MHC response was detected, the SVV-specific memory $CD4^+$ T-cell response was detected starting at 9 dpi (Figure 3D). Analogous to the frequency of grB^+ T-cells, most IFN-γ-secreting $CD4^+$ T-cells had a central memory phenotype (Figure 3Aiv and data not shown) as was also seen in grB+ T-cells (Figure 3C). Overall, all monkeys developed a virus-specific $CD4^+$ T-cell immune response beginning about 4 days after the peak in viremia.

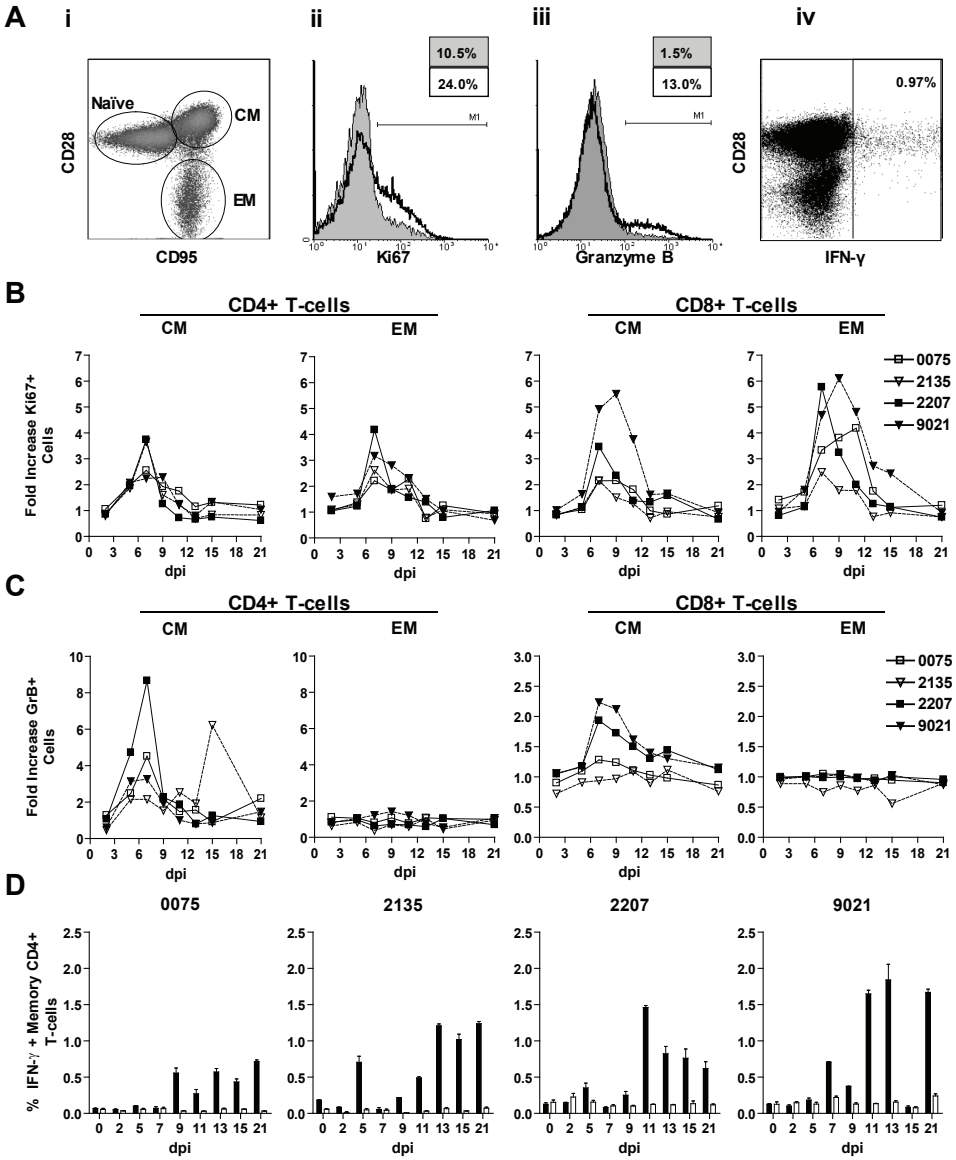

Figure 3. *Induction of systemic SVV-specific T-cell response in infected Chinese rhesus macaques. (Ai) Peripheral blood T-cells were identified based on expression of CD3 and categorized further based on expression of CD28 and CD95 as naïve ($CD28^+CD95^-$), central memory (CM; $CD28^+CD95^+$) and effector memory (EM; $CD28^-CD95^+$) T-cells. (Aii) Proliferating T-cells were identified by flow cytometric detection of cell proliferation marker Ki67, shown for CM CD4+ T-cells from animal 9021 at 0 (filled area) and 9 (black line) dpi. (Aiii) Granzyme B expression in CM $CD4^+$ T-cells from animal 2207 at 0 (filled area) and 7 (black line) dpi. (Aiv) SVV-specific IFN-γ-producing memory $CD4^+$ T-cells from animal 9021 at 21 dpi. (B) Kinetics of proliferation in T-cell subsets, with a peak in proliferation of CM and EM $CD4^+$ at 7 dpi and peak proliferation in CM and EM $CD8^+$ T-cells at 7 to 9 dpi and 7 to 11*

Figure 3 - continued. *dpi, respectively. (C) Kinetics of granzyme B expression in T-cell subsets, showing a relative increase in CM CD4⁺ and CD8⁺ at 7 dpi. (D) Percentage of IFN-γ producing peripheral blood memory CD4⁺ T-cells in response to protein lysates prepared from mock- and SVV- infected Vero cells (netto responses are shown in black bars) and mock-infected rhesus macaque FRhL-2 cells (white bars).*

Discussion

The present study showed that after primary infection with SVV, Chinese rhesus macaques developed viremia, ganglionic infection by the hematogenous route and virus-specific memory B- and T-cell responses in the absence of rash. The absence of rash contrasts with previous studies, which showed that inoculation of Indian rhesus macaques deep into the bronchial tree with similar virus loads of the same SVV strain lead to viremia, SVV-specific adaptive immune responses and varicella rash at 7 – 10 dpi [15, 19, 31]. While both the trachea and bronchi harbor cells susceptible to SVV infection, the anatomic location within the respiratory tract at which the virus is administrated might affect initial virus replication. Alternatively, the geographic origin of rhesus macaques may affect their susceptibility to SVV infection. Whole-genome sequencing has revealed extensive genetic differences in rhesus macaques of Indian and Chinese origin [32-33] that are likely to play a role in the different disease progression and host response seen after SIV infection [34-35].

VZV in humans is thought to enter ganglia either via hematogenous transport within infected lymphocytes or by retrograde axonal transport from varicella skin lesions [3-4]. The latter notion is based largely on studies with herpes simplex virus, while only indirect evidence exists for VZV. For example, VZV ORF29 protein is expressed in Schwann cells and axons of nerves in varicella, but not in zoster lesions [4]. Also, VZV can infect axons and undergo retrograde transport to neuronal cell bodies *in vitro* [36]. The data presented herein reveal that SVV replication in the skin of intratracheally infected rhesus macaques is not a prerequisite for virus to infect ganglia. The association between SVV DNA loads in blood and ganglia further supports the role of SVV-infected lymphocytes in the establishment of ganglionic infection. Analogous, the high correlation of VZV serostatus with the presence of VZV DNA in ganglia [37] indicates subclinical hematogenous infection in VZV seropositive humans without a history of chickenpox.

Compared to SVV infection of Indian rhesus macaques [15], a dampened adaptive B- and T-cell response, with reduced peak endpoint SVV-specific IgG titers, a lower proliferative B-cell response and a lower frequency of proliferating T-cells and SVV-specific T-cells were seen after SVV infection of Chinese rhesus macaques. Note that live attenuated VZV Oka vaccine typically does not cause varicella rash in humans and elicits an immune response that is less robust than that seen after natural VZV infection [38-39], although it is protective [29, 40-41]. The kinetics of the T-cell response found herein is similar to that found by Messaoudi et al. [15], who reported a peak in T-cell proliferation and grB expression shortly after peak viremia in ma-

caques. However, the SVV-specific immune response herein was dominated by T-cells exhibiting a central memory rather than an effector memory phenotype, consistent with studies on the phenotype of VZV-specific T-cells in humans which express the co-stimulatory molecule CD28 and the lymph node-homing receptors CCR7 and CD62L [42-43]. The close resemblance between SVV infection in rhesus macaques and humans vaccinated with the varicella vaccine emphasize the applicability of this animal model to develop novel therapeutic strategies against VZV infection.

Overall, our results demonstrate that acute SVV infection of Chinese rhesus macaques leads to ganglionic infection and the induction of a virus-specific adaptive B- and T-cell memory response in the absence of skin rash. Importantly, some humans have serum antibody to VZV without any history of varicella. Yet VZV is latent in ganglia of nearly all humans. A logical interpretation of these facts is that human ganglia are infected hematogenously, a notion supported by our demonstration that ganglia of Chinese rhesus macaques are infected hematogenously by SVV.

Acknowledgements

This work was supported in part by Public Health Service grant AG032958 from the National Institutes of Health. (W.J.D.O., R.M., V.T.D., M.W., D.G., G.M.G.M.V.). We thank Marina Hoffman for editorial assistance and Lori DePriest for manuscript preparation.

References

1. Heininger U, Seward JF. Varicella. Lancet 2006;368:1365-76
2. Asano Y, Itakura N, Hiroishi Y, et al. Viremia is present in incubation period in nonimmunocompromised children with varicella. J Pediatr 1985;106:69-71
3. Ozaki T, Kajita Y, Asano Y, Aono T and Yamanishi K. Detection of varicella-zoster virus DNA in blood of children with varicella. J Med Virol 1994;44:263-5
4. Annunziato PW, Lungu O, Panagiotidis C, et al. Varicella-zoster virus proteins in skin lesions: implications for a novel role of ORF29p in chickenpox. J Virol 2000;74:2005-10
5. Reichelt M, Zerboni L and Arvin AM. Mechanisms of varicella-zoster virus neuropathogenesis in human dorsal root ganglia. J Virol 2008;82:3971-83
6. Miller AE. Selective decline in cellular immune response to varicella-zoster in the elderly. Neurology 1980;30:582-7
7. Gilden DH, Kleinschmidt-DeMasters BK, LaGuardia JJ, Mahalingam R and Cohrs RJ. Neurologic complications of the reactivation of varicella-zoster virus. N Engl J Med 2000;342:635-45
8. Hope-Simpson RE. The Nature of Herpes Zoster: A Long-Term Study and a New Hypothesis. Proc R Soc Med 1965;58:9-20
9. Levin MJ, Smith JG, Kaufhold RM, et al. Decline in varicella-zoster virus (VZV)-specific cell-mediated immunity with increasing age and boosting with a high-dose VZV vaccine. J Infect Dis 2003;188:1336-44
10. Levin MJ, Oxman MN, Zhang JH, et al. Varicella-zoster virus-specific immune responses in elderly recipients of a herpes zoster vaccine. J Infect Dis 2008;197:825-35
11. Gray WL, Williams RJ, Chang R and Soike KF. Experimental simian varicella virus infection of St. Kitts vervet monkeys. J Med Primatol 1998;27:177-83
12. Mahalingam R, Smith D, Wellish M, et al. Simian varicella virus DNA in dorsal root ganglia. Proc Natl Acad Sci U S A 1991;88:2750-2
13. Mahalingam R, Traina-Dorge V, Wellish M, et al. Simian varicella virus reactivation in cynomolgus monkeys. Virology 2007;368:50-9
14. Gray WL, Starnes B, White MW and Mahalingam R. The DNA sequence of the simian varicella virus genome. Virology 2001;284:123-30
15. Messaoudi I, Barron A, Wellish M, et al. Simian varicella virus infection of rhesus macaques recapitulates essential features of varicella zoster virus infection in humans. PLoS Pathog 2009;5:e1000657
16. Mahalingam R, Clarke P, Wellish M, et al. Prevalence and distribution of latent simian varicella virus DNA in monkey ganglia. Virology 1992;188:193-7
17. Mahalingam R, Wellish M, Soike K, White T, Kleinschmidt-DeMasters BK and Gilden DH. Simian varicella virus infects ganglia before rash in experimentally infected monkeys. Virology 2001;279:339-42
18. Mahalingam R, Wellish M, White T, et al. Infectious simian varicella virus expressing the green fluorescent protein. J Neurovirol 1998;4:438-44
19. Mahalingam R, Traina-Dorge V, Wellish M, et al. Effect of time delay after necropsy on analysis of simian varicella-zoster virus expression in latently infected ganglia of rhesus macaques. J Virol 2010;84:12454-7
20. Bruce AG, Bakke AM, Thouless ME and Rose TM. Development of a real-time QPCR assay for the detection of RV2 lineage-specific rhadinoviruses in macaques and baboons. Virol J 2005;2:2
21. Soike KF, Huang JL, Zhang JY, Bohm R, Hitchcock MJ and Martin JC. Evaluation of infrequent dosing regimens with (S)-1-[3-hydroxy-2-(phosphonylmethoxy)propyl]-cytosine (S-HPMPC) on simian varicella infection in monkeys. Antiviral Res 1991;16:17-28
22. Vugmeyster Y, Howell K, Bakshi A, Flores C, Hwang O and McKeever K. B-cell subsets in blood and lymphoid organs in Macaca fascicularis. Cytometry A 2004;61:69-75
23. Pitcher CJ, Hagen SI, Walker JM, et al. Development and homeostasis of T cell memory in rhesus macaque. J Immunol 2002;168:29-43
24. Kennedy PG, Cohrs RJ. Varicella-zoster virus human ganglionic latency: a current summary. J Neurovirol 2010;16:411-8
25. Kennedy PG, Grinfeld E, Traina-Dorge V, Gilden DH and Mahalingam R. Neuronal localization of simian varicella virus DNA in ganglia of naturally infected African green monkeys. Virus Genes

2004;28:273-6
26. Srivastava B, Lindsley RC, Nikbakht N and Allman D. Models for peripheral B cell development and homeostasis. Semin Immunol 2005;17:175-82
27. Scholzen T, Gerdes J. The Ki-67 protein: from the known and the unknown. J Cell Physiol 2000;182:311-22
28. Weinberg A, Levin MJ. VZV T cell-mediated immunity. Curr Top Microbiol Immunol 2010;342:341-57
29. Hayward AR, Buda K, Jones M, White CJ and Levin MJ. Varicella zoster virus-specific cytotoxicity following secondary immunization with live or killed vaccine. Viral Immunol 1996;9:241-5
30. Malavige GN, Jones L, Black AP and Ogg GS. Rapid effector function of varicella-zoster virus glycoprotein I-specific CD4+ T cells many decades after primary infection. J Infect Dis 2007;195:660-4
31. Mahalingam R, Traina-Dorge V, Wellish M, et al. Latent simian varicella virus reactivates in monkeys treated with tacrolimus with or without exposure to irradiation. J Neurovirol 2010;16:342-54
32. Gibbs RA, Rogers J, Katze MG, et al. Evolutionary and biomedical insights from the rhesus macaque genome. Science 2007;316:222-34
33. Hernandez RD, Hubisz MJ, Wheeler DA, et al. Demographic histories and patterns of linkage disequilibrium in Chinese and Indian rhesus macaques. Science 2007;316:240-3
34. Ling B, Veazey RS, Luckay A, et al. SIV(mac) pathogenesis in rhesus macaques of Chinese and Indian origin compared with primary HIV infections in humans. AIDS 2002;16:1489-96
35. Trichel AM, Rajakumar PA and Murphey-Corb M. Species-specific variation in SIV disease progression between Chinese and Indian subspecies of rhesus macaque. J Med Primatol 2002;31:171-8
36. Markus A, Grigoryan S, Sloutskin A, et al. Varicella-zoster virus (VZV) infection of neurons derived from human embryonic stem cells: direct demonstration of axonal infection, transport of VZV, and productive neuronal infection. J Virol 2011;85:6220-33
37. Verjans GM, Hintzen RQ, van Dun JM, et al. Selective retention of herpes simplex virus-specific T cells in latently infected human trigeminal ganglia. Proc Natl Acad Sci U S A 2007;104:3496-501
38. Watson B. Humoral and cell-mediated immune responses in children and adults after 1 and 2 doses of varicella vaccine. J Infect Dis 2008;197 Suppl 2:S143-6
39. Weinberg A, Lazar AA, Zerbe GO, et al. Influence of age and nature of primary infection on varicella-zoster virus-specific cell-mediated immune responses. J Infect Dis 2010;201:1024-30
40. Levin MJ, Murray M, Zerbe GO, White CJ and Hayward AR. Immune responses of elderly persons 4 years after receiving a live attenuated varicella vaccine. J Infect Dis 1994;170:522-6
41. Takahashi M, Otsuka T, Okuno Y, Asano Y and Yazaki T. Live vaccine used to prevent the spread of varicella in children in hospital. Lancet 1974;2:1288-90
42. Malavige GN, Jones L, Black AP and Ogg GS. Varicella zoster virus glycoprotein E-specific CD4+ T cells show evidence of recent activation and effector differentiation, consistent with frequent exposure to replicative cycle antigens in healthy immune donors. Clin Exp Immunol 2008;152:522-31
43. Malavige GN, Jones L, Kamaladasa SD, et al. Viral load, clinical disease severity and cellular immune responses in primary varicella zoster virus infection in Sri Lanka. PLoS One 2008;3:e3789

Chapter 3

T-Cell Tropism of Simian Varicella Virus During Primary Infection

Werner J.D. Ouwendijk,[1] Ravi Mahalingam,[2] Rik L. de Swart,[1] Bart L. Haagmans,[1] Geert van Amerongen,[1] Sarah Getu,[1] Don Gilden,[2, 3] Albert D.M.E. Osterhaus,[1] and Georges M.G.M. Verjans[1]

[1]Department of Viroscience, Erasmus Medical Center, Rotterdam, the Netherlands; Departments of [2]Neurology and [3]Microbiology, University of Colorado Denver Medical School, Aurora, Colorado, USA

PLoS Pathog. 2013 May;9(5):e1003368

Abstract

Varicella-zoster virus (VZV) causes varicella, establishes a lifelong latent infection of ganglia and reactivates to cause herpes zoster. The cell types that transport VZV from the respiratory tract to skin and ganglia during primary infection are unknown. Clinical, pathological, virological and immunological features of simian varicella virus (SVV) infection of non-human primates parallel those of primary VZV infection in humans. To identify the host cell types involved in virus dissemination and pathology, we infected African green monkeys intratracheally with recombinant SVV expressing enhanced green fluorescent protein (SVV-EGFP) and with wild-type SVV (SVV-wt) as a control. The SVV-infected cell types and virus kinetics were determined by flow cytometry and immunohistochemistry, and virus culture and SVV-specific real-time PCR, respectively. All monkeys developed fever and skin rash. Except for pneumonitis, pathology produced by SVV-EGFP was less compared to SVV-wt. In lungs, SVV infected alveolar myeloid cells and T-cells. During viremia the virus preferentially infected memory T-cells, initially central memory T-cells and subsequently effector memory T-cells. In early non-vesicular stages of varicella, SVV was seen mainly in perivascular skin infiltrates composed of macrophages, dendritic cells, dendrocytes and memory T-cells, implicating hematogenous spread. In ganglia, SVV was found primarily in neurons and occasionally in memory T-cells adjacent to neurons. In conclusion, the data suggest the role of memory T-cells in disseminating SVV to its target organs during primary infection of its natural and immunocompetent host.

Author Summary

Varicella-zoster virus (VZV) causes varicella, establishes lifelong latent infection in ganglia and reactivates later in life to cause zoster. VZV is acquired via the respiratory route, with skin rash occurring up to 3 weeks after exposure. The cell types that transport VZV to skin and ganglia during primary infection are unknown. Simian varicella virus (SVV) infection of non-human primates mimics clinical, pathological and immunological features of human VZV infection. African green monkeys were infected with recombinant SVV expressing enhanced green fluorescent protein (SVV-EGFP) or wild-type SVV (SVV-wt) as a control. By visualizing SVV-EGFP-infected cells in the living animal and in tissue samples, we identified the virus-infected cell types in blood, lungs, skin and ganglia during primary infection. Our data demonstrate that during viremia, SVV predominantly infects peripheral blood memory T-cells. Detection of SVV-infected memory T-cells in lungs, in early varicella skin lesions and also, albeit to a lesser extent, in ganglia suggests a role for memory T-cells in transporting virus to these organs. Our study provides novel insights into the cell types involved in virus dissemination and the overall pathology of varicella in a non-human primate model.

Introduction

Varicella-zoster virus (VZV) is a ubiquitous human neurotropic alphaherpesvirus that causes varicella (chickenpox) as a primary infection and herpes zoster (shingles) upon reactivation of latent virus [1]. Primary VZV infection is acquired via the respiratory route and varicella occurs 2-3 weeks after exposure [2-3]. The pathogenesis of varicella is largely unknown, mostly due to the prolonged incubation period and restricted host range of the virus. VZV is detected in lymphocytes of varicella patients [4], suggesting that the virus spreads to susceptible organs including skin and ganglia via a cell-associated viremia. However, the low number of VZV-infected lymphocytes has precluded their identification during natural infection in humans [5].

Most of the current understanding of VZV pathogenesis is based on experimental infection of human fetal tissue transplanted in severe combined immunodeficient mice (SCID-hu model) [6-7]. In this model, VZV has a tropism for T-cells within thymus and liver xenografts [8]. It has been postulated that VZV initially replicates in respiratory epithelial cells and is transferred to T-cells within tonsilar lymphoid tissue contacting the upper respiratory tract [9-10]. Virus transport to human fetal skin and ganglia explants in SCID-hu mice can be mediated by T-cells [11-12], most likely activated memory CD4 T-cells expressing the skin homing markers C-C type chemokine receptor type 4 (CCR4) and cutaneous lymphocyte antigen (CLA) [10]. However, the VZV SCID-hu mouse model does not reproduce the complex and dynamic virus-host interactions involved in the dissemination of VZV to its target organs during primary infection in its natural and immunocompetent host [6-7].

Simian varicella virus (SVV) produces a naturally occurring disease in non-human primates with clinical, pathological and immunological features that parallel human VZV infection [13-14]. The prevalence of SVV in free-ranging non-human primates is largely unknown. However, SVV outbreaks in primate centers have been associated with the introduction of monkeys captured from the wild into the colony [15]. The genomes of SVV and VZV are similar in size, structure and genetic organization, with an estimated 70 – 75% DNA homology [16]. SVV causes varicella, becomes latent in ganglionic neurons and reactivates after stress and immunosuppression to cause herpes zoster [17-18]. A cell-associated viremia is detected from 3 days post-infection (dpi), with the highest number of infected lymphocytes just before the onset of skin rash [14,19]. SVV reaches the ganglia before skin rash [20-21], indicating viremic spread to ganglia.

The aim of the present study was to characterize the kinetics of virus infection and the cell types involved in the dissemination of SVV during primary infection. We have previously shown that infection of macaques with recombinant measles virus expressing EGFP (rMV-EGFP) facilitated the identification of the cell types involved in MV pathogenesis with unprecedented sensitivity [22-25]. To detect SVV-infected cells at the low frequencies expected in blood and lungs, we infected African green monkeys (AGMs) with recombinant SVV expressing EGFP (SVV-EGFP) and, as a

control, wild-type SVV (SVV-wt) to study SVV pathogenesis at the whole organism, tissue and cellular levels in its natural and immunocompetent host. The data presented suggest a crucial role for memory T-cells in the dissemination of SVV during primary infection.

Materials and Methods

Ethics statement

This study was performed in strict accordance with European guidelines (EU Directive on Animal Testing 86/609/EEC) and Dutch legislation (Experiments on Animals Act, 1997). The protocol was approved by the independent animal experimentation ethical review committee DCC in Driebergen, the Netherlands (Erasmus MC permit number EMC2374). Animals were housed in groups, received standard primate feed and fresh fruit daily, and had access to water *ad libitum*. Cages also contained sources of "environmental enrichment" such as hiding places and hanging ropes, tires and other toys. During infection, study animals were housed in HEPA-filtered, negatively pressurized BSL-3 isolator cages. Animal welfare was monitored daily and all animal handling was performed under light anesthesia (ketamine) or deep anesthesia (ketamine and medetomidine) to minimize animal discomfort. After deep anesthesia, atipamezole was administered to antagonize the effect of medetomidine. Animals were euthanized by sedation with ketamine and medetomidine followed by exsanguination.

Viruses

Low-passage clinical isolates of the Delta herpesvirus strain of SVV-wt and SVV-EGFP were obtained from PBMC of acutely infected AGM and propagated less than 5 times in AGM- kidney epithelial cell line BSC-1 (American Tissue Type Culture no. CCL-26) to generate virus stocks as described [26]. Virus stocks were confirmed as Mycoplasma-free. SVV-EGFP was generated by insertion of the EGFP gene downstream from a Rous sarcoma virus promoter between SVV ORF66 and ORF67 [20, 27].

SVV infection of PBMC *in vitro*

PBMC from SVV-naive AGM were infected by co-cultivating PBMC ($5x10^5$) with SVV-EGFP–infected Vero cells ($0.5\text{-}1x10^5$), showing 70% virus-induced cytopathic effect (CPE), in 0.5 ml DMEM supplemented with antibiotics and 10% heat-inactivated fetal bovine serum (FBS) for 24 hr in 24-well plates at 37°C in a CO_2-incubator. Mock-infected PBMC were similarly generated by co-cultivating PBMC with uninfected Vero cells. SVV-EGFP-infected PBMC were stained and analyzed by flow cytometry or spotted on microscope slides, fixed and stained by immunofluorescence for SVV as described below.

Experimental SVV infection of AGM, necropsy and collection of tissues

Five adult (10- to 12-year-old) SVV-seronegative AGMs (*Cercopithecus aethiops*)

with intraperitoneally implanted temperature transponders were inoculated intratracheally with ~10^6 plaque-forming units (pfu) of SVV-EGFP (n=3 animals; 1 male and 2 females) or SVV-wt (n=2 animals; 1 male and 1 female) diluted in 5 ml of phosphate-buffered saline [21]. Just before infection, animals were sedated with ketamine and medetomidine. The abdomen and back of the animals were shaved to allow careful examination for skin rash every other day until necropsy. Heparinized blood samples were collected under light ketamine sedation at 0, 2, 7, 11, 13, 17 and 20 dpi. Bronchoalveolar lavage (BAL) samples and peripheral blood (PB) samples were collected under deep anesthesia at 5 and 9 dpi. Three punch biopsies (3 mm) of varicella rashes and EGFP fluorescent skin tissue, while showing no characteristic varicella-like skin rash by the naked eye, were obtained from anesthetized animals at 9 dpi under anesthesia. SVV-EGFP-infected animals were checked for macroscopic EGFP fluorescence using a custom-made lamp containing 6 LEDs (peak emission 490-495 nm) mounted with D480/40 bandpass filters [22]. Fluorescence was detected by an amber cover of a UV transilluminator used for screening DNA gels [22]. Photographs were taken using a Nikon D80 SLR camera. SVV-infected animals were euthanized at 9 dpi (n=2; one SVV-wt- and one SVV-EGFP-infected animal), 13 dpi (n=2; one SVV-wt and one SVV-EGFP-infected animal) and 20 dpi (one SVV-EGFP-infected animal). Multiple tissues including lung, lymph nodes, spleen, tonsils, skin and ganglia were collected at necropsy and either snap-frozen or fixed and paraffin-embedded.

Collection and processing of PB and BAL samples

PBMC were isolated by density-gradient centrifugation and used for virus isolation, DNA isolation and flow cytometry or cryopreserved as viable cells as described [24]. Cells recovered from BAL samples were centrifuged, dissolved in RPMI-1640 medium supplemented with 10% FBS plus antibiotics (R10F medium), and used for virus isolation, DNA isolation and flow cytometry as described [22].

Virus isolation from PB and BAL samples

Infectious SVV was isolated from PB and BAL cells by incubating 1-2x10^6 cells in 10-fold serial dilutions in R10F medium on confluent monolayers of BSC-1 cells in 6-well plates. Cells were monitored for SVV-induced CPE or EGFP expression after 7 days of co-cultivation and results were expressed as numbers of SVV-infected cells per 10^6 input PBMC and BAL cells.

Nucleic acid extraction and quantitative PCR (qPCR)

DNA was isolated from PBMC, BAL cells, pooled ganglia, pooled lymph nodes, tonsils and spleen using a QIAamp DNA Mini Kit (Qiagen). qPCR was performed in triplicate on a ABI Prism 7500 using Taqman 2x PCR Universal Master Mix (Applied Biosystems) with primers and probes specific for SVV open reading frame 21 (ORF21) and the pan-primate single-copy gene oncostatin-M (OSM) as described [14, 21, 28]. DNA dilutions obtained from uninfected PBMC were used to validate the OSM Taqman assay.

Flow cytometry

PBMC were either directly used for flow cytometry to detect $EGFP^+$ cells or stained for indicated markers using fluorochrome-conjugated mAbs: $CD3^{APC\text{-}Cy7}$ (clone SP34-2), $CD4^{AmCyan}$ (L200), $CD8^{PerCp}$ (SK1), $CD14^{PE}$ (M5E2), $CD16^{AF647}$ (3G8), $CD20^{PE\text{-}Cy7}$ (L27) and HLA-$DR^{PacificBlue}$ (L243) (all from BD Biosciences) to delineate SVV-infected PBMC subsets. To identify SVV-infected T-cell subtypes, PBMC from infected AGMs were stained with mAbs specific for $CD3^{APC\text{-}Cy7}$ (SP34-2), $CD4^{PacificBlue}$ (L200), $CD8^{AmCyan}$ (SK1), $CD28^{APC}$ (28.2), $CD95^{PerCp}$ (DX2), $CCR4^{PE\text{-}Cy7}$ (1G1) (all from BD Biosciences) and $CD137^{PE}$ (4B4-1; Miltenyi biotec). T-cells were categorized into naive, central memory (CM) and effector memory (EM) T-cells based on differential expression of CD28 and CD95 (Fig. S2) [29]. In contrast to humans and macaque species, AGMs have three distinct $CD3^{pos}$ T-cell populations based on expression of CD4 and CD8α: $CD4^{pos}CD8\alpha^{neg}$ ($CD4^{pos}$), $CD4^{neg}$ $CD8\alpha^{dim}$ ($CD8^{dim}$) and $CD4^{neg}CD8\alpha^{bright}$ ($CD8^{bright}$) (Fig. S2)[29]. BAL cells were stained as described for PBMC, except for inclusion of anti-$CD45^{APC}$ (MB4-6D6; Miltenyi biotec) instead of anti-CD16 mAb. Fluorescence was detected on a FACS Canto II and analyzed using FACS Diva software (BD Biosciences). At least 10^6 viable cells were measured to accurately identify $EGFP^{pos}$ cells.

***In situ* analyses**

Immunohistochemical and immunofluorescence staining was performed using predefined optimal dilutions of primary mAbs directed against: CD3 (clone F7.2.38; Dako), CD11c (NCL-L-CD11c-563; Novocastra), CD20 (L26; Dako), CD68 (KP1; Dako), NCAM (123C3.D5; Thermo Fischer Scientific), GFAP (4A11; BD Biosciences), keratin (AE1/AE3; Thermo Fischer Scientific), α-smooth muscle actin (1A4; Sigma-Aldrich) and rabbit polyclonal antibodies directed against GFP (IgG fraction; Invitrogen) and SVV nucleocapsid proteins [19]. As isotype controls, sections were incubated with mouse IgG1, IgG2a and IgG2b and rabbit immunoglobulins (Dako). Paraformaldehyde-fixed (4%), paraffin-embedded tissue sections were deparaffinized, rehydrated, subjected to heat-induced antigen retrieval in citrate buffer (10 mM, pH= 6.0), blocked and incubated with primary antibodies overnight at 4°C as described [30-31]. Immunohistochemical staining was visualized using the avidin-biotin system (Dako) in combination with 3-amino-9-ethylcarbazole (AEC) (Sigma-Aldrich) and sections were counterstained with hematoxylin (Sigma-Aldrich) as described [30-31].

For immunofluorescence staining, sections were incubated with secondary Alexa Fluor 488 (AF488)- or AF594-conjugated goat-anti-mouse and/or goat-anti-rabbit antibodies and mounted in Prolong Gold Antifade reagent with 4′,6-diamidino-2-phenylindole (Invitrogen) [28]. Sections were analyzed on a Zeiss LSM 700 confocal laser scanning microscope fitted on an Axio Observer Z1 inverted microscope (Zeiss). Images were obtained using 2-4X frame averaging and the pinhole adjusted to 1 airy unit. ZEN 2010 software (Zeiss) was used to adjust brightness and contrast.

Results/Discussion

SVV-infected African green monkeys develop transient fever and skin rash
Five SVV-seronegative adult AGMs were infected intratracheally with SVV-wt (n=2) or SVV-EGFP (n=3). A transient increase in body temperature was seen between 6 and 11 dpi (Fig. 1A and B). SVV-wt-infected animals developed skin rash starting at 6 dpi, which increased in severity until 9 to 10 dpi and resolved thereafter (Fig. 1C). Macroscopic EGFP fluorescent lesions were detected on the skin and lips of all SVV-EGFP-infected animals starting at 7 dpi, which increased in severity until 9 dpi and resolved by 13 dpi (Fig. 1D and data not shown). EGFP fluorescent lesions were also detected on the tongue of SVV-EGFP-infected monkeys, coinciding with appearance of skin rash (data not shown). No lesions were observed on the lips and tongues of SVV-wt-infected animals, demonstrating the increased sensitivity of using SVV-EGFP to study varicella pathogenesis. Skin rash was more severe in SVV-wt compared to SVV-EGFP-infected monkeys. Collectively, the findings indicate the close resemblance of the clinical signs associated with experimental SVV-EGFP infection of AGMs and those of primary VZV infection in humans.

SVV infection of alveolar myeloid cells and T-cells in the lung
All SVV-infected animals became dyspneic at the time of skin rash. Macroscopic examination of lungs showed multifocal pulmonary consolidation and hemorrhage affecting at least one lobe in all animals euthanized 9 or 13 dpi (Fig. 2A). Diffuse EGFP fluorescence was detected in an SVV-EGFP-infected monkey at 9 dpi (Fig. 2B and

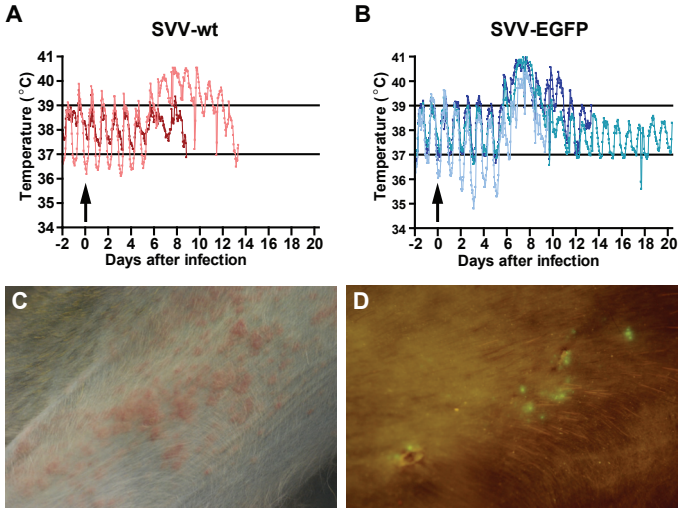

Figure 1. *Experimental SVV infection of African green monkeys results in transient fever and skin rash. (A, B) Fluctuations in body temperature after infection with SVV-wt and SVV-EGFP, respectively, were measured by intraperitoneally implanted temperature transponders during primary infection. Arrows indicate time of SVV inoculation; horizontal lines indicate normal range in body temperature before infection. (C) Vesicular skin rash at 8 dpi with SVV-wt. (D) Macroscopic detection of EGFP fluorescence on skin at 8 dpi with SVV-EGFP.*

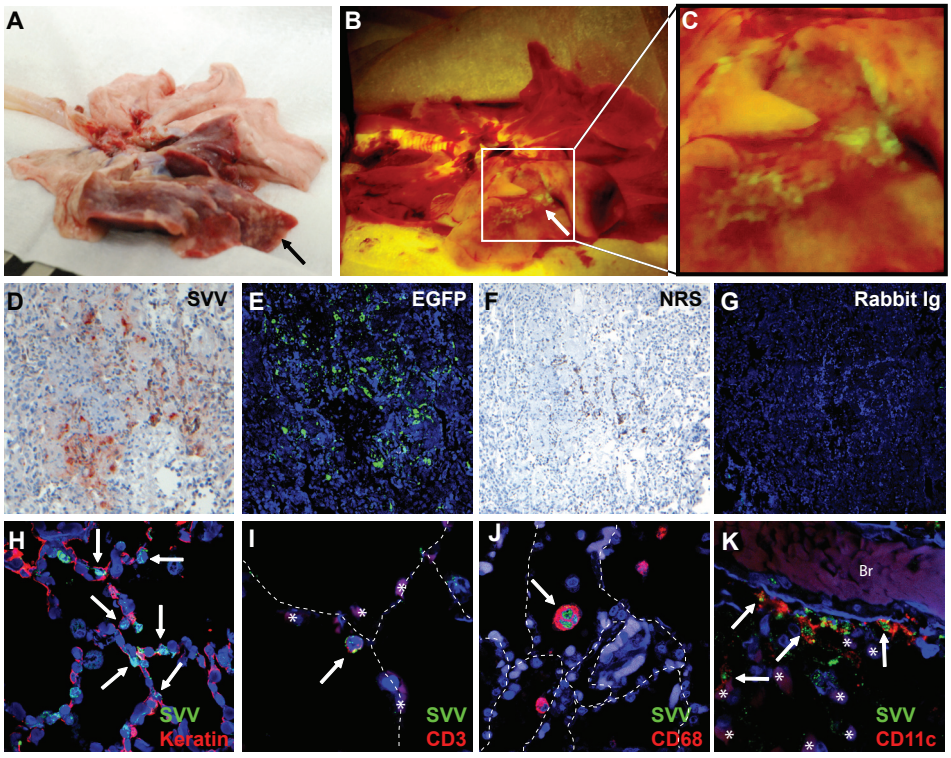

Figure 2. *Macroscopic and microscopic detection of SVV-infected cells in lungs of infected African green monkeys. (A) Macroscopic appearance of consolidated dark-red lesions (black arrow) in the lung of an SVV-wt-infected monkey at 13 dpi. (B) Macroscopic detection of EGFP fluorescence in affected area of lung (white arrow) of an SVV-EGFP-infected monkey at 9 dpi. (C) Magnification of the affected area in panel B shows EGFP fluorescence. (D-G) Serial lung sections obtained from an SVV-EGFP-infected monkey at 9 dpi analyzed by immunohistochemistry (IHC) for SVV antigens (D) or by immunofluorescence (IF) for EGFP (E), with two sections analyzed by IHC (F) or IF (G) using normal rabbit serum (NRS) and isotype control antibodies, respectively. Lung sections obtained from an SVV-wt-infected monkey at 9 dpi were analyzed using dual IF for SVV (green) and: cytokeratin (red) (H), CD3 (red) (I), CD68 (red) (J), and CD11c (red) (K) antigens. Arrows indicate double-positive cells. Asterisks indicate autofluorescent erythrocytes. Dashed lines indicate alveolar septa. Br: bronchus. Nuclei were counterstained with DAPI. D-G: 100X magnification; H, J: 400X magnification; I, K: 400X magnification and 2X digital zoom.*

C). Combined immunohistochemical (IHC) and immunofluorescence (IF) analyses for SVV antigens and EGFP on consecutive sections of lung showed that EGFP expression was restricted to SVV antigen-positive cells (Fig. 2D-G), demonstrating that EGFP is a valid marker to identify SVV-infected cells in the monkeys. To investigate SVV-infected cell types *in situ*, lung tissue sections were analyzed by dual-IF staining with SVV-specific antiserum and anti-keratin, -CD3, -CD68 and -CD11c mouse monoclonal antibodies (mAbs). SVV-infected cells were readily detected in lungs at 9 dpi, but not at later times (data not shown). At 9 dpi, abundant SVV^{pos}keratin^{pos} lung

epithelial cells were observed (Fig. 2H), as well as SVV^{pos}CD3^{pos} T-cells (Fig. 2I). In addition, SVV antigens were found in intra-alveolar cells that co-expressed CD68 and/or CD11c, consistent with alveolar macrophages (AM), some of which appeared to have phagocytosed SVV-infected cells (Fig. 2J). Occasionally, SVV^{pos}CD11c^{pos} dendritic cell (DC)-like cells displaying multiple branched projections were observed adjacent to bronchi (Fig. 2K).

To define the kinetics of virus replication and the cell types infected in the respiratory tract during primary SVV infection, bronchoalveolar lavage (BAL) cells were obtained at 5 dpi, 9 dpi and at necropsy (9, 13 or 20 dpi). SVV DNA load and infectious virus titers in BAL cells peaked at 5 dpi and declined rapidly thereafter (Fig. 3A and B). Infectious virus was not recovered from BAL cells at 13 and 20 dpi (Fig. 3B and data not shown). The viral DNA load and infectious SVV titer in BAL samples were similar in SVV-wt and SVV-EGFP-infected monkeys at 5 dpi, indicating a similar level of replication of both viruses in lung.

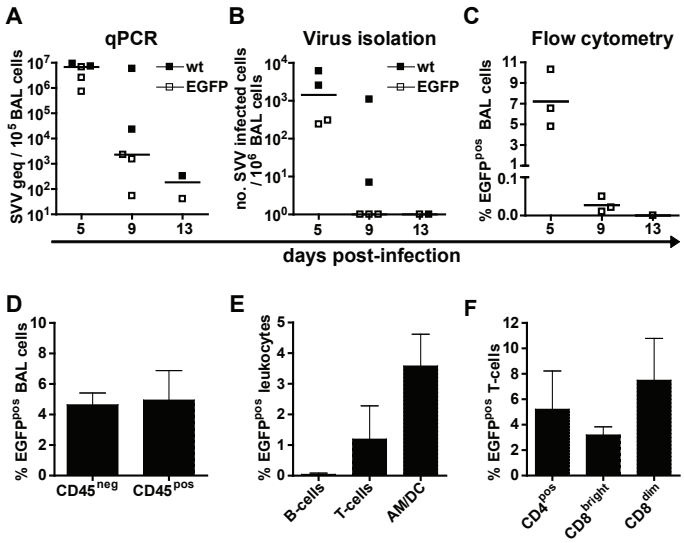

Figure 3. *SVV preferentially infects myeloid cells and T-cells in lungs of infected African green monkeys. (A) Bronchoalveolar lavage (BAL) cells obtained at 5, 9 and 13 dpi were analyzed for viral DNA by SVV-specific real-time qPCR. Data are expressed as genome equivalent copies (geq) per 10^5 BAL cells. (B) BAL cells were analyzed for infectious virus by co-cultivation with BSC-1 cells. (C-F) Percentage of EGFP-positive cells as assessed by flow cytometry in: all BAL cells (C); leukocytes (CD45^{pos} cells), non-leukocytes (CD45^{neg} cells) from BAL samples (D) and leukocyte subsets within BAL (E). Leukocyte subsets were identified based on the differential expression of the following markers: AM/DC= CD45^{pos}CD3^{neg}CD20^{neg}MHC-II^{pos}CD14$^{pos/dim}$, T-cells= CD45^{pos}CD3^{pos}, B-cells= CD45^{pos}CD20^{pos}MHC-II^{pos}; and the indicated T-cell subsets (F). AM/DC are BAL-derived lymphocytes expressing markers shared by dendritic cells (DC) and alveolar macrophages (AM). Horizontal bars indicate median values. (D-F) BAL cells were obtained at 5 dpi and data are given as means ± SEM.*

At 5 dpi, 7.2% of BAL cells from SVV-EGFP-infected monkeys were $EGFP^{pos}$ (Fig. 3C). In $EGFP^{pos}$ BAL cells, equal numbers of $CD45^{pos}$ (leukocytes) and $CD45^{neg}$ cells, most likely bronchial and alveolar epithelial cells, were detected (Fig. 3D and Fig. S1). $CD45^{pos}$ BAL cells could be categorized as T-cells, B-cells and alveolar myeloid cells, i.e. large granular cells expressing high levels of both CD14 and HLA-DR (Fig. S1). These myeloid cells could be alveolar macrophages (AM) and/or DC. At 5 dpi, 82% of $CD45^{pos}$ BAL cells were alveolar myeloid cells, 17% were T-cells and only 1% were B-cells (data not shown). Most $EGFP^{pos}CD45^{pos}$ BAL cells were alveolar myeloid cells and T-cells (Fig. 3E). $CD4^{pos}$, $CD8^{dim}$ and $CD8^{bright}$ T-cells were infected at equal frequencies (Fig. 3F). The number of BAL-derived T-cells was too low to determine their differentiation status unequivocally (data not shown). At 9 dpi, frequencies of $EGFP^{pos}CD45^{pos}$ BAL cells were too low to conclusively identify the SVV-infected leukocyte subsets (Fig. 3C).

SVV infection of memory T-cells in blood during viremia

To determine the kinetics of virus infection and identify the blood lymphocyte subsets infected during the viremic phase of varicella, peripheral blood mononuclear cells (PBMC) isolated at multiple dpi from SVV-infected monkeys were analyzed. SVV DNA was detected in PBMC from 2 dpi until necropsy (Fig. 4A). Viral DNA load in PBMC peaked at 7 dpi and was higher in SVV-wt compared to SVV-EGFP-infected monkeys (Fig. 4A). Infectious virus was isolated from PBMC of both SVV-EGFP and SVV-wt-infected monkeys until 9 and 11 dpi (Fig. 4B). $EGFP^{pos}$ lymphocytes were detected from 5 to 11 dpi, peaking at 7 dpi (Fig. 4C). Together, the data indicate that the kinetics of viral DNA load and infectious virus titer represent the temporal change in the number of circulating SVV-infected lymphocytes, but not in the replication of SVV in blood lymphocytes during viremia. The rapid loss of SVV-infected lymphocytes from the circulation could be caused by virus-induced apoptosis [32] or, alternatively, infected lymphocytes may be cleared from the circulation by the SVV-specific adaptive immune response [14, 21, 33].

At 5 dpi, $EGFP^{pos}$ cells were detected at similar frequencies in all major PBMC subsets (i.e., T-cells, B-cells, natural killer cells, monocytes and dendritic cells) (Fig. 4D and Fig. S2). However, given that most PBMC are T-cells (Fig. S2), T-cells were identified as the main SVV-infected lymphocyte subset in blood (Fig. 4D). Moreover, at the peak of viremia (7 dpi) T-cells were the only SVV-infected cells demonstrated in blood. Unlike humans and macaques, AGMs have three distinct T-cell subsets: $CD8^{bright}$, $CD8^{dim}$ and $CD4^{pos}$ T-cells (Fig. S2)[29]. While CD8bright T-cells correspond to classical human $CD8^{+}$ T-cells, $CD4^{pos}$ T-cells and $CD8^{dim}$ T-cells are considered dynamic populations of AGM T-helper cells functionally equivalent to human $CD4^{+}$ T-cells [29]. Similar levels of $CD8^{bright}$, $CD8^{dim}$ and $CD4^{pos}$ T-cells were SVV-infected, most of which were memory T-cells (Fig. 4E and F). Importantly, at 5 and 7 dpi, predominantly central memory (CM) T-cells and effector memory (EM) T-cells, respectively, were infected (Fig. 4F). The apparent dual phase of SVV-infected CM and EM T-cells may reflect the organ in which the T-cells have been infected. CM T-cells are preferentially found in lymphoid tissues, whereas EM T-cells are migratory memory T-cells that home to peripheral tissues to orchestrate local

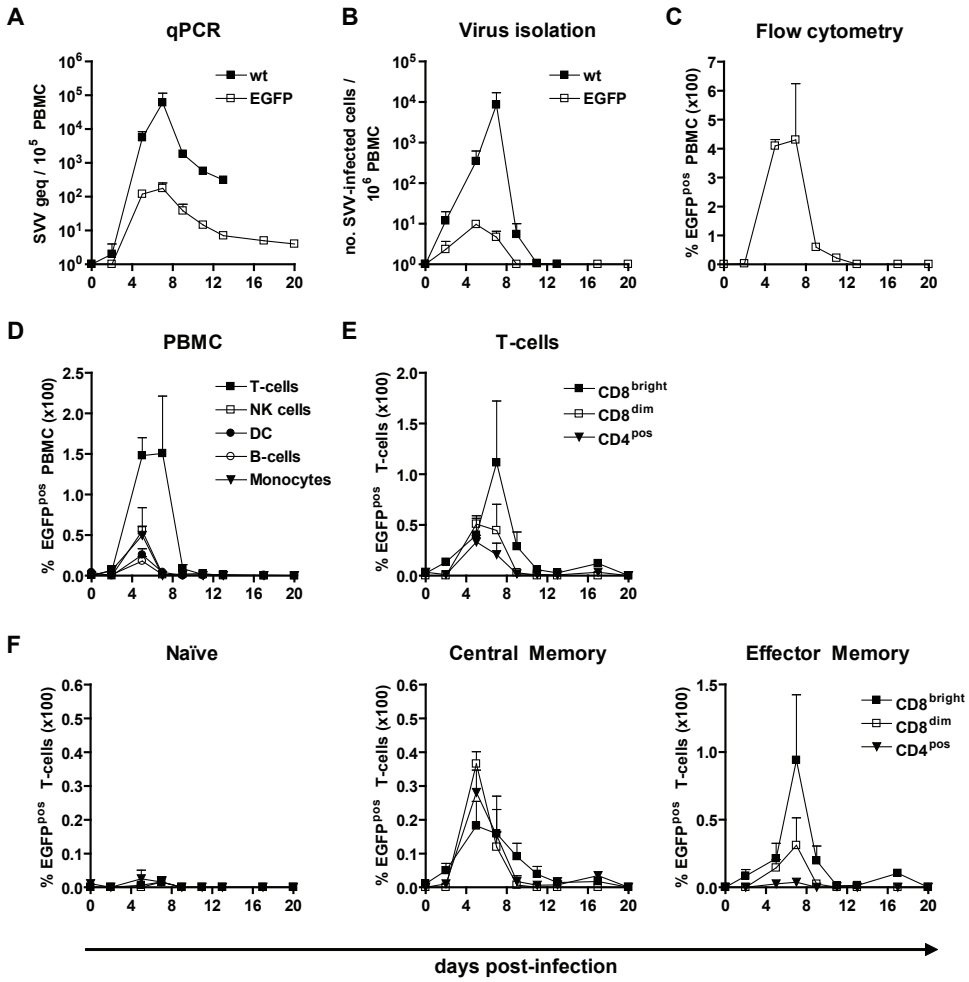

Figure 4. *SVV infects predominantly memory T-cells in blood after infection in African green monkeys. (A) Average SVV DNA load in PBMC of SVV-wt (closed squares) and SVV-EGFP (open squares) infected monkeys determined by SVV-specific real-time qPCR. (B) PBMC from SVV-wt (closed squares) and SVV-EGFP (open squares) infected monkeys were analyzed for infectious SVV by co-cultivation with BSC-1 cells. (C) PBMC from SVV-EGFP-infected monkeys were analyzed for EGFP expression by flow cytometry. (D) EGFP expression in PBMC subsets from SVV-EGFP-infected monkeys. Data are given as percentage of $EGFP^{pos}$ cells within each lymphocyte subset relative to the total number of PBMC, as determined by flow cytometry. Lymphocyte subsets were defined by differential expression of the following markers: T-cells= $CD3^{pos}CD16^{neg}$ cells, B-cells= $CD20^{pos}MHC\text{-}II^{pos}$ cells, natural killer (NK) cells = $CD3^{neg}CD16^{pos}$ cells, dendritic cells (DC)= $CD3^{neg}CD14^{neg}CD16^{neg}CD20^{neg}CD14^{neg}$ $MHC\text{-}II^{pos}$ cells, and monocytes= $CD3^{neg}CD14^{pos}MHC\text{-}II^{pos}$ cells. (E and F) Percentage of $EGFP^{pos}$ cells among each T-cell subset relative to the number of $CD8^{bright}$, $CD8^{dim}$ and $CD4^{pos}$ T-cells (E) and in naive, central memory and effector memory T-cells (F) from SVV-EGFP-infected monkeys as evaluated by flow cytometry. In all panels, data are means ± SEM.*

immune responses and may ultimately function as tissue-resident T-cells to sense the cognate antigen locally for extended periods of time [34-35]. CM T-cells may have been infected in lymphoid tissues and EM T-cells in lungs. Alternatively, SVV infection might have altered the expression of membrane markers used herein to identify AGM-derived CM and EM T-cells. Finally, virus infection may have induced differentiation of CM T-cells into EM T-cells *in vivo*.

In vitro infection studies on human tonsil-derived lymphocytes showed that VZV preferentially infects T-cells expressing the activation marker CD69 and skin-homing markers CCR4 and CLA [10]. To address this issue in SVV-EGFP-infected monkeys, peripheral blood-derived $EGFP^{pos}$ T-cells obtained at 5 and 7 dpi were analyzed for expression of both CCR4 and the T-cell activation marker CD137, the latter marker is selectively expressed by T-cells early after recognition of their cognate antigen [36-37]. No preference of SVV for memory T-cells expressing CCR4 or CD137 was seen *in vivo* (Fig. S3), suggesting that SVV did not infect virus-specific T-cells that recognized SVV-infected antigen presenting cells like macrophages or DCs.

To determine whether the predominant infection of memory T-cells *in vivo* reflects viral tropism for a specific lymphocyte subset, PBMC from SVV-naive AGMs were infected *in vitro* with SVV-EGFP. Expression of EGFP was restricted to lymphocytes that expressed SVV antigens (Fig. S4A), supporting the use of EGFP as a surrogate marker for SVV-infected cells in flow cytometry. While all major PBMC subsets appeared to be equally susceptible to SVV infection, T-cells were the prominent SVV-infected PBMC subset *in vitro* (Fig. S4B), with similar infection levels in $CD4^{pos}$, $CD8^{dim}$ and $CD8^{bright}$ T-cells (Fig. S4C). In particular, significantly more memory T-cells were infected compared to naive T-cells ($p<0.05$; Mann-Whitney test) (Fig. S4D). Thus, SVV preferentially infects memory T-cells rather than naive T-cells both *in vivo* (Fig. 4) and *in vitro* (Fig. S4).

Detection of SVV in lymphoid organs

Alveolar macrophages and lung-resident DC transport antigens to lung-draining lymph nodes for presentation to T-cells [38-39], and VZV-infected human DCs can transfer infectious virus to T-cells *in vitro* [40]. We hypothesized that SVV-infected alveolar myeloid cells transport SVV to draining lymph nodes for subsequent virus transfer to memory T-cells. High SVV DNA loads were detected in lymph nodes, tonsils and spleens of SVV-infected monkeys at 9 dpi, declining rapidly thereafter (Fig. 5A). Cells in lymph nodes and tonsils of SVV-infected monkeys contained intranuclear inclusions bodies and SVV antigen (Fig. 5B and C). Tracheobronchial lymph nodes showed more pronounced SVV-induced histopathology compared to peripheral lymph nodes (data not shown). However, SVV DNA loads were comparable in different lymph nodes collected at 9 dpi (Fig. 5A), emphasizing the need to investigate lymph nodes at earlier times after infection. In addition, detection of SVV-infected memory T-cells in blood may represent lung-resident T-cells involved in SVV dissemination. SVV infects alveolar epithelial cells leading to alveolar wall damage (data not shown) [19, 33, 41], which may result in egress of SVV-infected T-cells into the circulation.

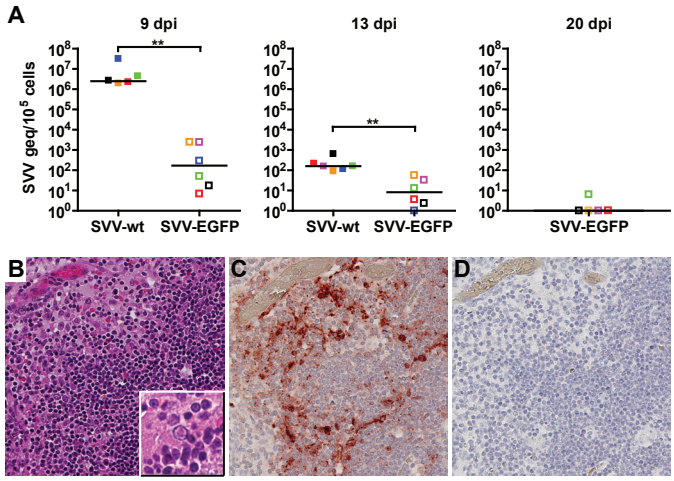

Figure 5. *Detection of SVV in lymphoid organs from infected African green monkeys. (A) Real-time qPCR analysis of SVV DNA load in tonsil, lymph nodes and spleen from SVV-wt- (closed squares) and SVV-EGFP- (open squares) infected monkeys at 9, 13 and 20 dpi. Squares indicate individual tissues, i.e., tonsils (red), tracheobronchial lymph nodes (LN) (green), axillary LN (pink), mandibular LN (blue), inguinal LN (orange) and spleen (black). Horizontal bar indicates the median value. (B-D) Serial sections of tonsil from an SVV-wt-infected monkey stained with hematoxylin and eosin (inset shows a Cowdry type A intranuclear inclusion body) (B) or examined immunohistochemically using rabbit anti-SVV antibodies (C) or control normal rabbit serum (D). Magnification: 200X. The area of tonsils containing multiple intranuclear inclusion bodies contained numerous cells expressing SVV protein. **p<0.01 by Mann-Whitney test.*

SVV-infected perivascular lymphocytes in early varicella lesions implicate hematogenous spread of SVV to the skin

Detailed *in situ* analysis was performed to identify the SVV-infected cell types in varicella skin lesions. Macroscopic detection of EGFP fluorescence corresponded to SVV infection of the skin, as demonstrated by the co-localization of SVV protein and EGFP in consecutive skin sections obtained from an SVV-EGFP–infected monkey (Fig. 6A and B). In vesicular skin lesions, SVV predominantly infected keratinocytes (Fig. 6C and D). In deeper skin layers, SVV protein was frequently detected in hair follicles (Fig. 6E and F) and sebaceous glands (Fig. 6G and H).

Analysis of skin biopsies from SVV-EGFP-infected monkeys allowed investigation of the early stages of varicella, as evidenced on the skin by the appearance of EGFP fluorescent areas in the absence of lesions visible to the naked eye. In these biopsies, SVV protein expression was consistently located within perivascular lymphocytes (Fig. 6I–K). Dual-IF staining for EGFP and specific lymphocyte markers identified SVV-infected perivascular cell subsets as $CD68^{pos}$ macrophages (Fig. 6L), $CD11c^{pos}$ DCs (Fig. 6M) and $CD3^{pos}$ T-cells (Fig. 6N). The remaining SVV-infected cells, which stained negative for lymphocyte markers, phenotypically resembled dendrocytes (data not shown) [42]. Interestingly, SVV-infected T-cells were also observed in the epidermis of SVV-wt infected monkeys at 9 dpi (Fig. 6O). Flow cy

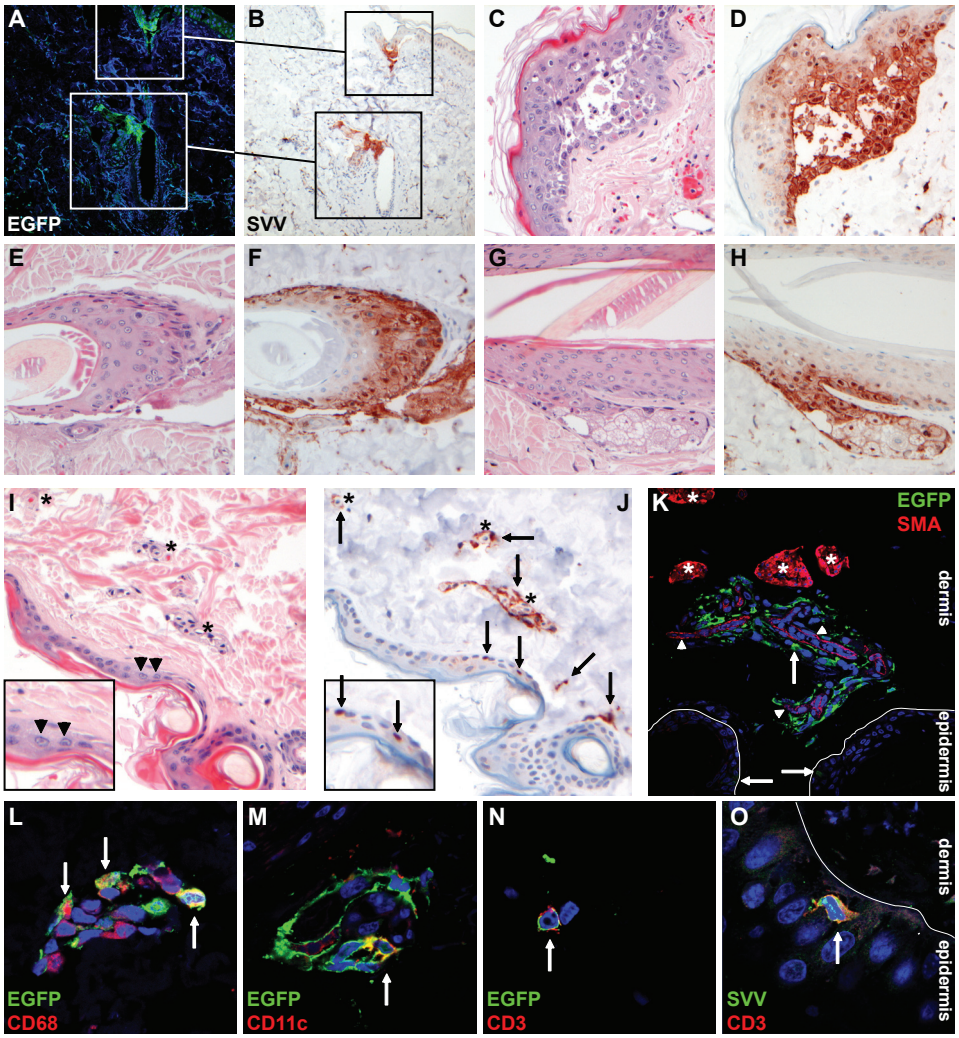

Figure 6. *Detection of SVV-infected cells in varicella skin lesions from infected African green monkeys. (A, B) Consecutive sections of skin obtained from an SVV-EGFP-infected monkey at 9 dpi and stained by immunofluorescence (IF) for EGFP (A) and by immunohistochemistry (IHC) for SVV antigens (B) show co-localization of SVV proteins and EGFP. Squares indicate the same area of tissue. (C-H) Consecutive sections of skin obtained from an SVV-wt-infected animal at 9 dpi and examined by staining with hematoxylin and eosin (H&E) or by IHC for SVV show virus-induced histopathology and viral proteins in epidermal blisters (C and D), dermal hair follicles (E and F) and dermal sebaceous glands (G and H). (I, J) Consecutive skin sections obtained from an SVV-EGFP-infected monkey at 9 dpi and stained with H&E (I) or by IHC for SVV antigens (J) show blood vessels (asterisks) surrounded by SVV protein-positive cells (arrows). Inset: magnification of the epidermis showing Cowdry type A intranuclear inclusion bodies in panel I (arrowheads) and SVV protein-positive cells in panel J (arrows). (K) Skin section from an SVV-EGFP-infected animal obtained at 9 dpi and double-stained for EGFP (green) and alpha-smooth muscle actin (SMA; red). Asterisks indicate SMA-positive*

Figure 6 - continued. *sweat glands, arrowheads indicate SMA-positive blood vessels, and arrows indicate EGFP-positive cells. (L-N) Skin sections obtained at 9 dpi and double-stained for EGFP (green) and: CD68 (red) (L); CD11c (red) (M); and CD3 (red) (N). Arrows indicate dual-stained cells. (O) Skin section obtained at 9 dpi and double-stained for SVV (green) and CD3 (red). Arrows indicate dual-stained cells. A, B: 100X magnification; C-K: 200X magnification; L-O: 400X magnification and 2X digital zoom.*

tometric analysis of skin-resident T-cells showed exclusively memory T-cells, mostly EM T-cells (data not shown).

Collectively, these data suggest that SVV reaches the skin hematogenously. Since the skin vasculature is composed of an upper horizontal superficial vascular plexus just beneath the epidermal surface and a deep vascular plexus that supplies the hair bulbs and sweat glands [43], it seems likely that SVV-infected memory T-cells transfer the virus to skin-resident perivascular macrophages, DCs or dendrocytes, which in turn transfer SVV to adjacent epidermal or hair follicle keratinocytes via cell-to-cell spread. Alternatively, epidermal SVV-infected T-cells may transfer the virus directly to skin epithelial cells (Fig. 6O).

Neurons are the main SVV-infected cell types in ganglia

The hallmark of primary SVV and VZV infection is the capacity of virus to infect and establish latency in ganglionic neurons along the entire neuraxis [1, 13, 42]. Virus may reach ganglia hematogenously or by retrograde axonal transport along axons innervating varicella lesions [12, 20, 48-49]. We determined the kinetics of virus infection and the cell types infected in ganglia during primary SVV infection. The SVV DNA load in ganglia was significantly higher in SVV-wt compared to SVV-EGFP-infected monkeys ($p<0.01$; Mann-Whitney test) (Fig. 7A), peaking at 9 dpi and decreasing thereafter (Fig. 7A), as might be expected during the establishment of latency. Despite high SVV DNA loads, no virus-mediated cytopathology was seen in ganglia (data not shown). Virus antigen was more abundant at 9 dpi than at 13 and 20 dpi (data not shown). SVV-infected cells in ganglia were detected *in situ* by IHC using SVV-specific antiserum (Fig. 7B-D). Dual-IF staining for SVV and the neuron-specific marker NCAM (neural cell adhesion molecule) showed that most SVV^{pos} cells were neurons (Fig. 7E). Occasionally, SVV antigens were seen at the neuronal cell surface or potentially within satellite glial cells (SGC) (Fig. 7D). SGC form a sheet that completely enwraps neuronal cell bodies, providing physical and metabolic support to the neurons and contributing to regulation of the immune response in the peripheral nervous system [30, 50]. Virus-infected cells located in vicinity to neurons did not express the SGC-specific marker glial fibrillary acidic protein (GFAP) [50], implicating that SGC were not infected with SVV at 9, 13 and 20 dpi (Fig. 7F and data not shown). To address the possibility of T-cell–mediated transfer of SVV to neurons, ganglia were examined using dual-IF staining for SVV antigens and CD3. In an SVV-wt-infected monkey euthanized at 9 dpi, SVV-infected T-cells were detected in close proximity to neurons (Fig. 7G). Notably, this animal also had the highest SVV DNA load in blood and ganglia. Flow cytometric analysis of ganglion-derived single-cell suspensions demonstrated that ganglion-resident T-cells were memory T-cells, predominantly EM T-cells (Fig. 7H).

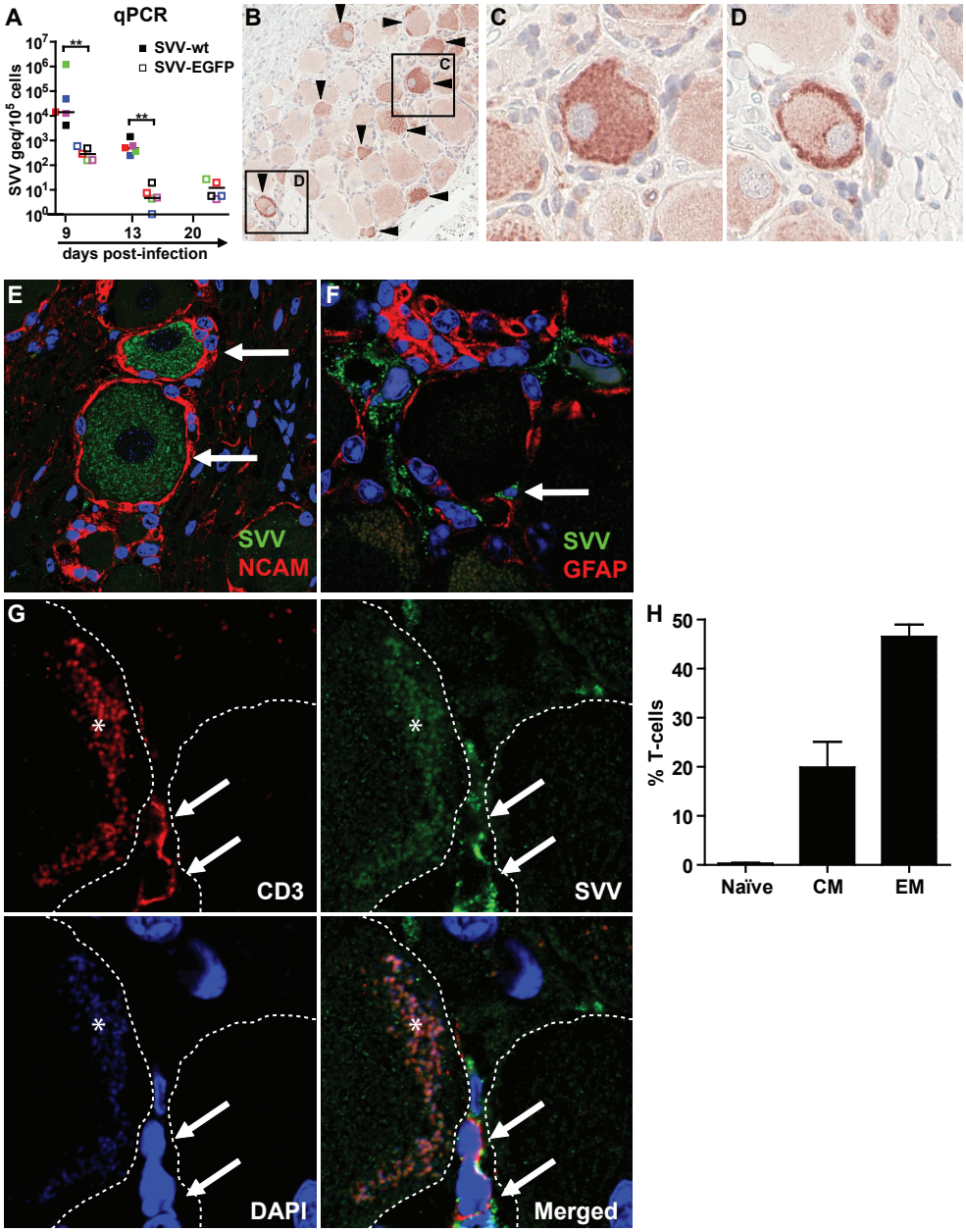

Figure 7. *Detection of SVV-infected cells in ganglia of infected African green monkeys. (A) Virus DNA load was determined in ganglia at 9, 13 and 20 dpi by SVV-specific real-time qPCR. Filled and open squares represent pooled ganglia from the same level of the neuraxis from animals infected with SVV-wt and SVV-EGFP, respectively. Colors indicate level of the neuraxis: trigeminal (black), cervical (red), thoracic (blue), lumbar (green) and sacral (pink) ganglia. Horizontal bars represent mean viral DNA load per animal. (B) Immunohistochemical detection of SVV proteins (arrowheads) in a cervical ganglion at 9 dpi.*

Figure 7 - continued. *Squares indicate corresponding tissue areas shown at higher magnification in (C) and (D). (E) Dual-immunofluorescence (IF) staining of a thoracic ganglion at 9 dpi for SVV proteins (green) and neural cell adhesion molecule (NCAM; red). Arrows indicate SVV-positive neurons. (F) Dual-IF staining of a thoracic ganglion at 9 dpi for SVV protein (green) and glial fibrillary acidic protein (GFAP; red). Arrow indicates neuron-adjacent SVV-positive cell. (G) Dual-IF staining of a thoracic ganglion from a monkey at 9 dpi for SVV protein (green) and CD3 (red). Arrows indicate SVV-positive T-cells. Asterisks indicate autofluorescent lipofuscin and the borders of the neuronal cell bodies are indicated with dashed lines. (H) Ganglion-derived single-cell suspensions were analyzed by flow cytometry and T-cells were categorized as naive, central memory (CM) and effector memory (EM) T-cells. E-G: nuclei were counterstained with DAPI (blue). ** p<0.01 by Mann-Whitney test. B: 200X magnification; C, D: 400X magnification, 2X digital zoom; E: 400X magnification; F, G: 400X magnification, 2X digital zoom.*

Our findings in ganglia contrast with the pronounced VZV-induced histopathology of both SGCs and neurons found in VZV-infected human fetal ganglia xenografts in the SCID-hu mouse model [21, 51]. Most likely, these differences are due to the use of fetal human ganglia and the lack of adaptive immune responses in the SCID-hu mouse model. The absence of SVV-induced histopathology in ganglia is consistent with previous studies [19,33] and the inability to recover infectious virus from ganglia [15] at 10 dpi. Nonetheless, virus-induced cytopathology of ganglia may have occurred during the peak of viremia (5 – 7 dpi), which will be considered in future studies. The detection of SVV protein in the cytoplasm of neurons, but not in the interacting SGC (Fig. 6B-F), supports the notion of retrograde axonal route of virus entry into ganglia [48-49, 52-53]. In contrast with this hypothesis, the SVV DNA load did not differ among ganglia, including those that innervated the dermatomes showing varicella rash (Fig. 7A and data not shown). The alternative scenario is that virus traffics to ganglia during viremia within lymphocytes. Indeed, both SVV and VZV enter ganglia before the onset of rash, arguing for hematogenous virus spread [1, 20, 21]. VZV-infected T-cells infiltrate human ganglion xenografts and transmit VZV to neurons in the VZV SCID-hu mouse model [12]. The occasional detection of neuron-interacting, SVV-infected memory T-cells within ganglia (Fig. 7G) supports the role of memory T-cells in virus dissemination to ganglia. Further studies on ganglia from SVV-EGFP-infected monkeys euthanized at earlier times after primary infection are warranted to test this hypothesis.

The current study is the first to present experimental evidence (summarized in Fig. 8) that supports the role of memory T-cells in the inter-organ dissemination of varicella virus in its natural and immunocompetent host. Our current hypothesis on the pathogenesis of primary SVV infection is presented in Figure 9. We hypothesize that upon intratracheal inoculation, SVV replicates in the respiratory tract and infects epithelial cells, alveolar myeloid cells (AM and/or DC) and T-cells in the lungs. Subsequently, the virus enters the circulation as cell-associated virus predominantly within memory T-cells, first within CM and subsequently within EM T-cells. Most likely, virus-infected alveolar myeloid cells transport SVV to lung-draining lymph nodes, with subsequent transfer of SVV to memory T-cells. Peak viremia coincided with onset of fever and appearance of skin rash. SVV reached the skin by the hematogenous route, most

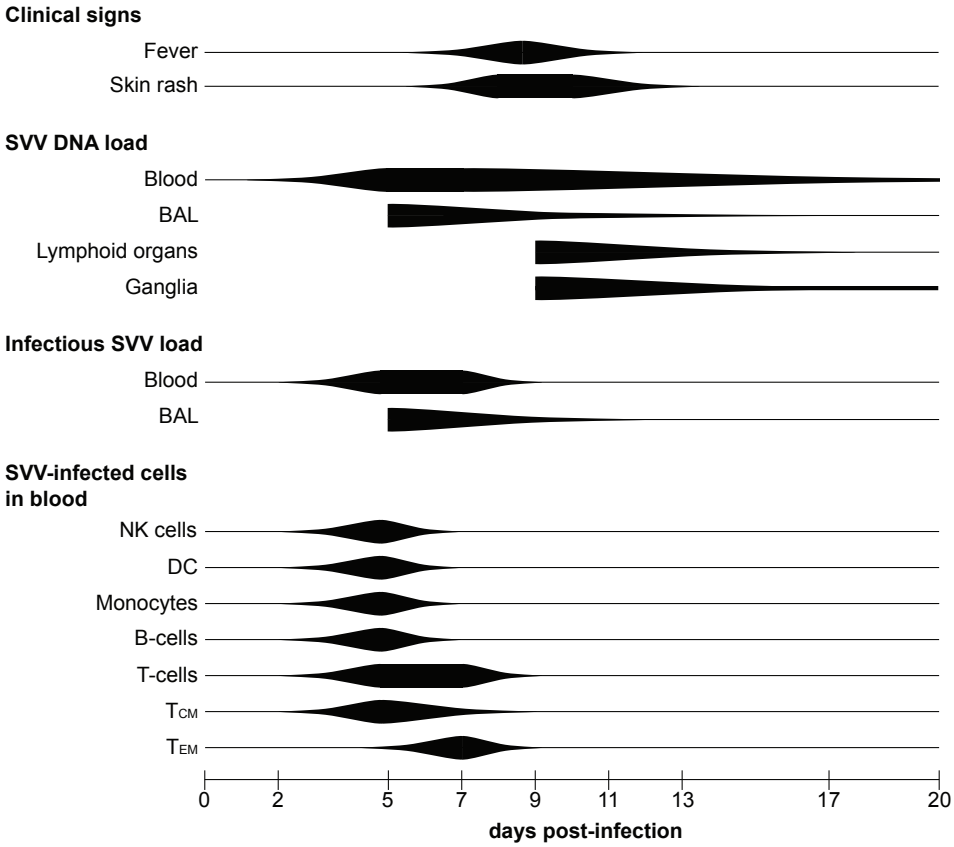

Figure 8. *Schematic presentation of primary SVV infection. Figure shows the kinetics of SVV infection and virus-infected cell types in African green monkeys during primary SVV infection. Horizontal lines indicate the time-frame covered by the sampling days. Width of the black bars indicates onset and severity of clinical signs, amount of SVV DNA detected in blood and the sampled organs, and the frequency of SVV-infected cells in peripheral blood during primary SVV infection. Note that BAL samples were obtained no earlier than 5 dpi and animals were euthanized no earlier than 9 dpi. BAL: bronchoalveolar lavage; NK cells: natural killer cells; DC: dendritic cell; T_{CM}: central memory T-cells; T_{EM}: effector memory T-cells.*

likely via virus-infected memory T-cells. SVV may enter ganglia by retrograde axonal transport from the infected epithelia and/or by the hematogenous route. In addition to memory T-cells, other lymphocyte subsets may also contribute to the viremic spread of SVV. Virus-infected DC, NK cells, B-cells and monocytes were detected in peripheral blood at 5 dpi, albeit at low frequencies compared to memory T-cells. The contribution of each lymphocyte population in transfer of SVV to its target organs will be addressed in future studies by analyzing virus-infected lymphocytes in tissues of animals euthanized during peak viremia at 5 – 7 dpi.

Like VZV, SVV is considered to spread to naive monkeys via aerosols and therefore most likely targets mucosal epithelial cells of the upper respiratory tract, although –

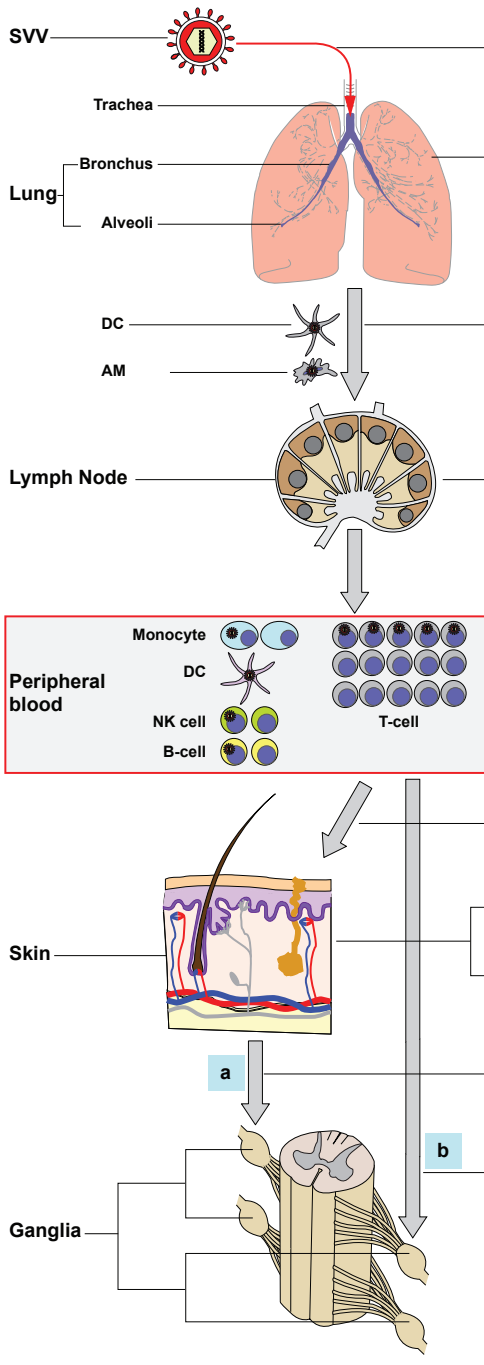

- Intratracheal inoculation with SVV
- Infection of epithelial cells, alveolar macrophages (AM), dendritic cells (DC) and T-cells
- Infected AM and DC transport SVV to lung-draining lymph nodes
- Transfer of SVV to lymphocytes
- Cell-associated viremia: predominant infection of memory T-cells
- Hematogenous spread of SVV to skin
- SVV infection of perivascular macrophages, DC and dendrocytes
- Cell-to-cell spread and infection of keratinocytes: skin rash
- Retrograde axonal transport of SVV to sensory ganglion neurons

and/or

- Hematogenous spread of SVV to ganglia

Figure 9. *Model of the pathogenesis of primary SVV infection. Upon intratracheal inoculation of African green monkeys, SVV replicates in the lower respiratory tract and infects lung epithelial cells, alveolar macrophages (AM), dendritic cells (DC) and T-cells. SVV-infected AM and DC may transport the virus to draining lymph nodes and subsequently transfer SVV to local lymphocytes resulting in a cell-associated viremia. Memory T-cells are the predominant SVV-infected lymphocyte subset during viremia and may play a central role in dissemination of SVV to its target organs. SVV reaches the skin by the hematogenous route, presumable via virus-infected memory T-cells, which results in the infection of perivascular macrophages, DC and dendrocytes. Subsequently, SVV may infect epidermal and hair follicle keratinocytes via cell-to-cell spread and cause vesicular skin lesions. SVV may enter ganglia by (a) retrograde axonal transport and/or (b) by viremic spread via virus-infected lymphocytes.*

depending on the size of the aerosols – some virus may also directly reach the lower respiratory tract [1,13,14,25]. In the current study, we have used intratracheal inoculation of monkeys with SVV, bypassing the putative initial site of local SVV replication in the upper respiratory tract or tonsils [1,13,14]. Primary VZV infections in adults are more severe than in children and frequently complicated by varicella pneumonia [1]. Consequently, the adult status of SVV-infected AGM may have enhanced disease severity, although pneumonia is a common feature in SVV-infected monkeys due to the intratracheal route of inoculation [19,33]. Recombinant SVV-EGFP was attenuated *in vivo* compared to SVV-wt, possibly due to insertion of the EGFP gene between open reading frames (ORFs) 66 and ORF67 [27]. Recombinant VZV lacking ORF67 is severely impaired for growth in cell culture [54]. Although attenuated in severity, SVV-EGFP–induced disease resembled that of a SVV-wt infection and attenuation did not alter the cell tropism of SVV-EGFP. Both SVV-wt and SVV-EGFP infected the same cell types in lung, lymph nodes, ganglia and skin *in vivo*, and identical PBMC types *in vitro*. The recent cloning of the SVV-wt full-length genome in a bacterial artificial chromosome facilitates the generation of a potentially less attenuated recombinant EGFP-expressing SVV by inserting the EGFP gene adjacent to SVV genes dispensable for growth *in vitro* [54,55].

Future studies on juvenile African green monkeys, infected with less-attenuated SVV-EGFP strains and via alternative inoculation routes (e.g., via the nose or throat), are warranted. Particularly, analysis of tissues obtained from infected animals euthanized shortly after primary infection are needed to unequivocally determine the early target cell types of SVV, their role in virus dissemination to the target organs affected during primary infection and the route of SVV entry into sensory ganglia [25]. Our current SVV-EGFP/AGM model, which largely covers the clinical and pathological features seen in both SVV-wt-infected monkeys and human varicella patients, provides novel opportunities to elucidate the virus-host cell interactions involved in varicella pathogenesis. This will open new avenues to develop and test new VZV vaccination and therapeutic interventions that limit viremic spread, while inducing long-lasting adaptive VZV-specific immunity.

Acknowledgments

We thank Rory D. de Vries, Monique van Velzen, Freek B. van Loenen and Gijsbert P. van Nierop for technical assistance.

References

1. Cohen JI, Straus, SE, and Arvin, AM. Varicella-zoster virus replication, pathogenesis, and management. In: Knipe DM, Howley PM, Griffin DE, et al., eds. Fields Virology. 5th ed. Vol. 2. Philadelphia, PA: Lippincott, Williams and Wilkins, 2007:2773-2818
2. Grose C. Variation on a theme by Fenner: the pathogenesis of chickenpox. Pediatrics 1981;68: 735-7
3. Heininger U, Seward JF. Varicella. Lancet 2006;368:1365-76
4. Asano Y, Itakura N, Hiroishi Y, et al. Viremia is present in incubation period in nonimmunocompromised children with varicella. J Pediatr 1985;106:69-71
5. Koropchak CM, Graham G, Palmer J, et al. Investigation of varicella-zoster virus infection by polymerase chain reaction in the immunocompetent host with acute varicella. J Infect Dis 1991;163:1016-22
6. Arvin AM, Moffat JF, Sommer M, et al. Varicella-zoster virus T cell tropism and the pathogenesis of skin infection. Curr Top Microbiol Immunol 2010;342:189-209
7. Zerboni L, Reichelt M and Arvin A. Varicella-zoster virus neurotropism in SCID mouse-human dorsal root ganglia xenografts. Curr Top Microbiol Immunol 2010;342:255-76
8. Moffat JF, Stein MD, Kaneshima H and Arvin AM. Tropism of varicella-zoster virus for human CD4+ and CD8+ T lymphocytes and epidermal cells in SCID-hu mice. J Virol 1995;69:5236-42
9. Ku CC, Besser J, Abendroth A, Grose C and Arvin AM. Varicella-Zoster virus pathogenesis and immunobiology: new concepts emerging from investigations with the SCIDhu mouse model. J Virol 2005;79:2651-8
10. Ku CC, Padilla JA, Grose C, Butcher EC and Arvin AM. Tropism of varicella-zoster virus for human tonsillar CD4(+) T lymphocytes that express activation, memory, and skin homing markers. J Virol 2002;76:11425-33
11. Ku CC, Zerboni L, Jones CD, Zehnder JL and Arvin AM. Varicella-zoster virus transfer to skin by T cells and modulation of viral replication by epidermal cell interferon-alpha. J Exp Med 2004;200: 917-25
12. Zerboni L, Ku CC, Jones CD, Zehnder JL and Arvin AM. Varicella-zoster virus infection of human dorsal root ganglia in vivo. Proc Natl Acad Sci U S A 2005;102:6490-5
13. Mahalingam R, Messaoudi I and Gilden D. Simian varicella virus pathogenesis. Curr Top Microbiol Immunol 2010;342:309-21
14. Messaoudi I, Barron A, Wellish M, et al. Simian varicella virus infection of rhesus macaques recapitulates essential features of varicella zoster virus infection in humans. PLoS Pathog 2009;5:e1000657
15. Gray WL. Simian varicella: a model for human varicella-zoster virus infections. Rev Med Virol 2004;14:363-81
16. Gray WL, Starnes B, White MW and Mahalingam R. The DNA sequence of the simian varicella virus genome. Virology 2991;284:123-130
17. Mahalingam R, Traina-Dorge V, Wellish M, et al. Simian varicella virus reactivation in cynomolgus monkeys. Virology 2007;368:50-9
18. Mahalingam R, Traina-Dorge V, Wellish M, et al. Latent simian varicella virus reactivates in monkeys treated with tacrolimus with or without exposure to irradiation. J Neurovirol 2010;16:342-54
19. Dueland AN, Martin JR, Devlin ME, et al. Acute simian varicella infection. Clinical, laboratory, pathologic, and virologic features. Lab Invest 1992;66:762-73
20. Mahalingam R, Wellish M, Soike K, White T, Kleinschmidt-DeMasters BK and Gilden DH. Simian varicella virus infects ganglia before rash in experimentally infected monkeys. Virology 2001;279:339-42
21. Ouwendijk WJ, Mahalingam R, Traina-Dorge V, et al. Simian varicella virus infection of Chinese rhesus macaques produces ganglionic infection in the absence of rash. J Neurovirol 2012;18:91-9
22. de Swart RL, Ludlow M, de Witte L, et al. Predominant infection of CD150+ lymphocytes and dendritic cells during measles virus infection of macaques. PLoS Pathog 2007;3:e178
23. de Vries RD, Lemon K, Ludlow M, et al. In vivo tropism of attenuated and pathogenic measles virus expressing green fluorescent protein in macaques. J Virol 2010;84:4714-24
24. de Vries RD, McQuaid S, van Amerongen G, et al. Measles immune suppression: lessons from the macaque model. PLoS Pathog 2012;8:e1002885

25. Lemon K, de Vries RD, Mesman AW, et al. Early target cells of measles virus after aerosol infection of non-human primates. PLoS Pathog 2011;7:e1001263
26. Mahalingam R, Clarke P, Wellish M, et al. Prevalence and distribution of latent simian varicella virus DNA in monkey ganglia. Virology 1992;188:193-7
27. Mahalingam R, Wellish M, White T, et al. Infectious simian varicella virus expressing the green fluorescent protein. J Neurovirol 1998;4:438-44
28. Ouwendijk WJ, Flowerdew SE, Wick D, et al. Immunohistochemical detection of intra-neuronal VZV proteins in snap-frozen human ganglia is confounded by antibodies directed against blood group A1-associated antigens. J Neurovirol 2012;18:172-80
29. Beaumier CM, Harris LD, Goldstein S, et al. CD4 downregulation by memory CD4+ T cells in vivo renders African green monkeys resistant to progressive SIVagm infection. Nat Med 2009;15:879-85
30. van Velzen M, Laman JD, Kleinjan A, Poot A, Osterhaus AD and Verjans GM. Neuron-interacting satellite glial cells in human trigeminal ganglia have an APC phenotype. J Immunol 2009;183:2456-61
31. Verjans GM, Hintzen RQ, van Dun JM, et al. Selective retention of herpes simplex virus-specific T cells in latently infected human trigeminal ganglia. Proc Natl Acad Sci U S A 2007;104:3496-501
32. Konig A, Homme C, Hauroder B, Dietrich A and Wolff MH. The varicella-zoster virus induces apoptosis in vitro in subpopulations of primary human peripheral blood mononuclear cells. Microbes Infect 2003;5:879-89
33. Gray WL, Williams RJ, Chang R and Soike KF. Experimental simian varicella virus infection of St. Kitts vervet monkeys. J Med Primatol 1998;27:177-83
34. Gebhardt T, Mackay LK. Local immunity by tissue-resident CD8(+) memory T cells. Front Immunol 2012;3:340
35. Picker LJ, Terstappen LW, Rott LS, Streeter PR, Stein H and Butcher EC. Differential expression of homing-associated adhesion molecules by T cell subsets in man. J Immunol 1990;145:3247-55
36. Jing L, Haas J, Chong TM, et al. Cross-presentation and genome-wide screening reveal candidate T cells antigens for a herpes simplex virus type 1 vaccine. J Clin Invest 2012;122:654-73
37. Wolfl M, Kuball J, Ho WY, et al. Activation-induced expression of CD137 permits detection, isolation, and expansion of the full repertoire of CD8+ T cells responding to antigen without requiring knowledge of epitope specificities. Blood 2007;110:201-10
38. Kirby AC, Coles MC and Kaye PM. Alveolar macrophages transport pathogens to lung draining lymph nodes. J Immunol 2009;183:1983-9
39. Thornton EE, Looney MR, Bose O, et al. Spatiotemporally separated antigen uptake by alveolar dendritic cells and airway presentation to T cells in the lung. J Exp Med 2012;209:1183-99
40. Abendroth A, Morrow G, Cunningham AL and Slobedman B. Varicella-zoster virus infection of human dendritic cells and transmission to T cells: implications for virus dissemination in the host. J Virol 2001;75:6183-92
41. Roberts ED, Baskin GB, Soike K and Meiners N. Transmission and scanning electron microscopy of experimental pulmonary simian varicella (Delta herpesvirus) infection in African green monkeys (Cercopithecus aethiops). J Comp Pathol 1984;94:323-8
42. Nikkels AF, Debrus S, Sadzot-Delvaux C, et al. Comparative immunohistochemical study of herpes simplex and varicella-zoster infections. Virchows Arch A Pathol Anat Histopathol 1993;422:121-6
43. Braverman IM. The cutaneous microcirculation: ultrastructure and microanatomical organization. Microcirculation 1997;4:329-40
44. Gilden DH, Vafai A, Shtram Y, Becker Y, Devlin M and Wellish M. Varicella-zoster virus DNA in human sensory ganglia. Nature 1983;306:478-80
45. Kennedy PGE, Grinfeld E and Gow JE. Latent varicella-zoster virus is located predominantly in neurons in human trigeminal ganglia. Proc Natl Acad Sci U S A 1998;95:4658-62
46. Kennedy PGE, Grinfeld E, Traina-Dorge V, Gilden DH and Mahalingam R. Neuronal localization of simian varicella virus DNA in ganglia of naturally infected African green monkeys. Virus Genes 2004;28:273-6
47. Wang K, Lau TY, Morales M, Mont EK and Straus SE. Laser-capture microdissection: refining estimates of the quantity and distribution of latent herpes simplex virus 1 and varicella-zoster virus DNA in human trigeminal ganglia at the single-cell level. J Virol 2005;79:14079-87
48. Annunziato PW, Lungu O, Panagiotidis C, et al. Varicella-zoster virus proteins in skin lesions: implications for a novel role of ORF29p in chickenpox. J Virol 2000;74:2005-10
49. Hope-Simpsom RE. The nature of herpes zoster: a long-term study and a new hypothesis. Proc R

Soc med 1965;58:9-20
50. Hanani M. Satellite glial cells in sensory ganglia: from form to function. Brain Res Brain Res Rev 2005;48:457-76
51. Reichelt M, Zerboni L and Arvin AM. Mechanisms of varicella-zoster virus neuropathogenesis in human dorsal root ganglia. J Virol 2008;82:3971-83
52. Grigoryan S, Kinchington PR, Yang IH, et al. Retrograde axonal transport of VZV: kinetic studies in hESC-derived neurons. J Neurovirol 2012
53. Markus A, Grigoryan S, Sloutskin A, et al. Varicella-zoster virus (VZV) infection of neurons derived from human embryonic stem cells: direct demonstration of axonal infection, transport of VZV, and productive neuronal infection. J Virol 2011;85:6220-33
54. Zhang Z, Selariu A, Warden C, et al., Genome-wide mutagenesis reveals that ORF7 is a novel VZV skin-tropic factor. PLoS Pathog 2010;6:e1000971
55. Gray WL, Zhou F, Noffke J and Tischer BK. Cloning the simian varicella virus genome in E. coli as an infectious bacterial artificial chromosome. Arch Virol 2011; 156:739-46

Supporting Information

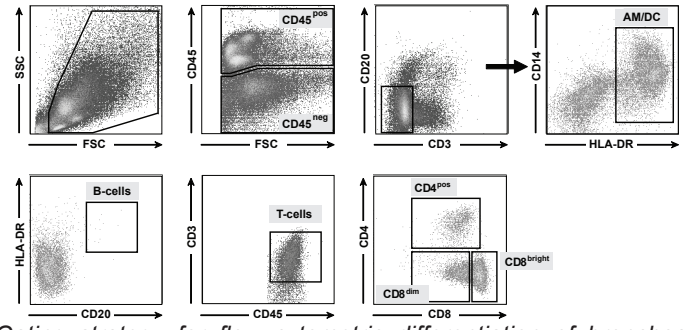

Figure S1. *Gating strategy for flow cytometric differentiation of bronchoalveolar lavage (BAL) cells of African green monkeys. BAL cells were gated on viable cells based on forward scatter (FSC) and sideward scatter (SSC) properties and defined as $CD45^{neg}$ cells or $CD45^{pos}$ leukocytes. $CD45^{pos}$ BAL leukocyte subsets were defined as follows: $CD3^{neg}CD20^{neg}$MHC-$II^{pos}CD14^{pos/dim}$ =alveolar macrophages (AM) or dendritic cells (DC); $CD20^{pos}$MHC-II^{pos} =B-cells; $CD3^{pos}$ =T-cells; $CD4^{neg}CD8\alpha^{high}$ =$CD8^{bright}$ T-cells, $CD4^{neg}CD8\alpha^{dim}$ =$CD8^{dim}$ T-cells, and $CD4^{pos}CD8\alpha^{neg}$ =$CD4^{pos}$ T-cells.*

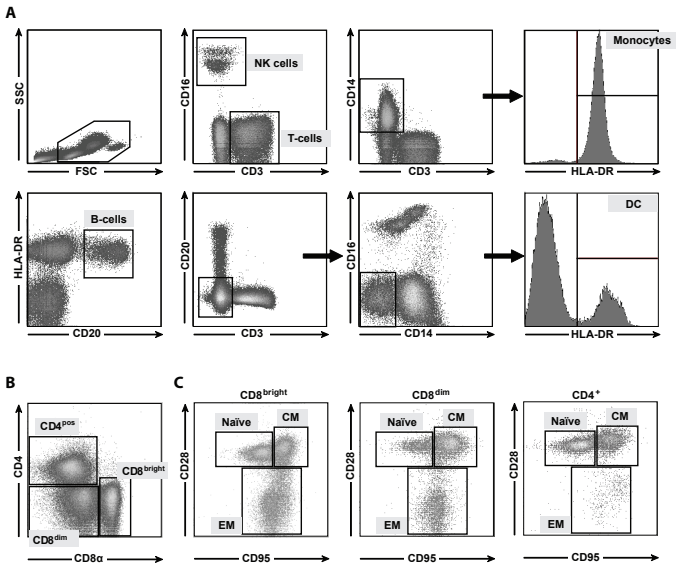

Figure S2. *Gating strategy for flow cytometric differentiation of PBMC subsets from African green monkeys. (A) Viable lymphocytes were selected based on forward scatter (FSC) and sideward scatter (SSC) properties and PBMC subsets were defined as follows: $CD3^{pos}CD16^{neg}$ =T-cells; $CD3^{neg}CD16^{pos}$ =natural killer (NK) cells; $CD3^{neg}CD14^{pos}$MHC-II^{pos} =monocytes; $CD20^{pos}$MHC-II^{pos} =B-cells; $CD3^{neg}CD20^{neg}CD14^{neg}CD16^{ne}$gMHC-$II^{pos}$ =dendritic cells (DC). (B) AGM-specific T-cell subsets were categorized based on the expression of CD8α and CD4: $CD4^{neg}CD8\alpha^{high}$ =$CD8^{bright}$ T-cells, $CD4^{neg}CD8\alpha^{dim}$ =$CD8^{dim}$ T-cells, and $CD4^{pos}CD8\alpha^{neg}$ =$CD4^{pos}$ T-cells. (C) Based on the differential expression of CD28 and CD95, T-cells were categorized as naive ($CD28^{pos}CD95^{neg}$), central memory (CM; $CD28^{pos}CD95^{pos}$) and effector memory (EM; $CD28^{neg}CD95^{pos}$) T-cells.*

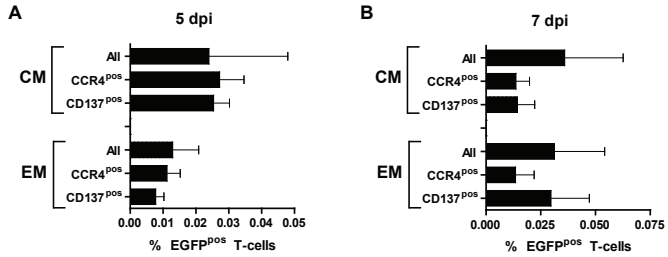

Figure S3. *Peripheral blood CCR4^{pos} and CD137^{pos} T-cells were not preferentially infected in African green monkeys. Flow cytometric detection of EGFP expression in central memory (CM) and effector memory (EM) T-cells at 5 dpi (A) and 7 dpi (B). Gating strategy was according to Figure S2. Data are given as means ± SEM.*

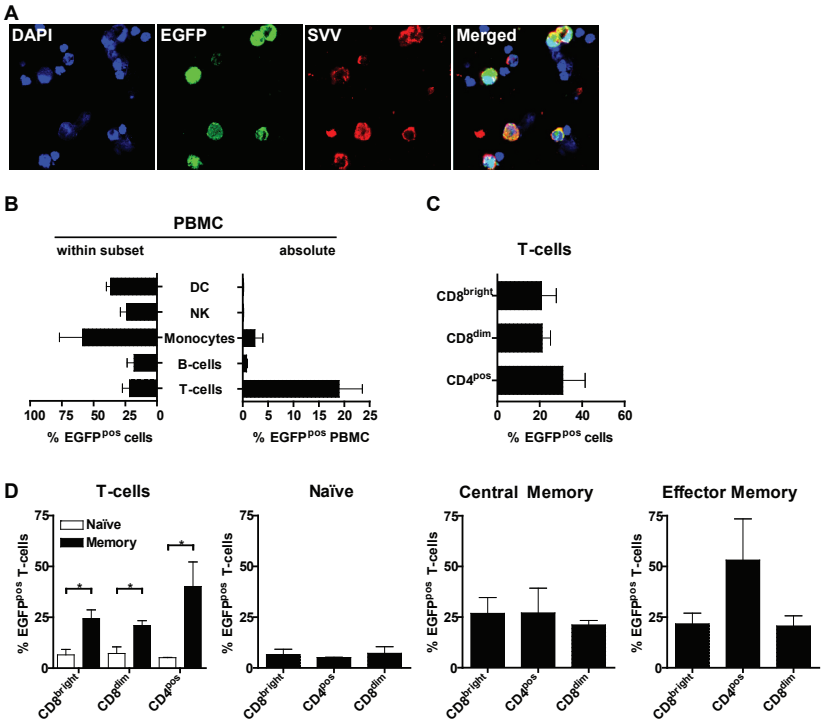

Figure S4. *Memory T-cells were preferentially infected in vitro. (A) SVV-naive African green monkey peripheral blood mononuclear cells (PBMC) were infected with SVV-EGFP in vitro and stained 24 hr later for SVV proteins to show that EGFP fluorescence (green) co-localized with SVV proteins (red). Nuclei were counterstained with DAPI (blue). Magnification: 400X. (B) African green monkey PBMC were infected with SVV-EGFP in vitro and analyzed 24 hr later by flow cytometry for EGFP expression in the indicated lymphocyte subsets. Data are plotted as the frequency of EGFP^{pos} cells within individual PBMC subsets (within subset) or as the percentage of EGFP^{pos} cells within each lymphocyte subset relative to the total number of PBMC (absolute). (C, D) Percentage of EGFP^{pos} cells in the indicated T-cell subsets as assessed by flow cytometry. The lymphocyte subsets were defined as described in Figure S2. Data represent means ± SEM of three independent experiments performed on PBMC from three animals. * p<0.05 by Mann-Whitney test.*

Chapter 4

Immunohistochemical detection of intra-neuronal VZV proteins in snap-frozen human ganglia is confounded by antibodies directed against blood group A1-associated antigens

Werner J.D. Ouwendijk,[1*] Sarah E. Flowerdew,[2,3*] Desiree Wick,[2,3] Anja K.E. Horn,[3,4] Inga Sinicina,[5] Michael Strupp,[2,3] Albert D.M.E. Osterhaus,[1] Georges M.G.M. Verjans,[1] and Katharina Hüfner,[2,3]

[1]Department of Viroscience, Erasmus Medical Center, Rotterdam, the Netherlands; [2]Department of Neurology, Klinikum Grosshadern, [3]Integrated Research and Treatment Center for Vertigo IFBLMU, [4]Institute of Anatomy, Department I and [5]Department of Legal Medicine, Ludwig-Maximilians University, Munich, Germany

*Authors contributed equally to the manuscript

J Neurovirol. 2012 Jun;18(3):172-80

Abstract

Varicella-zoster virus (VZV) causes chickenpox, establishes latency in trigeminal (TG) and dorsal root ganglia (DRG), and can lead to herpes zoster upon reactivation. The VZV proteome expressed during latency remains ill-defined and previous studies have shown discordant data on the spectrum and expression pattern of VZV proteins and transcripts in latently infected human ganglia. Recently, Zerboni and colleagues have provided new insight into this discrepancy [1]. They showed that VZV-specific ascites-derived monoclonal antibody (mAb) preparations contain endogenous antibodies directed against blood group A1 proteins, resulting in false-positive intra-neuronal VZV staining in formalin-fixed human DRG. The aim of the present study was to confirm and extend this phenomenon to snap-frozen TG (n=30) and DRG (n=9) specimens of blood group genotyped donors (n=30). The number of immunohistochemically stained neurons was higher with mAb directed to immediate early protein 62 (IE62) compared to IE63. The IE63 mAb positive neurons always co-stained for IE62, but not vice versa. The mAb staining was confined to distinct large intra-neuronal vacuoles and restricted to $A1^{POS}$ donors. Anti-VZV mAb staining in neurons, but not in VZV-infected cell monolayers, was obliterated after mAb adsorption against blood group A1 erythrocytes. The data presented demonstrate that neuronal VZV protein expression detected by ascites-derived mAb in snap-frozen TG and DRG of blood group $A1^{POS}$ donors can be misinterpreted due to the presence of endogenous antibodies directed against blood group A1-associated antigens present in ascites-derived VZV-specific mAb preparations.

Introduction

Varicella-zoster virus (VZV) is an endemic human alphaherpesvirus that is typically acquired in early childhood and is the causative agent of chickenpox [2]. After primary infection the virus establishes a lifelong latent infection of sensory neurons of the trigeminal ganglia (TG) and dorsal root ganglia (DRG). In about one in five latently infected individuals the virus reactivates later in life to cause herpes zoster (shingles), a number that can be approximately halved by VZV vaccination of adults [3-4]. Individuals with declining VZV-specific cellular immunity, including immunocompromised patients and the elderly, are at risk of developing herpes zoster. Factors such as the host restriction of VZV and the difficulty in obtaining high titers of cell-free virus have hindered advances in elucidating the virus and host factors involved in VZV latency and reactivation in humans.

DNA PCR analysis has long been used to identify virus-specific nucleic acids in human sensory ganglia, with VZV DNA present in about 90% of TG and slightly fewer DRG [5-6]. The frequency of individual VZV-positive neurons has been determined at about 4.1% [7]. The exact composition of the VZV latency-associated transcriptome and proteome is still a matter of debate. The VZV genome encompasses 68 unique open reading frames (ORF), which are coordinately expressed during lytic infection. In contrast to latent herpes simplex virus (HSV) infections, in which predominantly the non-coding latency-associated transcript (LAT) and no viral protein is detectable [8-9], transcripts of the VZV genes 21, 29, 62, 63 and 66 have been consistently detected in latently infected human sensory ganglia using a wide array of molecular biology techniques such as Northern Blot [10], *in situ* hybridization [11], PCR analysis of cDNA libraries [12-13], RT-PCR and qRT-PCR [14], as well as multiplex RT-PCR and the GeXPS System [15]. Transcripts of the VZV genes 4 and 18 have only incidentally been reported [11,16]. Recently, Nagel and colleagues have used multiplex RT-PCR to determine the entire VZV transcriptome in latently VZV infected human TG, reporting on the transcription of additional VZV genes including 11, 41, 43, 57 and 68 [15].

The VZV latency-associated proteome is even more enigmatic, having only been studied using immunohistochemistry (IHC), and with discordant results on the expression of viral proteins compared to their corresponding transcripts [17-21]. Also, a higher frequency of neurons was found positive for VZV protein compared to VZV DNA [7]. Proteins encoded by VZV ORF 4, 21, 29, 62, 63 and 66 have been detected in the cytoplasm of ganglionic neurons with variable results depending on the antibody format (rabbit polyclonal and mouse monoclonal antibodies; mAb), the antibody source (mAb clones) and the tissues examined (DRG and TG being either formalin-fixed or snap-frozen) [18-23]. The expression of the immediate early proteins 62 (IE62) and IE63 has been most widely studied. The frequency of IE62 and IE63 expressing neurons varied extensively between studies ranging from incidental positive neurons to about 1 in 4 neurons positive in human ganglia [18-23].

Recently, Zerboni and colleagues have provided new insight into the described discrepancies [1]. They showed that VZV-specific ascites-derived mAb and rabbit antibody preparations, but not tissue culture-derived VZV mAb, contain endogenous anti-human blood group A1 antibodies. Among other cells, sensory neurons express blood group A1-associated antigens within cytoplasmic vacuoles that are part of the Golgi apparatus [24-25] resulting in false-positive intra-neuronal VZV staining in formalin-fixed latently VZV infected human DRG [1]. This aberrant staining pattern could be attributed to the formalin fixation exposing the respective blood group antigenic epitopes for antibody recognition. The aim of the present study was to confirm and extend this aberrant VZV protein immunohistology finding to snap-frozen TG and DRG specimens of blood group genotyped donors.

Materials and Methods

Human tissue samples and preparation of VZV-infected cells
The current study was performed on 39 human sensory ganglia comprising 30 TG from 25 donors and 9 DRG from 7 donors (Table 1). The average age of the donors was 63.0 ± 4 yrs (± SEM) and the average post-mortem delay was 13.8 ± 1.8 hrs. Fifteen TG and 9 DRG were autopsy samples obtained at the Ludwig-Maximilians University (Munich, Germany) and the use thereof was approved by the Ethics Committee of the Medical Faculty of the Ludwig-Maximilians University in Munich. An additional 15 TG were obtained from The Netherlands Brain Bank (NBB) at the Netherlands Institute for Neuroscience (Amsterdam, Netherlands). All NBB-derived tissues have been collected from donors from whom a written informed consent for brain autopsy and the use of the material and clinical information for research purposes had been obtained. The cause of death of the donors analyzed was mainly due to trauma or neurodegenerative diseases but not related to herpesvirus infections. Ganglia were embedded directly in Tissue Tek compound (Sakura, Zoeterwoude, Netherlands) and stored at -80^{o}C for subsequent in situ analyses.

The human skin melanoma cell line MeWo was grown to confluent monolayers on coverslips and infected with the VZV strain pOka. At 16 hrs post-infection the cells were fixed with acetone and used for immunocytology.

***In situ* analyses**
Immunohistochemical (IHC) stainings were performed using predefined optimal dilutions of the following primary antibodies: mouse anti-VZV IE62 (clone MAB8616; Millipore, Schwalbach, Germany) at a dilution of 1:50 – 1:100, mouse anti-VZV IE63 (clone 9D12; a generous gift of Sebastien Bontems and Catherine Sadzot-Delvaux, Liège, Belgium) [26] at a dilution of 1:500 and mouse anti-VZV gE (clone MAB8612; Millipore) at a dilution of 1:200 using previously described protocols [23, 27]. Additionally hybridoma supernatant-derived IgG1 and IgG2a isotype control mAbs (R&D Systems, Abingdon, United Kingdom) were used. In brief, frozen tissue sections were cut, dried, fixed, endogenous peroxidase-blocked for 10 minutes using 1.5 - 3%

Table 1. Donor Blood Type and VZV Protein Immunohistochemistry Results on Human Sensory Ganglia Assayed

Nr	Ganglion Type[a]	Age (years); Sex[b]	Diagnosis at death	Anti-VZV mAb		ABO genotype	ABO phenotype
				IE62	IE63		
1	TG	93; F	Non-demented/Lewy bodies	+	+	A101 - B101	A1B
2	TG	87; F	Parkinson	+	+	A101 - A101	A1
3	TG	52; M	Pick's disease	-	-	A201 - O01	A2
4	TG	73; F	Alzheimer. Lewy bodies	+	-	A101 - A101	A1
5	TG	84; F	Alzheimer	+	+	A101 - O01	A1
6	TG	51; M	Pick's disease	-	-	A101 - A201	A1A2
7	TG	70; M	Pick's disease	-	-	A201 - A201	A2
8	TG	67; M	Parkinson	+	-	A101 - A201	A1A2
9	TG	81; F	Alzheimer	+	+	A101 - B101	A1B
10	TG	70; M	Alzheimer	-	-	O01 - O01	O
11	TG	68; F	Pick's disease	-	-	O01 - O01	O
12	TG	41; F	Pick's disease	-	-	A101 - A201	A1A2
13	TG	77; M	Parkinson	-	-	A101 - O03	A1
14	TG	93; F	non-demented control	-	-	O01 - O01	O
15	TG	77; F	Alzheimer	-	-	O01 - O01	O
16	TG	36; M	Pulmonary embolism	-	-	A101 – O01	A1
17	TG (L+R)	81; F	Cardiac cause	+	+	A101 – B101	A1B
18	TG	44; M	Aspiration	+	+	A101 – O01	A1
	DRG			+	+		
19	TG (L+R)	63; F	Trauma	-	-	O01 – O01	O
	DRG			-	-		
20	TG	43; M	Trauma	-	-	B101 – O01	B
21	TG (L+R)	44; M	Cardiac cause	+	+/-	A101 – O01	A1
22	TG (L+R)	81; n.a.	Bleeding from shunt	+	+	A101 – O01	A1
23	TG	48; F	Cardiac cause	-	-	O01 – O01	O
24	TG	80; F	Trauma	+	+	A101 – O01	A1
25	TG (L+R)	78; M	Cardiac cause	-	-	B101 – O01	B
26	DRG	60; F	Cardiac cause	-	-	O01 – O01	O
27	DRG	61; M	Trauma	-	-	O02 – O02	O
28	DRG (n=2)	17; M	Trauma	+	-	A101 – O01	A1
29	DRG	26; M	Trauma	+	-	A101 – O01	A1
30	DRG (n=2)	43; F	Trauma	-	-	O01 – O01	O

[a] TG (L), left trigeminal ganglion, TG (R), right trigeminal ganglion and DRG, dorsal root ganglion.
[b] F, female; M, male, and n.a., info not available.

H_2O_2 in methanol and incubated with 5-10% normal rabbit or goat serum followed by incubation with the primary antibody. Primary antibody reactivity was visualized using the avidin-biotin system (DakoCytomation, Heverlee, Belgium) in combination with the substrates 3-amino-9-ethylcarbazole (AEC) or 3,3'-diaminobenzidine (DAB) (both from Sigma-Aldrich, Deisenhofen, Germany). Finally, the tissue sections were counterstained with hematoxylin (Sigma-Aldrich). Acetone-fixed, VZV-infected MeWo cells were also stained using this protocol, without counterstaining. In case of immunofluorescence (IF) staining, sections were incubated with secondary goat anti-mouse Ig Alexa Fluor 594 (1:500; Invitrogen, Breda, Netherlands) and mounted in Prolong Gold Antifade Reagent with DAPI (Invitrogen).

All stainings were performed in duplicate or triplicate. For quantification, between 100 and 700 neurons per stained tissue section were assessed by two independent researchers. IHC stained tissue sections were assessed and imaged on an Olympus BX41 microscope (Olympus Europa Holding, Hamburg, Germany) with an Olympus C-4040 Zoom camera. Images were made at 400x magnification with an air objective. The IF stainings were analyzed on a Zeiss LSM 700 confocal laser scanning microscope (Zeiss, Sliedrecht, Netherlands). Z-stacks were generated by scanning 21 slices of 0.35 µm thick at 1,112X1,112 pixels, with a Plan-Apochromat 40X/1.3 Oil DIC M27 objective, 2.5X digital zoom, 8X frame averaging and the pinhole adjusted to 1 airy unit. ZEN 2010 software (Zeiss) was used to adjust brightness and contrast and to generate the 3D reconstruction.

The anti-VZV IE62 (MAB8616) and anti-VZV gE (MAB8612) mAbs were adsorbed against human blood group A1 erythrocytes as described [1, 28-29]. In brief, peripheral blood was extracted in EDTA, centrifuged to pellet the erythrocytes, which were then washed several times with physiological saline. Approximately 500µl packed erythrocytes were incubated with PBS-diluted antibody. After 1 hour at 37°C the erythrocytes were centrifuged and the respective supernatant was used for IHC as described [1, 28-29].

ABO genotyping

The ABO blood group genotype of TG and DRG donors studied was defined by determining the allelic variations in exons 6 and 7 of the donors' ABO gene [30]. DNA was extracted from tissue using the Qiagen DNA extraction kit (Qiagen, Valencia, CA, USA). Exons 6 and 7 from the ABO gene were amplified using the high-fidelity DNA polymerase pfuUltra (Stratagene, Amsterdam, The Netherlands) and primers Ex6-F, Ex6-R, Ex7-F1 and Ex7-R1 described in Table 2. Amplification conditions included denaturation for 2 min 95°C followed by 40 cycles 30 sec 95°C, 30 sec 57°C, 1 min 72°C and a final elongation of 3 min 72°C. The resulting amplicons were purified from agarose gel using the gel extraction kit from Qiagen and sequenced on the ABIprism 3130XL genetic analyzer with the BigDye Terminator v.1 cycle sequence kit using the above mentioned primers and the additional internal primers Ex7-F2 and Ex7-R2 (Table 2) for exon 7. The ABO genotype and resultant phenotype of the donor was defined on ABO allele-specific nucleotide alterations within exon 6 (nucleotide positions 261 and 297) and exon 7 (nucleotide positions 467, 526, 646, 657,

Table 2. Primers Used for PCR and Sequencing of ABO Gene Exons 6 and 7.

Primer	Sequence	Location[a]	Amplicon size (bp)	Reference
PCR + Sequencing				
Ex6-F	5′-AGCTCAGCTTGCTGTGTGTT-3′	Exon 6	528	31
Ex6-R	5′-AGATGCTGCATGAATGACC-3′	Exon 6		31
Ex7-F1	5′-GCCTGCCTTGCAGATACGTG-3′	Exon 7	1061[b]	31
Ex7-R1	5'-TATCTGCGATTGCGTGTCTG-3'	3'-UTR Exon 7[c]		
Sequencing				
Ex7-F2	5'-AGGTGGATTACCTGGTGTGC-3'	Exon 7	Not applicable	
Ex7-R2	5'-GTAGAAATCGCCCTCGTCCT-3'	Exon 7	Not applicable	

[a] Location within the ABO gene
[b] The PCR product size is 1060 bp for A*201 alleles, which have a deletion at position 1060 in exon 7
[c] 3'-untranslated region (UTR) of exon 7

681, 703, 796, 802, 803, 829, 930 and 1059) of the ABO gene [30-31].

Statistical Analyses
Data handling, analysis, and graphical representations were performed by using GraphPad Prism 4 software (GraphPad, San Diego, CA). All results are given as mean ± SEM. Statistical differences were determined by the paired t and chi-square test. P values <0.05 were considered significant.

Results

Intra-neuronal expression of VZV IE62 and IE63 in snap-frozen human TG and DRG
Thirty TG and 9 DRG were stained with mAb against the described latency-associated VZV proteins IE62 (clone MAB8616) and IE63 (clone 9D12) (Figure 1A and B). For both TG and DRG, more ganglia and neurons stained positive with the IE62 mAb compared to IE63. Fourteen of 30 (47%) TG and 4 of 9 (44%) DRG were IE62 mAb positive, whereas only 11 of 30 (37%) TG and 1 of 9 (11%) DRG stained positive with the IE63 mAb (Table 1). In TG, the frequency of IE62 mAb reactive neurons was significantly higher compared to IE63 (17.6% ± 2.6 vs 3.8% ± 1.3; p=0.0006). An equivalent frequency pattern was observed in the DRG (Figure 1C). Whereas 6 of 39 (15%) ganglia were only IE62 mAb positive, none of the ganglia stained solely with the IE63 mAb (Table 1). When analyzing serial sections we observed that IE63 mAb reactive neurons always co-stained with the IE62 mAb, but not vice versa (Figure1A , B and D). None of the ganglia stained positive with the appropriate isotype control mAb, which were derived from hybridoma supernatant of in vitro cultured hybdridoma cells (data not shown).

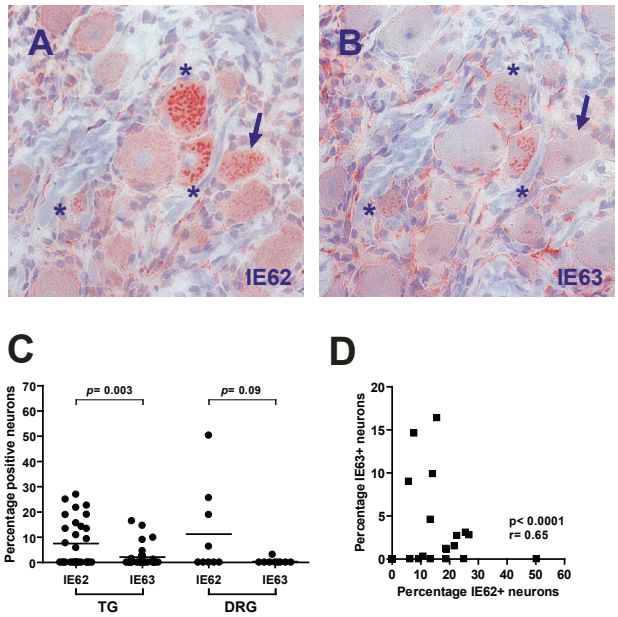

Figure 1. *Immunohistochemistry with anti-VZV IE62 and IE63 mAb on snap-frozen human TG and DRG. (A and B) Consecutive human TG sections were stained with anti-IE62 mAb (A) and IE63 mAb (B). Sections were developed and counterstained with AEC and hematoxylin resulting in a red colour and blue nuclei, respectively. Neurons reactive with both IE62 and IE63 mAbs, and those that are single IE62 mAb positive, are indicated by an asterisk and arrow, respectively. Magnification X400. (C) Percentage IE62 and IE63 mAb positive neurons in TG and DRG. (D) Intra-donor correlation between IE62 and IE63 mAb positive neurons.*

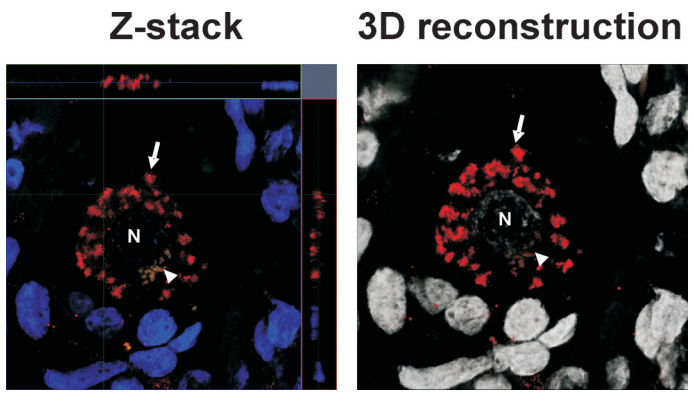

Figure 2. *Intracellular localization of the VZV IE62 mAb signal in human TG neurons. Human TG sections were stained for VZV IE62 (Alexa Fluor 594, red color) and nuclei were visualized using DAPI (blue and gray color in left and right panels, respectively). The specimen was analyzed in a Zeiss LSM 700 confocal microscope and a Z-stack (21 slices, 0.35 µm thick) of images at 400x magnification and 2.5x digital zoom was taken showing one VZV IE62 mAb positive TG neuron. Left panel shows slice 12 from the Z-stack with the smaller side panels showing the view from X and Y. Note that in the X and Y view the IE62 mAb-positive vesicles appear to be interconnected. Right panel shows a 3D reconstruction of the Z-stack, demonstrating that the IE62 mAb signal is located in vesicular-like structures that seem to be interconnected and are spread throughout the neuronal cytoplasm, consistent with the Golgi compartment. Long arrows indicate VZV IE62 mAb staining and arrow heads indicate lipofuscin. N, nucleus.*

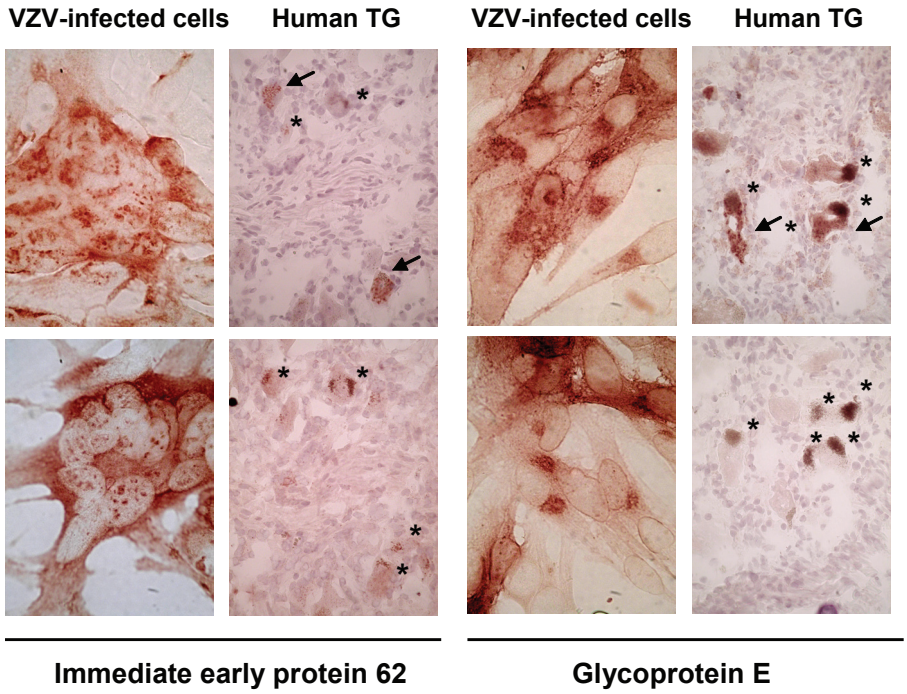

Figure 3. *Abrogation of neuronal VZV mAb reactivity in snap-frozen TG and DRG upon adsorption by blood group A1 erythrocytes. Mouse monoclonal ascites-derived VZV IE62- and glycoprotein E-specific mAbs were adsorbed against blood group A1 erythrocytes or left untreated. Both non-adsorbed (top row panels) and adsorbed (bottom row panels) anti-VZV mAbs equally reacted with their respective antigens in VZV-infected MeWo cells. In contrast, intra-neuronal immunoreactivity of both mAbs in snap-frozen human TG was completely abrogated by adsorption with blood group A1 erythrocytes.*

We determined the spatial distribution of the IE62 and IE63 mAb signal within individual neurons by laser scanning microscopy. This revealed that the observed signal was localized in vesicular-like structures throughout the cytoplasm (Figure 2; arrow). These structures were clearly discernible from the intracellular deposits of neuromelanin and lipofuscin that had a more punctuated dense structure and autofluorescent properties (Figure 2; arrowhead). When Z-stacks were examined in both the X- and Y-axis orientation, the VZV mAb reactive vesicles were partially interconnected within the cytoplasm of VZV latently infected human TG neurons (Figure 2; arrowhead).

Donor´s blood group A1 status correlates with IE62 and IE63 mAb reactivity

The exclusive cytoplasmic IE62 and IE63 mAb staining pattern in VZV latently infected neurons contrasts with the predominant nuclear localization of both proteins during lytic infection [19]. The high frequency of VZV-specific mAb reactive neurons is also discordant with the expected frequency of only 1 to 6.9% VZV DNA containing neurons in VZV latently infected neurons [7].

Recently, Zerboni and colleagues have shown that the IHC signal is most likely the result of a mouse ascites Golgi (MAG) reaction to human blood group A1-associated antigens [1]. The formalin fixation in that study may, however, have selectively released the MAG-specific epitopes. To ascertain the causal role of the donor's blood type to staining frequency and pattern, the blood group of the 30 donors under investigation was determined by sequencing exons 6 and 7 of the ABO blood group gene [31]. Seventeen donors had an A1 phenotype, consisting of donors with the following phenotypes A1;A2 (n=3), A1;B (n=3) and A1 (n= 11) (Table 1). Whereas none of the $A1^{NEG}$ donors had IE62 and IE63 mAb positive neurons, a significant correlation between the donor's A1 phenotype and IE62 ($p< 0.0001$) and IE63 ($p= 0.003$) mAb staining was detected. The frequency of VZV mAb positive neurons was not different between $A1^{POS}$ donors with different A1 genotypes. Among the 22 ganglia from $A1^{POS}$ donors, 12 of 22 (55%) stained positive with both mAbs and 6 of 22 (27%) were solely IE62 mAb positive. Notably, 4 of 22 (18%) ganglia from $A1^{POS}$ donors did not stain with either anti-VZV mAb (Table 1).

To consolidate that the observed anti-VZV mAb IHC signal was due to endogenous contaminating antibodies directed against blood group A1-associated antigens, anti-IE62 and glycoprotein E ascites-derived mAb preparations were adsorbed against blood group A1 erythrocytes. Whereas both the original and adsorbed mAbs stained VZV-infected cells without discernable differences (Figure 3), intra-neuronal mAb reactivity was completely eliminated upon adsorption by A1 erythrocytes (Figure 3).

Discussion

Elucidation of the virus and host factors involved during VZV latency in sensory ganglia is vital to optimize existing treatments and to develop new therapeutic intervention strategies to prevent recrudescent VZV infections. The application of VZV ORF multiplex RT-PCR, and more recently GeXPS technology covering the whole VZV transcriptome, has provided a comprehensive overview of the VZV transcripts expressed during latency [32]. Contrastingly, due to the limited availability of anti-VZV antibodies for in situ analysis, our knowledge of the VZV latency-associated proteome is far from complete.

The expression of the VZV proteins IE62 and IE63 has been studied extensively in latently infected human sensory ganglia since they are considered as the prototypic latency-associated VZV proteins [18-23]. Several groups have reported on the intra-neuronal expression of both proteins in human DRG and TG, but with discordant results on the number of ganglia positive and the frequency of protein expressing neurons per ganglion. IE62 has been detected in 6-10% neurons of all DRG tested using mouse ascites mAb and polyclonal rabbit antibodies [19], with 5-10% of neurons positive in all tested TG using a polyclonal antibody [18], and with 2.5-8% of neurons positive in 8 of 21 TG analyzed using the same mouse IE62 antibody used in the present study [23]. For IE63 the varying detection frequencies between labo-

ratories are also significant and can be related to the antibodies used: very rare neurons in 5 of 21 ganglia [20] and 5 of 20 TG [11] were found to be IE63 positive using the same polyclonal rabbit antibody, while using a different rabbit anti-IE63 antibody also gave few positive neurons in only 1 of 27 tested ganglia [21]. Other studies, however, show a more abundant apparent VZV protein expression, with 3-9% of neurons from all DRG positive using a polyclonal rabbit antibody [19], and using a mouse monoclonal antibody from ascites in TG from 10 subjects with 5 to 10% of neurons positive [18, 26]. Herein, we used the same IE62 and IE63 mAb to detect the respective VZV proteins in snap-frozen human TG and DRG and found a high number of positive ganglia with relatively high frequencies of mAb reactive neurons. Notably, IE63 mAb reactivity correlated with IE62, suggesting an interaction between both stainings (Table 1 and Figure 1).

One important cause for the aforementioned discordant IE62 and IE63 IHC results was recently highlighted in a study by Zerboni and colleagues [1]. They demonstrated that VZV-specific ascites-derived mouse mAb and rabbit polyclonal antibodies contain endogenous contaminating antibodies reacting with blood group A1-associated antigens in formalin-fixed and paraffin-embedded human DRG. The present study on human snap-frozen DRG and TG supports this concept. First, the intra-neuronal IE62 and IE63 mAb reactivity correlated significantly with the TG/DRG donor's blood group A1 genotype status and second the IHC staining was abolished by adsorption of VZV mAb against blood group A1 erythrocytes (Table 1 and Figure 3). There was no correlation between the frequency of neuronal staining and post-mortem delay, suggesting that neither this variable nor the fixation method is important for the availability of blood group A1-associated antigens.

Staining of particular tissues and cells from blood group $A1^{POS}$ donors with mouse ascites-derived mAb is due to the so-called MAG reaction. The MAG epitopes are considered blood group A1 oligosaccharides [33], which are also expressed by sensory neurons within Golgi-associated vacuoles that closely resemble the VZV mAb positive vesicular structures shown in Figure 2 [24-25]. The expression of the MAG epitopes varies between ganglia (e.g. cervical vs thoracic) and is limited to certain sub-classes of neurons [25]. In the present study, we found differences in IE62 and IE63 mAb reactivity between ganglia from the same individual, as well as differences in the percentage of neurons positively stained with each mAb over the studied population. The limited expression of the MAG epitopes in only certain ganglion and neuron types, could explain such varying anti-VZV antibody staining frequencies described previously and those reported here. Alternatively, different antibody preparations may contain variable concentrations of MAG-reactive antibodies. However, despite using multiple lots of VZV IE62-specific antibodies we did not observe differences in antibody reactivity within donors using different antibody batches (data not shown).

In conclusion, the data presented here consolidate the previous report by Zerboni and colleagues [1] and extend the MAG reaction of ascites-derived anti-VZV mAbs to snap-frozen human sensory ganglion tissues. As a synthesis of both studies it

emerges that ascites-derived mAb preparations should be screened for reactivity against blood group A1-associated antigens to avoid misinterpretation of intra-cellular detection of virus and host proteins in both formalin-fixed and snap-frozen human ganglia. The described blood group A1 erythrocyte adsorption procedure allows depletion of the MAG reactive contaminating antibodies from ascites-derived mAb preparations to circumvent aberrant IHC staining patterns in the future. The MAG reaction is not restricted to sensory ganglia, nor anti-viral antibodies, as highlighted by several other publications on this phenomenon [33-34]. The extent of VZV translation during latency remains an important issue, that will require careful re-evaluation using both current IHC methods and new tools.

Acknowledgements

The authors thank Sebastien Bontems and Catherine Sadzot-Delvaux (Liège, Belgium) for the generous gift of the VZV IE63 mAb, Susanne Bailer (Munich, Germany) for providing the VZV-infected MeWo cells and Freek van Loenen (Rotterdam, the Netherlands) for technical assistance with the ABO blood group genotyping. This study was supported by a grant from the BMBF (German Ministry for Education and Research) IFB-01EO0901 to K.H.

References

1. Zerboni L, Sobel RA, Lai M, et al. Apparent expression of varicella-zoster virus proteins in latency resulting from reactivity of murine and rabbit antibodies with human blood group a determinants in sensory neurons. J Virol 2012;86:578-583.
2. Arvin AM. Varicella-zoster virus. Clin Microbiol Rev 1996;9:361-381.
3. Mick G. Vaccination: a new option to reduce the burden of herpes zoster. Expert Rev Vaccines 2010;9:31-35.
4. Oxman MN, Levin MJ, Johnson GR, et al. A vaccine to prevent herpes zoster and postherpetic neuralgia in older adults. N Engl J Med 2005;352:2271-2284.
5. Inoue H, Motani-Saitoh H, Sakurada K, et al. Detection of varicella-zoster virus DNA in 414 human trigeminal ganglia from cadavers by the polymerase chain reaction: a comparison of the detection rate of varicella-zoster virus and herpes simplex virus type 1. J Med Virol 2010;82:345-349.
6. Mahalingam R, Wellish MC, Dueland AN, Cohrs RJ and Gilden DH. Localization of herpes simplex virus and varicella zoster virus DNA in human ganglia. Ann Neurol 1992;31:444-448.
7. Wang K, Lau TY, Morales M, Mont EK and Straus SE. Laser-capture microdissection: refining estimates of the quantity and distribution of latent herpes simplex virus 1 and varicella-zoster virus DNA in human trigeminal Ganglia at the single-cell level. J Virol 2005;79:14079-14087.
8. Croen KD, Ostrove JM, Dragovic LJ, Smialek JE and Straus SE. Latent herpes simplex virus in human trigeminal ganglia. Detection of an immediate early gene “anti-sense” transcript by in situ hybridization. N Engl J Med 1987;317:1427-1432.
9. Stevens JG, Wagner EK, vi-Rao GB, Cook ML and Feldman LT. RNA complementary to a herpesvirus alpha gene mRNA is prominent in latently infected neurons. Science 1987;235:1056-1059.
10. Meier JL, Holman RP, Croen KD, Smialek JE and Straus SE. Varicella-zoster virus transcription in human trigeminal ganglia. Virology 1993;193:193-200.
11. Kennedy PG, Grinfeld E and Bell JE. Varicella-zoster virus gene expression in latently infected and explanted human ganglia. J Virol 2000;74:11893-11898.
12. Cohrs RJ, Srock K, Barbour MB, et al. Varicella-zoster virus (VZV) transcription during latency in human ganglia: construction of a cDNA library from latently infected human trigeminal ganglia and detection of a VZV transcript. J Virol 1994;68:7900-7908.
13. Cohrs RJ, Barbour M and Gilden DH. Varicella-zoster virus (VZV) transcription during latency in human ganglia: detection of transcripts mapping to genes 21, 29, 62, and 63 in a cDNA library enriched for VZV RNA. J Virol 1996;70:2789-2796.
14. Cohrs RJ and Gilden DH. Prevalence and abundance of latently transcribed varicella-zoster virus genes in human ganglia. J Virol 2007;81:2950-2956.
15. Nagel MA, Choe A, Traktinskiy I, et al. Cordery-Cotter R, Gilden D and Cohrs RJ. Varicella-zoster virus transcriptome in latently infected human ganglia. J Virol 2011;85:2276-2287.
16. Kennedy PG, Grinfeld E and Gow JW. Latent Varicella-zoster virus in human dorsal root ganglia. Virology 1999;258:451-454.
17. Cohrs RJ and Gilden DH. Varicella zoster virus transcription in latently-infected human ganglia. Anticancer Res 2003;23:2063-2069.
18. Grinfeld E and Kennedy PG. Translation of varicella-zoster virus genes during human ganglionic latency. Virus Genes 2004;29:317-319.
19. Lungu O, Panagiotidis CA, Annunziato PW, Gershon AA and Silverstein SJ. Aberrant intracellular localization of Varicella-Zoster virus regulatory proteins during latency. Proc Natl Acad Sci U S A 1998;95:7080-7085.
20. Mahalingam R, Wellish M, Cohrs R, et al. Expression of protein encoded by varicella-zoster virus open reading frame 63 in latently infected human ganglionic neurons. Proc Natl Acad Sci U S A 1996;93:2122-2124.
21. Zerboni L, Sobel RA, Ramachandran V, et al. Expression of varicella-zoster virus immediate-early regulatory protein IE63 in neurons of latently infected human sensory ganglia. J Virol 2010;84:3421-3430.
22. Cohrs RJ, Gilden DH, Kinchington PR, Grinfeld E and Kennedy PG. Varicella-zoster virus gene 66 transcription and translation in latently infected human Ganglia. J Virol 2003;77:6660-6665.
23. Theil D, Derfuss T, Paripovic I, et al.Latent herpesvirus infection in human trigeminal ganglia causes

chronic immune response. Am J Pathol 2003;163:2179-2184.
24. Dodd J and Jessell TM. Lactoseries carbohydrates specify subsets of dorsal root ganglion neurons projecting to the superficial dorsal horn of rat spinal cord. J Neurosci 1985;5:3278-3294.
25. Mollicone R, Davies DR, Evans B, Dalix AM and Oriol R. Cellular expression and genetic control of ABH antigens in primary sensory neurons of marmoset, baboon and man. J Neuroimmunol 1986;10:255-269.
26. Kennedy PG, Grinfeld E, Bontems S and Sadzot-Delvaux C. Varicella-Zoster virus gene expression in latently infected rat dorsal root ganglia. Virology 2001;289:218-223.
27. Verjans GM, Hintzen RQ, van Dun JM, et al. Selective retention of herpes simplex virus-specific T cells in latently infected human trigeminal ganglia. Proc Natl Acad Sci U S A 2007;104:3496-3501.
28. Gorzynski EA, Brodhage H and Neter E. Hemagglutination by mixtures of enterobacterial antigen and Shigella sonnei antiserum. Z Hyg Infektionskr 1964;150:1-9.
29. Wolf MF, Koerner U and Schumacher K. Specificity of reagents directed to the Thomsen-Friedenreich antigen and their capacity to bind to the surface of human carcinoma cell lines. Cancer Res 1986;46:1779-1782.
30. Gassner C, Schmarda A, Nussbaumer W and Schonitzer D. ABO glycosyltransferase genotyping by polymerase chain reaction using sequence-specific primers. Blood 1996;88:1852-1856.
31. Watanabe K, Ikegaya H, Hirayama K, et al. A novel method for ABO genotyping using a DNA chip. J Forensic Sci 2011;56 Suppl 1:S183-S187.
32. Kennedy PG and Cohrs RJ. Varicella-zoster virus human ganglionic latency: a current summary. J Neurovirol 2010;16:411-418.
33. Kliman HJ, Feinberg RF, Schwartz LB, Feinman MA, Lavi E and Meaddough EL. A mucin-like glycoprotein identified by MAG (mouse ascites Golgi) antibodies. Menstrual cycle-dependent localization in human endometrium. Am J Pathol 1995;146:166-181.
34. Finstad CL, Yin BW, Gordon CM, Federici MG, Welt S and Lloyd KO. Some monoclonal antibody reagents (C219 and JSB-1) to P-glycoprotein contain antibodies to blood group A carbohydrate determinants: a problem of quality control for immunohistochemical analysis. J Histochem Cytochem 1991;39:1603-1610.

Chapter 5

Restricted Varicella-Zoster Virus Transcription in Human Trigeminal Ganglia Obtained Soon after Death

Werner J.D. Ouwendijk,[1] Alexander Choe,[2] Maria A. Nagel,[2] Don Gilden,[2,3] Albert D.M.E. Osterhaus,[1] Randall J. Cohrs,[2] and Georges M.G.M. Verjans[1]

[1]Department of Viroscience, Erasmus Medical Center, Rotterdam, the Netherlands; Departments of [2]Neurology and [3]Microbiology, University of Colorado Denver Medical School, Aurora, CO, USA

J Virol. 2012 Sep;86(18):10203-6

Abstract

We analyzed the varicella-zoster virus (VZV) transcriptome in 43 latently infected human trigeminal ganglia (TG) with post-mortem intervals (PMIs) ranging from 3.7 to 24 h. Multiplex RT-PCR revealed no VZV transcripts with a PMI <9 h. Real-time PCR indicated a significant increase ($p = 0.02$) in VZV ORF63 transcript levels, but not the virus DNA burden with longer PMI. Overall, both the breadth of the VZV transcriptome and the VZV ORF63 transcript levels in human cadaver TG increased with longer PMI

Primary varicella-zoster virus (VZV) infection causes varicella, after which the virus becomes latent in ganglia along the entire neuraxis; reactivation decades later results in herpes zoster [1]. Studies of VZV latency have been restricted to analysis of human ganglia obtained at autopsy and have reported discrepant numbers and abundance of VZV transcripts [2-9]. The discrepancies may be due to methodological differences and/or the undefined [7-9], inexact (<24 h) [2,4-5,10] and long post-mortem intervals (PMI) (average 17–25 h) [3,11] in obtaining cadaver ganglia. Herein, we searched for VZV transcripts in human trigeminal ganglia (TG) acquired not only at the usual intervals (PMI of 9-24 h), but also at earlier time points after death (PMI of 3-9 h).

Multiplex RT-PCR reveals no VZV transcripts in human TG with a PMI <9 h.
Our recent use of multiplex RT-PCR to examine human TG with an average PMI of 17 h revealed a wide variability among the VZV genes transcribed in human TG [11-12]. Here, we extended the TG cohort with 17 additional samples obtained early after death (mean PMI: 7.75 h; range: 3.7 - 23.25 h) (Table 1), resulting in a total of 43 TG from 25 donors with PMIs ranging from 3.7 to 24 h (Table 2). Poly(A) mRNA was extracted from ganglia, and 100 ng mRNA was reverse-transcribed and amplified in each of five multiplex PCR reactions covering all 68 VZV open reading frames (ORFs) [11]. No VZV transcripts were detected with a PMI <9 h, while the cellular control transcripts GAPdH, neurofilament (NF) and β-actin were detected in all samples by reverse transcriptase-linked real-time PCR (RT-qPCR) (Table 2 and data not shown). In TG with a PMI of 9 h or more, transcripts mapping to VZV immediate-early ORFs 63 (65%), 4 (42%) and 62 (39%), early ORF 29 (32%), or late ORFs 11 (23%), 68 (19%), 40 (13%), 43 (6%), 41 (3%) and 57 (3%) were detected (Table 2). The number of VZV genes transcribed correlated significantly with longer PMI (Fig. 1A) ($r = 0.59$, $p < 0.0001$; Pearson's correlation test).

Table 1. Clinical Features of Human Trigeminal Ganglia Donors

Subject	Age; Sex[a]	Cause of death	PMI[b]
A	87; M	Cachexia and dehydration	03:40
B	91; F	Dementia	03:45
C	83; F	Dehydration	04:55
D	90; F	Cachexia and dehydration	05:35
E	62; M	Brain tumor	07:43
F	74; M	Suicide	07:45
G	44; M	Cachexia and sedation	10:15
H	51; M	Unknown	11:00
I	44: M	Pneumonia	12:00
J	59; M	Cardiac arrest	12:30
K	90; F	Unknown	23:16

[a] M, male; F, female
[b] PMI, post-mortem interval (hours:minutes).

Table 2. Detection of VZV Transcripts in Human Trigeminal Ganglia[a]

			Multiplex RT-PCR										RT-qPCR Result
			IE[b]			E[b]	L[b]						
PMI[c]	Subject[d]	Location[e]	63[f]	4	62	29	11	68	40	43	41	57	ORF63
03:40	A	R	–	–	–	–	–	–	–	–	–	–	+
		L	–	–	–	–	–	–	–	–	–	–	+
03:45	B	R	–	–	–	–	–	–	–	–	–	–	–
		L	–	–	–	–	–	–	–	–	–	–	–
04:55	C	R	–	–	–	–	–	–	–	–	–	–	+
		L	–	–	–	–	–	–	–	–	–	–	+
05:35	D	R	–	–	–	–	–	–	–	–	–	–	–
		L	–	–	–	–	–	–	–	–	–	–	+
07:43	E	R	–	–	–	–	–	–	–	–	–	–	+
		L	–	–	–	–	–	–	–	–	–	–	+
07:45	F	R	–	–	–	–	–	–	–	–	–	–	–
		L	–	–	–	–	–	–	–	–	–	–	–
9:00	12	R	–	+	–	–	–	+	+	–	–	–	+
		L	–	–	–	–	–	+	–	–	+	–	+
10:15	G	L	–	+	+	–	–	–	–	–	–	–	+
11:00	9	R	–	–	–	–	–	–	–	–	–	–	+
11:00	H	L	–	+	+	–	–	–	–	–	–	–	+
12:00	6	R	+	–	+	+	–	+	–	+	–	–	+
		L	+	–	–	–	–	+	–	+	–	–	+
12:00	I	L	–	+	+	–	–	–	–	–	–	–	+
12:30	J	L	+	+	+	–	–	–	–	–	–	–	+
14:00	3	R	–	–	–	–	–	–	–	–	–	–	+
		L	–	–	–	–	–	–	–	–	–	–	+
14:00	13	R	+	–	+	–	+	–	–	–	–	–	–
		L	+	–	+	–	+	–	–	–	–	–	–
15:00	1	R	–	–	–	–	–	–	–	–	–	+	+
		L	–	–	–	–	–	–	–	–	–	–	+
17:00	14	R	+	–	+	–	+	–	–	–	–	–	+
		L	+	+	+	–	–	–	–	–	–	–	+
18:00	4	R	+	–	–	–	–	–	–	–	–	–	–
		L	+	–	–	+	–	–	+	–	–	–	+
18:00	7	R	+	+	–	+	–	–	+	–	–	–	+
		L	+	+	–	+	–	–	+	–	–	–	+
18:00	8	R	+	+	+	–	+	–	–	–	–	–	–
		L	+	+	+	+	+	–	–	–	–	–	–
22:00	2	R	–	–	–	–	–	–	–	–	–	–	–
23:00	10	R	+	–	–	+	+	+	–	–	–	–	+
		L	+	+	–	+	–	–	–	–	–	–	+
23:00	11	R	+	–	–	+	–	+	–	–	–	–	+
		L	+	+	–	+	–	–	–	–	–	–	–
23:16	K	L	+	+	+	–	–	–	–	–	–	–	+
24:00	5	R	+	–	–	+	+	–	–	–	–	–	+
		L	+	–	–	–	–	–	–	–	–	–	+

[a] Viral transcripts were determined by VZV transcriptome-wide multiplex RT-PCR and VZV ORF63-specific real-time quantitative PCR (RT-qPCR; last column) on cDNA generated from human TG-derived RNA. +, transcript detected; –, transcript not detected.
[b] Putative kinetic class of the VZV open reading frame with respect to HSV-1 [2, 18]. IE, immediate early.
[c] PMI, post-mortem interval (hours:minutes).
[d] See reference 16 for VZV multiplex RT-PCR data on subjects 1-14.
[e] Left (L) or right (R) trigeminal ganglion.
[f] VZV open reading frame.

VZV ORF63 transcript levels in human TG increased with longer PMI. VZV ORF63 is the most frequent and abundant VZV gene transcribed in latently infected human TG [2-3, 7-9, 11]. To determine whether VZV transcript abundance was affected by the PMI, cDNA was synthesized from 100 ng poly(A) RNA extracted from all 43 TG and subjected to RT-qPCR analysis using primers and probes specific for VZV ORF63 along with cellular GAPdH and NF [3,11]. GAPdH and NF were amplified in all ganglia, but not when reverse transcriptase was omitted from the cDNA synthesis reaction (data not shown). Consistent with earlier findings [2-3, 7-9, 11], ORF63 was the most prevalent VZV transcript detected in latently infected human TG. VZV ORF63 transcripts were detected in 31 of 43 (72%) ganglia (Table 2; last column), including those obtained when PMI was <9 h, and the abundance of VZV ORF63 transcripts increased significantly with longer PMIs (Fig. 1B) ($r = -0.42$, $p = 0.02$; Pearson's correlation test). There was no significant difference ($p = 0.27$; Fisher's exact test) in the number of TG that contained VZV ORF63 transcripts in donors with a PMI of <9 h (7 of 12 TG; 58%) compared to a PMI >9 h (24 of 31 TG; 77%). The NF transcript levels were not affected by the PMI (Fig. 1C). There was no significant difference in the abundance VZV ORF63 transcription in paired left and right TG from individual donors (Fig. 1D, $p = 0.02$; Wilcoxon matched-pairs signed-rank test) suggesting that the PMI-related increase of VZV ORF63 transcription found in paired TG reflects a general host response, which may involve cellular stress due to hypoxia, nutrient deprivation or hypothermia [13]. Vascular endothelial growth factor (VEGF) is a cellular gene whose transcription is induced by hypoxia [14]. Analysis of cDNA synthesized from 16 TG mRNAs (12 donors) by RT-qPCR showed that the number of VEGF transcripts did not correlate with longer PMIs (Fig. 1E) ($r = 0.48$, $p = 0.06$; Pearson's correlation test) or with VZV ORF63 transcription (Fig. 1F) ($r = -0.21$, $p = 0.52$; Pearson's correlation test), indicating that the increase in VZV gene transcription is virus-specific and not likely to be due to hypoxia.

No correlation of VZV DNA load in human TG with longer PMI.
The increased number of VZV transcripts (multiplex RT-PCR) and ORF63 transcript abundance (RT-qPCR) with longer PMI suggest post-mortem VZV reactivation. Quantitative PCR analysis confirmed the presence of VZV DNA in 42 of 43 ganglia (VZV DNA was not detected in subject I), but the viral DNA load did not correlate with the PMI (Fig. 1G and data not shown). Thus, if VZV reactivated after death, reactivation had not yet advanced to virus DNA replication within the time frame investigated. Finally, the lack of correlation between VZV ORF63 transcript levels and ganglionic VZV DNA load (Fig. 1H) indicated that ORF63 transcription was independent of the latent VZV DNA burden.

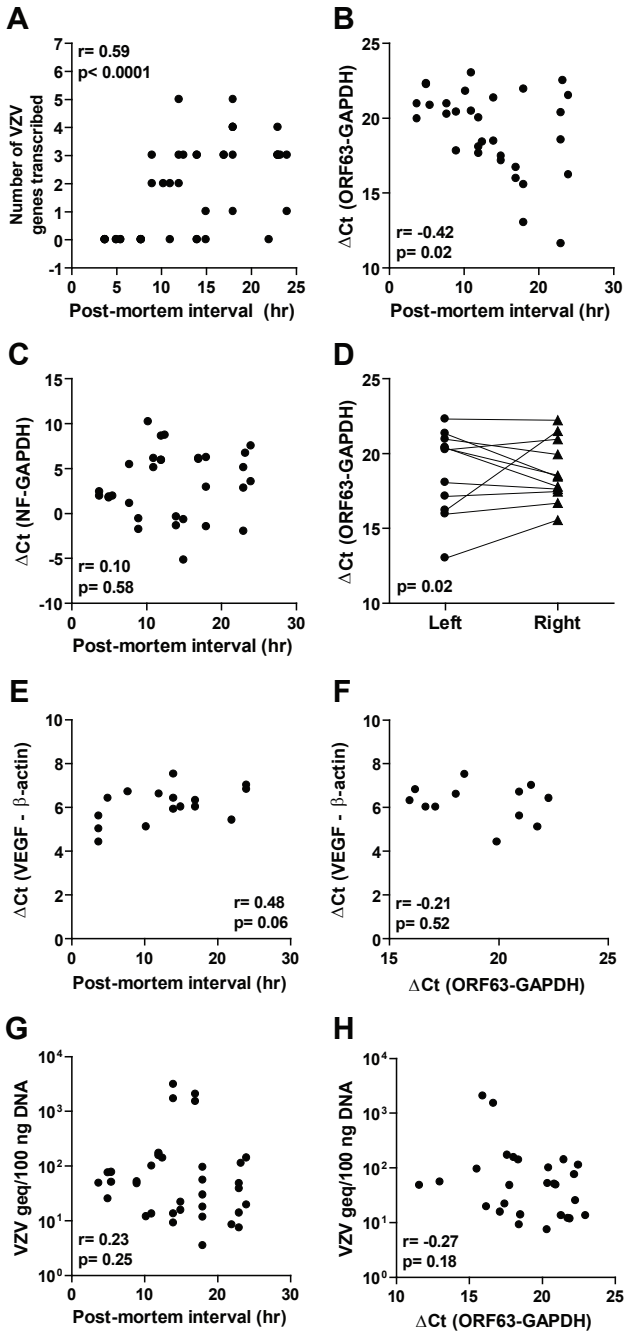

Figure 1. *VZV ORF63 transcript levels, but not VZV DNA load, in human trigeminal ganglia (TG) correlate with the post-mortem interval (PMI). (A) Correlation between PMI and number of VZV transcripts detected by multiplex RT-PCR. (B) Correlation between PMI and abundance of ORF63 transcripts. (C) No correlation between PMI and abundance of neurofilament (NF) transcripts. (D) Correlation of the abundance of ORF63 transcripts in paired left and right TG. (E) No correlation between vascular endothelial growth factor (VEGF) transcript levels and PMI. (F) No correlation between VEGF and ORF63 transcript levels. (G) No correlation between ganglionic VZV DNA load and PMI or (H) abundance of ORF63 transcripts. Statistical analyses were performed using Pearson's correlation test (A-C, E, and F-H) and Wilcoxon matched-pairs signed-rank test (D). Figures A, and E and F, contain VZV transcript data and VZV genome load levels that in part have been published previously, respectively (see Table 2 and reference 11).*

This study is the first to investigate the entire VZV transcriptome in human ganglia with a short PMI. Multiplex RT-PCR did not detect VZV transcription early (<9 h) after death by, but did reveal multiple VZV transcripts in TG at >9 h post-mortem as well as an increased abundance of VZV ORF63 transcripts with a longer PMI. The sensitivity of ORF63 transcript detection was greater for RT-qPCR than for multiplex RT-PCR. The sensitivity of multiplex RT-PCR is 1 to 10 copies for 82% of VZV transcripts and 100 to 500 copies for the remaining 18% VZV transcripts [11-12]. Table 2 shows that 7 of 10 (70%) VZV genes were detected at a sensitivity of 1 mRNA copy per sample, 2 of 10 (20%) VZV genes were detected with a sensitivity of 10 mRNA copies per sample, and 1 of 10 (10%) VZV genes were detected with a sensitivity of 100 mRNA copies per sample [11-12]. Thus, differential VZV gene sensitivity of the multiplex RT-PCR assay did not account for VZV transcripts detected in the TGs. The data contrast with a previous study reporting no difference in simian varicella virus (SVV) transcription in ganglia removed immediately and 30 h after death, although ganglia from just 2 monkeys were analyzed for 7 transcripts and only at 2 post-mortem intervals [15].

The current study raises an important question regarding ongoing low-level VZV gene transcription during latency or *de novo* VZV gene transcription after death. Until an appropriate *in vitro* culture model of VZV latency is developed, studies of VZV latency must be restricted to human ganglia [2-9]. While our data is consistent with continued VZV ORF63 transcription during latency with transcription of other VZV genes initiated only after death, a definitive answer would require analysis of human ganglia obtained during life, a situation not possible. The SVV non-human primate model of varicella latency provide an experimental setting to definitively determine the extent of virus transcription during latency [16].

Our data showed that the VZV immediate early genes are the most frequently transcribed in human TG (Table 2). However, the absence of increasing VZV DNA loads with longer PMI argues against viral replication that would be expected during VZV reactivation (Fig 1E). No immediate explanation for the detection of multiple VZV transcripts at >9 h post-mortem, but not apparent at earlier times, can be provided but may reflect the epigenetic state of the VZV genome. We have previously shown that late VZV genes 14 and 36 are epigenetically silenced, whereas genes 63 and 62 are maintained in a euchromatic configuration in human TG [17]. Future studies will address VZV genome-wide epigenetic modifications along with the detection and role of specific VZV transcripts, including ORF63, in human ganglia with a short versus long PMI.

Acknowledgments

This work was supported in part by the Public Health Service grants AG032958 (W.J.D.O., D.G., R.J.C., G.M.G.M.V.), AG006127 (D.G.) and NS067070 (M.A.N.) from the National Institutes of Health. The TG specimens, provided by the Netherlands Brain Bank (Netherlands Insitute for Neuroscience; Amsterdam), were collected from donors from whom a written informed consent for brain autopsy and the use of the material and clinical information for research purposes had been obtained.

References

1. Cohen JI, Straus SE and Arvin AM. Varicella-zoster virus replication, pathogenesis, and management, p 2773-2818. In: Knipe DM, Howley PM, Griffin DE, et al., eds. Fields Virology, 5th ed, Vol 2. Philadelphia: Lippincott, Williams and Wilkins, 2007:2773-2818.
2. Cohrs RJ, Barbour M and Gilden DH. Varicella-zoster virus (VZV) transcription during latency in human ganglia: detection of transcripts mapping to genes 21, 29, 62, and 63 in a cDNA library enriched for VZV RNA. J Virol, 1996;70:2789-96.
3. Cohrs RJ and Gilden DH. Prevalence and abundance of latently transcribed varicella-zoster virus genes in human ganglia. J Virol 2007;81:2950-6.
4. Cohrs RJ, Gilden DH, Kinchington PR, Grinfeld E and Kennedy PG. Varicella-zoster virus gene 66 transcription and translation in latently infected human ganglia. J Virol, 2003;77:6660-5.
5. Cohrs RJ, Strock K, Barbour MB, et al. Varicella-zoster virus (VZV) transcription during latency in human ganglia: construction of a cDNA library from latently infected human trigeminal ganglia and detection of a VZV transcript. J Virol, 1994;68:7900-8.
6. Croen KD, Ostrove JM, Dragovic LJ and Straus SE. Patterns of gene expression and sites of latency in human nerve ganglia are different for varicella-zoster and herpes simplex viruses. Proc Natl Acad Sci U S A 1988;85:9773-7.
7. Kennedy PG, Grinfeld E and Bell JE. Varicella-zoster virus gene expression in latently infected and explanted human ganglia. J Virol 2000;74:11893-8.
8. Kennedy PG, Grinfeld E and Gow JW. Latent varicella-zoster virus in human dorsal root ganglia. Virology 1999;258:451-4.
9. Kennedy PG, Grinfeld E and Gow JW. Latent varicella-zoster virus is located predominantly in neurons in human trigeminal ganglia. Proc Natl Acad Sci U S A 1998;95:4658-62.
10. Meier JL, Holman RP, Croen KD, Smialek JE and Straus SE. Varicella-zoster virus transcription in human trigeminal ganglia. Virology 1993;193:193-200.
11. Nagel MA, Choe A, Traktinskiy I, et al. Varicella-zoster virus transcriptome in latently infected human ganglia. J Virol, 2011;85:2276-87.
12. Nagel MA, Gilden D, Shade T, Gao B, and Cohrs RJ. Rapid and sensitive detection of 68 unique varicella zoster virus gene transcripts in five multiplex reverse transcription-polymerase chain reactions. J Virol Methods 2009;157:62-8.
13. Birdsill AC, Walker DG, Lue L, Sue LI and Beach TG. Postmortem interval effect on RNA and gene expression in human brain tissue. Cell Tissue Bank 2011;12:311-8.
14. Marti HH and Risau W. Systemic hypoxia changes the organ-specific distribution of vascular endothelial growth factor and its receptors. Proc Natl Acad Sci U S A 1998;95: 15809-14.
15. Mahalingam R, Traina-Dorge V, Wellish M, et al. Effect of time delay after necropsy on analysis of simian varicella-zoster virus expression in latently infected ganglia of rhesus macaques. J Virol 2010;84:12454-7
16. Messaoudi I, Barron A, Wellish M, et al. Simian varicella virus infection of rhesus macaques recapitulates essential features of varicella zoster virus infection in humans. PLoS Pathog 2009;5: e1000657.
17. Gary L, Gilden DH and Cohrs RJ. Epigenetic regulation of varicella-zoster virus open reading frames 62 and 63 in latently infected human trigeminal ganglia. J Virol 2006;80:4921-6
18. Roizman B, Knipe DM and Whitley RJ. Herpes simplex viruses. In: Knipe DM, Howley PM, Griffin DE, et al., eds. Fields Virology, 5th ed, Vol 2. Philadelphia: Lippincott, Williams and Wilkins, 2007:2501-2601.

Chapter 6

Longitudinal Study on Oral Shedding of Herpes Simplex Virus 1 and Varicella-Zoster Virus in Individuals Infected with HIV

Monique van Velzen,[1] Werner J.D. Ouwendijk,[1] Stacy Selke,[2] Suzan D. Pas,[1] Freek B. van Loenen,[1,3] Albert D.M.E. Osterhaus,[1] Anna Wald,[1,4,5] and Georges M.G.M. Verjans[1]

[1]Department of Viroscience, Erasmus Medical Center, Rotterdam, the Netherlands; [2]Department of Laboratory Medicine, University of Washington, Seattle, WA, USA; [3]Rotterdam Eye Hospital, Rotterdam, the Netherlands; [4]Department of Medicine, University of Washington, Seattle, WA, USA; [5]Vaccine and Infectious Disease Division, Fred Hutchinson Cancer Research Center, Seattle, WA, USA.

J Med Virol. 2013 Sep;85(9):1669-77

Abstract

Primary herpes simplex virus 1 (HSV-1) and varicella-zoster virus (VZV) infection leads to a life-long latent infection of ganglia innervating the oral mucosa. HSV-1 and VZV reactivation is more common in immunocompromised individuals and may result in viral shedding in saliva. We determined the kinetics and quantity of oral HSV-1 and VZV shedding in HSV-1 and VZV seropositive individuals infected with HIV and to assess whether HSV-1 shedding involves reactivation of the same strain intra-individually. HSV-1 and VZV shedding was determined by real-time PCR of sequential daily oral swabs (n = 715) collected for a median period of 31 days from 22 individuals infected with HIV. HSV-1 was genotyped by sequencing the viral thymidine kinase gene. Herpesvirus shedding was detected in 18 of 22 participants. Shedding of HSV-1 occurred frequently, on 14.3% of days, whereas solely VZV shedding was very rare. Two participants shed VZV. The median HSV-1 load was higher compared to VZV. HSV-1 DNA positive swabs clustered into 34 shedding episodes with a median duration of 2 days. The prevalence, duration and viral load of herpesvirus shedding did not correlate with CD4 counts and HIV load. The genotypes of the HSV-1 viruses shed were identical between and within shedding episodes of the same person, but were different between individuals. One-third of the individuals shed an HSV-1 strain potentially refractory to acyclovir therapy. Compared to HSV-1, oral VZV shedding is rare in individuals infected with HIV. Recurrent oral HSV-1 shedding is likely due to reactivation of the same latent HSV-1 strain.

Introduction

Herpes simplex virus 1 (HSV-1) and varicella-zoster virus (VZV) are closely related neurotropic human alpha-herpesviruses (αHHV) that are endemic worldwide. A hallmark of both viruses is the ability to establish a lifelong latent infection of sensory ganglia with intermittent reactivation and neuronal spread of the virus to innervating tissues [1]. αHHV shedding in bodily secretions and fluids, particularly saliva, contributes to virus transmission throughout the population [2-5]. Virus shedding is commonly asymptomatic, but may lead to recurrent herpetic lesions most commonly as cold sores for HSV-1 and as shingles for VZV. Recurrent HSV infections of the same anatomical location may be due to reactivation of the latent virus strain or superinfection with an exogenous strain. Whereas most sequential HSV-1 isolates from the same anatomical location of an individual are identical, HSV-1 isolates with different genome profiles have been described in patients with oral, genital and corneal herpesvirus infections [6-9]. Alternatively, multiple virus strains may have established latency in the same ganglion. Indeed, different HSV-1 strains have been detected in the same latently infected human ganglion, including the oral mucosa innervating trigeminal ganglion, indicating that recurrent oral HSV-1 shedding may be due to reactivation of genetically different latent HSV-1 strains [10-11]. The host immune system is pivotal to limit reactivation from its ganglionic stronghold [12-14]. As such, individuals infected with HIV experience more severe and persistent herpetic lesions and may be at risk for central nervous system disease [12, 15-17].

Previous studies have described high oral HSV shedding frequencies in individuals infected with HIV compared to healthy persons seropositive for the respective herpesviruses [15, 18, 19]. Oral lesions present in individuals infected with HIV have been associated with shedding of herpesviruses in the oral cavity [20-21]. Moreover, oral detection of herpesviruses is decreased in individuals treated with anti-retroviral or anti-herpesvirus drugs [22-24]. Limited number of studies have reported on VZV shedding in saliva or oral swabs of herpes zoster patients [25-26], healthy individuals [26] and in one study on individuals infected with HIV [27]. These studies were mainly restricted to the detection of VZV only and limited to the analysis of one or a few consecutive saliva samples per individual. The trigeminal ganglion, which innervates the oral mucosa and eye, commonly contains both latent HSV-1 and VZV in co-infected individuals. Hence, the aim of this study was to determine the prevalence and kinetics of oral HSV-1 and VZV shedding in HSV-1 and VZV seropositive individuals infected with HIV and to assess whether HSV-1 shedding involves reactivation of the same strain intra-individually.

Materials and Methods

Study Population

Individuals infected with HIV-1 were recruited between 1995 and 2007 at the Univer-

Table 1. Demographic and Clinical Characteristics of Study Subjects.

Baseline Characteristics[a]	n = 22 subjects
Median age (range) in yrs	42 (22-61)
Male, n (%)	20 (91)
HSV serostatus, n (%)	
HSV-1 only	7 (32)
HSV-1 and HSV-2	15 (68)
Race/ethnicity, n (%)	
White	18 (82)
Black	2 (9)
Other	2 (9)
Anti-retroviral use during study, n (%)	6 (27)
Median (IQR) CD4 count, cells/μL	268 (202-476)
HAART treatment: yes	367 (153-645)
HAART treatment: no	240 (202-412)
Median (IQR) HIV RNA, geq/mL	37,900 (15,656-109,316)
HAART treatment: yes	7,141 (25-46,608)
HAART treatment: no	59,500 (25,400-113,500)

[a] HSV-1, herpes simplex virus 1; VZV, varicella-zoster virus; HAART, highly active anti-retroviral therapy; IQR, interquartile range; geq, genome equivalent copies

sity of Washington Virology Research Clinic (Seattle, WA, USA) from a pool of unrelated research study participants known to comply with an intensive study protocol and asked to collect oral swab specimens at home daily for at least 30 days (Table I). The median duration of HIV infection was 8 years (range 3 months to 18 years). Participants were instructed to rub a Dacron swab across the buccal mucosa and tongue in the morning prior to showering or brushing their teeth, to place the oral swab in 1 mL of PCR transport medium and to store the sample at -20°C until laboratory processing [18]. Participants were eligible if they were HSV-1 and VZV seropositive, and agreed not to use anti-herpesvirus drugs, such as acyclovir (ACV) during the study. The use of anti-herpesvirus drugs was only monitored if prescribed by the University of Washington Virology Research Clinic (Seattle, WA). Participants #11 and #16 used famciclovir bidaily for 60 days in the year prior to collection of the oral specimens, but treatment was stopped two weeks before start of the study. At baseline, plasma HIV RNA load and blood CD4 T-cell counts were determined as described [18]. A log book recording symptomatic (herpetic) oral lesions was filed. Participants had routine clinic visits at the start and end of the study and irregularly during the study. During these visits brief visual oral exams were performed and a history of suspected herpetic oral lesions since the last visit was reviewed by the clinician and noted in the participant's chart. Except for participant #6, no evident abnormalities of the mouth (e.g. bleeding gum) or the neck were recorded and reported by the participants themselves during the sampling period. Written informed consent

was given by the participants and the protocol was approved by the Institutional Review Board at the University of Washington (Seattle, WA). The study was performed according to the tenets of the Declaration of Helsinki.

Quantitative αHHV PCR Analyses and HSV-1 Thymidine Kinase Sequencing from Oral Swabs

DNA was extracted from swab medium as described [18]. Quantitative PCR (qPCR) assay for HSV-1 and VZV DNA was performed using an ABI prism 7500 and Taqman Universal Master Mix (both from Applied Biosystems, Foster City, CA) as reported [28]. The HSV-1 and VZV qPCR used published virus-specific primers and probes [29]. For standardization of HSV-1 and VZV Taqman assays, electron microscopy counted high-titer virus preparations and commercially available quantified DNA control panels (Advanced Biotechnologies) were used [29]. The lower limit of detection of both qPCR assays was 50 genome equivalent copies (geq)/mL. Cycle threshold values outside the linear range of the qPCR assay were considered as positive results, but could not be reliably quantified.

From a selected number of HSV-1 positive swabs (n=39), the entire HSV-1 thymidine kinase (TK) gene was amplified and sequenced as described [30]. The TK sequences were aligned to the consensus TK sequence of reference HSV-1 strain H129 (GenBank: GU_734772). The obtained HSV-1 TK sequences were deposited in the GenBank database under accession numbers JQ895543-JQ895556. Phylogenetic analysis was performed by estimating a maximum-likelihood unrooted tree of HSV-1 TK nucleotide sequences under the Kimura 2-parameter model and 1,000 bootstrap replications (MEGA 5.0 software).

Statistical Analysis

Herpesvirus shedding episodes were defined as one virus DNA positive swab or a series of DNA positive swabs that were collected before and after at least two negative swabs. Any shedding episode could include one missing or one negative swab within the episode [18]. Statistical analyses were done using GraphPad Prism 4. Spearman's correlation tests were used to determine correlations between herpesvirus shedding frequency, HIV viral load, CD4 T-cell counts or highly active anti-retroviral therapy (HAART). Mann-Whitney tests were used to compare shedding rates and median HSV-1 viral loads in HAART versus non-HAART persons and among shedding episodes of variable length. Differences were considered significant if $P<0.05$.

Results

Oral HSV-1 and VZV Shedding in Individuals Infected with HIV

Twenty-two HSV-1 and VZV seropositive individuals infected with HIV were enrolled in the study. The median age was 42 years (range 22-61 years) and 20 were male. Fifteen participants were HSV-2 seropositive, and 6 persons (27%) were taking

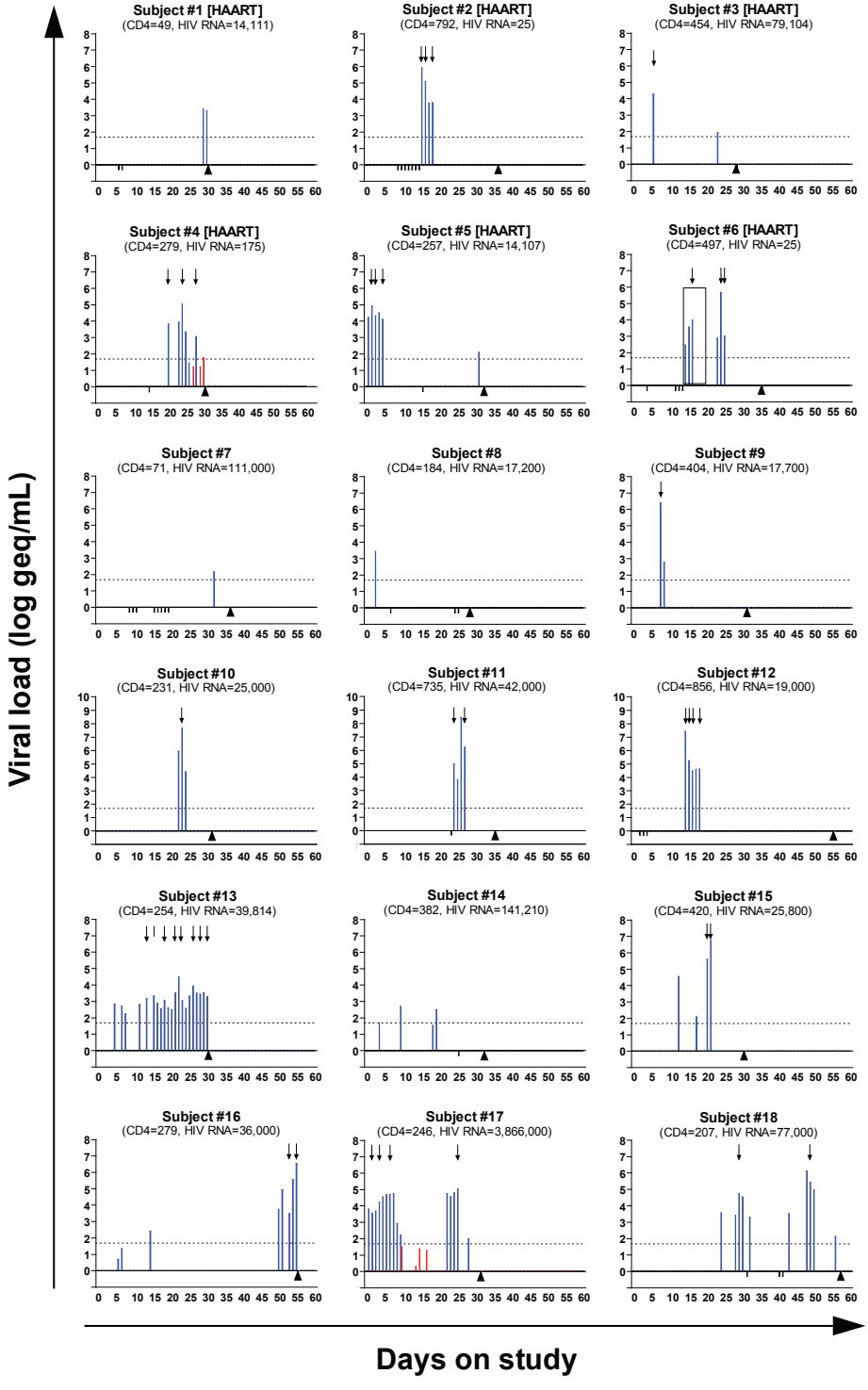
Subject #1 [HAART]
(CD4=49, HIV RNA=14,111)
Subject #2 [HAART]
(CD4=792, HIV RNA=25)
Subject #3 [HAART]
(CD4=454, HIV RNA=79,104)
Subject #4 [HAART]
(CD4=279, HIV RNA=175)
Subject #5 [HAART]
(CD4=257, HIV RNA=14,107)
Subject #6 [HAART]
(CD4=497, HIV RNA=25)
Subject #7
(CD4=71, HIV RNA=111,000)
Subject #8
(CD4=184, HIV RNA=17,200)
Subject #9
(CD4=404, HIV RNA=17,700)
Subject #10
(CD4=231, HIV RNA=25,000)
Subject #11
(CD4=735, HIV RNA=42,000)
Subject #12
(CD4=856, HIV RNA=19,000)
Subject #13
(CD4=254, HIV RNA=39,814)
Subject #14
(CD4=382, HIV RNA=141,210)
Subject #15
(CD4=420, HIV RNA=25,800)
Subject #16
(CD4=279, HIV RNA=36,000)
Subject #17
(CD4=246, HIV RNA=3,866,000)
Subject #18
(CD4=207, HIV RNA=77,000)
Viral load (log geq/mL)
Days on study

Figure 1 (previous page). *Oral herpes simplex virus 1 (HSV-1) and varicella-zoster virus (VZV) shedding patterns in individuals infected with HIV. Viral loads [genome equivalent copies (geq) per mL] are plotted on the y-axis and the days on study on the x-axis. For each patient, CD4 T-cell counts (cells/μL) and HIV RNA loads (geq/mL) are specified. Individuals #1 to #6 were taking anti-retroviral therapy (HAART). The dotted line represents the lower limit of detection of the qPCR. Blue bars indicate HSV-1 shedding, red bars indicate VZV, and black bars below the x-axis indicate missing swabs. The solid box (graph of patient #6) indicates the presence of symptomatic herpetic oral lesions. Arrowheads denote the end of the swabbing period per individual and arrows indicate swabs that were used for HSV-1 thymidine kinase-based genotyping (see Table III).*

HAART (i.e. participants #1 to #6) (Table I and Figure 1). Participants had a median CD4 T-cell count of 268 cells/mL with an interquartile range (IQR) of 202-476 cells/mL and a median HIV RNA load of 37,900 copies/mL (IQR: 15,656-109,316 copies/mL) (Table I). Whereas the CD4 T-cell counts were not different (Mann-Whitney test; P=0.45), the HIV RNA load was significantly lower in persons taking HAART compared to those not receiving HAART (Mann-Whitney test; P=0.01), respectively. A total of 715 oral swabs were obtained and analyzed for the presence and amount of HSV-1 and VZV DNA by qPCR. Samples were collected for a median of 31 days (IQR: 28-33 days), with 19 participants collecting for ≥30 days (Figure 1). Except for individual #6, none of the participants reported symptomatic herpetic oral lesions during the study period.

Four of the 22 (18%) persons shed neither HSV-1 nor VZV DNA during the study. From the 18 remaining persons, HSV-1 DNA was detected on 102 out of 715 sample days (14.3%) (Table II). The HSV-1 DNA load was quantified in 97 swabs, with a median DNA load of 5,603 geq/mL (IQR: 1,073-56,050 geq/mL). Very low VZV DNA levels were detected in 7 swabs from two persons, and could be quantified in 1 sample (participant #4; 58 geq/mL). The median number of episodes of HSV-1 shedding was 2 and 1.5 episodes per 30 days among participants receiving HAART and those who were not receiving HAART (Mann-Whitney test; P=0.48), respectively. The frequency of HSV-1 and VZV shedding, and the maximum detected HSV-1 load, did not correlate with the participants' CD4 T-cell counts or HIV RNA load (Figure 1 and data not shown). All VZV DNA positive swabs were HSV-1 negative, with the exception of one swab from participant #17 in which both HSV-1 and VZV were detected (Figure 1).

The 102 HSV-1 positive swabs clustered into 34 distinct shedding episodes, with a median duration of 2 days (range 1-20 days) (Table II). During the study period, 14 episodes (41%) of 1 day duration were detected with a median HSV-1 DNA load of 256 geq/mL (IQR: 124-3,555 geq/mL). Eleven episodes (32%) lasted ≥ 4 days, and 7 episodes where of unknown duration because swabs were positive at the beginning or end of the study (Figure 1 and Table II). The median HSV-1 load of 3-day episodes (909,842 geq/mL) or ≥ 4-day episodes (106,000 geq/mL) was significantly higher compared to one-day episodes (Mann-Whitney test; P=0.005 and P=0.0001, respectively) (Figure 2). One of the participants (#6) reported symptomatic herpetic oral lesions at days 15 to 20 of the study. HSV-1 DNA was detected in mucosal

Table 2. Proportion of Days, Time Points, and Study Participants with HSV-1 or VZV Detected in at Least One Oral Swab.

Baseline Characteristics[a]	n = 22 subjects
Days sample collected, n	715
VZV DNA positive participants, n (%)	2 (9)
Days VZV detected, n (%)	7 (1)
HSV-1 DNA positive participants, n (%)	18 (82)
Days HSV-1 detected, n (%)	102 (14)
Duration of HSV-1 DNA positive episodes	34
1 day (%)	14 (41)
2 days (%)	5 (15)
3 days (%)	4 (12)
≥4 days (%)	11 (32)

[a] HSV-1, herpes simplex virus 1; VZV, varicella-zoster virus; n (%), indicates the number, between parentheses the percentage, of the indicated parameters within the whole study group or the total number oral swabs obtained.

swabs at the start of symptoms and was undetectable during the resolution phase. Notably, the participant's second HSV-1 shedding episode, with a 2-log higher HSV-1 DNA load, was asymptomatic (Figure 1).

Genotyping of Oral HSV-1 in Individuals Infected with HIV

To determine if oral HSV-1 shedding involves reactivation of the same latent strain within and between shedding episodes, the entire TK gene from a selected set of HSV-1 DNA positive oral swabs was sequenced (Figure 1). Besides the causative role of TK mutations in ACV resistance (ACV^R), the hypervariability of the TK gene provides insight into the genetic composition of a virus isolate [11, 30, 31]. The HSV-1 TK genotype was determined from 14 participants with a median of 2.5 (range 1-8) oral swabs analyzed per person. The analyzed sequential oral swabs were obtained during one (n=10 participants) or of two subsequent HSV-1 shedding episodes (n=4 participants) (Table III). Alignment of the TK sequences obtained with the corresponding sequence of the HSV-1 reference strain H129 revealed numerous TK gene nucleotide substitutions, including those resulting in amino acid mutations in the encoding TK protein. Notably, HSV-1 TK sequences of sequential oral swabs from each individual, both within and between shedding episodes, were identical suggesting reactivation and subsequent oral shedding of the same endogenous HSV-1 strain (Table III). Most of the viruses shed by each individual had a unique TK nucleotide sequence clustering into distinct participant-specific phylogenetic clades (Figure 3). However, HSV-1 shed by participants #2 and #18, and participants #6 and #13, could not be differentiated based on the TK gene genotypes (Table III and Figure 3). The TK sequence homology was not due to contamination, since the participants' samples were processed at different time points, all sequential swabs of each participant were identical (Table III), and none of the aforementioned participants were family members or in any way related.

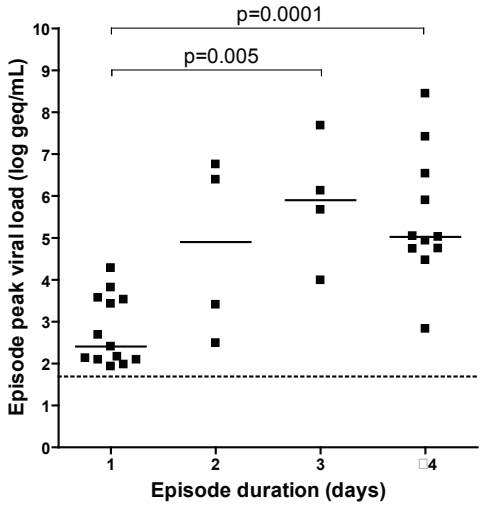

Figure 2. *Oral herpes simplex virus 1 (HSV-1) shedding characteristics of individuals infected with HIV. Episode duration (in days) is plotted against the peak HSV-1 viral load per individual (log-transformed geq/mL). Bars indicate the median viral load. The dotted line represents the lower limit of detection of the qPCR. The Mann-Whitney test was used to compare median viral loads and significant differences are indicated.*

ACV^R HSV-1 is predominantly due to specific mutations in the drug-targeted TK protein leading to its defective or limited ability to convert ACV to ACV-monophosphate necessary to block HSV-1 replication [31]. Whereas the majority of the HSV-1 TK amino acid changes identified in the oral swabs were natural polymorphisms, 4 of 14 (29%) participants (#6, #10, #13 and #17) shed HSV-1 strains expressing ACV^R–associated TK protein variants suggesting that the respective viruses are unresponsive to ACV therapy (Table III) [11, 31-33]. Notably, participants #6 and #17 shed the respective HSV-1 strain on two subsequent shedding episodes suggesting that this inferred ACV^R virus had reactivated from latency. For participant #6, one of these shedding episodes coincided with symptomatic oral lesions.

Discussion

The aim of this study was to examine the kinetics and quantity of oral HSV-1 and VZV shedding during a one-month daily sampling in individuals infected with HIV. It was found that shedding of HSV-1 occurs frequently, on 14.3% of days, whereas VZV shedding is very rare and at significantly lower genome copies. Based on the TK genotypes of sequential HSV-1 DNA positive oral swabs it was demonstrated that the participants shed genetically identical HSV-1 viruses, within and between HSV-1 shedding episodes, which were generally patient-unique. One-third of the participants shed a virus with an ACV^R TK genotype that potentially results in an HSV-1 strain refractory to ACV therapy.

Oral shedding of αHHV likely contributes to the epidemic spread within the human population [2-5]. Estimates on the frequency of HSV-1 shedding in immunocompetent individuals range from 0.5-76%. The sensitivity of virus detection techniques used, the number of persons and consecutive swabs sampled, and the time course

Table 3. Herpes Simplex Virus 1 Thymidine Kinase Variants Detected in Sequential Oral Swabs of HIV Patients.

Subject ID	Sampling day[a]	Thymidine kinase (TK) protein amino acid changes[b]	GenBank Accession No.[c]
2	16, 17 & 19	I138V	JQ895543
3	6	S23N, E36K, Q89R, I138V, G240E & R281Q	JQ895544
4	21, 25 & 29	S23N, E36K, Q89R, I138V, G240E & R281Q	JQ895545
5	2, 3 & 5	L42P, Q89R, I138V, G251C, V267L, P268T, D286E & N376H	JQ895546
6	17, 25 & 26	C6G, R41H, Q89R, I138V, A192V, G251C, V267L, P268T, D286E & N376H	JQ895547
9	8	I138V & A316V	JQ895548
10	24	S23N, E36K, Q89R, I138V, G240E, R281Q & C336R	JQ895549
11	25 & 28	C6G, L42P, Q89R, I138V, L267T, P268T & D286E	JQ895550
12	15, 16, 17 & 19	I138V & G240E	JQ895551
13	14, 16, 19, 22, 23, 27, 29 & 31	C6G, R41H, Q89R, I138V, A192V, G251C, V267L, P268T, D286E, N376H	JQ895552
15	21 & 22	C6G, I138V & G240E	JQ895553
16	54 & 56	I138V	JQ895554
17	2, 4, 7 & 26	C6G, del36E, R41H, Q89R, I138V, A192V, G251C, V267L, P268T, D286E & N376H	JQ895555
18	30, 50	I138V	JQ895556

[a] Sampling day refers to the oral HSV-1 shedding day of which the corresponding TK sequence of the indicated subject was determined. The analyzed sampling days are also depicted with arrows in Fig. 1.

[b] Amino acid changes are listed that are different from the HSV-1 TK reference sequence (GenBank No.: GU_734772). All sequential HSV-1 DNA positive swabs of the indicated days were identical within each subject. Underlined and bold/italic TK residue changes are unknown to affect acyclovir (ACV) sensitivity and published TK mutations leading to an ACV-resistant phenotype of the respective HSV-1 strain, respectively [11, 31-33]. All other residue changes are TK polymorphisms that are described not to affect ACV sensitivity. The mutation “del36E” refers to a deletion of “glutamic acid” at residue position 36 of the TK protein. HSV-1 DNA positive oral swabs of subjects #2 and #18, and #6 and #13, had identical HSV-1 TK nucleotide and protein sequences, respectively. In contrast, the TK sequences of the HSV-1 shed by subject #16 was different at the nucleotide level compared to the TK sequences of subjects #2 and #18.

[c] The GenBank Accession numbers of the HSV-1 TK sequences of the indicated oral swabs are provided.

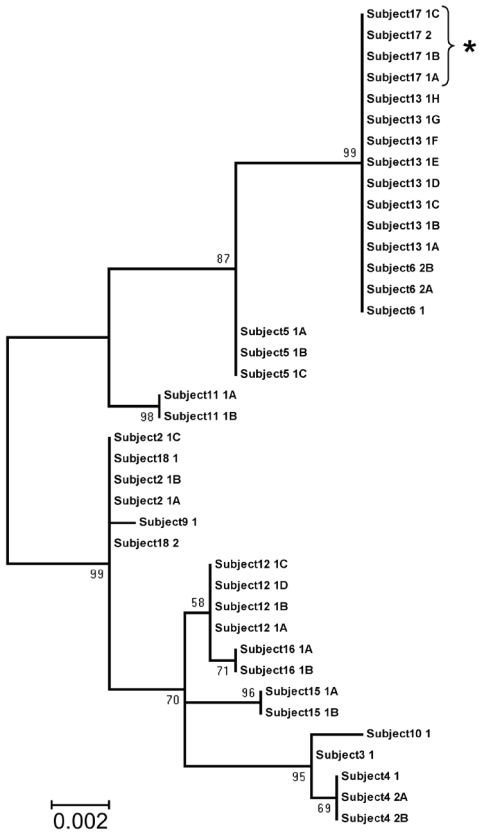

Figure 3. *Distinct oral herpes simplex virus 1 (HSV-1) thymidine kinase (TK) genotypes in individuals infected with HIV. Maximum likelihood unrooted phylogenetic tree of HSV-1 TK sequences was estimated under the Kimura 2-parameter model. The HSV-1 TK variants shown are coded by the participant's number, episode number (1 or 2), and swab within an episode (A to H). Selected bootstrap values are given. Scale bar represents number of nucleotide substitutions per site. *The TK variants from participant #17 are identical to those of individuals #1 and #6, except for a 3-nucleotide deletion (see Table III).*

of the studies may have attributed to the high variation reported [3, 34-37]. Studies that sampled saliva multiple times a day have revealed that 39% of oral HSV-2 reactivations are cleared within 12 hours [19]. A study in individuals infected with HIV demonstrated that HSV reactivations are also of short duration and usually resolve before the onset of symptoms [18]. Consistent with previous reports, the current study detected HSV-1 shedding in 82% of the individuals infected with HIV at a frequency comparable to immunocompetent individuals [3, 18, 34-37]. The results corroborate with earlier data describing that a large proportion of the oral shedding episodes were cleared within 2 days and maximal viral loads per episode were significantly higher in episodes of prolonged duration [18-19]. In this study, one participant (#6) reported oral lesions during one shedding episode that coincided with the detection of HSV-1 DNA in the mucosal swabs. Notably, the concurrent shedding episode of this participant, which was asymptomatic, had 2-log higher HSV-1 DNA copy numbers suggesting that the viral DNA load was not related to symptomatic herpetic oral lesions [21].

Subclinical reactivation of VZV has been less well studied and is largely evident in the elderly, in immunocompromised individuals and in herpes zoster patients [25-26, 38-39]. One study evaluated the prevalence of VZV in saliva of individuals infected

with HIV and demonstrated low copy numbers in 3 of 59 (5.1%) participants [27]. A similarly low incidence and low copy numbers of oral VZV shedding was reported in the current study. The low prevalence of VZV shedding did not allow investigation of the potential interrelatedness of oral HSV-1 and VZV reactivation and shedding in individuals infected with HIV. Deprived VZV-specific T-cell immunity, as seen in immunocompromised individuals and the elderly, is a risk factor for VZV reactivation [14]. Future studies on more severe immunocompromised individuals, e.g. stem cell transplant patients, are warranted to study a potential interrelation between oral HSV-1 and VZV shedding [12, 27, 38].

HSV-1 and VZV are closely related human herpesviruses that establish a lifelong latent infection of sensory ganglia, yet HSV-1 shedding is much more frequent compared to VZV shedding. The different patterns in virus shedding resemble the differences observed in recurrent symptomatic HSV-1 and VZV infections. Recurrent HSV-1 lesions occur frequently, whereas individuals typically develop herpes zoster only once in a life time [40]. In contrast to HSV-1, VZV establishes latency in ganglia along the entire neuraxis, hence VZV reactivation from ganglia other than the trigeminal ganglia may be undetectable in saliva. However, previous studies have shown that VZV DNA and infectious virus can be detected during asymptomatic reactivation in astronauts and in zoster patients, irrespective of the affected dermatome [2, 25-26]. Likewise, elderly vaccinated with the live-attenuated VZV vaccine shed viral DNA in saliva, suggesting that VZV reaches the saliva by viremic spread upon vaccination or viral reactivation [41].

It was previously shown that HSV-1/VZV co-infection correlates with the detection of both viruses in human trigeminal ganglia [42-43]. Both viruses can be detected in the same trigeminal ganglion and even HSV-1 and VZV double-infected neurons have been described [44]. The higher ganglionic HSV-1 DNA load compared to VZV DNA load [43-45] may account for a higher HSV-1 reactivation frequency. Alternatively, viral determinants of HSV-1 latency, including intra-neuronal expression of latency-associated transcripts and microRNAs [46-49], which are not shared by VZV, may contribute to the differential αHHV reactivation patterns. Finally, CD8 T-cells are considered pivotal to control HSV-1, but not VZV latency in human trigeminal ganglia suggesting that different immune mechanisms act on the control of latency of both αHHVs [42-43].

In addition to the genetic hypervariability of the HSV-1 TK gene, ACV resistance is mostly associated with specific mutations in the drug-targeted viral TK protein [31]. The current study demonstrated that for each participant the sequential HSV-1 strains shed were identical within and between oral HSV-1 shedding episodes and expressed an overall individual-unique genotype. The data are in line with a recent study demonstrating that paired trigeminal ganglia are latently infected with a person-specific HSV-1 strain [11]. Recurrent symptomatic ACV^R HSV-1 infections have been described in ocular infections demonstrating that ACV^R HSV-1 can reactivate from latency [6]. Four of 14 (28.6%) participants shed HSV-1 strains with ACV^R-associated TK protein variants, including 2 patients on two different episodes, suggest-

ing that the inferred ACV^R HSV-1 strains have established latency and reactivated from latency [6, 11]. Recurrent therapy-induced ACV^R HSV-1 have been described in immunocompromised individuals, illustrating the importance of local immunity in viral clearance from infected mucosal tissues [50-53]. Due to the low prevalence of ACV^R HSV-1 in the population [54], the participants likely developed ACV^R HSV-1 during the course of ACV treatment prior to study entry. Alternatively, ACV^R HSV-1 could arise locally as the result of natural variation. HSV-1 TK genotyping can be an additional diagnostic tool to determine the anti-viral sensitivity of clinical samples [6, 30]. Rationalized selection of the appropriate antiviral agents may prevent the development of severe herpetic disease in immunocompromised patients, including individuals infected with HIV.

The limitations of the current study are the relatively small sample size with male predominance and the relatively long swabbing interval. Assessment of herpesvirus shedding in the oral cavity in persons infected with HIV can be improved by a dense time interval of mucosal sampling in addition to a detailed description of clinical symptoms (e.g., cold or flu-like symptoms) and dental procedures that may be associated with herpesvirus reactivation. Moreover, a next generation sequencing approach would allow monitoring of drug-resistant minority virus variants present in the isolate.

In summary, the current study demonstrated that short episodes of oral HSV-1 reactivations occur frequently in individuals infected with HIV. Within a daily swabbing interval, HSV-1 shedding episodes were detected with a median of 2 days. HSV-1 TK genotyping demonstrated that each individual sheds a unique HSV-1 strain among episodes, which can express ACV^R-associated mutations. VZV shedding was detected in two of 22 participants at very low copy numbers, demonstrating the low incidence of VZV shedding even in immunocompromised individuals. Future studies should address the mechanism underlying the different shedding kinetics between these two closely related human alpha-herpesviruses.

Acknowledgments

The authors acknowledge S. Deniz and S. Victor for technical assistance (Dept. of Viroscience, Erasmus MC, Rotterdam, the Netherlands). This work was financially supported by NIAID PO1 AI3073 (to AW and SS).

References

1. Roizman B, Knipe DM, Whitley RJ. Herpes simplex viruses. In: Knipe DM, Howley PM and Griffin DE, et al., eds. Fields Virology. 5th ed. Vol. 2. Philadelphia, PA: Lippincott, Williams and Wilkins, 2007:2501-2601
2. Cohrs RJ, Mehta SK, Schmid DS, Gilden DH and Pierson DL. Asymptomatic reactivation and shed of infectious varicella zoster virus in astronauts. J Med Virol 2008;80:1116-1122.
3. Kaufman HE, Azcuy AM, Varnell ED, et al. HSV-1 DNA in tears and saliva of normal adults. Invest Ophthalmol Vis Sci 2005;46:241-247.
4. Koelle DM and Wald A. Herpes simplex virus: the importance of asymptomatic shedding. J Antimicrob Chemother 2000;45 (Suppl T3):1-8.
5. Wald A, Zeh J, Selke S, Ashley RL and Corey L. Virologic characteristics of subclinical and symptomatic genital herpes infections. N Engl J Med 1995;333:770-775.
6. Duan R, de Vries RD, van Dun JM, et al. Acyclovir susceptibility and genetic characteristics of sequential herpes simplex virus type 1 corneal isolates from patients with recurrent herpetic keratitis. J Infect Dis 2009;200:1402-1414.
7. Liljeqvist JA, Tunback P and Norberg P. Asymptomatically shed recombinant herpes simplex virus type 1 strains detected in saliva. J Gen Virol 2009;90:559-566.
8. Roest RW, Carman WF, Maertzdorf J, et al. Genotypic analysis of sequential genital herpes simplex virus type 1 (HSV-1) isolates of patients with recurrent HSV-1 associated genital herpes. J Med Virol 2004;73:601-604.
9. Umene K, Yamanaka F, Oohashi S, Koga C and Kameyama T. Detection of differences in genomic profiles between herpes simplex virus type 1 isolates sequentially separated from the saliva of the same individual. Journal of Clinical Virology 2007;39:266-270.
10. Lewis ME, Leung WC, Jeffrey VM and Warren KG. Detection of multiple strains of latent herpes simplex virus type 1 within individual human hosts. J Virol 1984;52:300-305.
11. van Velzen M, van Loenen FB, Meesters RJ, et al. Latent Acyclovir Resistant Herpes Simplex Type 1 in Trigeminal Ganglia of Immunecompetent Individuals. J Infect Dis 2012;205:1539-43.
12. Birlea M, Arendt G, Orhan E, et al. Subclinical reactivation of varicella zoster virus in all stages of HIV infection. J Neurol Sci 2011;304:22-24.
13. Griffin E, Krantz E, Selke S, Huang ML and Wald A. Oral mucosal reactivation rates of herpesviruses among HIV-1 seropositive persons. J Med Virol 2008;80:1153-1159.
14. Miller AE. Selective decline in cellular immune response to varicella-zoster in the elderly. Neurology 1980;30:582-587.
15. Kim HN, Meier A, Huang ML, et al. Oral herpes simplex virus type 2 reactivation in HIV-positive and -negative men. J Infect Dis 2006;194:420-427.
16. Schacker T, Zeh J, Hu HL, Hill E and Corey L. Frequency of symptomatic and asymptomatic herpes simplex virus type 2 reactivations among human immunodeficiency virus-infected men. J Infect Dis 1998;178:1616-1622.
17. Cinque P, Vago L, Marenzi R, et al. Herpes simplex virus infections of the central nervous system in human immunodeficiency virus-infected patients: clinical management by polymerase chain reaction assay of cerebrospinal fluid. Clin Infect Dis 1998;27:303-309.
18. Mark KE, Wald A, Magaret AS, et al. Rapidly cleared episodes of oral and anogenital herpes simplex virus shedding in HIV-infected adults. J Acquir Immune Defic Syndr 2010;54:482-488.
19. Mark KE, Wald A, Magaret AS, et al. Rapidly cleared episodes of herpes simplex virus reactivation in immunocompetent adults. J Infect Dis 2008;198:1141-1149.
20. Contreras A, Mardirossian A and Slots J. Herpesviruses in HIV-periodontitis. Journal of clinical periodontology 2001;28:96-102.
21. Miller CS, Berger JR, Mootoor Y, et al. High prevalence of multiple human herpesviruses in saliva from human immunodeficiency virus-infected persons in the era of highly active antiretroviral therapy. J Clin Microbiol 2006;44:2409-2415.
22. Ceballos-Salobrena A, Gaitan-Cepeda LA, Ceballos-Garcia L and Lezama-Del Valle D. Oral lesions in HIV/AIDS patients undergoing highly active antiretroviral treatment including protease inhibitors: a new face of oral AIDS? AIDS patient care and STDs 2000;14:627-635.
23. Miller CS, Avdiushko SA, Kryscio RJ, Danaher RJ and Jacob RJ. Effect of prophylactic valacyclovir on the presence of human herpesvirus DNA in saliva of healthy individuals after dental treatment.

J Clin Microbiol 2005;43:2173-2180.
24. Posavad CM, Wald A, Kuntz S, et al. Frequent reactivation of herpes simplex virus among HIV-1-infected patients treated with highly active antiretroviral therapy. J Infect Dis 2004;190:693-696.
25. Mehta SK, Tyring SK, Gilden DH, et al. Varicella-zoster virus in the saliva of patients with herpes zoster. J Infect Dis 2008;197:654-657.
26. Nagel MA, Choe A, Cohrs RJ, et al. Persistence of varicella zoster virus DNA in saliva after herpes zoster. J Infect Dis 2011;204:820-824.
27. Wang CC, Yepes LC, Danaher RJ, et al. Low prevalence of varicella zoster virus and herpes simplex virus type 2 in saliva from human immunodeficiency virus-infected persons in the era of highly active antiretroviral therapy. Oral Surg Oral Med Oral Pathol Oral Radiol Endod 2010;109:232-237.
28. Remeijer L, Duan R, van Dun JM, et al. Prevalence and clinical consequences of herpes simplex virus type 1 DNA in human cornea tissues. J Infect Dis 2009;200:11-19.
29. van Doornum GJ, Guldemeester J, Osterhaus AD and Niesters HG. Diagnosing herpesvirus infections by real-time amplification and rapid culture. J Clin Microbiol 2003;41:576-580.
30. Duan R, de Vries RD, Osterhaus AD, Remeijer L and Verjans GM. Acyclovir-resistant corneal HSV-1 isolates from patients with herpetic keratitis. J Infect Dis 2008;198:659-663.
31. Morfin F and Thouvenot D. Herpes simplex virus resistance to antiviral drugs. Journal of Clinical Virology 2003;26:29-37.
32. Graham D, Larder BA and Inglis MM. Evidence that the 'active centre' of the herpes simplex virus thymidine kinase involves an interaction between three distinct regions of the polypeptide. J Gen Virol 1986;67:753-758.
33. Sauerbrei A, Deinhardt S, Zell R and Wutzler P. Phenotypic and genotypic characterization of acyclovir-resistant clinical isolates of herpes simplex virus. Antiviral Res 2010;86:246-252.
34. Gilbert SC. Oral shedding of herpes simplex virus type 1 in immunocompetent persons. J Oral Pathol Med 2006;35:548-553.
35. Knaup B, Schunemann S and Wolff MH. Subclinical reactivation of herpes simplex virus type 1 in the oral cavity. Oral Microbiol Immunol 2000;15:281-283.
36. Miller CS and Danaher RJ. Asymptomatic shedding of herpes simplex virus (HSV) in the oral cavity. Oral Surg Oral Med Oral Pathol Oral Radiol Endod 2008;105:43-50.
37. Scott DA, Coulter WA and Lamey PJ. Oral shedding of herpes simplex virus type 1: a review. J Oral Pathol Med 1997;26:441-447.
38. Ljungman P, Lonnqvist B, Gahrton G, et al. Clinical and subclinical reactivations of varicella-zoster virus in immunocompromised patients. J Infect Dis 1986;153:840-847.
39. Schunemann S, Mainka C and Wolff MH. Subclinical reactivation of varicella-zoster virus in immunocompromised and immunocompetent individuals. Intervirology 1998;41(2-3):98-102.
40. Steiner I, Kennedy PG and Pachner AR. The neurotropic herpes viruses: herpes simplex and varicella-zoster. Lancet Neurol 2007;6:1015-1028.
41. Pierson DL, Mehta SK, Gilden D, et al. Varicella zoster virus DNA at inoculation sites and in saliva after Zostavax immunization. J Infect Dis 2011;203:1542-1545.
42. Theil D, Derfuss T, Paripovic I, et al. Latent herpesvirus infection in human trigeminal ganglia causes chronic immune response. Am J Pathol 2003;163:2179-2184.
43. Verjans GM, Hintzen RQ, van Dun JM, et al. Selective retention of herpes simplex virus-specific T cells in latently infected human trigeminal ganglia. Proc Natl Acad Sci USA 2007;104:3496-3501.
44. Theil D, Paripovic I, Derfuss T, et al. Dually infected (HSV-1/VZV) single neurons in human trigeminal ganglia. Ann Neurol 2003;54:678-682.
45. Cohrs RJ, Laguardia JJ and Gilden D. Distribution of latent herpes simplex virus type-1 and varicella zoster virus DNA in human trigeminal Ganglia. Virus Genes 2005;31:223-227.
46. Umbach JL, Kramer MF, Jurak I, et al. MicroRNAs expressed by herpes simplex virus 1 during latent infection regulate viral mRNAs. Nature 2008;454:780-783.
47. Umbach JL, Nagel MA, Cohrs RJ, Gilden DH and Cullen BR. Analysis of human alphaherpesvirus microRNA expression in latently infected human trigeminal ganglia. J Virol 2009;83:10677-10683.
48. Stevens JG, Wagner EK, Devi-Rao GB, Cook ML and Feldman LT. RNA complementary to a herpesvirus alpha gene mRNA is prominent in latently infected neurons. Science 1987;235:1056-1059.
49. Tang S, Bertke AS, Patel A, et al. An acutely and latently expressed herpes simplex virus 2 viral microRNA inhibits expression of ICP34.5, a viral neurovirulence factor. Proc Natl Acad Sci

U S A 2008;105:10931-10936.
50. Levin MJ, Bacon TH and Leary JJ. Resistance of herpes simplex virus infections to nucleoside analogues in HIV-infected patients. Clin Infect Dis 2004;39 (Suppl 5):S248-257.
51. Morfin F, Thouvenot D, Aymard M and Souillet G. Reactivation of acyclovir-resistant thymidine kinase-deficient herpes simplex virus harbouring single base insertion within a 7 Gs homopolymer repeat of the thymidine kinase gene. J Med Virol 2000;62:247-250.
52. Saijo M, Suzutani T, Itoh K, et al. Nucleotide sequence of thymidine kinase gene of sequential acyclovir-resistant herpes simplex virus type 1 isolates recovered from a child with Wiskott-Aldrich syndrome: evidence for reactivation of acyclovir-resistant herpes simplex virus. J Med Virol 1999;58:387-393.
53. Zhu J, Koelle DM, Cao J, et al. Virus-specific CD8+ T cells accumulate near sensory nerve endings in genital skin during subclinical HSV-2 reactivation. J Exp Med 2007;204:595-603.
54. Bacon TH, Levin MJ, Leary JJ, Sarisky RT and Sutton D. Herpes simplex virus resistance to acyclovir and penciclovir after two decades of antiviral therapy. Clin Microbiol Rev 2003;16:114-128.

Chapter 7

T-cell Infiltration Correlates with CXCL10 Expression in Ganglia of Cynomolgus Macaques with Reactivated Simian Varicella Virus

Werner J.D. Ouwendijk,[1] Allison Abendroth,[2] Vicki Traina-Dorge,[3] Sarah Getu,[1] Megan Steain,[2] Mary Wellish,[4] Arno C Andeweg,[1] Albert D.M.E. Osterhaus,[1] Don.Gilden,[4,5] Georges M.G.M. Verjans,[1] and Ravi Mahalingam[4]

[1]Department of Viroscience, Erasmus Medical Center, Rotterdam, the Netherlands; [2]Centre for Virus Research, Westmead Millennium Institute, Sydney, Australia; [3]Division of Microbiology, Tulane National Primate Research Center, Tulane University, Covington, Louisiana, USA; Departments of [4]Neurology and [5]Microbiologye, University of Colorado School of Medicine, Aurora, Colorado, USA

J Virol. 2013 Mar;87(5):2979-82

Abstract

Ganglia of monkeys with reactivated simian varicella virus (SVV) contained more $CD8^+$ than $CD4^+$ T-cells around neurons. The abundance of $CD8^+$ T-cells was greater less than 2 months after reactivation than that at later times and correlated with CXCL10 RNA but not with SVV protein or open reading frame (ORF61) antisense RNA. CXCL10 RNA colocalized with T-cell clusters. After SVV reactivation, transient T-cell infiltration, possibly mediated by CXCL10, parallels varicella-zoster virus (VZV) reactivation in humans.

Varicella-zoster virus (VZV) causes varicella (chickenpox) and becomes latent in ganglia, producing zoster (shingles) upon reactivation. Because VZV infects only humans, studies of virus latency and reactivation have been restricted to autopsy tissues. Analyses of ganglia obtained after death from individuals with recent zoster revealed lymphocytic infiltration [1-2], possibly mediated by antigenic stimuli or chemokines, including CXCL10 (3). VZV-specific T cells have not been identified in human ganglia latently infected with VZV [4-5]. Simian varicella virus (SVV) infection in monkeys closely resembles VZV infection in humans [6]. Earlier, we demonstrated reactivation of latent SVV in immunosuppressed monkeys [7]. Herein, we extended those studies by examining ganglia containing reactivated SVV for infiltrating T cells. Four cynomolgus macaques (GP02, -04, -06 and -07) were naturally infected with SVV [7]. Ten to 14 days later, all monkeys developed varicella (Figure 1). At 4 months postinfection, monkeys were immunosuppressed with tacrolimus, resulting in a 34% reduction in mean white blood cell counts at 6 weeks posttreatment [7]. Monkeys GP02, -06 and -07 developed zoster at 23, 3 and 10 days, respectively, after starting tacrolimus treatment. Monkeys were euthanized at monthly intervals post-tacrolimus treatment (Figure 1). Detection of SVV glycoproteins in lungs and multiple ganglia in monkey GP04, which did not develop skin rash, confirmed subclinical reactivation [6].

Immunohistochemical analysis of consecutive ganglion tissue sections from these monkeys and from an uninfected control monkey (CTRL) for CD3, CD4 and CD8 expression showed that SVV reactivation was associated with T-cell infiltration, mostly $CD8^+$ T-cells, in ganglia along the entire neuraxis (Figure 2). T-cells were dispersed throughout ganglia. T-cell clusters, both $CD4^+$ and $CD8^+$ T-cells, were occasionally detected adjacent to neurons (Figure 2A). Rare granzyme B^+ (grB) cells, not restricted to T-cell clusters, were observed in ganglia from all monkeys (Figure 2A), suggesting that ganglion-infiltrating T-cells did not encounter their cognate antigen [8]. Ganglion-

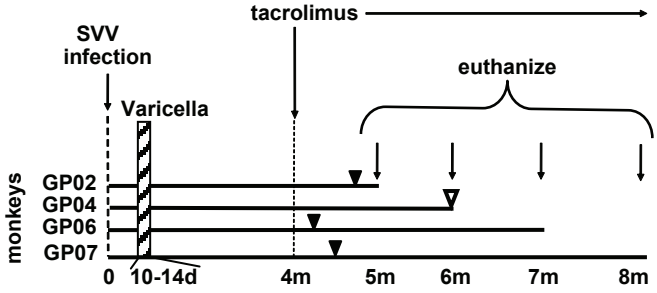

Figure 1. *Establishment of latent SVV infection in cynomologus macaques and reactivation by tacrolimus-induced immunosuppression. Four cynomolgus macaques (GP02, GP04, GP06 and GP07) were exposed to monkeys inoculated intratracheally with 10^4 plaque forming units of SVV and developed varicella rash 10 to 14 days later. At 4 months (4m) pos-exposure, all 4 monkeys received tacrolimus for the remainder of their lives. Zoster rash developed 26, 3 and 10 days (closed triangles) after tacrolimus treatment in monkeys GP02, -06 and -07, respectively. All 4 monkeys were euthanized 1-4 months postimmunosuppression. Subclinical reactivation of SVV was confirmed in monkey GP04 by detection of SVV glycoproteins in ganglia removed at necropsy (open triangle) [6].*

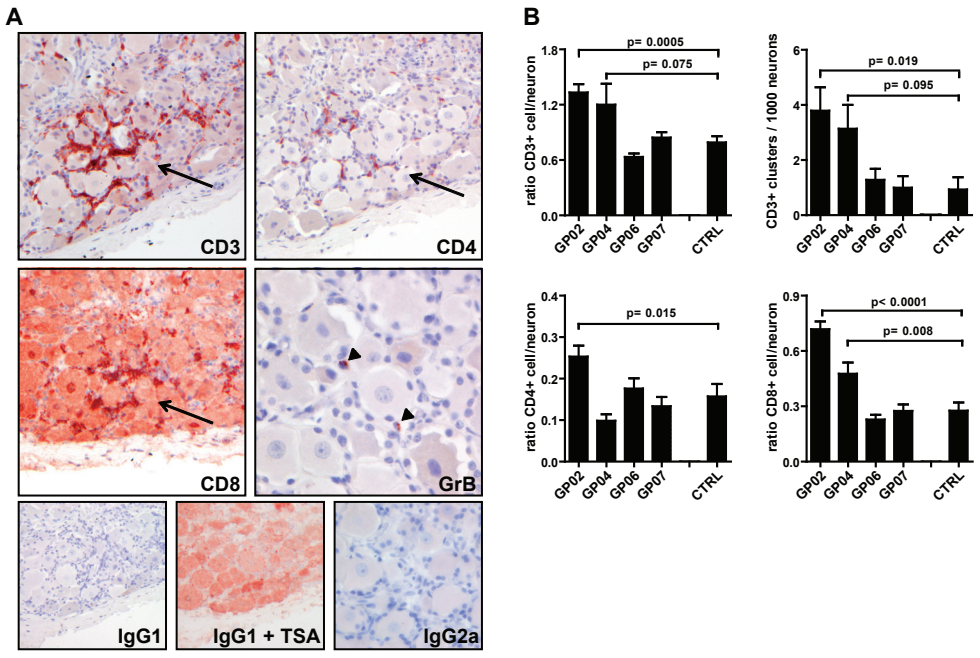

Figure 2. *Increased number of ganglion-infiltrating T-cells and T-cell clusters early after SVV reactivation in monkeys. (A) Immunohistochemical staining of consecutive sections of lumbar ganglia from monkey GP02 at 4 days after zoster rash for CD3, CD4, CD8 and granzyme B (grB) antigens or IgG1 and IgG2a isotype control antibodies. Staining was enhanced in sections stained for CD8 and the corresponding IgG1 isotype control using tyramide signal amplification (TSA). Arrows indicate T-cell clusters. Arrowheads indicate occasional grB+ cells. Stainings were visualized using the substrate 3-amino-9-ethylcarbazole (AEC) (red) and nuclei were counterstained with hematoxylin (blue). Magnifications: X200 for CD3, CD4, CD8 and the corresponding isotype controls IgG1 and IgG1 plus TSA, and X400 for grB and the corresponding isotype control IgG2a. (B) Numbers of positive T-cells and T-cell clusters (≥10 T-cells clustered around a single neuron) compared to the number of neurons in the same section. Stainings were performed as described previously (5). Data are average ratios/ monkey + standard error of the mean. The Mann-Whitney test was used for statistical analysis.*

infiltrating CD8$^+$ T-cells in zoster patients are also predominantly grB-negative [9].

We analyzed 11 to 19 ganglia from each monkey to determine the number of T cells per neuron. The number of ganglionic neurons counted in sections from each anatomical level of the neuraxis ranged from 657 to 3,991 (Table 1). Ganglia obtained from monkey GP02, euthanized at 1 week post-zoster rash, contained significantly greater numbers of CD3$^+$ (p= 0.0005), CD4$^+$ (p= 0.015) and CD8$^+$ (p<0.0001) T-cells/neuron compared to those in the control monkey (Fig. 2B) (Table 1). Monkey GP02 also contained significantly more CD3$^+$ T-cell clusters, defined as >10 T-cells surrounding a single neuron, compared to the control monkey (p= 0.019). Similarly, ganglia from monkey GP04, euthanized at 2 months postimmunosuppression, contained significantly more CD8$^+$ T-cells (p = 0.008) and had more CD3$^+$ cells (p= 0.075) and T-cell clusters (p= 0.095) than the control monkey. In contrast, T-cells and

Table 1. CXCL10 Transcript Expression and Numbers of Infiltrating T-cells in Sensory Ganglia from SVV-Infected Cynomolgus Macaques.

Monkey	Ganglion	No. of copies of CXCL10/ ng of GAPDH	Ratio (mean ± SD)				
			Total no.of neurons counted	T-cells / neurons	$CD4^+$ T-cells / neurons	$CD8^+$ T-cells / neurons	$CD8^+$ / $CD4^+$ T-cells
GP02	Cervical	NA[a]	NA	NA	NA	NA	NA
	Thoracic[b]	3.6	2,080	1.18 ± 0.18	0.24 ± 0.44	0.64 ± 0.09	2.85 ± 0.80
	Lumbar	12.0	1,265	1.48 ± 0.44	0.23 ± 0.11	0.74 ± 0.17	3.67 ± 1.46
	Sacral	11.6	1,766	1.41 ± 0.29	0.28 ± 0.09	0.83 ± 0.12	3.31 ± 1.06
GP04	Cervical	1.3	1,684	0.70 ± 0.17	0.11 ± 0.05	0.30 ± 0.08	2.91 ± 1.57
	Thoracic	1.5	1,862	0.97 ± 0.24	0.13 ± 0.02	0.43 ± 0.06	3.32 ± 0.84
	Lumbar	1.8	1,610	1.91 ± 1.66	0.03 ± 0.01	0.71 ± 0.37	31.29 ± 17.18
	Sacral	2.5	709	1.52 ± 0.19	0.08 ± 0.11	0.50 ± 0.15	9.93 ± 1.06
GP06	Cervical	0.4	3,521	0.58 ± 0.13	0.23 ± 0.11	0.23 ± 0.05	1.10 ± 0.27
	Thoracic	0.9	2,514	0.45 ± 0.05	0.11 ± 0.07	0.14 ± 0.00	1.56 ± 1.05
	Lumbar	0.8	3,991	0.70 ± 0.07	0.18 ± 0.11	0.29 ± 0.14	2.48 ± 1.66
	Sacral[b]	0.9	1,908	0.80 ± 0.14	0.13 ± 0.04	0.18 ± 0.03	1.70 ± 0.71
GP07	Cervical	0.3	704	0.80 ± 0.14	0.19 ± 0.09	0.31 ± 0.08	2.11 ± 1.25
	Thoracic[b]	0.4	2,636	0.82 ± 0.08	0.07 ± 0.02	0.19 ± 0.05	3.03 ± 0.99
	Lumbar	0.4	3,884	1.02 ± 0.25	0.23 ± 0.10	0.41 ± 0.18	1.88 ± 0.37
	Sacral	0.2	1,421	0.68 ± 0.28	0.12 ± 0.07	0.33 ± 0.16	2.93 ± 0.55
BI79	Cervical	NA	657	1.00 ± 0.42	0.30 ± 0.18	0.42 ± 0.10	1.59 ± 0.61
	Thoracic	NA	1,260	0.83 ± 0.11	0.13 ± 0.03	0.37 ± 0.07	3.05 ± 1.14
	Lumbar	NA	2,181	0.68 ± 0.22	0.10 ± 0.03	0.12 ± 0.09	1.09 ± 0.86
	Sacral	NA	1,854	0.75 ± 0.07	0.18 ± 0.01	0.30 ± 0.01	1.67 ± 0.02

[a] NA, not available
[b] Site of zoster rash [7]

T-cell clusters in monkeys euthanized at 3 and 4 months postimmunosuppression (monkeys GP06 and GP07) were similar to those of the control monkey (Fig. 2B). Overall, SVV reactivation led to a transient T-cell infiltration of ganglia, predominantly $CD8^+$ T-cells, which clustered around neurons. Notably, T-cell numbers and clusters were not increased in ganglia corresponding to the site of zoster rash (Table 1).

SVV open reading frame 61 (ORF61) antisense transcripts are abundant in latently infected ganglia of rhesus macaques [10-11]. Thus, we analyzed consecutive ganglionic sections after reactivation by *in situ* hybridization (ISH) for SVV ORF61 antisense RNA and by immunohistochemistry (IHC) for CD3 expression and SVV antigen to determine if SVV infection might mediate T-cell infiltration of ganglia. T-

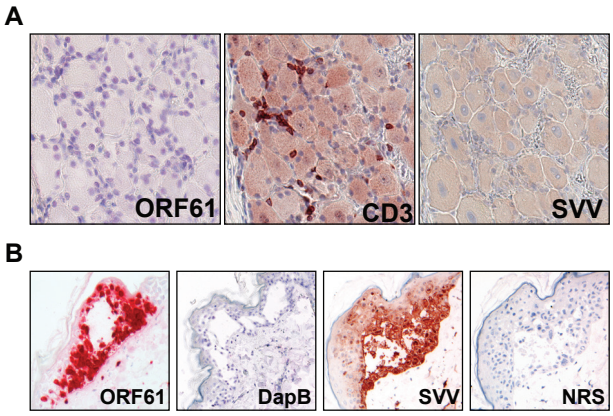

Figure 3. *CD8⁺ T-cell infiltration in ganglia of cynomolgus macaques after SVV reactivation did not correlate with local expression of SVV antigens or with the ORF61 antisense transcript. (A) Consecutive ganglionic sections from monkey GP02 at 4 days after zoster rash stained for the SVV ORF61 antisense transcript by in situ hybridization (ISH) or stained for CD3 and SVV antigens by immunohistochemistry. (B) Biopsied skin rash sections from an acutely infected African green monkey stained for the SVV ORF61 antisense transcript by ISH or for SVV antigens by IHC. Controls were biopsied skin stained for E.coli diaminopimelate B (DapB) and normal rabbit serum (NRS) by ISH and IHC, respectively. IHC stainings (5) were visualized using substrate 3-amino-9-ethylcarbazole (AEC) (red), and ISH staining was visualized using the substrate Fast Red (pink). The ISH probes were designed by Advanced Cell Diagnostics (Hayward, CA) and ISH was performed according to the manufacturer's instructions. Nuclei were counterstained with hematoxylin (blue). Magnification: 200X.*

cells did not cluster with neurons expressing SVV ORF61 antisense RNA and SVV antigens (Figure. 3A). Figure 3B is a positive control showing that SVV ORF61 antisense RNA and SVV antigens were readily detected in skin of an acutely infected monkey. The absence of SVV ORF61 antisense RNA in ganglia of our cynomolgus monkeys could reflect a difference in species studied or the well documented variability of ganglionic infection within a single subject [7]. T-cell infiltration in ganglia of monkeys after SVV reactivation did not correlate with local expression of SVV ORF61 antisense transcripts or SVV antigens.

Increased expression of the chemokine CXCL10, which recruits activated T-cells and NK cells by binding to their receptor CXCR3 [12-13], has been described in human ganglia after VZV infection *in vitro* and *in situ* in human ganglia of deceased zoster patients [3]. To test the role of CXCL10 in the SVV monkey model, consecutive ganglionic sections were stained for CD3, CD4 and CD8 by IHC and for CXCL10 transcripts by ISH. CXCL10 transcripts were readily detected within T-cell clusters, but not within neurons (Figure 4A). CXCL10-positive cells were more abundant in monkeys at 1 or 2 months than at 3 to 4 months postimmunosuppression (data not shown). The number of CXCR3-positive cells in ganglia at reactivation did not differ from that in uninfected ganglia (data not shown).

To determine whether CXCL10 transcript levels correlated with infiltrating T-cells,

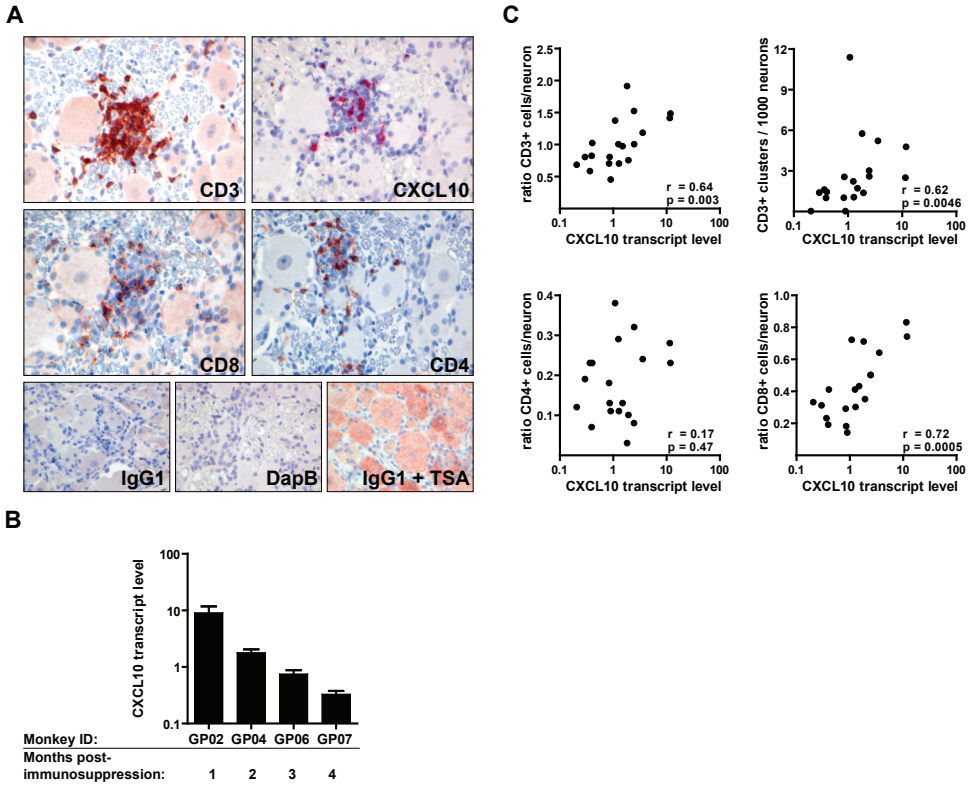

Figure 4. *T-cell infiltration correlates with CXCL10 mRNA expression in ganglia of cynomolgus macaques after SVV reactivation. (A) Consecutive tissue sections of ganglia from monkey GP02 stained for CD3, CD4 and CD8 antigens by immunohistochemistry (IHC) as described previously [5] and for CXCL10 transcript by in situ hybridization (ISH) or stained using the corresponding IgG1 isotype control antibodies by IHC (with or without tyramide signal amplification [TSA]) and the negative-control probe directed to the E.coli gene diaminopimelate B (DapB) by ISH. Stainings were TSA enhanced in sections tested for CD8 and the corresponding IgG1 isotype control. IHC stainings were visualized using the substrate 3-amino-9-ethylcarbazole (AEC) (red) and ISH staining was visualized using Fast Red (pink). The ISH probes were designed by Advanced Cell Diagnostics (Hayward, CA) and ISH was performed according to the manufacturer's instructions. Nuclei were counterstained with hematoxylin (blue). Magnification: X400. (B) Average CXCL10 transcript levels (copies of CXCL10 mRNA/ng of GAPDH mRNA ± standard error of the mean) per monkey (C) Scatter plots of CXCL10 transcript levels versus average number of CD3⁺ T-cells/neuron, CD4⁺ T-cells/neuron, or CD8⁺ T-cells/neuron and the number of T-cell clusters/1,000 neurons in the contralateral ganglia of the same monkey. Spearman's correlation test was used for statistical analysis. Real-time RT-PCR analysis was performed as described previously [11].*

RNA extracted from ganglia contralateral to the ones used for IHC were analyzed for CXCL10 transcription by quantitative RT-PCR (qPCR) using oligonucleotide primers specific for human CXCL10 (CXCL10 forward: GCCAATTTTGTCCACGTGTTG; CXCL10 reverse: GGCCTTCGATTCTGGATTCA; CXCL10 probe: TCATTGCTACAATGAAAAAGAAGGGTGAGAAGAG). Consistent with CXCL10 detection by ISH,

CXCL10 transcript levels were greatest in monkeys GP02 and GP04 at 1 and 2 months after immunosuppression (Figure 4B and Table 1), and correlated significantly with the number of T-cells (p= 0.003) and T-cell clusters (p= 0.0046). Note that the number of $CD8^+$ (p=0.0005), but not $CD4^+$ T-cells (p=0.47) correlated with CXCL10 transcript levels (Figure 4C).

Our findings demonstrate that SVV reactivation induced a transient $CD8^+$ T-cell infiltration in monkey ganglia, possibly mediated by the chemokine CXCL10. The magnitudes of CXCL10 expression and T-cell infiltration did not differ among ganglia, including those that corresponded to the dermatome associated with zoster rash. Our study parallels the previous findings that VZV reactivation induces CXCL10 expression and T-cell infiltration in human ganglia [3] and underscores the usefulness of equivalent findings in monkey ganglia containing reactivated SVV and SVV infection of primates as a useful model to study VZV pathogenesis [6]. In both settings, however, it remains unclear whether CXCL10 is the primary cause of T-cell influx or secondarily due to interferon-γ secreted by activated infiltrating lymphocytes [14-15]. Future studies of latently infected ganglia and ganglia from monkeys with zoster may help to differentiate between the two possibilities.

Acknowledgments

This work was supported in part by Public Health Service grants AG032958 (W.J.D.O, V.T.-D., D.G., G.M.G.M.V. and R.M.) and AG06127 (D.G.) from the National Institutes of Health, and grants 2M01RR005096, 1G20RR016930, 1G20RR018397, 1G20RR019628, 1G20RR013466, 1G20RR012112 and 1G20RR015169, P51 RR00164-50 (V.T.-D.) from the National Center for Research and Resources and the Office of Research Infrastructure Programs (ORIP) or the National Institutes of Health. The authors ADMEO, SG and ACA are supported by the Virgo consortium, funded by the Dutch government project number FES0908, and by the Netherlands Genomics Initiative (NGI) project number 050-060-452. We thank Dr. Subbiah Pugazhenthi for providing CXCL10 primers, Marina Hoffman for editorial assistance and Lori DePriest for manuscript preparation.

References

1. Head H and Campbell AW. The pathology of herpes zoster and its bearing on sensory localization. Brain 1900;23:353-523.
2. Kleinschmidt-DeMasters BK and Gilden DH. Varicella-Zoster virus infections of the nervous system: clinical and pathologic correlates. Arch. Pathol. Lab Med. 2001;125:770-780.
3. Steain M, Gowrishankar K, Rodriguez M, Slobedman B and Abendroth A. Upregulation of CXCL10 in human dorsal root ganglia during experimental and natural varicella zoster virus infection. J. Virol. 2011;85:626-631.
4. Theil D, Derfuss T, Paripovic I, et al.Latent herpesvirus infection in human trigeminal ganglia causes chronic immune response. Am. J. Pathol. 2003;163:2179-2184.
5. Verjans GM, Hintzen RQ, van Dun JM, et al. Selective retention of herpes simplex virus-specific T cells in latently infected human trigeminal ganglia. Proc. Natl. Acad. Sci. U. S. A. 2007;104:3496-3501.
6. Mahalingam R, Traina-Dorge V, Wellish M, et al. Latent simian varicella virus reactivates in monkeys treated with tacrolimus with or without exposure to irradiation. J. Neurovirol. 2010;16:342-354.
7. Mahalingam R, Messaoudi I and Gilden D. Simian varicella virus pathogenesis. Curr. Top. Microbiol. Immunol. 2010;342:309-321.
8. van Lint AL, Kleinert L, Clarke SRM, et al. Latent infection with herpes simplex Virus Is associated with ongoing CD8+ T-cell stimulation by parenchymal cells within sensory ganglia. J. Virol. 2005;79:14843-14851.
9. Gowrishankar K, Steain M, Cunningham AL, et al. Characterization of the host immune response in human ganglia after herpes zoster. J. Virol. 2010;84:8861-8870.
10. Ou Y, Davis KA, Traina-Dorge V and Gray WL. Simian varicella virus expresses a latency-associated transcript that is antisense to open reading frame 61 (ICP0) mRNA in neural ganglia of latently infected monkeys. J. Virol. 2007;81:8149-8156.
11. Messaoudi I, Barron A, Wellish M, et al. Simian varicella virus infection of rhesus macaques recapitulates essential features of varicella zoster virus infection in humans. PLoS. Pathog. 2009;5:e1000657. doi:10.1371/journal.ppat.1000657.
12. Loetscher M, Gerber B, Loetscher P, et al. Chemokine receptor specific for IP10 and mig: structure, function, and expression in activated T-lymphocytes. J. Exp. Med. 1996;184:963-969.
13. Wald O, Weiss ID, Wald H, et al. IFN-gamma acts on T cells to induce NK cell mobilization and accumulation in target organs. J. Immunol. 2006;176:4716-4729.
14. Groom JR and Luster AD. CXCR3 ligands: redundant, collaborative and antagonistic functions. Immunol. Cell Biol. 2011;89:207-215.
15. Derfuss T, Segerer S, Herberger S, et al. Presence of HSV-1 immediate early genes and clonally expanded T-cells with a memory effector phenotype in human trigeminal ganglia. Brain Pathol. 2007;17:389-398.

Chapter 8

Functional Characterization of Ocular-Derived Human Alphaherpesvirus Cross-Reactive CD4 T-cells

Werner J.D. Ouwendijk,[1] Annemieke Geluk,[2] Saskia L. Smits,[1] Sarah Getu,[1] Albert D.M.E. Osterhaus,[1] and Georges M.G.M. Verjans[1]

[1]Department of Viroscience, Erasmus Medical Center, Rotterdam, the Netherlands; [2] Department of Infectious Diseases, Leiden University Medical Center, Leiden, the Netherlands

Submitted, 2013

Abstract

Intraocular varicella-zoster virus (VZV) and HSV type 1 (HSV-1) infections cause sight-threatening uveitis. The disease is characterized by an intraocular inflammatory response involving herpesvirus-specific T-cells. T-cell reactivity to the non-causative human alphaherpesvirus (αHHV) is commonly detected in the affected eyes of herpetic uveitis patients, suggesting the role of cross-reactive T-cells in the disease. This study aimed to identify and functionally characterize intraocular αHHV cross-reactive T-cells. VZV protein IE62, which shares extensive homology with HSV ICP4, is a major T-cell target in VZV uveitis. Two VZV-specific CD4 T-cell clones (TCC), recovered from the eye of a VZV uveitis patient, recognized the same $IE62_{918-927}$ peptide using different TCR and HLA-DR alleles. The $IE62_{918-927}$ peptide bound with high affinity to multiple HLA-DR alleles and was recognized by blood-derived T-cells of 5 of 17 HSV-1/VZV-seropositive healthy adults, but not in cord blood donors (n=5). Despite complete conservation of the IE62 epitope in the orthologous protein ICP4 of HSV-1 and HSV-2, the TCC recognized VZV and HSV-1 but not HSV-2 infected B-cells. This was not attributed to proximal epitope-flanking amino acid polymorphisms in HSV-2 ICP4. Notably, VZV/HSV-1 cross-reactive CD4 T-cells controlled VZV, but not HSV-1 infection of human primary retinal pigment epithelium (RPE) cells. In conclusion, we report on the first VZV/HSV-1 cross-reactive CD4 T-cell epitope, which is HLA-DR promiscuous and immuneprevalent in co-infected individuals. Moreover, ocular-derived peptide-specific CD4 TCC controlled VZV but not HSV-1 infection of RPE cells, suggesting that HSV-1 actively inhibits CD4 T-cell activation by infected human RPE cells.

Introduction

Varicella-zoster virus (VZV) and HSV type 1 (HSV-1) are closely related endemic human alphaherpesviruses (αHHV) [1-2]. Primary VZV and HSV-1 infections are acquired during childhood and lead to the establishment of a lifelong latent infection of sensory neurons [1-2]. VZV causes varicella (chickenpox) as a primary infection and herpes zoster (shingles) upon reactivation [2]. Primary and recurrent HSV-1 infections typically cause oral and ocular lesions [1]. Herpesvirus infections induce CD4 and CD8 T-cell responses that are essential to control acute infection and to prevent recrudescent disease [3-6]. T-cell responses are beneficial to the host, but on occasion and depending on the anatomic site of the body (e.g., brain and eye) localized αHHV-specific T-cell responses may orchestrate immunopathology leading to irreversible tissue damage [7].

Acute retinal necrosis (ARN) is a rapidly progressing and potentially blinding uveitis entity, which is commonly initiated by an intraocular infection with HSV-1 or VZV in immunecompetent individuals [8-10]. The clinical pictures of HSV-1 and VZV ARN are identical suggesting a common pathological mechanism [9]. The pathogenesis of ARN involves the destruction of uveal tissue by both the cytopathic effect of the triggering αHHV and local innate and adaptive inflammatory responses [11-15]. Studies on the experimental HSV-1 ARN mouse model have demonstrated the pathogenic role of ocular infiltrating T-cells [11, 16]. The intraocular virus-specific T-cell response in αHHV uveitis patients, mediated by cytotoxic CD4 and CD8 Th0/Th1-like T-cells, is preferentially directed to the causative herpesvirus [17-21]. Herpesvirus particles and antigens have been detected in the neural retina and retinal pigment epithelial (RPE) cell layer of patients with HSV and VZV posterior uveitis [22-24]. The co-localization of T-cells in these lesions suggests the role of RPE cells as APC in herpetic uveitis [24].

The VZV and HSV proteomes are highly homologous [25], suggesting that αHHV-specific T-cells may cross-react with orthologous herpesvirus proteins. Indeed, T-cell reactivity to the non-causative αHHV is commonly detected, albeit at low frequency, in affected eyes of both HSV-1 and VZV uveitis patients [19]. We have identified VZV immediate early protein 62 (IE62) as a major target antigen of the intraocular VZV-specific T-cell response in VZV uveitis patients [18]. VZV open reading frame (ORF) 62 encodes for the 175 kDa tegument protein IE62, which is expressed with immediate early kinetics and functions as the major transactivator protein during VZV infection [26-27]. VZV IE62 is highly homologous with the orthologous infected cell polypeptide 4 (ICP4) of HSV-1 and HSV-2 (~30% amino acid homology) and complements ICP4 in HSV-1 [28]. Consequently, VZV IE62 is a promising candidate antigen of αHHV cross-reactive T-cells in VZV uveitis patients. The aim of this study was to identify and functionally characterize intraocular αHHV cross-reactive T-cells in relation to the pathology of αHHV uveitis.

Materials and Methods

Cell lines and T-cell clones

Human melanoma MeWo cells (American Type Culture collection (ATCC) ID; HTB-65) and African green monkey kidney epithelial Vero cells (ATCC ID: CCL-81) were grown in DMEM (Lonza) containing 10% heat-inactivated fetal bovine serum (FBS) (Sigma) and antibiotics. The human RPE cell line ARPE-19 (ATCC ID: CRL-2302) was cultured in a 1:1 ratio (vol/vol) of DMEM and Ham's F12 nutrient mixture (both Lonza) supplemented with 10% heat-inactivated FBS and antibiotics (hereafter referred to as S10F). The generation of two primary human RPE cell lines, designated RPE 171 and 172, has been described [17]. The primary RPE cell lines were used from passage 6 to 12.

The intraocular fluid (IOF)-derived VZV-specific CD4 T-cell clones (TCC) 7 and TCC 53 were obtained from the affected eye of a VZV ARN patient (patient #3 in reference 18). The IOF-derived HSV-1–specific CD4 TCC 44 was obtained from the affected eye of a HSV-1 ARN patient (patient #1 in reference 21). Autologous B-cell lines (BLCL) were obtained by transformation of peripheral blood B-cells with Epstein-Barr virus as described [19, 21]. TCC were cultured in U-bottom 96-well plates (Greiner Bio-One) in RPMI-1640 (Lonza) supplemented with 10% heat-inactivated human pooled serum and antibiotics (hereafter referred to as T-cell medium; TCM) [18, 21]. The study was approved by the local ethical committee and informed consent was provided by the uveitis patients and blood donors and the parents of the cord blood donors according to the Declaration of Helsinki.

Viruses and viral antigens

Recombinant HSV-1 (HSV-1.EGFP-VP16) and VZV (VZV.EGFP-ORF66) strains express enhanced green fluorescent protein (EGFP) conjugated to the viral proteins VP16 and ORF66 under control of the HSV-1 UL48 and VZV ORF66 promoter, respectively [29-30]. Wild-type VZV (strain Dumas), HSV-1 (strain KOS) and HSV-2 (strain MS) were used. HSV and VZV strains were grown in Vero cells and ARPE-19 cells, respectively [19, 21]. Monolayers of virus-infected cells showing >80% cytopathic effect, and mock-infected cells as controls, were scraped in PBS, lysed by three successive freeze-thaw cycles and cleared by centrifugation (1000 x g for 5 min). The antigen preparations were inactivated by UV-irradiation ($2.5x10^{-2}mW/mm^2$) and stored in aliquots at -80°C.

Flow cytometry

The following fluorochrome-conjugate mouse mAbs were used for flow cytometry: anti-CD3 (clone SP34-2; APC), anti-CD4 (clone SK3; PerCP) and anti-HLA-DR (clone L243; PerCP) (all BD Biosciences). The TCR Vβ gene usage of TCC 7 and 53 was determined using the flow cytometric IOTest Beta Mark assay according to the manufacturer's protocol (Beckman Coulter). Fluorescence intensity was measured on a BD FACS Canto II and analyzed using FACS Diva software (BD Biosciences) and WinMDI 2.9 software.

Sequence analysis of TCR gene rearrangement
Total RNA and DNA were isolated from TCC 7 and 53 using TRIzol combined with the RNeasy mini kit (Roche), and the MagnaPure DNA Tissue Kit II (Roche) by using the MagnaPure LC Isolation station (Roche), respectively. RNA was converted into cDNA using oligo(dT) and reverse transcriptase as described [31]. DNA and cDNA were used as templates for the amplification of TCRB and TCRA, respectively. TCRB multiplex PCR was performed according to the BIOMED-2 multiplex PCR protocol, while TCRA rearrangements were analysed by cDNA-based multiplex PCR reactions [32]. TCRB- and TCRA-specific PCR products from the valid size ranges were excised from agarose gels, purified, and subjected to sequence analysis using an ABI3730XL sequencer (Applied Biosystems). Sequence reactions were performed in both directions separately in a multiplex setting [32]. To identify TCR V, D and J gene usage, sequence data were compared with TCR sequences deposited in the ImMunoGeneTics database (http://www.imgt.org).

Synthetic peptides and HLA-DR allele binding affinity
The N-terminal FITC-conjugated and non-modified peptides, varying in length from 9 to 12 amino acids (aa), were synthesized by Sigma Aldrich and GeneCust, respectively, to >70% purity. The HLA-DR binding potential was predicted using the following HLA-II binding epitope prediction software packages: Propred [33], ARB [34], MHCPred [35], NetMHCII [36], NetMHCIIpan [36] and SVRMHC [37]. Peptides were considered to bind to a specific HLA-DR allele if ≥4 out of 6 programs predicted high affinity peptide binding. The HLA-DR allele-specific peptide binding affinity was determined as described previously [38] using affinity-purified HLA-DR molecules and FITC-conjugated peptides known to bind with high affinity to the respective HLA-DR alleles, combined with an increasing concentration of the virus-derived peptide of interest. Binding affinities were considered to be high (<1 μM), intermediate (1–10 μM), weak (10–100 μM) or absent (>100 μM) [38].

Plasmids
Sequences coding for HSV-1 ICP4 residues 945-1054 (Genbank accession number: ACM62283) and HSV-2 ICP4 residues 972-1082 (Genbank accession number: NP_044530) were amplified by PCR from DNA isolated from Vero cells infected with wild-type HSV-1 (KOS strain) and HSV-2 (strain MS) DNA using the following primers: HSV-1_Fw (5'-gaagatctccaccatgGGCGGGGCCTCGGGGGGGCCG-3'), HSV-1_Rv (5'ggaattcgCTCGCACGCCAGGTAGGCGTG-3'), HSV-2_Fw (5'-gaagatctccaccatgGGCCGCGCCGGGGGCGGGCCC-3') and HSV-2_Rv (5'-ggaattcgCTCGCAGGCCAGGTAGGCGTG-3'). Amplification was performed using Pfu Turbo DNA polymerase (Stratagene) and the following conditions: denaturation for 5 min at 95°C, 40 cycles (1 min at 95°C, 1 min at 65°C and 30 sec at 72°C) and final extension for 10 min at 72°C. The resulting amplicons were purified using the MinElute Gel Extraction kit (Qiagen) and cloned into pEGFP-N1 plasmid (BD Biosciences) in frame with the open reading frame of EGFP, using restriction enzymes BglII and EcoRI. Plasmid DNA was isolated using the Qiagen Plasmid Midi kit to confirm appropriate in-frame insertion of the target sequence in the vector by sequence analysis using the BigDye Terminator (version 3.1) cycle sequencing kit (Applied Biosystems) and the ABI

Prism 3100 Genetic Analyzer (Applied Biosystems).

IFNγ ELISPOT assay
Autologous BLCL were used as APC for IFNγ ELISPOT assays in three different ways. First, BLCL were infected overnight with HSV at a multiplicity of infection (MOI) of 10 or pulsed overnight with predefined optimal concentrations of protein lysates obtained from VZV-, HSV- and mock-infected cells. Second, BLCL were pulsed overnight with the indicated synthetic peptides in RPMI-1640 medium (2 μM, or as indicated) [20]. Third, BLCL were nucleofected with pEGFP-N1 control plasmid and plasmids expressing HSV-1 ICP4 aa 945 – 1054 (pEGFP-N1/HSV-1:ICP4945-1054) or HSV-2 ICP4 aa 972 – 1082 (pEGFP-N1/HSV-2:ICP4972-1082) using Amaxa Cell Line Nucleofector kit V (Lonza). IFNγ ELISPOT assays were performed in triplicate, according to the manufacturer's instructions (Mabtech AB). Briefly, T-cells (5-20 x 10^3 cells/well) were pre-incubated with BLCL (2 x 10^4 cells/well) for 1.5 h at 37°C in U-bottom 96-well plates (Greiner Bio-One) followed by an additional 6 h incubation at 37°C in anti-IFNγ pre-coated Multiscreen HTS-IP ELISPOT plates (Millipore) [20]. T-cells were washed away and the secondary anti-IFNγ mAb followed by the streptavidin-alkaline-phosphatase mAb were added to the wells. Spots were visualized by adding nitroblue tetrazolium 5-bromo-4-chloro-3-indoylphosphate (NBT/BCIP) substrate (Lucron Elitech). Resulting blue IFNγ spots were counted with an automated ELISPOT reader (Sanquin Reagents). Each experiment was repeated at least twice.

VZV peptide $IE62_{915-929}$ reactive T-cell responses in blood samples
PBMC were isolated from heparized peripheral blood samples of 17 HLA-typed HSV-1 and VZV seropositive healthy adult individuals and 5 cord blood (CB) donors. The donor's HLA-DR genotype was determined as described [17]. The PBMC and CBMC fractions (10^6 each) were incubated with the VZV peptide $IE62_{915-929}$ (0.1 μM) in TCM with IL-2 added after 3 days and supplemented after an additional 5 days of culture. After 1.5 to 2 weeks of culture, the resulting short-term PB- and CB-derived T-cell cultures were assayed for reactivity to VZV $IE62_{915-929}$ peptide, and medium as negative control, by IFNγ ELISPOT as described above.

T-cell responses to virus-infected or viral antigen pulsed human RPE cells
Primary human RPE cell lines were grown to confluence in 48-well plates and the expression of HLA-II and co-stimulatory molecules was induced by incubation with recombinant human IFNγ (500 U/mL; PeproTech) for 3 days in S10F as described [17]. The HLA-II genotype of the uveitis patients and RPE cell lines, and the HLA-II restriction of TCCs were previously determined [17-18, 20]. The RPE 171 cell line expresses HLA-DRB1*0301;0701 compatible with the HLA-DRB1*0703 restriction element of TCC 53, whereas RPE 172 cells express HLA-DRB1*1201;1501 compatible with the HLA-DRB1*1501 restriction element of TCC 44 [17-18, 20]. Human RPE cells were infected with HSV-1.EGFP-VP16 or VZV.EGFP-ORF66, washed extensively and 7.5-15 x 10^4 T-cells were added to each well. At the indicated times cell-free conditioned medium was collected, RPE cells were harvested by trypisinization and the frequency of viable EGFP-expressing RPE cells was determined by flow cytometry. Supernatants were clarified by centrifugation for 5 min at 400 x

g, stored at -20°C for subsequent assayed by ELISA for IFNγ levels (eBioscience). Experiments were performed in triplicate and repeated at least three times. Alternatively, RPE cells were incubated with predefined optimal concentrations of viral Ag overnight at 37°C. Antigen-pulsed RPE cells were washed and 7.5-15 x 10^4 T-cells was added to each well for 24 h. Cell-free conditioned TCM was assayed for the amount of secreted IFNγ by ELISA (eBioscience). Experiments were performed in triplicate and repeated at least twice.

Immunofluorescent staining and confocal microscopy
Primary human RPE cell lines were grown to confluence on glass cover slips in 24-well plates, stimulated with IFNγ (500 U/ml) for 3 days in S10F and infected with HSV-1.EGFP-VP16 and VZV.EGFP-ORF66 for 24 h at 37°C. Virus-infected RPE cells were fixed using 4% (w/v) paraformaldehyde dissolved in PBS for 15 min at room temperature (RT), permeabilized with 0.1% (v/v) Triton-X dissolved in PBS for 10 min and incubated with mAb anti-HSV-1 ICP0 (Santa Cruz Biotechnology) or polyclonal rabbit serum directed to VZV glycoprotein E (gE; kind gift from Dr. P.R. Kinchington) for 1 h at RT. The RPE cells were incubated with Alexa Fluor 594-conjugated secondary goat anti-mouse or anti-rabbit antibodies (Invitrogen) and mounted in Vectashield containing 4',6-diamidino-2-phenylindole (DAPI) (Vector Labs). Cells were analyzed using a Zeiss LSM 700 confocal laser scanning microscope fitted on an Axio Observer Z1 inverted microscope (Zeiss). Images were obtained using 2X frame averaging and the pinhole adjusted to 1 airy unit. ZEN 2010 software (Zeiss) was used to adjust brightness and contrast.

Results

Two ocular-derived CD4 TCC recognize VZV peptide IE62$_{918-927}$ using discordant HLA-DR alleles and TCR
Two protein domains of VZV IE62 and the orthologous HSV-1 protein ICP4 are highly conserved among alphaherpesvirinae: a domain that contains sites for DNA binding and homo-dimerization (IE62$_{463-636}$ and ICP4$_{326-482}$) and the large C-terminal region (IE62$_{750-1187}$ and ICP4$_{814-1254}$) involved in transactivation of virus genes [28, 39]. Previously, we reported that IE62 is a major target antigen of the intraocular VZV-specific T-cell response in VZV uveitis patients [18]. Two IE62-specific CD4 TCC (TCC 7 and TCC 53), which were recovered from intraocular fluid from the same affected eye of a VZN ARN patient, reacted to the same VZV IE62 region (IE62$_{901-930)}$ using HLA-DR*1404 and -DR*0703 as HLA restriction element, respectively [18]. Herein, we determined the minimal T-cell epitope of both TCC using partially overlapping 9- to 12-meric peptides that cover the IE62$_{901-930}$ region (Figure 1A and data not shown). Both TCC recognized IE62$_{918-926}$ and IE62$_{919-927}$ peptides, indicating that the TCC are directed to the same T-cell epitope (IE62$_{918-927}$; LLLSTRDLAF). Because both TCC recognized the same IE62 peptide by disparate HLA-DR alleles, we determined their TCRA and TCRB genotype. First, the TCC's TCR Vβ gene (TRBV) usage was determined by flow cytometry using a panel of

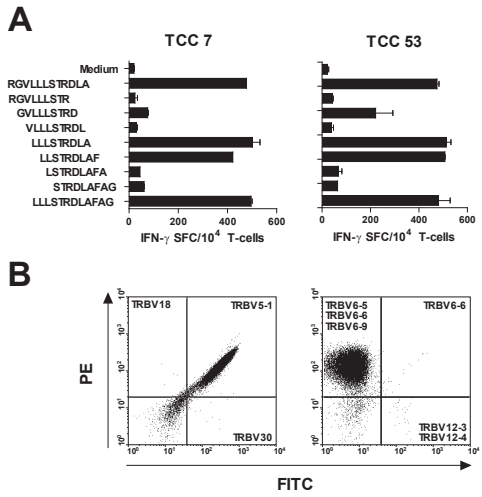

Figure 1. *Identification of the minimal T-cell epitope and TCR Vβ gene usage of TCC 7 and 53. (A) T-cell clones (TCC) were cultured for 6 h with autologous EBV-transformed B-cell lines (BLCL) pulsed with the indicated peptides or medium as a negative control. T-cell reactivity was determined by IFNγ ELISPOT. Data are presented as mean ± SEM number of IFNγ spot-forming cells (SFC)/10⁴ T-cells. (B) TCR Vβ gene (TRBV) usage was determined by flow cytometry using a panel of commercial single or dual FITC- and PE-conjugated human TRBV-specific mAbs. Dot plots showing discriminatory TRBV staining of TCC 7 (left panel) and TCC 53 (right panel) are presented. TRBV gene annotation is according to reference 40. T-cells were gated on viable CD3+CD4+ cells and quadrants were set with reference to isotype controls.*

Table 1. TCRαβ Gene Usage and CDR3 Region of T-cell Clones 7 and 53

	TCR gene usage[a]			
TCC[b]	**TCR V**	**TCR D**	**TCR J**	**Aa sequence CDR3 region**
7	TRAV3*01	NA[c]	TRAJ6*01	CAVRDMGTGGSYIPTF
7	TRBV5-1*01	TRBD2*01	TRBJ2-5*01	CASSSSGGQETQYF
53	TRAV23/DV6*01	NAc	TRAJ27*01	CAAGGSTNAGKSTF
53	TRBV6-5*01	TRBD1*01	TRBJ1-5*01	CASSPTGALRGNQPQHF

[a]TCR variable (V), diversity (D) and joining (J) gene annotation of the TCR α (TRA) and β (TRB) chains are according to reference 40.
[b]TCC, T-cell clone.
[c]NA, not applicable.

commercial single or dual FITC- and PE-conjugated human TRBV-specific mAbs. TCC 7 expressed TRBV5-1 and TCC 53 reacted with a mAb recognizing TRBV6-5, TRBV6-6 and TRBV6-9 (Figure 1B). Finally, the TCR variable (V), joining (J) and diversity (D) gene usage, and the corresponding CDR3 region, of the TCC's TCRα and TCRβ chain were defined by multiplex RT-PCR and sequencing. The data showed that both TCC expressed not only different TCR V, J and D gene segments, but also

Table 2. Characteristics and Protein Sequences of Alphaherpesvirinae Proteins Homologous to VZV Protein IE62.

Genus	Host	Name	Genbank ID[a]	Location[b]	Amino acid sequence of homologous herpesvirus proteins[c]
Simplexvirus	Human	Human herpesvirus 1	ACM62283	979 - 1,029	AWAGNWTGAPDVSALGAQGV**LLLSTRDLAF**AGAVEFLGLLASAGDRRLIV
	Human	Human herpesvirus 2	NP_044530	1,007 - 1,057	----------G-C------
	Monkey	Cercopithecine herpesvirus 2	YP_164502	856 - 906	--------P----------A-AG---V-
	Monkey	Papiine herpesvirus 2	YP_443906	856 - 906	--------P----------A-AG---V-
	Monkey	Macacine herpesvirus 1	NP_851919	877 - 927	--------P----------Y-----A-AG---V-
Varicellovirus	Human	Human herpesvirus 3	AAK19968	898 - 1,048	--------P------N-R----------Y-SRLASAR----L-
	Monkey	Cercopithecine herpesvirus 9	AAA03549	667 - 717	------S-P----Q-N-R-I----------Y-SR-----R-L--L
	Cow	Bovine herpesvirus 1	NP_045364	975 - 1,025	----R----------R----Y-CARLA-AR-----
	Cow	Bovine herpesvirus 5	NP_954953	1,037 - 1,087	----S----------**A**------R----Y-C-RLA-AR-----
	Dog	Canid herpesvirus 1	BAA32781	1,050 - 1,100	--------K-VIDS-NS----------**K**------C--Y-C-RLGSAR-----
	Horse	Equid herpesvirus 1	BAD83403	1,145 - 1,195	----------N----------**G**----T-C--Y-C-RLGSAR-K-L-
	Horse	Equid herpesvirus 4	NP_045296	1,111 - 1,161	--------P------N----------**G**----T-CI-Y-C-RLGSAR-K-L-
	Gazelle	Equid herpesvirus 9	YP_002333545	1,134 - 1,184	----------N----------**G**----T-C--Y-C-RLGSAR-K-L-
	Cat	Felid herpesvirus 1	YP_003331583	1,057 - 1,107	S-----S-P--IRR-N----------**G**------C--Y-C-RLGSAR-----
	Pig	Suid herpesvirus 1	YP_068382	1,115 - 1,165	--------R--IGR-N----------**A**---**G**------Y-CSRLG-AR-----

[a] Genbank accession number of the reference viral protein used in the alignment.
[b] Location of N- and C-terminal residues of the respective protein fragment used in the alignment.
[c] Alignment of the homologous herpesvirus proteins with reference to human herpesvirus 1 protein ICP4. Shown are the amino acid sequences of the proteins' region homologous to the VZV peptide $IE62_{918-927}$ and its flanking residues. Residue changes are shown. The region of the VZV $IE62_{918-927}$ T-cell epitope is boxed.

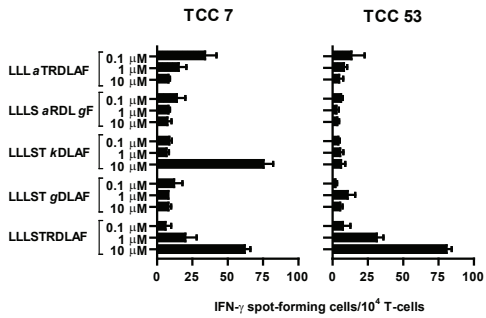

Figure 2. *Cross-reactivity of T-cell clones 7 and 53 towards VZV IE62$_{918-927}$ alphaherpesvirinae orthologous peptides. T-cell clones (TCC) were cultured for 6 h with autologous EBV-transformed B-cells pulsed with increasing concentrations of the indicated alphaherpesvirinae-derived peptides or medium as a negative control. Peptide sequences are based on the homologous alphaherpesvirinae protein sequences presented in Table II. Residue changes compared to the consensus human alphaherpesvirus-specific peptide sequence (i.e. LLLSTRDLAF) are shown in italics. T-cell reactivity was determined by IFNγ ELISPOT. Data are presented as mean ± SEM number of IFNγ spot-forming cells per 10^4 T-cells.*

had distinct TCR CDR3 regions (Table 1). Collectively, the data demonstrate that two ocular-derived VZV-specific CD4 TCC recognize the same IE62$_{918-927}$ T-cell epitope, located within the highly conserved C-terminal region of VZV IE62, using discordant HLA-DR alleles and TCR.

The VZV IE62$_{918-927}$ CD4 T-cell epitope is highly conserved among alphaherpesvirinae

We aligned the aa sequences of published orthologous alphaherpesvirus proteins to determine if the VZV IE62$_{918-927}$ T-cell epitope is conserved among alphaherpesvirinae of diverse animal species. Notably, VZV IE62$_{918-927}$ is completely conserved among human and monkey simplexviruses and varicelloviruses, whereas orthologous proteins of more distant varicelloviruses varied only 1 to 2 residues (Table 2). Autologous BLCL were pulsed with increasing concentrations of peptides corresponding to the IE62$_{918-927}$ variants to determine cross-species T-cell reactivity (Table 2 and Figure 2). TCC 7 recognized its cognate IE62$_{918-927}$ epitope and cross-reacted - only at high concentrations - with the orthologous canid herpesvirus 1 peptide (LLLSTKDLAF). TCC 53 recognized only its cognate IE62$_{918-927}$ T-cell epitope. Collectively, the data indicated that two VZV-specific CD4 TCC recognize a peptide that is highly conserved among primate alphaherpesvirinae.

The VZV IE62 peptide binds to multiple HLA-DR alleles and is a common target of memory T-cells in blood of HSV-1 and VZV co-infected healthy individuals

In contrast to MHC-I, the binding motifs of MHC-II molecules are highly degenerative enabling certain peptides, so-called promiscuous peptides, to bind to multiple MHC-II alleles [41-42]. Based on the disparate HLA-DR allele usage of the IE62$_{918-927}$ reactive TCC 7 and 53, we determined the HLA-DR promiscuity of the IE62 epitope in detail by in silico binding analyses. Notably, peptide IE62$_{915-929}$ was predicted to

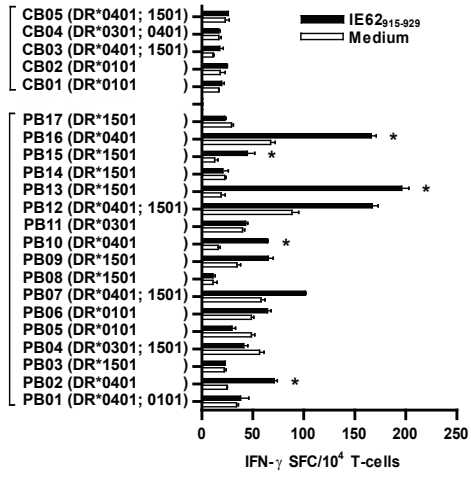

Figure 3. *Detection of VZV peptide IE62$_{915-929}$ reactive CD4 T-cells in peripheral blood (PB)- and cord blood (CB)-derived mononuclear cells (MC) of HLA class II typed healthy adults and newborns, respectively. PBMC and CBMC, isolated from HSV-1 and VZV co-infected individuals (n=17) and naïve cord blood donors (n=5), were stimulated with peptide IE62$_{915-929}$ for 1 week in vitro and subsequently analyzed for reactivity to peptide IE62$_{915-929}$ by IFNγ ELISPOT. The donors' HLA-DR genotypes presented are those able to bind the IE62 peptide with high affinity (see Table 3). Data are presented as mean ± SEM number of IFNγ spot-forming cells (SFC)/10^4 T-cells. *Short-term T-cell cultures with ≥2-times IFNγ SFC in response to IE62$_{915-929}$ compared to medium.*

bind with high affinity to multiple HLA-DR alleles, including HLA-DR*0101, -DR*0301, -DR*0401, -DR*0701, -DR*1101, -DR*1301 and -DR*1501 (data not shown). Next, we determined the binding affinity of the peptides IE62$_{915-926}$, IE62$_{918-926}$, IE62$_{919-927}$ and IE62$_{918-929}$ for HLA-DR*0101, -DR*0201, -DR*0301 and -DR*0401 using an *in vitro* competition assay [38]. Except for IE62$_{919-927}$ binding to HLA-DR*0301, all peptides bound with high (<1 μM) or intermediate (1–10 μM) affinity to HLA-DR*0101, -DR*0201, -DR*0301 and -DR*0401 molecules (Table 3).

Based on the HLA-DR promiscuity and the conservation of the IE62 T-cell epitope among αHHV we hypothesized that the peptide is a target of memory T-cells in blood of HSV-1 and VZV co-infected individuals. PBMC of 17 HSV-1 and VZV seropositive healthy adults, and as control CBMC of 5 donors, were incubated with the IE62$_{915-929}$ peptide to enrich for peptide-specific memory T-cells. Donors were selected for expression of the following predicted epitope-binding HLA-DR alleles: HLA-DR*0101, -DR*0301, -DR*0401 and -DR*1501. The resulting short-term T-cell cultures were assayed for peptide-specific T-cell reactivity by IFNγ ELISPOT. Five of 17 HSV-1 and VZV seropositive healthy donors, including three HLA-DR*0401^{POS} and two HLA-DR*1501^{POS} donors, responded to IE62$_{918-929}$ (Figure 3). No T-cell responses to IE62$_{915-929}$ were observed in 5 cord blood donors, demonstrating the specificity of the observed T-cell responses. Overall, these data demonstrated that the identified VZV IE62 epitope is HLA-DR promiscuous and is a common target antigen of memory

Table 3. Binding Affinity of VZV Protein IE62-Derived Peptides to Different HLA-DRB1 Alleles

Location[a]	Aa sequence[b]	DRB1*0101	DRB1*0201	DRB1*0301	DRB1*0401
915-926	RGVLLLSTRDLA	0.04[c]	0.3	0.2	0.006
918-926	LLLSTRDLA	0.1	4.0	0.1	0.2
919-927	LLSTRDLAF	1.0	10	>20	0.3
918-929	LLLSTRDLAFAG	0.06	1.1	0.08	0.02

[a] Location of N- and C-terminal residues (Aa) of the respective peptide in VZV IE62.
[b] Amino acid (Aa) sequence according to a reference VZV protein IE62 sequence (Genbank accession number NP_040184.1).
[c] Binding affinity of each peptide is expressed as the IC50 value, referred to as the test peptide concentration (μM) at which binding of the HLA-DR allele-specific standard fluorescence labelled peptide is reduced to 50% of its maximal value. IC50 < 1 μM: high binding affinity; IC50 1 – 10 μM: intermediate binding affinity; IC50 10 – 100 μM: weak binding affinity; IC50 >100 μM: no binding affinity [38].

CD4 T-cells in blood of HSV-1 and VZV co-infected healthy individuals.

VZV IE62-specific CD4 TCC recognize HSV-1, but not HSV-2 infected B-cells
The complete conservation of the identified CD4 T-cell epitope among αHHV suggests that the respective VZV-specific TCC recognize both HSV-1 and HSV-2 infected cells. Surprisingly, both TCC 7 and 53 recognized HSV-1, but not HSV-2 infected autologous BLCL (Figure 4A). Because VZV does not infect BLCL efficiently (data not shown), we used BLCL pulsed with a VZV protein lysate as APC. In contrast to HSV-1 and VZV, HSV-2 antigen pulsed BLCL were not recognized (Figure 4A and data not shown).

Epitope-flanking residues affect antigen processing and subsequent presentation of the cognate peptide to T-cells [43-45]. Alignment of the HSV ICP4 protein sequences revealed 9 aa substitutions and 1 aa insertion in the epitope-flanking region of HSV-2 compared to HSV-1 ICP4 (Figure 4B). To determine if these epitope-flanking residues were involved in the differential T-cell recognition of HSV ICP4, fragments of HSV-1 ICP4 (aa 945-1054) and HSV-2 ICP4 (aa 972-1082) encompassing the αHHV conserved T-cell epitope plus 54 (HSV-1) or 55 (HSV-2) N-terminal flanking residues and 46 C-terminal residues were cloned into an expression vector. The TCC were cultured with autologous BLCL nucleofected with plasmids encoding HSV-1 $ICP4_{945-1054}$ and HSV-2 $ICP4_{972-1082}$ (Figure 4C). Notably, both TCC recognized BLCL that expressed the HSV-1 and HSV-2 ICP4 protein fragments implicating that the failure to recognize the αHHV conserved CD4 T-cell epitope in the context of HSV-2 infection was not due to proximal epitope-flanking aa polymorphisms.

VZV/HSV-1 cross-reactive CD4 T-cells control VZV, but not HSV-1 infection in human RPE cells
To determine the functional properties of VZV/HSV-1 cross-reactive CD4 T-cells, we assayed the capacity of TCC 53 to inhibit VZV and HSV-1 replication in target cells relevant to the pathogenesis of ARN: human RPE cells [22-24]. Under physiological

conditions and in cell culture human RPE cells do not express HLA-DR. The expression of inflammatory cytokines, including IFNγ and TNFα, in affected eyes of uveitis patients shape resident RPE cells to potent APC [46-48]. This can be mimicked in vitro by stimulating human primary RPE cell cultures with IFNγ for 3 days, resulting in increased HLA-I and the induction of HLA-II and the T-cell co-stimulatory molecules CD40 and CD54 surface expression [17, 47-48]. First, we determined if IFNγ stimulation of human RPE influenced productive HSV-1 and VZV infection in vitro. Compared to untreated RPE cells, only a higher virus inoculum was essential to accomplish a productive virus infection that can be monitored for multiple days in cell culture (Figure 5 and data not shown). At 24 h post-infection, IFNγ stimulated RPE infected with EGFP-expressing HSV-1 and VZV expressed immediate early (HSV-1 ICP0), early (VZV ORF66) and late viral proteins (HSV-1 VP16 and VZV gE; Figure 5A). Herpesvirus genes are expressed in a coordinated temporal fashion, such that

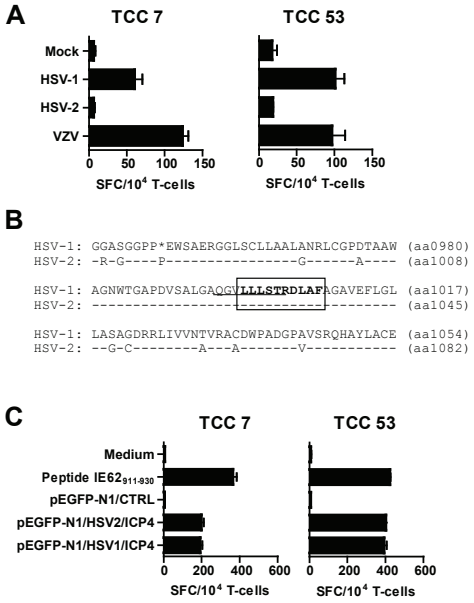

Figure 4. *T-cell clones 7 and 53 recognize VZV and HSV-1, but not HSV-2 infected B-cells. (A) The T-cell clones (TCC) were cultured for 6 h with autologous EBV-transformed B-cells (BLCL) infected overnight with HSV-1 and HSV-2, or pulsed with protein lysates of mock and VZV infected Vero cells. T-cell reactivity was determined by IFNγ ELISPOT. (B) Alignment of the HSV-1 and HSV-2 ICP4 orthologous protein sequences of the VZV IE62$_{918-927}$ T-cell epitope (boxed residues) and their flanking regions (Genbank accession numbers ACM62283 and NP_044530, respectively). The location of N- and C-terminal residues of the respective protein sequences are indicated in brackets. Dashes and asterisks indicate identical amino acids and insertion introduced to align the protein sequences, respectively. (C) TCC were cultured with autologous BLCL pulsed with peptide or medium. Alternatively, BLCL were nucleofected with the vectors pEGFP-N1/HSV-1:ICP4$_{945-1054}$ (encoding HSV-1 ICP4 residues 945-1054), pEGFP-N1/HSV-2:ICP4$_{972-1082}$ (encoding HSV2 ICP4 residues 972-1082), or pEGFP-N1/CTRL (no insert) as negative control. T-cell reactivity was determined by IFNγ ELISPOT. (A and C) Data are presented as mean ± SEM number of IFNγ spot-forming cells (SFC)/10⁴ T-cells.*

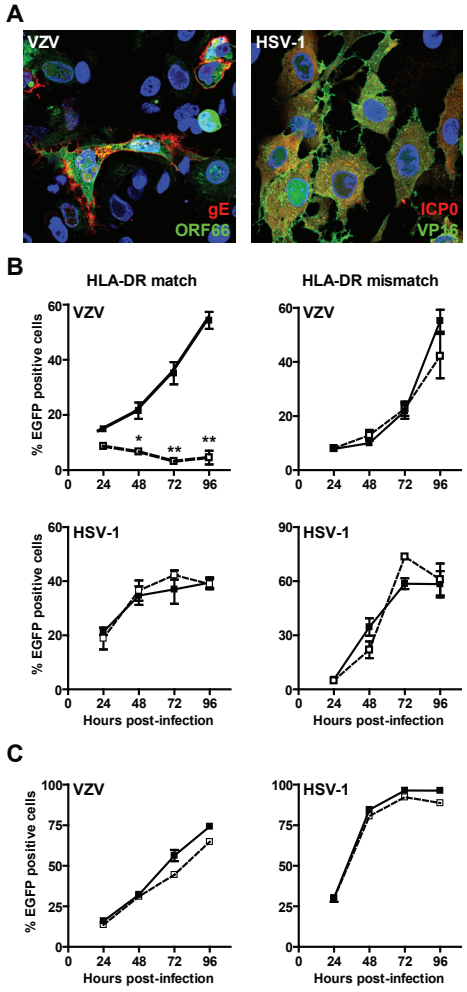

Figure 5. *VZV/HSV-1 cross-reactive CD4 T-cells inhibit VZV, but not HSV-1 infection in human retinal pigmented epithelial cells (RPE). (A) IFNγ–stimulated RPE cells were infected with recombinant EGFP expressing VZV (VZV.EGFP-ORF66) and HSV-1 (HSV-1. EGFP-VP16) strains for 24 h and stained for VZV glycoprotein E (gE; red) or HSV-1 protein ICP0 (red). Nuclei were stained with DAPI (blue). EGFP is fused to VZV protein ORF66 or HSV-1 protein VP16 (green). Magnification: 400X. (B) VZV.EGFP-ORF66 or HSV-1.EGFP-VP16 infected IFNγ-stimulated RPE cells were cultured with (open squares) or without (filled squares) the VZV/HSV-1 cross-reactive CD4 T-cell clone 53 (TCC 53). (C) HLA-DR matched IFNγ-stimulated VZV.EGFP-ORF66 or HSV-1. EGFP-VP16 infected RPE cells were cultured with (open squares) or without (filled squares) the solely HSV-1 specific TCC 44. (B and C) At the indicated times the percentage of EGFP-positive RPE cells (i.e. $CD3^{NEG}HLA\text{-}DR^{POS}$ cells) was determined by flow cytometry. HLA-DR (mis)matched RPE cells refer to the TCC's HLA-DR restricting allele. Data are presented as mean ± SEM. Differences in the number of $EGFP^{pos}$ RPE cells with TCC compared with no TCC added were analyzed by the paired Student's t-test. *P < 0.05; **P < 0.01.*

the detection of late proteins implicates that viral DNA replication has occurred [1-2]. Thus, EGFP expression is a valid marker to detect a productive HSV-1 and VZV infection in IFNγ-stimulated human primary RPE cells.

Next, the capacity of TCC 53 to control VZV and HSV-1 replication in human RPE cells *in vitro* was determined (Figure 5B). TCC 53 significantly inhibited VZV replication in HLA-DR matched, but not mismatched RPE cells. The data are in line with our previous studies, demonstrating that IFNγ-stimulated human primary RPE cells efficiently process and present the TCC's cognate VZV peptide in an HLA-DR restricted fashion [17]. Contrastingly, TCC 53 did not inhibit HSV-1 replication in both HLA-DR matched and mismatched RPE cells. To demonstrate that this differential effect was not due to the TCC and RPE cell line used, the experiments were repeated with a different TCC/RPE combination. We used TCC 44, a CD4 TCC originally obtained from a vitreous fluid sample of a patient with HSV-1 ARN (patient #1 in reference 21), which recognizes HSV-1, but not HSV-2 and VZV (reference 20) and data not

shown). Analogous to TCC 53, TCC 44 did not inhibit HSV-1 replication in RPE cells (Figure 5C), demonstrating that HSV-1 reactive CD4 T-cells are unable to control HSV-1 infection in human RPE cells.

HSV-1 infection inhibits CD4 T-cell activation by human RPE cells

Deficient CD4 T-cell control of HSV-1 infection in RPE cells may be due to a virus-mediated inhibition of T-cell recognition of infected cells. To test this hypothesis, we determined IFNγ levels, as a marker of T-cell activation, in conditioned medium of TCC 53 co-cultured with HSV-1 and VZV infected RPE cells (Figure 6A). Notably, the TCC secreted high levels of IFNγ in response to VZV-, but not HSV-1 infected HLA-DR matched RPE cells. Similar data were obtained with TCC 44 (Figure 6B), indicating that this effect was not TCC, target protein and RPE cell line specific.

The inhibitory effect may be attributed to the inability of RPE cells to process and present the cognate peptide or may involve an HSV-1-specific evasion strategy that counteracts CD4 T-cell activation by the infected RPE cells. To differentiate between both options αHHV antigen pulsed RPE cells were used as APC. In contrast to HSV-1 infected RPE cells, HSV-1 antigen pulsed RPE cells activated TCC 53 efficiently (Figure 6C). As expected both VZV-infected and VZV antigen pulsed RPE cells were recognized by TCC 53. Collectively, the data indicate that HSV-1 infection selectively inhibited CD4 T-cell activation by RPE cells (Figure 6), but not BLCL (Figure 4A).

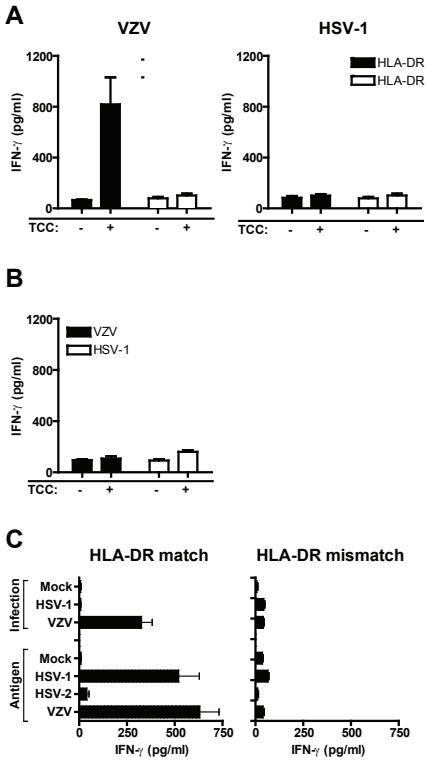

Figure 6. *HSV-1 infection of human retinal pigmented epithelial cells (RPE) abrogates CD4 T-cell activation. (A) IFNγ-stimulated HLA-DR matched or mismatched RPE cells were infected with recombinant EGFP expressing VZV (VZV.EGFP-ORF66) and HSV-1 (HSV-1.EGFP-VP16) and subsequently co-cultured with the VZV/ HSV-1 cross-reactive CD4 T-cell clone 53 (TCC 53). (B) IFNγ-stimulated HLA-DR matched RPE cells were infected with VZV. EGFP-ORF66 or HSV-1.EGFP-VP16 and co-cultured with the solely HSV-1 specific TCC 44. (C) TCC 53 was co-cultured with IFNγ-stimulated HLA-DR matched or mismatched RPE that were mock, VZV. EGFP-ORF66 or HSV-1.EGFP-VP16 infected, or alternatively pulsed with protein lysates of virus and mock infected cells. (A-C) Conditioned medium harvested after 24 h of TCC/RPE co-culture were analyzed for secreted IFNγ by ELISA. Data are presented as mean ± SEM.*

Discussion

HSV and VZV are closely related endemic αHHV that establish latency in sensory neurons and reactive intermittingly to cause recrudescent disease [1-2]. Based on the extensive homology between the HSV and VZV proteomes cross-reactive adaptive immune responses are anticipated. These responses are of potential interest for vaccine development to confer cross-protection, but may also be involved in immunopathogenesis. Whereas various αHHV cross-reactive B-cell target antigens have been identified [49-51], T-cell immunity directed to multiple αHHV is restricted to HSV-1 and HSV-2 [52-54]. The current study reports three main findings. First, we report on the first HLA-DR promiscuous VZV/HSV-1 cross-reactive CD4 T-cell epitope, located within VZV IE62 and HSV-1 ICP4, which is immuneprevalent in HSV-1 and VZV co-infected healthy individuals. Second, despite complete conservation of this epitope in HSV-2 ICP4, HSV-2 infected cells were not recognized by the cross-reactive CD4 TCC. Third, VZV/HSV-1 cross-reactive CD4 TCC selectively controlled VZV, but not HSV-1 infection in human RPE cells suggesting that HSV-1 actively inhibits CD4 T-cell activation.

Dominance and prevalence of pathogen-derived immunogens are determined by various factors including the host T-cell repertoire, antigen abundance, size and structure, antigenic competition and antigen processing [55-57]. VZV IE62 and HSV ICP4 are abundantly expressed viral proteins that are transported from the nucleus to the cytoplasm for incorporation in the tegument of the virion during lytic infection [27, 58-60]. Both viral proteins are large (~1,300 aa long) and contain a DNA-binding and a large C-terminal transactivator domain that are both highly conserved among alphaherpesvirinae of diverse animal species [28, 39, 61]. Previous studies showed that viral tegument proteins, including VZV IE62 and HSV-1 ICP4, are immuneprevalent targets of αHHV-specific CD4 and CD8 T-cells in blood of healthy HSV-1 and/or VZV infected adults [52, 62-64], lesions of genital herpes patients [65], affected eyes of herpetic uveitis and keratitis patients [18-20, 66] and at the site of HSV-1 latency in human trigeminal ganglia [67]. The identification of a HLA-DR promiscuous and broadly recognized CD4 T-cell epitope, located within VZV IE62 and HSV-1 ICP4, underscores the immunogenicity of both viral proteins as T-cell targets.

The identified VZV IE62 CD4 T-cell epitope was highly conserved among *alphaherpesvirinae* of multiple animal species, with complete conservation in VZV, HSV-1 and HSV-2. Nonetheless, the epitope-specific CD4 TCC 7 and 53 did not recognize the non-αHHV orthologous peptides at low concentrations. All non-reactive peptides diverged from the αHHV conserved epitope at HLA-II anchor residues P4, P6 and P9 [42, 55]. Possibly, the peptides are unable to form stable peptide:HLA-DR complexes or do not functionally engage with the TCR of both TCC. Despite complete conservation of the IE62/ICP4 epitope among αHHV, both TCC failed to recognize HSV-2 infected BLCL. Antigen processing is affected by the context of the respective antigen via its tertiary structure and protease susceptibility in epitope-flanking residues [41-45]. Compared to HSV-1 ICP4, the epitope-containing domain of HSV-

2 ICP4 includes several aa substitutions. However, nucleofected BLCL expressing a HSV-2 ICP4 fragment, including the αHHV conserved T-cell epitope along with about 50 N- and C-terminal residues, were readily recognized by both TCC indicating that the proximal epitope-flanking polymorphic residues in HSV-2 ICP4 did not affect processing and presentation of the cognate peptide to the TCC. HSV-1 and HSV-2 ICP4 proteins are highly homologous [68], suggesting that differential protease susceptibility due to more distal residues rather than the overall tertiary ICP4 structure are most likely involved in the inability to present the cognate epitope by HSV-2 infected BLCL.

ARN is a potentially blinding inflammatory eye disease that is predominantly caused by ocular HSV and VZV infections [8-10]. Most ARN patients have pre-existing serum IgG towards the initiating herpesvirus indicating that reactivation of latent virus rather than primary infection triggers the disease [7]. Reactivated virus may reach the retina by axonal transport via the optic nerve [69], explaining the increased risk of developing ARN following herpetic encephalitis [70]. Whereas under normal physiological conditions RPE cells are involved in creating and maintaining ocular immune privilege, inflammatory reactions evoked by intraocular infections shape RPE cells into potent APC to coordinate local T-cell responses [46-48]. Given the potential uveitogenic role of intraocular virus-specific T-cells in herpetic uveitis patients and corresponding animal models [11-16], the functional properties of the ocular-derived IE62/ICP4 cross-reactive TCC towards HSV-1 and VZV infected human RPE was analyzed in detail. In agreement with our previous study [17], VZV infection was controlled in human RPE cells by the IE62/ICP4 cross-reactive CD4 TCC in vitro. The mechanisms involved are both T-cell mediated cytolysis of infected RPE cells and the antiviral effect of secreted cytokines like IFNγ and TNFα [17].

In contrast, the same cross-reactive CD4 TCC did not recognize and consequently failed to control HSV-1 infection in RPE cells. Because the TCC recognized both HSV-1 infected autologous BLCL and HSV-1 antigen pulsed RPE cells, the data suggest that productive HSV-1 infection selectively renders RPE cells unable to activate CD4 T-cells. Currently, two HSV-1 specific immune evasion strategies have been reported that reduce, but do not completely abrogate, CD4 T-cell recognition of infected cells [71-73]. The first mechanism involves HLA-II downregulation on infected cells through the combined actions of the virion host shut-off protein, γ34.5 protein and gB [72-73]. The second pathway is mediated by HSV-1 ICP22 protein that impairs antigen presentation, but not antigen processing [71]. The high HLA-II surface expression on IFNγ stimulated RPE cells, used as APC throughout the current study, was only modestly reduced upon HSV-1 infection (data not shown). Consequently, the HSV-1 ICP22 pathway or a novel immune evasion mechanism is potentially involved in the inhibition of CD4 T-cell recognition of HSV-1 infected RPE cells.

In conclusion, we report on the first HLA-DR promiscuous and immune-prevalent VZV/HSV-1 cross-reactive CD4 T-cell epitope located within VZV IE62 and HSV ICP4. The data warrant further studies on the applicability of both proteins, preferentially the conserved C-terminal domain that contains the αHHV conserved CD4

T-cell epitope, in future vaccines to confer αHHV-specific and possibly αHHV cross-protective T-cell immunity. Furthermore, the use of ocular-derived VZV/HSV-1 cross-reactive TCC revealed that HSV-1 infection selectively rendered human RPE, but not B-cells, invisible to CD4 T-cell control. Studies are in progress to identify the HSV-1 protein, potentially ICP22 [71], and the mechanism involved in the CD4 T-cell immune evasion strategy recognized.

Acknowledgements

The authors thank Paul R. Kinchington for providing the rabbit polyclonal VZV gE antiserum, Johannes C.M. Milikan for technical support and Anton W Langerak for TCR sequencing.

References

1. Roizman B, Knipe DM, and Whitley RJ. Herpes simplex viruses. In: Knipe DM, Howley PM and Griffin DE, et al., eds. Fields Virology. 5th ed. Vol. 2. Philadelphia, PA: Lippincott, Williams and Wilkens, 2007:2501-2601
2. Cohen JI, Straus SE, and Arvin AM. Varicella-zoster virus replication, pathogenesis, and management. In: Knipe DM, Howley PM, Griffin DE, et al., eds. ields Virology. 5th ed. Vol. 2. Philadelphia, PA: Lippincott, Williams and Wilkens, 2007: 2773-2818
3. Arvin AM, Koropchak CM, Williams BR, Grumet FC, and Foung SK. Early immune response in healthy and immunocompromised subjects with primary varicella-zoster virus infection. J Infect Dis 1986;154:422-429.
4. Khanna KM, Bonneau RH, Kinchington PR, and Hendricks RL. Herpes simplex virus-specific memory CD8+ T cells are selectively activated and retained in latently infected sensory ganglia. Immunity 2003;18:593-603.
5. Miller AE. Selective decline in cellular immune response to varicella-zoster in the elderly. Neurology 1980;30:582-587.
6. Nash AA, Jayasuriya A, Phelan J, Cobbold SP, Waldmann H, and Prospero T. Different roles for L3T4+ and Lyt 2+ T cell subsets in the control of an acute herpes simplex virus infection of the skin and nervous system. J Gen Virol 1987;68 (Pt 3):825-833.
7. Verjans GMGM, and Heiligenhaus A. Herpes simplex virus-induced ocular diseases: detrimental interaction between virus and host. Current immunology reviews 2011;7:310-327.
8. Hillenkamp J, Nolle B, Bruns C, Rautenberg P, Fickenscher H, and Roider J. Acute retinal necrosis: clinical features, early vitrectomy, and outcomes. Ophthalmology 2009. 16:1971-1975 e1972.
9. Ritterband DC, and Friedberg DN. Virus infections of the eye. Rev Med Virol 1998;8:187-201.
10. Zamir E. Herpetic posterior uveitis. Int Ophthalmol Clin 2005;45:89-97.
11. Azumi A, and Atherton SS. T cells in the uninjected eye after anterior chamber inoculation of herpes simplex virus type 1. Invest Ophthalmol Vis Sci 1998;39:78-83.
12. Cousins SW, Gonzalez A, and Atherton SS. Herpes simplex retinitis in the mouse. Clinicopathologic correlations. Invest Ophthalmol Vis Sci 1989;30:1485-1494.
13. Deschenes J, Freeman WR, Char DH, and Garovoy MR. Lymphocyte subpopulations in uveitis. Arch Ophthalmol 1986;104:233-236.
14. Matsuo T, Nakayama T, Koyama T, and Matsuo N. Cytological and immunological study of the aqueous humor in acute retinal necrosis syndrome. Ophthalmologica 1987;195:38-44.
15. Pettit TH, Kimura SJ, Uchida Y, and Peters H. Herpes Simplex Uveitis: An Experimental Study with the Fluorescein-Labeled Antibody Technique. Invest Ophthalmol 1965;4:349-357.
16. Whittum-Hudson J, Farazdaghi M, and Prendergast RA. A role for T lymphocytes in preventing experimental herpes simplex virus type 1-induced retinitis. Invest Ophthalmol Vis Sci 1985. 26:1524-1532
17. Milikan JC, Baarsma GS, Kuijpers RW, Osterhaus AD, and Verjans GM. Human ocular-derived virus-specific CD4+ T cells control varicella zoster virus replication in human retinal pigment epithelial cells. Invest Ophthalmol Vis Sci 2009;50:743-751.
18. Milikan JC, Kinchington PR, Baarsma GS, Kuijpers RW, Osterhaus AD, and Verjans GM. Identification of viral antigens recognized by ocular infiltrating T cells from patients with varicella zoster virus-induced uveitis. Invest Ophthalmol Vis Sci 2007;48:3689-3697.
19. Milikan JC, Kuijpers RW, Baarsma GS, Osterhaus AD, and Verjans GM. Characterization of the varicella zoster virus (VZV)-specific intra-ocular T-cell response in patients with VZV-induced uveitis. Exp Eye Res 2006;83:69-75.
20. Verjans GM, Dings ME, McLauchlan J, et al. Intraocular T cells of patients with herpes simplex virus (HSV)-induced acute retinal necrosis recognize HSV tegument proteins VP11/12 and VP13/14. J Infect Dis 2000;182:923-927.
21. Verjans GM, Feron EJ, Dings ME, et al. T cells specific for the triggering virus infiltrate the eye in patients with herpes simplex virus-mediated acute retinal necrosis. J Infect Dis 1998;178:27-34.
22. Culbertson WW, Blumenkranz MS, Haines H, Gass DM, Mitchell KB, and Norton EW. The acute retinal necrosis syndrome. Part 2: Histopathology and etiology. Ophthalmology 1982;89:1317-1325.
23. Culbertson WW, Blumenkranz MS, Pepose JS, Stewart JA, and Curtin VT. Varicella zoster virus is a cause of the acute retinal necrosis syndrome. Ophthalmology 1986;93:559-569.

24. Kuppermann BD, Quiceno JI, Wiley C, et al. Clinical and histopathologic study of varicella zoster virus retinitis in patients with the acquired immunodeficiency syndrome. Am J Ophthalmol 1994;118:589-600.
25. Davison AJ, and Scott JE. The complete DNA sequence of varicella-zoster virus. J Gen Virol 1986;67 (Pt 9):1759-1816.
26. Cohen JI, Heffel D, and Seidel K. The transcriptional activation domain of varicella-zoster virus open reading frame 62 protein is not conserved with its herpes simplex virus homolog. J Virol 1993;67:4246-4251.
27. Kinchington PR, Fite K, and Turse SE. Nuclear accumulation of IE62, the varicella-zoster virus (VZV) major transcriptional regulatory protein, is inhibited by phosphorylation mediated by the VZV open reading frame 66 protein kinase. J Virol 2000;74:2265-2277.
28. Felser JM, Kinchington PR, Inchauspe G, Straus SE, and Ostrove JM. Cell lines containing varicella-zoster virus open reading frame 62 and expressing the "IE" 175 protein complement ICP4 mutants of herpes simplex virus type 1. J Virol 1988;62:2076-2082.
29. Eisfeld AJ, Yee MB, Erazo A, Abendroth A, and Kinchington PR. Downregulation of class I major histocompatibility complex surface expression by varicella-zoster virus involves open reading frame 66 protein kinase-dependent and -independent mechanisms. J Virol 2007;81:9034-9049.
30. La Boissiere S, Izeta A, Malcomber S, and O'Hare P. Compartmentalization of VP16 in cells infected with recombinant herpes simplex virus expressing VP16-green fluorescent protein fusion proteins. J Virol 2004;78:8002-8014.
31. Verjans GM, Hintzen RQ, van Dun JM, et al. Selective retention of herpes simplex virus-specific T cells in latently infected human trigeminal ganglia. Proc Natl Acad Sci U S A 2007;104:3496-3501.
32. Langerak AW, Groenen PJ, Bruggemann M, et al. EuroClonality/BIOMED-2 guidelines for interpretation and reporting of Ig/TCR clonality testing in suspected lymphoproliferations. Leukemia 2012;26:2159-2171.
33. Singh H, and Raghava GP. ProPred: prediction of HLA-DR binding sites. Bioinformatics 2001;17:1236-1237.
34. Bui HH, Sidney J, Peters B, et al. Automated generation and evaluation of specific MHC binding predictive tools: ARB matrix applications. Immunogenetics 2005;57:304-314.
35. Guan P, Hattotuwagama CK, Doytchinova IA, and Flower DR. MHCPred 2.0: an updated quantitative T-cell epitope prediction server. Appl Bioinformatics 2006;5:55-61.
36. Nielsen M, Lundegaard C, and Lund O. Prediction of MHC class II binding affinity using SMM-align, a novel stabilization matrix alignment method. BMC Bioinformatics 2007;8:238.
37. Wan J, Liu W, Xu Q, Ren Y, Flower DR, and Li T. SVRMHC prediction server for MHC-binding peptides. BMC Bioinformatics 2006;7:463.
38. Geluk A, Taneja V, van Meijgaarden KE, et al.Identification of HLA class II-restricted determinants of Mycobacterium tuberculosis-derived proteins by using HLA-transgenic, class II-deficient mice. Proc Natl Acad Sci U S A 1998;95:10797-10802.
39. Tyler JK, and Everett RD. The DNA binding domains of the varicella-zoster virus gene 62 and herpes simplex virus type 1 ICP4 transactivator proteins heterodimerize and bind to DNA. Nucleic Acids Res 1994;22:711-721.
40. Lefranc MP. Nomenclature of the human T cell receptor genes. Curr Protoc Immunol 2001;Appendix 1:Appendix 1O.
41. Neefjes J, Jongsma ML, Paul P, and Bakke O. Towards a systems understanding of MHC class I and MHC class II antigen presentation. Nat Rev Immunol 2011;11:823-836.
42. Painter CA, and Stern LJ. Conformational variation in structures of classical and non-classical MHCII proteins and functional implications. Immunol Rev 2012;250:144-157.
43. Schneider SC, Ohmen J, Fosdick L, et al. Cutting edge: introduction of an endopeptidase cleavage motif into a determinant flanking region of hen egg lysozyme results in enhanced T cell determinant display. J Immunol 2000;165:20-23.
44. Sercarz EE, Lehmann PV, Ametani A, Benichou G, Miller A, and Moudgil K. Dominance and crypticity of T cell antigenic determinants. Annu Rev Immunol 1993;11:729-766.
45. Shastri N, Miller A, and Sercarz EE. Amino acid residues distinct from the determinant region can profoundly affect activation of T cell clones by related antigens. J Immunol 1986;136:371-376.
46. Chan CC, Detrick B, Nussenblatt RB, Palestine AG, Fujikawa LS, and Hooks JJ. HLA-DR antigens on retinal pigment epithelial cells from patients with uveitis. Arch Ophthalmol 1986;104:725-729.
47. Liversidge JM, Sewell HF, and Forrester JV. Human retinal pigment epithelial cells differentially

express MHC class II (HLA, DP, DR and DQ) antigens in response to in vitro stimulation with lymphokine or purified IFN-gamma. Clin Exp Immunol 1988;73:489-494.
48. Percopo CM, Hooks JJ, Shinohara T, Caspi R, and Detrick B. Cytokine-mediated activation of a neuronal retinal resident cell provokes antigen presentation. J Immunol 1990;145:4101-4107.
49. Kalantari-Dehaghi M, Chun S, Chentoufi AA, et al. Discovery of potential diagnostic and vaccine antigens in herpes simplex virus 1 and 2 by proteome-wide antibody profiling. J Virol 2012;86:4328-4339.
50. Kuhn JE, Klaffke K, Munk K, and Braun RW. HSV-1 gB and VZV gp-II crossreactive antibodies in human sera. Arch Virol 1990;112:203-213.
51. Wolff MH, Buchel F, and Zoll A. Serological studies on the antigenic relationship between herpes simplex virus and varicella-zoster virus. Immunobiology 1979;156:76-82.
52. Jing L, Haas J, Chong TM, et al. Cross-presentation and genome-wide screening reveal candidate T cells antigens for a herpes simplex virus type 1 vaccine. J Clin Invest 2012;122:654-673.
53. Johnston C, Koelle DM, and Wald A. HSV-2: in pursuit of a vaccine. J Clin Invest 2011;121:4600-4609.
54. Ouwendijk WJ, Laing KJ, Verjans GM, and Koelle DM. T-cell immunity to human alphaherpesviruses. Curr Opin Virol. 2013;3(4):452-460
55. Cole DK, Gallagher K, Lemercier B, et al. Modification of the carboxy-terminal flanking region of a universal influenza epitope alters CD4(+) T-cell repertoire selection. Nat Commun 2012;3:665.
56. Moon JJ, Chu HH, Pepper M, et al. Naive CD4(+) T cell frequency varies for different epitopes and predicts repertoire diversity and response magnitude. Immunity 2007;27:203-213.
57. Weaver JM, Chaves FA, and Sant AJ. Abortive activation of CD4 T cell responses during competitive priming in vivo. Proc Natl Acad Sci U S A 2009;106:8647-8652.
58. Eisfeld AJ, Turse SE, Jackson SA, Lerner EC, and Kinchington PR. Phosphorylation of the varicella-zoster virus (VZV) major transcriptional regulatory protein IE62 by the VZV open reading frame 66 protein kinase. J Virol 2006;80:1710-1723.
59. Imbalzano AN, Coen DM, and DeLuca NA. Herpes simplex virus transactivator ICP4 operationally substitutes for the cellular transcription factor Sp1 for efficient expression of the viral thymidine kinase gene. J Virol 1991;65:565-574.
60. Loret S, and Lippe R. Biochemical analysis of infected cell polypeptide (ICP)0, ICP4, UL7 and UL23 incorporated into extracellular herpes simplex virus type 1 virions. J Gen Virol 2012;93:624-634.
61. McGeoch DJ, Dolan A, Donald S, and Brauer DH. Complete DNA sequence of the short repeat region in the genome of herpes simplex virus type 1. Nucleic Acids Res 1986;14:1727-1745.
62. Arvin AM, Sharp M, Moir M, et al. Memory cytotoxic T cell responses to viral tegument and regulatory proteins encoded by open reading frames 4, 10, 29, and 62 of varicella-zoster virus. Viral Immunol 2002;15:507-516.
63. Arvin AM, Sharp M, Smith S, et al. Equivalent recognition of a varicella-zoster virus immediate early protein (IE62) and glycoprotein I by cytotoxic T lymphocytes of either CD4+ or CD8+ phenotype. J Immunol 1991;146:257-264.
64. Jing L, Schiffer JT, Chong TM, et al. CD4 T-cell memory responses to viral infections of humans show pronounced immunodominance independent of duration or viral persistence. J Virol 2013;87:2617-2627.
65. Laing KJ, Magaret AS, Mueller DE, et al. Diversity in CD8(+) T cell function and epitope breadth among persons with genital herpes. J Clin Immunol 2010;30:703-722.
66. Koelle DM, Reymond SN, Chen H, et al. Tegument-specific, virus-reactive CD4 T cells localize to the cornea in herpes simplex virus interstitial keratitis in humans. J Virol 2000;74:10930-10938.
67. van Velzen M, Jing L, Osterhaus ADME, Sette A, Koelle DM, and Verjans GMGM. Local CD4 and CD8 T-cell reactivity to HSV-1 antigens documents broad viral protein expression and immune competence in human ganglia. PLoS Pathog. 2013;9(8):e1003547.
68. Wyrwicz LS, and Rychlewski L. Fold recognition insights into function of herpes ICP4 protein. Acta Biochim Pol 2007;54:551-559.
69. Atherton SS, and Streilein JW. Two waves of virus following anterior chamber inoculation of HSV-1. 1987. Ocul Immunol Inflamm 2007;15:195-204.
70. Vandercam T, Hintzen RQ, de Boer JH, and Van der Lelij A. Herpetic encephalitis is a risk factor for acute retinal necrosis. Neurology 2008;71:1268-1274.
71. Barcy S, and Corey L. Herpes simplex inhibits the capacity of lymphoblastoid B cell lines to stimulate CD4+ T cells. J Immunol 2001;166:6242-6249.

72. Temme S, Eis-Hubinger AM, McLellan AD, and Koch N. The herpes simplex virus-1 encoded glycoprotein B diverts HLA-DR into the exosome pathway. J Immunol 2010;184:236-243.
73. Trgovcich J, Johnson D, and Roizman B. Cell surface major histocompatibility complex class II proteins are regulated by the products of the gamma(1)34.5 and U(L)41 genes of herpes simplex virus 1. J Virol 2002;76:6974-6986.

Chapter 9

Summarizing Discussion

Summarizing Discussion

Varicella-zoster virus (VZV) is a ubiquitous human alphaherpesvirus (αHHV). Most individuals become infected with VZV during childhood typically resulting in generalized vesicular skin rash, although a minority of individuals will not develop evident skin rash. During primary infection the virus gains access to ganglia along the entire neuraxis, where it establishes a life-long latent infection of mostly sensory neurons. Due to the long incubation period and restricted host range of the virus, the cell types involved in the dissemination of VZV from the site of primary infection to the virus' target organs are largely unknown. Clinical, pathological, virological and immunological features of simian varicella virus (SVV) infection of nonhuman primates parallel those of primary VZV infection in humans. Consequently, the virus-host interactions involved in primary infection were studied in the SVV nonhuman primate model in **Chapters 2 and 3** of this thesis. The latent phase of VZV is completely refractory to antiviral treatment and provides the virus the opportunity to reactivate later in life and cause herpes zoster. The mechanisms by which VZV latency is established and maintained remain enigmatic. Although cumulative data suggest that VZV latency is associated with restricted gene expression and possibly protein expression, considerable discrepancies have been reported in literature. The expression of VZV proteins and genes was reinvestigated in **Chapters 4 and 5** of this thesis, providing novel insights into VZV latency. VZV reactivation as a result of declined virus-specific T-cell immunity causes herpes zoster or may occur asymptomatically. Asymptomatic shedding of the closely related αHHV HSV-1 occurs frequently, but the incidence of VZV shedding and its relation to HSV-1 shedding in that same individual is largely unknown. This was addressed in **Chapter 6** of this thesis. Herpes zoster results from intraganglionic VZV replication followed by transaxonal spread of virus to the skin. Consequently, immune cells, mainly T-cells, infiltrate ganglia following herpes zoster most likely to control local virus replication. The stimulus driving T-cell infiltration and subsequent retention after VZV reactivation is ill-defined. The aim of the study described in **Chapter 7** was to investigate this issue in ganglia of cynomolgus macaques obtained at variable intervals following SVV reactivation. Although virus-specific T-cells are essential for uncomplicated recovery from varicella and herpes zoster, VZV-specific T-cells may cause immunopathology in patients with VZV-induced uveitis. **Chapter 8** describes the identification and functional characterization of ocular-derived VZV/HSV-1 cross-reactive $CD4^+$ T-cells.

1. Simian Varicella Virus

Varicella in Apes and Old World Monkeys

VZV is a human-restricted pathogen that does not cause disease in experimental animal models. Possible exceptions are closely related primate species that belong to the family of Hominoidae: e.g. chimpanzees, bonobos, gorillas and orangutans [1]. A juvenile gorilla living in a zoo developed a varicella-like disease during an epi-

demic of varicella in the community [2]. Restriction fragment length polymorphism analyses revealed that the causative virus was genetically identical to VZV [2]. Chimpanzees confer limited susceptibility to VZV infection as subcutaneous injection of VZV-infected cells produces a localized skin rash [3], whereas intratracheal VZV inoculation does not cause varicella-like disease [4]. Similarly, infection of Old World monkeys, like patas monkeys and cynomolgus macaques, with VZV results in an abortive infection and does not produce any clinical signs [4-5]. Nonetheless, outbreaks of varicella-like disease in African green monkeys, patas monkeys and various species of macaque monkeys occurred in the 1960s and 1970s at multiple primate centers worldwide [6-7]. The causative virus was identified as a varicellovirus, referred to as SVV, which was both antigenetically [8] and genetically [9] highly similar to VZV. Phylogenetic analysis of SVV and VZV genomes suggests that both viruses originated from an ancestral virus that most likely emerged in the earliest primates in Africa [10-11]. About 20 – 30 million years ago Hominoidae diverged from Old World monkeys [1], each carrying their own primordial varicellovirus, eventually giving rise to two closely related viruses that co-evolved with their respective hosts [10-11]. Thus, rather than studying a human herpesvirus in its non-natural host, e.g. HSV infection of mice, SVV infection of Old World monkeys provides a model to study the pathogenesis of varicella and herpes zoster in its natural host.

Natural Host and Prevalence of SVV

The prevalence of SVV and the species infected by SVV in the wild are largely unknown. One study reported that only 0.8% of macaques in Malaysia had detectable serum antibodies to SVV [12]. The true frequency of SVV latently infected monkeys is most likely higher as most monkeys do not develop detectable virus-neutralizing antibodies upon “natural” infection (see below) [13] and outbreaks in multiple primate centers occurred after the introduction of monkeys captured from the wild into the monkey colony [6]. Although various species of Old World monkeys are susceptible to SVV infection [6-7], it is not clear which species are infected by SVV in the wild. Given that SVV originated an estimated 20 – 30 million years ago [1, 10-11], it is likely that different monkey species carry closely related, but diverse, SVV strains. Not surprisingly, therefore, the susceptibility to and severity of SVV infection varies among different monkey species. African green monkeys, patas monkeys and cynomolgus macaques are highly susceptible to SVV infection and may develop severe, potentially life-threatening, disease [6, 14-15]. Contrastingly, rhesus macaques are less susceptible to SVV infection and disease severity is limited compared to the other nonhuman primate species [12, 16-17]. Notably, the geographic origin of rhesus macaques may also affect their susceptibility to SVV infection. Intrabronchial inoculation of Indian rhesus macaques with SVV results in cutaneous rash 7 – 10 days post infection (dpi) and the establishment of ganglionic viral latency [18-19]. In contrast, intratracheal SVV infection of Chinese rhesus macaques results in SVV latency, without clinical signs of primary SVV infection **(Chapter 2)** [20]. Recent whole-genome sequencing has revealed extensive genetic differences in rhesus macaques of Indian and Chinese origin [21-22] that are likely to play a role in the different disease progression and host response seen after e.g. SIV infection [23-24] or SVV infection [20].

SVV Nonhuman Primate Models

The studies described in **Chapters 2, 3 and 7** of this thesis used Chinese rhesus macaques, African green monkeys and cynomolgus macaques, respectively. The prototypic Delta herpesvirus strain of SVV, which was used in all studies, was originally derived from a naturally infected patas monkey that is closely related to the African green monkey [9]. The pathogenesis of primary SVV infection in various nonhuman primate species is comparable and parallels VZV infection in humans [6-7, 15, 19]. However, as outlined above, our studies demonstrated that Chinese rhesus macaques were less susceptible to SVV than Indian rhesus macaques **(Chapter 2)** [20]. The relatively low levels of viremia in both rhesus macaque subspecies [19-20] prompted us to study the pathogenesis of primary SVV infection in the highly susceptible African green monkeys [6-7]. The anticipated low frequencies of virus-infected lymphocytes in blood of SVV-infected monkeys necessitates a high viremia to define the lymphocyte subsets involved in the virus dissemination in the host **(Chapter 3)** [25]. However, low levels of SVV DNA and transcripts, but not infectious virus, may persist in peripheral blood and organs for prolonged periods of time after resolution of varicella in African green monkeys and cynomolgus macaques following intratracheal inoculation [7, 26-27]. To study latency a model of "natural" SVV infection has been developed in which naïve monkeys were exposed to an intratracheally inoculated monkey, resulting in a mild viremia, skin rash after 10 – 14 days and establishment of latency [28]. Similar to primary VZV infection in humans SVV DNA cannot be detected in non-ganglionic tissues after resolution of skin rash [28]. However, the amount of virus received by the animals cannot be controlled and most monkeys do not develop a detectable viremia using this model [28-29]. SVV reactivation can be experimentally induced in "naturally" infected African green monkeys and cynomolgus macaques using various combinations of immunosuppression and stress [13, 29]. Thus, experimentally induced SVV reactivation in cynomolgus macaques provides an excellent model to study the pathogenesis of herpes zoster at variable periods following reactivation.

2. Pathogenesis of Primary VZV Infection

Early Target Cells

VZV is transmitted from varicella or herpes zoster patients to susceptible individuals by aerosols or by direct contact to vesicular fluid [30-31]. It has been proposed that VZV gains access to the human body by infecting epithelial cells of the upper respiratory tract [30-31]. Presumably, initial virus replication occurs in the pharyngeal lymphoid tissue comprising Waldeyer's tonsilar ring resulting in transmission of VZV to lymphocytes, mostly T-cells [30]. This view is supported by the detection of VZV in tonsils obtained from a child undergoing tonsillectomy three days prior to the onset of varicella [32]. Additionally, or alternatively, VZV may target epithelial cells of the conjunctiva or lower respiratory tract. Conjunctivitis is a common feature of primary VZV infection and – depending on the size of the aerosols – viruses may directly reach the lower respiratory tract [30, 33]. In **Chapter 3** it was shown that SVV infects

both respiratory epithelial cells and airway-resident antigen presenting cells (APC), such as alveolar macrophages and lung-resident dendritic cells (DC), after intracheal infection of African green monkeys [25]. Alveolar macrophages and lung-resident DC traffic to lung-draining lymph nodes for antigen presentation to T-cells [34-35]. In cell culture VZV productively infects macrophages and DC, and the latter cells can transmit the virus to T-cells [36-37]. These data suggest that SVV and VZV infection of APC in the respiratory tract may spread virus to draining lymph nodes. Consistent with this hypothesis, pronounced histopathology and high viral loads were detected in lymphoid organs of African green monkeys at 9 dpi **(Chapter 3)** [25]. Abundant DC are present in the sub-epithelium of both upper and lower respiratory tract [38], suggesting that – regardless the site of initial VZV and SVV infection – these cells may play an essential role in transporting the virus to lymphoid organs for subsequent transfer to memory T-cells. The APC-mediated transfer of VZV to lymph nodes can be bypassed through direct injection of VZV into the bloodstream, which reduces the incubation period by four to six days [31].

Tropism for Memory T-cells

During primary infection VZV is disseminated to susceptible organs via a cell-associated viremia. Although various infected lymphocyte subsets can be detected at low levels in humans and nonhuman primates with varicella, the majority of virus-infected cells are T-cells **(Chapter 3)** [25, 39-40]. Both VZV and SVV have an inherent tropism for memory T-cells over naïve T-cells [25, 40-42]. Tonsil-derived activated memory $CD4^+$ T-cells can be productively infected by VZV in cell culture and can transfer virus to melanoma cells [42-43]. Although VZV was shown to preferentially infect T-cells expressing the skin-homing markers CLA and CCR4 *in vitro* [42], we did not observe any preference of SVV for memory T-cells expressing CCR4 or CD137 (a marker expressed by T-cells early after recognition of their cognate antigen [44-45]) *in vivo* or *in vitro* **(Chapter 3)** [25]. Nonetheless, memory T-cells are enriched for activated T-cells and cells expressing CCR4 ([42] and Ouwendijk et al., 2013, unpublished data), and have an increased propensity to traffic to peripheral tissues for immune surveillance, making these cells the ideal “Trojan Horse” for VZV and SVV. Of interest, we observed a dual phase of initially predominantly SVV-infected central memory (CM) T-cells and subsequently effector memory (EM) T-cells during primary SVV infection of African green monkeys **(Chapter 3)** [25]. CM T-cells are preferentially found in lymphoid organs, whereas EM T-cells are migratory T-cells that home to peripheral tissues to orchestrate local immune responses [46-47], indicating that the tissue or differentiation status of SVV-infected T-cells differ at various times after infection. Although direct T-cell-mediated transfer of SVV to its target organs cannot be demonstrated in the SVV nonhuman primate model, VZV-infected T-cells can transport the virus to skin and ganglia in the SCID-hu mouse model [48-49]. In addition to memory T-cells, other lymphocyte subsets may also contribute to viremic spread of the virus. VZV-infected B-cells and monocytes are detected in blood of varicella patients at low frequencies [40, 50] and we have detected low numbers of SVV-infected DC, B-cells, NK cells and monocytes at 5 dpi, but not at 7 dpi **(Chapter 3)** [25]. VZV- and SVV-infected lymphocytes are rapidly cleared from the circulation, presumably due to a combination of virus-induced apoptosis [51] and

the virus-specific adaptive immune responses evoked [19-20, 52].

Lymphocytes Transfer the Virus to the Skin

VZV reaches the skin via hematogenous spread during primary infection, resulting in a generalized cuteaneous rash. Virus-infected lymphocytes can be detected in peripheral blood just prior to and immediately after the onset of skin rash [6, 30] and the magnitude of viremia is correlated with the severity of the rash during primary VZV [53] and SVV infection [19]. The first cells in the skin to become infected with SVV are the dermal perivascular cells [25, 54]. A prominent role for T-cells in the viremic transport of virus to skin is assumed based on the predominant infection of memory T-cells in blood during primary SVV infection **(Chapter 3)** [25]. Moreover, memory T-cells traffic VZV to human fetal skin xenografts in the SCID-hu mouse model [48]. The skin vasculature is composed of an upper horizontal superficial vesicular plexus just beneath the epidermal surface and a deep vascular plexus that supplies the hair bulbs and sweat glands [55]. Therefore, virus-infected memory T-cells most likely transfer virus to skin-resident perivascular macrophages, DCs or dendrocytes, which in turn transfer VZV to adjacent epidermal or hair follicle keratinocytes via cell-to-cell spread. Although VZV-infected T-cells may already reach the skin at early stages of primary infection, the virus needs to overcome local epidermal innate immune responses to produce rash [48, 56-58]. It has been proposed that secondary “crops” of skin lesions result from memory T-cells trafficking through early lesions, becoming infected and transferring virus to distal cutaneous sites [48]. This hypothesis might explain the dominance of SVV-infected EM T-cells at 7 dpi in African green monkeys **(Chapter 3)** [25], because most skin-infiltrating T-cells have an EM phenotype (Ouwendijk et al., 2013, unpublished data).

VZV Infects Ganglia by the Transaxonal and/or Hematogenous Route

VZV infects ganglionic neurons by retrograde axonal transport from cutaneous lesions and/or hematogenously via virus-infected lymphocytes, most likely memory T-cells. Herpes zoster predominantly occurs at the site of varicella vaccine inoculation or sites most severely affected by varicella [59-60], suggesting transaxonal transport of VZV. The capacity of VZV to infect axons followed by retrograde axonal transport to neuronal cell bodies was only recently demonstrated in cell culture [61-62]. The axonal route is further supported by the predominant detection of SVV proteins in neuronal cell bodies, but not non-neuronal cells, in ganglia of African green monkeys at 9, 13 and 20 dpi **(Chapter 3)** [25]. Importantly, extensive virus replication in skin is not a prerequisite for the establishment of latent SVV or VZV infections, as observed in Chinese rhesus macaques inoculated with SVV **(Chapter 2)** [20] and demonstrated by the detection of VZV serum antibodies in humans without a history of varicella [30]. Given that sensory nerve endings in skin are also located in close proximity to the cutaneous vasculature at the dermal-epidermal junction and hair follicles [63], VZV may concurrently infect epidermal or hair follicle keratinocytes and neurons via local cell-to-cell spread. This implies that VZV infects neurons prior to the appearance of skin rash. The velocity of VZV retrograde axonal transport was recently estimated to be approximately 1.4 μm/s in cell culture [61], suggesting that axonal transport of virus from skin to most sensory neuron cell bodies could occur

within 1 – 2 days (corresponding to a distance of 121 – 242 mm). Alternatively, or additionally, virus may be transported to ganglia via a cell-associated viremia. In support of this hypothesis, SVV DNA load in ganglia is dependent on the viremic SVV DNA load [19-20], but not associated with the severity of varicella in the innervated dermatome [25]. The detection of SVV-infected T-cells adjacent to neurons suggests that memory T-cells have the capacity to transport virus to ganglia **(Chapter 3)** [25]. Indeed, intravenous injection of VZV-infected T-cells produces infection of human fetal ganglia in the SCID-hu mouse model [49]. Thus, definitive identification of the route(s) by which VZV and SVV enter sensory ganglia needs to be addressed in future research in the SVV nonhuman primate model, preferably at earlier times post infection.

Induction of Adaptive Immune Response during Primary Infection

Primary SVV and VZV infections induce robust B- and T-cell responses that become detectable around the onset of skin rash [19, 52]. VZV-specific T-cell immunity, but not humoral immunity, is essential for the termination of viremia and recovery from varicella [52-53]. By depleting individual lymphocyte subsets in nonhuman primates it was recently demonstrated that T-cells, and especially $CD4^+$ T-cells, were pivotal for controlling primary SVV infection [64]. Consequently, the magnitude of VZV- and SVV-specific T-cell immunity induced determines the severity of varicella [52-53, 64]. Conversely, the extent of the SVV-specific B- and T-cell responses induced are affected by the level of virus replication during primary infection. SVV-specific adaptive immune responses are more vigorous in Indian rhesus macaques, which develop skin rash during primary SVV infection, compared to Chinese rhesus macaques that do not develop skin rash **(Chapter 2)** [19-20, 64]. Furthermore, most pronounced virus-specific T-cell immunity is induced in animals with higher SVV DNA loads in ganglia and those demonstrating more extensive skin rash [19]. Notably, the adaptive immune response elicited in VZV Oka vaccinees is less robust compared to individuals who experienced a natural VZV infection [65-67].

3. VZV Latency Revisited

VZV Latency is Characterized by Highly Restricted Viral Gene Expression and No Viral Protein Expression

VZV latency can be operationally defined as the presence of the viral genome in host cells without production of infectious progeny, specified that the virus retains the capacity to reactivate and produce infectious virus (i.e. not an abortive infection). The time after primary infection at which neuronal VZV latency is established is unknown and presumably depends on various factors, such as the virus genotype, severity of varicella and viremia, ganglionic viral load and host factors involved in infection (e.g. virus receptors) and immunity. Studies on SVV infection of nonhuman primates suggest that virus is mostly restricted to ganglia at 21 dpi **(Chapters 2 and 3)** [20, 25] and that complete viral latency is established prior to 10 weeks after infection [19]. Classically, VZV latency is defined by the restricted expression of several immediate

early (IE) and early (E) transcripts and their protein products in ganglionic neurons: open reading frames (ORFs) 4, 21, 29, 62, 63 and 66 [68-77]. Previous studies on VZV protein expression in latently infected human ganglia have reported disparate results. Some groups described high frequencies of VZV protein expressing neurons, predominantly localized within specific cytoplasmatic compartments [72, 75, 77], whereas others reported that VZV protein expression in human ganglia is rare [73, 76, 78]. Recent studies performed by Zerboni et al. [80] and our group **(Chapter 4)** demonstrated that ascites-derived VZV IE62- and IE63-specific mouse monoclonal antibodies (mAbs) contain traces of endogenous anti-human blood group A1 antibodies that react with blood group A1-associated antigens within neuronal cytoplasmatic Golgi-related vacuoles [79-80]. Consequently, ganglia from blood group A1 positive donors showed pronounced immunohistochemical staining of the Golgi zones within a subset of sensory neurons, which was previously misinterpreted as genuine detection of IE62 and IE63 protein in previous studies. Note that this so-called mouse ascites Golgi (MAG) reaction is a common phenomenon observed with both ascites-derived mAbs and rabbit polyconal antibody preparations, is not removed by immunoglobulin purification and can result in false-positive staining of various tissues [81-85]. Although the anti-VZV IE62 and IE63 mAbs used in these studies recognized VZV proteins in cell culture and skin punch biopsies of herpes zoster patients, we have never observed specific VZV IE62 or IE63 protein staining – other than MAG reactivity – in ganglia of more than 20 donors (**Chapter 4** and Ouwendijk et al., 2013, unpublished data). Recent generation of a novel collection of mouse monoclonal anti-VZV antibodies [86] allowed us to reinvestigate expression of VZV proteins corresponding to ORFs 4, 21, 62, 63 and 66. No VZV proteins were detected in 12 TG donors using the novel VZV mAbs (Ouwendijk et al., 2013, unpublished data), nor was any MAG reactivity observed. The observation that in contrast to HSV-1, VZV latency is not associated with the local retention of VZV-specific T-cells strengthens our *in-situ* analyses that VZV proteins are not overtly expressed in human latently infected ganglia [87].

In addition to the six most frequently detected IE and E VZV transcripts, late gene products corresponding to VZV ORFs 18 and 40 are occasionally detected in latently infected human ganglia [73]. Moreover, recent VZV transcriptome-wide analysis of human latently infected cadaveric ganglia detected 10 VZV transcripts corresponding to all kinetic classes [88]. In **Chapter 5**, we have shown that the breadth and magnitude of the detected VZV latency transcriptome in human ganglia correlates with the postmortem interval (PMI), i.e. the interval between death and obtaining the ganglia for research purposes [89]. VZV transcriptome-wide multiplex RT-PCR did not reveal any viral transcripts in ganglia obtained prior to 9 hours after death [89]. Quantitative real-time PCR detected ORF63 transcripts in ganglia irrespective of the PMI [89]. However, ORF63 transcript levels, but not VZV DNA levels, increased with advancing PMI **(Chapter 5)** [89]. Thus, the large variability in number and abundance of VZV transcripts reported previously by others groups are caused by differences in PMI of the ganglia analyzed. All previous studies used human cadaveric ganglia that were obtained at >12 hrs, commonly >24 hrs after death [68-71, 73-74, 90]. Collectively, the data presented in **Chapters 4 and 5** refute the current dogmas on

both VZV transcript and protein expression during VZV latency [30]. Our data demonstrate that VZV gene expression is restricted during latency – possibly limited to ORF63 – and that no VZV proteins are expressed in latently infected human ganglia.

Epigenetic Silencing of the Latent VZV Genome

The virus and host factors involved in the establishment and maintenance of VZV latency are largely unknown. VZV contrasts the closely related viruses HSV and SVV in that it does not encode a specific transcript that is predominantly expressed during latent infection. During latency both HSV-1 and HSV-2 encode the non-coding latency-associated transcripts (referred to as LAT) and SVV transcribes the anti-sense ORF61 RNA [19, 91]. Instead, the most frequently and abundantly VZV transcript detected in latently infected human ganglia is ORF63 **(Chapter 5)** [70, 88-89], an IE gene that is also abundantly expressed during lytic infection [30]. Note that not all VZV latently infected ganglia express detectable levels of ORF63 transcript **(Chapter 5)** [70, 89] and that the function of ORF63 transcripts in VZV latently infected ganglia is unknown. The host may control VZV latency at multiple levels, e.g. by silencing the viral genome or by immune control of virus replication [87]. In general, gene expression is regulated by its location within the nuclear architecture, epigenetic chromatin modifications and the availability of transcription factors [92-93]. For HSV, it has been shown that some, but not all, viral genomes localize to promyelocytic leukemia protein nuclear bodies (PML-NBs) and centromeres subnuclear domains in latently infected mouse neurons leading to restriction of viral gene expression [94]. Latent VZV and HSV genomes are bound to histones in the nucleus of the infected neuron and therefore subjected to epigenetic chromatin modifications. Specific post-translational acetylation and methylation of histone protein H3 determine the accessibility of genes for transcription: transcriptional permissive genes (euchromatin) are associated with acetylation of histone H3 on lysines 9 and 14 (H3K9ac/14ac) and di-methylation on lysine 4 (H3K4me2). Contrastingly, transcriptionally repressed genes (heterochromatin) are associated with H3K9me2, H3K9me3 and H3K27me3 [95]. Whereas most HSV genes are enriched for heterochromatic marks the HSV LAT locus is enriched for euchromatic marks, consistent with the abundant expression of LAT during latency [96]. Similar analysis of the epigenetic configuration of the latent VZV genome in ganglia obtained within 24 hours after death showed that VZV ORFs 14 and 36 are maintained in heterochromatic states, whereas ORFs 62 and 63 are kept in a euchromatic configuration [97]. CCCTC-binding factor (CTCF) binds to specific HSV DNA sequences, which facilitates the formation of chromatin insulators that maintain the boundary between euchromatin and heterochromatin and block the interaction between enhancers and promoters [96, 98]. Stress stimuli may release CTCF from the viral genome, resulting in expression of lytic genes and ultimately reactivation [96, 99]. Most HSV CTCF motifs are conserved in the VZV genome and VZV contains a number of additional CTCF motifs [98]. Noteworthy, these findings corroborate our observation that the VZV transcriptome in latently infected human ganglia is affected by the PMI and associated neuronal stress **(Chapter 5)** [89]. The pattern of VZV gene expression observed ≥9 hour postmortem may reflect epigenetic modifications of the viral genome [89]. Conceptually, steady-state low level transcription of VZV ORF63 may prevent complete silencing of the viral genome in

latently infected ganglia.

Innate Immune Control of VZV Latency

A two-stage model for the reactivation of latent alphaherpesviruses has been proposed based on HSV reactivation in rodent neurons [100]. Phase I, recently termed "animation" [100], does not depend on *de novo* synthesis of (viral) proteins and includes disordered gene expression [101]. Phase II depends on *de novo* synthesis of HSV virion protein 16 (VP16), and involves a regulated cascaded viral gene expression resembling lytic infection that results in production of infectious virus [100]. VP16 binds to cytoplasmatic host cell factor-1 (HCF-1), after which the complex relocates to the nucleus to combine with the host transcription factor Oct1 leading to initiation of viral gene expression [102-103]. However, VZV ORF10 transcripts, the ortholog of HSV VP16, cannot be detected in latently infected human ganglia [89]. Possibly, the VZV genome is more refractory to reactivation compared to HSV, e.g. due to the lack of LAT or microRNAs [30, 104], such that ORF10 expression is an extremely rare event. Alternatively, the major viral transactivator protein IE62 may interact with HCF-1 to initiate lytic gene expression [105], as ORF62 transcripts are frequently expressed in ganglia ≥9 hour postmortem [89]. Presumably, neurons are able to block progression of most reactivation events from progressing from phase I to phase II via the epigenetic silencing mechanisms outlined above. Additional control of viral latency is conferred by local host innate and adaptive immune responses. VZV can establish latency in the absence of an adaptive immune system in the SCID-hu mouse model [49], suggesting that ganglionic innate immune responses are sufficient to control viral replication and force VZV into latency. Although impaired $CD4^+$ T-cell immunity during primary infection may affect the establishment of SVV latency [106], VZV latency is not associated with the retention of virus-specific T-cells in human ganglia [87]. Both neurons and the neuron-interacting satellite glial cells (SGC) may contribute to ganglionic innate anti-alphaherpesvirus immunity. Neurons may produce type I IFNs, sequester viral proteins in PML-NBs or degrade viral proteins/particles in autophagosomes [56, 107]. The latter antiviral defense may be of particular importance for VZV as the virus does not encode a homologue of HSV ICP34.5, a neurovirulence factor known to inhibit autophagy [108]. SGC are ganglion-resident APCs that have the capacity to synthesize inflammatory mediators and cytokines such as prostaglandins, TNF-α, IL-6 and IL-15, and may modulate local T-cell responses [109-110]. Direct evidence for the role of SGC in controlling ganglionic alphaherpesvirus latency comes from the detection of TNF-α and IL-6 in SGC surrounding HSV-1 infected neurons [111-112].

4. Reactivation

Symptomatic and Asymptomatic VZV Reactivation

Herpes zoster results from reactivation of endogenous latent virus, after which VZV is transported along axons to the skin innervated by that particular sensory nerve. Although the stimuli that drive VZV reactivation are unknown, the risk of developing

herpes zoster increases with advancing age as a consequence of declining VZV-specific T-cell immunity [113-115]. Most individuals develop only episode of herpes zoster [116], but the presence of VZV DNA in PBMC [117-118] and saliva [119-121] of healthy individuals without clinical signs of VZV infection indicates that intermittent asymptomatic VZV reactivation does occur. Like VZV, HSV-1 establishes latency in neurons of the trigeminal ganglia (TG) [30, 103] and both viruses may even infect the same neuron [122]. Subclinical HSV reactivation occurs frequently and results in asymptomatic shedding of infectious virus at mucosal surfaces [123-124]. Under the presumption that the frequency of symptomatic virus reactivation is predictive for subclinical HSV and VZV reactivation, it was expected that asymptomatic shedding of VZV is less frequent compared to HSV. HSV-1 and VZV reactivation is more common in immunocompromised individuals and may result in viral shedding in saliva [113-115]. Therefore, we determined the kinetics and quantity of oral HSV-1 and VZV shedding in HSV-1 and VZV seropositive individuals infected with HIV **(Chapter 6)** [125]. Longitudinal analysis of daily saliva samples obtained for a median of 31 days from 22 individuals infected with HIV showed that while all persons shed HSV-1 at one or more time points, only two study participants shed very low levels of VZV in their saliva [125]. Unfortunately, the low frequency of asymptomatic VZV shedding – even in immunocompromised individuals – prohibited investigation of the potential interrelatedness of oral HSV-1 and VZV reactivation and shedding within the same individuals **(Chapter 6)** [125]. The increased propensity of HSV to reactivate compared to VZV may result from a variety of virus and host factors. Differential reactivation frequencies could be caused by the higher HSV DNA load compared to VZV DNA load in ganglia [77, 87, 126], since the HSV reactivation rate increases with higher ganglionic HSV DNA levels [127]. Alternatively, inhibitory epigenetic chromatin modifications on the VZV genome may be more resilient to reactivation compared to HSV-1. Abundant non-coding RNAs, including LAT and microRNAs, expressed by latent HSV [128-129] are not shared by VZV [30, 104], thereby potentially contributing to differential reactivation patterns. Further, an initial phase of intraganglionic virus replication and spread is believed to occur upon VZV reactivation before the virus descends down the sensory nerve endings to the skin, whereas this is not required for HSV [30, 103]. The resulting delay in VZV transfer to the skin or lymphocytes may provide the host immune system more time to control infection. Finally, the host may utilize different immune mechanisms to control the latency of both alphaherpesviruses: e.g. $CD8^+$ T-cells are considered pivotal to control HSV-1, but not VZV latency in human TG [77, 87].

Reactivation Induces Infiltration of T-cells into Ganglia

The direct correlation between the risk of developing herpes zoster and VZV-specific T-cell immunity [113-115, 130] contrasts the apparent lack of virus-specific T-cells in VZV latently infected human ganglia [77, 87]. However, upon herpes zoster the rash-innervating ganglia may show profound inflammation [131-132]. Immune infiltrates, mainly composed of noncytolytic T-cells, persist for weeks to months after reactivation [133]. Recruitment of $CD8^+$ T-cells to the genital mucosa following HSV infection is dependent on local expression of the chemokine CXCL10 [134-135]. VZV infection of intact human fetal ganglia *in vitro* induced production and secretion

of CXCL10 [136], which may provide the trigger for T-cells to infiltrate ganglia upon reactivation. Alternatively, infiltration of T-cells into ganglia may be antigen-driven. Similar to the human situation, only few T-cells are observed in ganglia of uninfected or SVV latently infected nonhuman primates (**Chapter 6** [137] and Ouwendijk et al., 2013, unpublished data). Analogous to VZV, SVV reactivation induces a transient infiltration of predominantly noncytolytic $CD8^+$ T-cells [137]. The number of ganglion-infiltrating $CD8^+$ T-cells and T-cell clusters correlated significantly with local expression of CXCL10 transcripts, but not SVV transcripts or antigens, suggesting that the influx of $CD8^+$ T-cells at the analyzed stages following SVV reactivation is mainly chemokine- rather than antigen-driven [137]. Notably, CXCL10 expression and associated T-cell infiltration did not differ among ganglia, including those that corresponded to the dermatome associated with zoster rash **(Chapter 6)** [137]. These findings suggest that virus reactivation is initiated in multiple ganglia simultaneously, not restricted to the herpes zoster lesion innervating ganglia, as evidenced by the detection of late SVV transcripts in various ganglia [13, 29]. HSV reactivation induces proliferation of both tissue-resident and newly recruited virus-specific T-cells in ganglia [138-139]. Optimal intraganglionic $CD8^+$ T-cell proliferation is dependent on efficient antigen presentation by recruited dendritic cells and/or ganglion-resident SGC, as well as $CD4^+$ T-cell help [139]. Alternatively or additionally, SVV reactivation likely stimulates (systemic) virus-specific T-cells that subsequently infiltrate multiple ganglia due their activated phenotype, which is sufficient for T-cells to enter latently infected HSV ganglia in mice [140]. Although tissue-resident memory T-cells (T_{RM} cells) present within ganglia are retained locally, both systemic and newly recruited intraganglionic virus-specific activated T-cells may enter additional sensory ganglia [138-139]. Thus, VZV and SVV reactivation induce the influx of T-cells into sensory ganglia most likely to contain local virus replication, analogous to the potential role of $CD8^+$ T-cells in restricting HSV reactivation [87, 141-142].

Recent studies suggest that HSV-specific T_{RM} cells are retained in both ganglia and skin to control virus replication locally [138, 143-145]. As outlined above, HSV reactivation induces local proliferation of both T_{RM} cells and newly recruited T-cells [138-139]. Combined with the observations that (1) (subclinical) reactivation of HSV occurs much more frequently compared to VZV [125] and (2) that SVV reactivation, but not latency, is associated with influx of T-cells into ganglia [137], these data suggest that virus-specific T-cells in ganglia are mainly involved in controlling reactivation rather than latency. Most likely HSV-specific T-cells are highly abundant in HSV-infected ganglia as a result of more frequent reactivation [77, 87, 137]. Currently, no VZV-specific T-cells have been detected in VZV latently infected human ganglia [87]. Because ganglia from herpes zoster patients are extremely rare to obtain, the SVV nonhuman primate model provides the ideal setting to study the immune response in ganglia during and following reactivation. Future studies should address the source of ganglionic T-cells (recruitment or local proliferation), their antigen specificity, their phenotype at various stages after reactivation and the role of ganglion-resident or infiltrating APCs. Skin-resident T_{RM} cells are induced by various virus infections, including HSV and vaccinia virus, and persist in the epidermis for sustained periods of time and are potentially involved in protecting the host for reactivations and re-infec-

tions [138, 145-146]. However, VZV and HSV infections differ in several fundamental aspects: (1) whereas HSV infection is localized, primary VZV infection results in generalized skin rash; (2) HSV reactivation occurs frequently, whereas VZV reactivation is rare with most individuals developing only one episode of herpes zoster several decades after varicella. Therefore, the potential role of skin-resident T_{RM} cells in the pathogenesis of VZV infection remains to be determined.

Ocular VZV Disease

Although VZV-specific T-cell immunity is essential for uncomplicated recovery from varicella and herpes zoster [52, 115], tissue-infiltrating virus-specific T-cells may also initiate severe disease in organs with limited regenerative capacities like the brain and eye [147]. Acute retinal necrosis (ARN) is a rare, rapidly progressing and potentially blinding inflammatory eye disease that is commonly caused by reactivation of latent VZV or HSV-1 in immunecompetent individuals [148-150]. Most likely, alphaherpesviruses gain access to the retinal pigment epithelial (RPE) cells by axonal transport via the optic nerve [151], explaining the increased risk of herpetic encephalitis and meningitis patients to develop ARN [152]. ARN is the outcome of a combination of an initial virus-induced cytopathology and the subsequent immunopathology caused by ocular-infiltrating virus-specific T-cells [153-155]. Intraocular fluid (IOF)-derived T-cells predominantly recognize the causative alphaherpesvirus, secrete cytokines consistent with a Th0/Th1 phenotype, and demonstrate HLA class I- and HLA class II-restricted cytotoxicity [156-160]. Previous studies have shown that some IOF-derived T-cells recognize non-causative alphaherpesviruses too, suggesting that αHHV-cross-reactive T-cells infiltrate the eyes of herpetic uveitis patients [157-160]. In **Chapter 8**, we have identified a HLA class II allele promiscuous $CD4^+$ T-cell epitope located within VZV IE62 that was recognized by two distinct T-cell clones obtained from the affected eye of the same VZV ARN patient. The IE62 epitope was completely conserved in its HSV counterpart ICP4 and a common target for blood-derived $CD4^+$ T-cells in HSV-1/VZV immune individuals. Furthermore, the IE62/ICP4-specific IOF-derived T-cells recognized both VZV and HSV-1 in autologous B-cell lines. The data are in agreement with previous studies showing that immunodominant T-cell responses are mostly directed to viral tegument proteins, such as IE62/ICP4, in blood of healthy VZV/HSV-seropositive individuals and genital herpes patients, as well as in the affected eyes of herpetic uveitis patients [161]. Furthermore, a recent HSV-1 ORFeome-wide screen for $CD4^+$ and $CD8^+$ T-cell targets revealed that ICP4 is an immunodominant T-cell antigen in HSV-1 seropositive individuals [44]. Notably, experiments on RPE cells – used as a disease-relevant cell type – demonstrated that the αHHV-cross-reactive T-cells controlled VZV, but not HSV-1 infection *in vitro* **(Chapter 8)**. This differential effect was not observed using RPE cells pulsed with HSV-1 and VZV protein lysates, indicating that HSV-1 employs an immune evasion strategy to prevent $CD4^+$ T-cell recognition. Further studies are warranted to identify the HSV-1 protein(s) and the mechanisms involved.

5. Future Perspectives

VZV reactivation occurs in 20% – 30% of latently infected individuals and is a significant cause of neurological and ophthalmological disease [162-164]. Vaccination of elderly individuals with the zoster vaccine reduces the incidence of herpes zoster only by 51% and post-herpetic neuralgia by 67% [165]. Childhood vaccination prevents varicella in 80 – 87% (1-dose regimen) [166-167] and up to 98% (2-dose regimen) [168] of vaccinated children, but produces a life-long latent VZV infection in 100% of vaccinated individuals. The VZV vaccine strain vOka is not attenuated for replication in human T-cells and fetal ganglia [49, 169], which poses the lifelong risk of reactivation and associated disease or even death in vaccinees [170]. Thus, there is an unmet need for a safer and more efficacious 2nd generation VZV vaccine. Since the latent phase is imperceptible for adaptive immune control novel intervention strategies should be aimed at limiting the VZV latent load and prevention of VZV reactivation. To achieve this, it will be essential to combine studies on the virus-host factors involved in VZV infection in humans and the SVV nonhuman primate model. Full VZV genome-wide screens of the systemic VZV-specific CD4$^+$ and CD8$^+$ T-cell repertoire in healthy and diseased VZV immune individuals are needed to identify the protective VZV T-cell targets. It will be important to understand why VZV-specific T-cell immunity is declining with ageing and why not all elderly individuals vaccinated with the zoster vaccine develop protective virus-specific immune responses. SVV infection of nonhuman primates provides the only animal model to study the pathogenesis of varicella and herpes zoster. In order to limit the establishment of latency it will be essential to define the cell types and effector molecules that control SVV infections during the early phase of primary SVV infection in the respiratory tract and ganglia. Further, experimental reactivation of SVV in nonhuman primates provides a model system in which both systemic and tissue-resident (e.g., skin and ganglia) virus-specific T-cell responses induced by herpes zoster can be studied. Thus, future integrated research on VZV and SVV will provide novel intervention strategies to limit the establishment of VZV latency and prevent reactivation.

References

1. Stevens NJ, Seiffert ER, O'Connor PM, et al. Palaeontological evidence for an Oligocene divergence between Old World monkeys and apes. Nature 2013;497:611-4
2. Myers MG, Kramer LW and Stanberry LR. Varicella in a gorilla. J Med Virol 1987;23:317-22
3. Cohen JI, Moskal T, Shapiro M and Purcell RH. Varicella in Chimpanzees. J Med Virol 1996;50:289-92
4. Felsenfeld AD, Schmidt NJ. Varicella-zoster virus immunizes patas monkeys against simian varicella-like disease. J Gen Virol 1979;42:171-8
5. Willer DO, Ambagala AP, Pilon R, et al. Experimental infection of Cynomolgus Macaques (Macaca fascicularis) with human varicella-zoster virus. J Virol 2012;86:3626-34
6. Gray WL. Simian varicella: a model for human varicella-zoster virus infections. Rev Med Virol 2004;14:363-81
7. Mahalingam R, Messaoudi I and Gilden D. Simian varicella virus pathogenesis. Curr Top Microbiol Immunol 2010;342:309-21
8. Fletcher TM, 3rd, Gray WL. Simian varicella virus: characterization of virion and infected cell polypeptides and the antigenic cross-reactivity with varicella-zoster virus. J Gen Virol 1992;73 (Pt 5):1209-15
9. Gray WL, Starnes B, White MW and Mahalingam R. The DNA sequence of the simian varicella virus genome. Virology 2001;284:123-30
10. Grose C. Pangaea and the Out-of-Africa Model of Varicella-Zoster Virus Evolution and Phylogeography. J Virol 2012;86:9558-65
11. McGeoch DJ, Rixon FJ and Davison AJ. Topics in herpesvirus genomics and evolution. Virus Res 2006;117:90-104
12. Blakely GA, Lourie B, Morton WG, Evans HH and Kaufmann AF. A varicella-like disease in macaque monkeys. J Infect Dis 1973;127:617-25
13. Mahalingam R, Traina-Dorge V, Wellish M, et al. Latent simian varicella virus reactivates in monkeys treated with tacrolimus with or without exposure to irradiation. J Neurovirol 2010;16:342-54
14. Dueland AN, Martin JR, Devlin ME, et al. Acute simian varicella infection. Clinical, laboratory, pathologic, and virologic features. Lab Invest 1992;66:762-73
15. Wenner HA, Barrick S, Abel D and Seshumurty P. The pathogenesis of simian varicella virus in cynomolgus monkeys. Proc Soc Exp Biol Med 1975;150:318-23
16. Kolappaswamy K, Mahalingam R, Traina-Dorge V, et al. Disseminated simian varicella virus infection in an irradiated rhesus macaque (Macaca mulatta). J Virol 2007;81:411-5
17. Ward TM, Traina-Dorge V, Davis KA and Gray WL. Recombinant simian varicella viruses expressing respiratory syncytial virus antigens are immunogenic. J Gen Virol 2008;89:741-50
18. Mahalingam R, Traina-Dorge V, Wellish M, et al. Effect of time delay after necropsy on analysis of simian varicella-zoster virus expression in latently infected ganglia of rhesus macaques. J Virol 2010;84:12454-7
19. Messaoudi I, Barron A, Wellish M, et al. Simian varicella virus infection of rhesus macaques recapitulates essential features of varicella zoster virus infection in humans. PLoS Pathog 2009;5:e1000657
20. Ouwendijk WJ, Mahalingam R, Traina-Dorge V, et al. Simian varicella virus infection of Chinese rhesus macaques produces ganglionic infection in the absence of rash. J Neurovirol 2012;18:91-9
21. Gibbs RA, Rogers J, Katze MG, et al. Evolutionary and biomedical insights from the rhesus macaque genome. Science 2007;316:222-34
22. Hernandez RD, Hubisz MJ, Wheeler DA, et al. Demographic histories and patterns of linkage disequilibrium in Chinese and Indian rhesus macaques. Science 2007;316:240-3
23. Ling B, Veazey RS, Luckay A, et al. SIV(mac) pathogenesis in rhesus macaques of Chinese and Indian origin compared with primary HIV infections in humans. AIDS 2002;16:1489-96
24. Trichel AM, Rajakumar PA and Murphey-Corb M. Species-specific variation in SIV disease progression between Chinese and Indian subspecies of rhesus macaque. J Med Primatol 2002;31:171-8
25. Ouwendijk WJ, Mahalingam R, de Swart RL, et al. T-Cell Tropism of Simian Varicella Virus during Primary Infection. PLoS Pathog 2013;9:e1003368
26. White TM, Mahalingam R, Traina-Dorge V and Gilden DH. Persistence of simian varicella virus DNA

in CD4(+) and CD8(+) blood mononuclear cells for years after intratracheal inoculation of African green monkeys. Virology 2002;303:192-8
27. White TM, Mahalingam R, Traina-Dorge V and Gilden DH. Simian varicella virus DNA is present and transcribed months after experimental infection of adult African green monkeys. J Neurovirol 2002;8:191-203
28. Mahalingam R, Traina-Dorge V, Wellish M, Smith J and Gilden DH. Naturally acquired simian varicella virus infection in African green monkeys. J Virol 2002;76:8548-50
29. Mahalingam R, Traina-Dorge V, Wellish M, et al. Simian varicella virus reactivation in cynomolgus monkeys. Virology 2007;368:50-9
30. Cohen JI, Straus, S.E., Arvin, A.M. . Varicella-zoster virus replication, pathogenesis, and management. In: Knipe DM, Howley, P.M. , ed. Field virology. 5 ed. Vol. 2. Philadelphia, PA: Lippincott Williams and Wilkins, 2007
31. Grose C. Variation on a theme by Fenner: the pathogenesis of chickenpox. Pediatrics 1981;68:735-7
32. Tomlinson TH. Giant cell formation in the tonsils in the prodromal stage of chickenpox: Report of a case. Am J Pathol 1939;15:523-526 3
33. Lemon K, de Vries RD, Mesman AW, et al. Early target cells of measles virus after aerosol infection of non-human primates. PLoS Pathog 2011;7:e1001263
34. Kirby AC, Coles MC and Kaye PM. Alveolar macrophages transport pathogens to lung draining lymph nodes. J Immunol 2009;183:1983-9
35. Thornton EE, Looney MR, Bose O, et al. Spatiotemporally separated antigen uptake by alveolar dendritic cells and airway presentation to T cells in the lung. J Exp Med 2012;209:1183-99
36. Abendroth A, Morrow G, Cunningham AL and Slobedman B. Varicella-zoster virus infection of human dendritic cells and transmission to T cells: implications for virus dissemination in the host. J Virol 2001;75:6183-92
37. Arbeit RD, Zaia JA, Valerio MA and Levin MJ. Infection of human peripheral blood mononuclear cells by varicella-zoster virus. Intervirology 1982;18:56-65
38. de Witte L, de Vries RD, van der Vlist M, et al. DC-SIGN and CD150 have distinct roles in transmission of measles virus from dendritic cells to T-lymphocytes. PLoS Pathog 2008;4:e1000049
39. Asano Y, Itakura N, Kajita Y, et al. Severity of viremia and clinical findings in children with varicella. J Infect Dis 1990;161:1095-8
40. Mainka C, Fuss B, Geiger H, Hofelmayr H and Wolff MH. Characterization of viremia at different stages of varicella-zoster virus infection. J Med Virol 1998;56:91-8
41. Koropchak CM, Graham G, Palmer J, et al. Investigation of varicella-zoster virus infection by polymerase chain reaction in the immunocompetent host with acute varicella. J Infect Dis 1991;163:1016-22
42. Ku CC, Padilla JA, Grose C, Butcher EC and Arvin AM. Tropism of varicella-zoster virus for human tonsillar CD4(+) T lymphocytes that express activation, memory, and skin homing markers. J Virol 2002;76:11425-33
43. Soong W, Schultz JC, Patera AC, Sommer MH and Cohen JI. Infection of human T lymphocytes with varicella-zoster virus: an analysis with viral mutants and clinical isolates. J Virol 2000;74:1864-70
44. Jing L, Haas J, Chong TM, et al. Cross-presentation and genome-wide screening reveal candidate T cells antigens for a herpes simplex virus type 1 vaccine. J Clin Invest 2012;122:654-73
45. Wolfl M, Kuball J, Ho WY, et al. Activation-induced expression of CD137 permits detection, isolation, and expansion of the full repertoire of CD8+ T cells responding to antigen without requiring knowledge of epitope specificities. Blood 2007;110:201-10
46. Gebhardt T, Mackay LK. Local immunity by tissue-resident CD8(+) memory T cells. Front Immunol 2012;3:340
47. Picker LJ, Terstappen LW, Rott LS, Streeter PR, Stein H and Butcher EC. Differential expression of homing-associated adhesion molecules by T cell subsets in man. J Immunol 1990;145:3247-55
48. Ku CC, Zerboni L, Ito H, Graham BS, Wallace M and Arvin AM. Varicella-zoster virus transfer to skin by T Cells and modulation of viral replication by epidermal cell interferon-alpha. J Exp Med 2004;200:917-25
49. Zerboni L, Ku CC, Jones CD, Zehnder JL and Arvin AM. Varicella-zoster virus infection of human dorsal root ganglia in vivo. Proc Natl Acad Sci U S A 2005;102:6490-5
50. Asano Y, Itakura N, Hiroishi Y, et al. Viremia is present in incubation period in nonimmunocompromised

children with varicella. J Pediatr 1985;106:69-71
51. Konig A, Homme C, Hauroder B, Dietrich A and Wolff MH. The varicella-zoster virus induces apoptosis in vitro in subpopulations of primary human peripheral blood mononuclear cells. Microbes Infect 2003;5:879-89
52. Arvin AM, Koropchak CM, Williams BR, Grumet FC and Foung SK. Early immune response in healthy and immunocompromised subjects with primary varicella-zoster virus infection. J Infect Dis 1986;154:422-9
53. Malavige GN, Jones L, Kamaladasa SD, et al. Viral load, clinical disease severity and cellular immune responses in primary varicella zoster virus infection in Sri Lanka. PLoS One 2008;3:e3789
54. Tyzzer EE. The Histology of the Skin Lesions in Varicella. J Med Res 1906;14:361-392 7
55. Braverman IM. The cutaneous microcirculation: ultrastructure and microanatomical organization. Microcirculation 1997;4:329-40
56. Reichelt M, Wang L, Sommer M, et al. Entrapment of viral capsids in nuclear PML cages is an intrinsic antiviral host defense against varicella-zoster virus. PLoS Pathog 2011;7:e1001266
57. Sen N, Che X, Rajamani J, et al. Signal transducer and activator of transcription 3 (STAT3) and survivin induction by varicella-zoster virus promote replication and skin pathogenesis. Proc Natl Acad Sci U S A 2012;109:600-5
58. Takahashi MN, Jackson W, Laird DT, et al. Varicella-zoster virus infection induces autophagy in both cultured cells and human skin vesicles. J Virol 2009;83:5466-76
59. Hardy I, Gershon AA, Steinberg SP and LaRussa P. The incidence of zoster after immunization with live attenuated varicella vaccine. A study in children with leukemia. Varicella Vaccine Collaborative Study Group. N Engl J Med 1991;325:1545-50
60. Hope-Simpson RE. The Nature of Herpes Zoster: A Long-Term Study and a New Hypothesis. Proc R Soc Med 1965;58:9-20
61. Grigoryan S, Kinchington PR, Yang IH, et al. Retrograde axonal transport of VZV: kinetic studies in hESC-derived neurons. J Neurovirol 2012;18:462-70
62. Markus A, Grigoryan S, Sloutskin A, et al. Varicella-zoster virus (VZV) infection of neurons derived from human embryonic stem cells: direct demonstration of axonal infection, transport of VZV, and productive neuronal infection. J Virol 2011;85:6220-33
63. Myers MI, Peltier AC and Li J. Evaluating dermal myelinated nerve fibers in skin biopsy. Muscle Nerve 2013;47:1-11
64. Haberthur K, Engelmann F, Park B, et al. CD4 T cell immunity is critical for the control of simian varicella virus infection in a nonhuman primate model of VZV infection. PLoS Pathog 2011;7:e1002367
65. Chaves SS, Gargiullo P, Zhang JX, et al. Loss of vaccine-induced immunity to varicella over time. N Engl J Med 2007;356:1121-9
66. Watson B. Humoral and cell-mediated immune responses in children and adults after 1 and 2 doses of varicella vaccine. J Infect Dis 2008;197 Suppl 2:S143-6
67. Weinberg A, Lazar AA, Zerbe GO, et al. Influence of age and nature of primary infection on varicella-zoster virus-specific cell-mediated immune responses. J Infect Dis 2010;201:1024-30
68. Cohrs RJ, Barbour M and Gilden DH. Varicella-zoster virus (VZV) transcription during latency in human ganglia: detection of transcripts mapping to genes 21, 29, 62, and 63 in a cDNA library enriched for VZV RNA. J Virol 1996;70:2789-96
69. Cohrs RJ, Gilden DH. Varicella zoster virus transcription in latently-infected human ganglia. Anticancer Res 2003;23:2063-9
70. Cohrs RJ, Gilden DH. Prevalence and abundance of latently transcribed varicella-zoster virus genes in human ganglia. J Virol 2007;81:2950-6
71. Cohrs RJ, Srock K, Barbour MB, et al. Varicella-zoster virus (VZV) transcription during latency in human ganglia: construction of a cDNA library from latently infected human trigeminal ganglia and detection of a VZV transcript. J Virol 1994;68:7900-8
72. Grinfeld E, Kennedy PG. Translation of varicella-zoster virus genes during human ganglionic latency. Virus Genes 2004;29:317-9
73. Kennedy PG, Grinfeld E and Bell JE. Varicella-zoster virus gene expression in latently infected and explanted human ganglia. J Virol 2000;74:11893-8
74. Kennedy PG, Grinfeld E and Gow JW. Latent varicella-zoster virus is located predominantly in neurons in human trigeminal ganglia. Proc Natl Acad Sci U S A 1998;95:4658-62
75. Lungu O, Panagiotidis CA, Annunziato PW, Gershon AA and Silverstein SJ. Aberrant intracellular localization of Varicella-Zoster virus regulatory proteins during latency. Proc Natl Acad Sci U S A

1998;95:7080-5
76. Mahalingam R, Wellish M, Cohrs R, et al. Expression of protein encoded by varicella-zoster virus open reading frame 63 in latently infected human ganglionic neurons. Proc Natl Acad Sci U S A 1996;93:2122-4
77. Theil D, Derfuss T, Paripovic I, et al. Latent herpesvirus infection in human trigeminal ganglia causes chronic immune response. Am J Pathol 2003;163:2179-84
78. Zerboni L, Sobel RA, Ramachandran V, et al. Expression of varicella-zoster virus immediate-early regulatory protein IE63 in neurons of latently infected human sensory ganglia. J Virol 2010;84:3421-30
79. Ouwendijk WJ, Flowerdew SE, Wick D, et al. Immunohistochemical detection of intra-neuronal VZV proteins in snap-frozen human ganglia is confounded by antibodies directed against blood group A1-associated antigens. J Neurovirol 2012;18:172-80
80. Zerboni L, Sobel RA, Lai M, et al. Apparent expression of varicella-zoster virus proteins in latency resulting from reactivity of murine and rabbit antibodies with human blood group a determinants in sensory neurons. J Virol 2012;86:578-83
81. Finstad CL, Yin BW, Gordon CM, Federici MG, Welt S and Lloyd KO. Some monoclonal antibody reagents (C219 and JSB-1) to P-glycoprotein contain antibodies to blood group A carbohydrate determinants: a problem of quality control for immunohistochemical analysis. J Histochem Cytochem 1991;39:1603-10
82. Kliman HJ, Feinberg RF, Schwartz LB, Feinman MA, Lavi E and Meaddough EL. A mucin-like glycoprotein identified by MAG (mouse ascites Golgi) antibodies. Menstrual cycle-dependent localization in human endometrium. Am J Pathol 1995;146:166-81
83. Mollicone R, Davies DR, Evans B, Dalix AM and Oriol R. Cellular expression and genetic control of ABH antigens in primary sensory neurons of marmoset, baboon and man. J Neuroimmunol 1986;10:255-69
84. Smith ZD, D'Eugenio-Gumkowski F, Yanagisawa K and Jamieson JD. Endogenous and monoclonal antibodies to the rat pancreatic acinar cell Golgi complex. J Cell Biol 1984;98:2035-46
85. Spicer SS, Spivey MA, Ito M and Schulte BA. Some ascites monoclonal antibody preparations contain contaminants that bind to selected Golgi zones or mast cells. J Histochem Cytochem 1994;42:213-21
86. Lenac Rovis T, Bailer SM, Pothineni VR, et al. A comprehensive analysis of varicella zoster virus proteins using a new monoclonal antibody collection. J Virol 2013
87. Verjans GM, Hintzen RQ, van Dun JM, et al. Selective retention of herpes simplex virus-specific T cells in latently infected human trigeminal ganglia. Proc Natl Acad Sci U S A 2007;104:3496-501
88. Nagel MA, Choe A, Traktinskiy I, Cordery-Cotter R, Gilden D and Cohrs RJ. Varicella-zoster virus transcriptome in latently infected human ganglia. J Virol 2011;85:2276-87
89. Ouwendijk WJ, Choe A, Nagel MA, et al. Restricted varicella-zoster virus transcription in human trigeminal ganglia obtained soon after death. J Virol 2012;86:10203-6
90. Croen KD, Ostrove JM, Dragovic LJ and Straus SE. Patterns of gene expression and sites of latency in human nerve ganglia are different for varicella-zoster and herpes simplex viruses. Proc Natl Acad Sci U S A 1988;85:9773-7
91. Ou Y, Davis KA, Traina-Dorge V and Gray WL. Simian varicella virus expresses a latency-associated transcript that is antisense to open reading frame 61 (ICP0) mRNA in neural ganglia of latently infected monkeys. J Virol 2007;81:8149-56
92. Sexton T, Schober H, Fraser P and Gasser SM. Gene regulation through nuclear organization. Nat Struct Mol Biol 2007;14:1049-55
93. Spector DL. The dynamics of chromosome organization and gene regulation. Annu Rev Biochem 2003;72:573-608
94. Catez F, Picard C, Held K, et al. HSV-1 genome subnuclear positioning and associations with host-cell PML-NBs and centromeres regulate LAT locus transcription during latency in neurons. PLoS Pathog 2012;8:e1002852
95. Jenuwein T, Allis CD. Translating the histone code. Science 2001;293:1074-80
96. Bloom DC, Giordani NV and Kwiatkowski DL. Epigenetic regulation of latent HSV-1 gene expression. Biochim Biophys Acta 2010;1799:246-56
97. Gary L, Gilden DH and Cohrs RJ. Epigenetic regulation of varicella-zoster virus open reading frames 62 and 63 in latently infected human trigeminal ganglia. J Virol 2006;80:4921-6
98. Amelio AL, McAnany PK and Bloom DC. A chromatin insulator-like element in the herpes simplex

virus type 1 latency-associated transcript region binds CCCTC-binding factor and displays enhancer-blocking and silencing activities. J Virol 2006;80:2358-68
99. Ertel MK, Cammarata AL, Hron RJ and Neumann DM. CTCF occupation of the herpes simplex virus 1 genome is disrupted at early times postreactivation in a transcription-dependent manner. J Virol 2012;86:12741-59
100. Kim JY, Mandarino A, Chao MV, Mohr I and Wilson AC. Transient reversal of episome silencing precedes VP16-dependent transcription during reactivation of latent HSV-1 in neurons. PLoS Pathog 2012;8:e1002540
101. Du T, Zhou G and Roizman B. HSV-1 gene expression from reactivated ganglia is disordered and concurrent with suppression of latency-associated transcript and miRNAs. Proc Natl Acad Sci U S A 2011;108:18820-4
102. Thompson RL, Preston CM and Sawtell NM. De novo synthesis of VP16 coordinates the exit from HSV latency in vivo. PLoS Pathog 2009;5:e1000352
103. Roizman B, Knipe DM and Whitley RJ. Herpes Simplex Viruses. In: Knipe DM, Howley PM, Griffin et al., eds. Fields Virology. 5th ed. Vol. 2. Philadelphia: Lippincott, Williams & Wilkins, 2007:2501 - 2601
104. Umbach JL, Nagel MA, Cohrs RJ, Gilden DH and Cullen BR. Analysis of human alphaherpesvirus microRNA expression in latently infected human trigeminal ganglia. J Virol 2009;83:10677-83
105. Narayanan A, Nogueira ML, Ruyechan WT and Kristie TM. Combinatorial transcription of herpes simplex virus and varicella zoster virus immediate early genes is strictly determined by the cellular coactivator HCF-1. J Biol Chem 2005;280:1369-75
106. Meyer C, Dewane J, Kerns A, et al. Age and immune status of rhesus macaques impacts simian varicella virus gene expression in sensory ganglia. J Virol 2013
107. Yordy B, Iijima N, Huttner A, Leib D and Iwasaki A. A neuron-specific role for autophagy in antiviral defense against herpes simplex virus. Cell Host Microbe 2012;12:334-45
108. Orvedahl A, Levine B. Autophagy and viral neurovirulence. Cell Microbiol 2008;10:1747-56
109. Hanani M. Satellite glial cells in sensory ganglia: from form to function. Brain Res Brain Res Rev 2005;48:457-76
110. van Velzen M, Laman JD, Kleinjan A, Poot A, Osterhaus AD and Verjans GM. Neuron-interacting satellite glial cells in human trigeminal ganglia have an APC phenotype. J Immunol 2009;183:2456-61
111. Mori I, Goshima F, Koshizuka T, et al. Iba1-expressing microglia respond to herpes simplex virus infection in the mouse trigeminal ganglion. Brain Res Mol Brain Res 2003;120:52-6
112. Shimeld C, Easty DL and Hill TJ. Reactivation of herpes simplex virus type 1 in the mouse trigeminal ganglion: an in vivo study of virus antigen and cytokines. J Virol 1999;73:1767-73
113. Burke BL, Steele RW, Beard OW, Wood JS, Cain TD and Marmer DJ. Immune responses to varicella-zoster in the aged. Arch Intern Med 1982;142:291-3
114. Levin MJ, Smith JG, Kaufhold RM, et al. Decline in varicella-zoster virus (VZV)-specific cell-mediated immunity with increasing age and boosting with a high-dose VZV vaccine. J Infect Dis 2003;188:1336-44
115. Miller AE. Selective decline in cellular immune response to varicella-zoster in the elderly. Neurology 1980;30:582-7
116. Dworkin RH, Johnson RW, Breuer J, et al. Recommendations for the management of herpes zoster. Clin Infect Dis 2007;44 Suppl 1:S1-26
117. Devlin ME, Gilden DH, Mahalingam R, Dueland AN and Cohrs R. Peripheral blood mononuclear cells of the elderly contain varicella-zoster virus DNA. J Infect Dis 1992;165:619-22
118. Schunemann S, Mainka C and Wolff MH. Subclinical reactivation of varicella-zoster virus in immunocompromised and immunocompetent individuals. Intervirology 1998;41:98-102
119. Cohrs RJ, Mehta SK, Schmid DS, Gilden DH and Pierson DL. Asymptomatic reactivation and shed of infectious varicella zoster virus in astronauts. J Med Virol 2008;80:1116-22
120. Mehta SK, Cohrs RJ, Forghani B, Zerbe G, Gilden DH and Pierson DL. Stress-induced subclinical reactivation of varicella zoster virus in astronauts. J Med Virol 2004;72:174-9
121. Nagel MA, Choe A, Cohrs RJ, et al. Persistence of varicella zoster virus DNA in saliva after herpes zoster. J Infect Dis 2011;204:820-4
122. Theil D, Paripovic I, Derfuss T, et al. Dually infected (HSV-1/VZV) single neurons in human trigeminal ganglia. Ann Neurol 2003;54:678-82
123. Mark KE, Wald A, Magaret AS, et al. Rapidly cleared episodes of herpes simplex virus reactivation

in immunocompetent adults. J Infect Dis 2008;198:1141-9
124. Schiffer JT, Corey L. Rapid host immune response and viral dynamics in herpes simplex virus-2 infection. Nat Med 2013;19:280-90
125. van Velzen M, Ouwendijk WJ, Selke S, et al. Longitudinal study on oral shedding of herpes simplex virus 1 and varicella-zoster virus in individuals infected with HIV. J Med Virol 2013
126. Cohrs RJ, Laguardia JJ and Gilden D. Distribution of latent herpes simplex virus type-1 and varicella zoster virus DNA in human trigeminal Ganglia. Virus Genes 2005;31:223-7
127. Hoshino Y, Pesnicak L, Cohen JI and Straus SE. Rates of reactivation of latent herpes simplex virus from mouse trigeminal ganglia ex vivo correlate directly with viral load and inversely with number of infiltrating CD8+ T cells. J Virol 2007;81:8157-64
128. Stevens JG, Haarr L, Porter DD, Cook ML and Wagner EK. Prominence of the herpes simplex virus latency-associated transcript in trigeminal ganglia from seropositive humans. J Infect Dis 1988;158:117-23
129. Umbach JL, Kramer MF, Jurak I, Karnowski HW, Coen DM and Cullen BR. MicroRNAs expressed by herpes simplex virus 1 during latent infection regulate viral mRNAs. Nature 2008;454:780-3
130. van Besouw NM, Verjans GM, Zuijderwijk JM, Litjens NH, Osterhaus AD and Weimar W. Systemic varicella zoster virus reactive effector memory T-cells impaired in the elderly and in kidney transplant recipients. J Med Virol 2012;84:2018-25
131. Head H, Campbell AW. The pathology of herpes zoster and its bearing on sensory localisation. Brain 1900;23:170
132. Nagashima K, Nakazawa M and Endo H. Pathology of the human spinal ganglia in varicella-zoster virus infection. Acta Neuropathol 1975;33:105-17
133. Gowrishankar K, Steain M, Cunningham AL, et al. Characterization of the host immune response in human Ganglia after herpes zoster. J Virol 2010;84:8861-70
134. Nakanishi Y, Lu B, Gerard C and Iwasaki A. CD8(+) T lymphocyte mobilization to virus-infected tissue requires CD4(+) T-cell help. Nature 2009;462:510-3
135. Shin H, Iwasaki A. A vaccine strategy that protects against genital herpes by establishing local memory T cells. Nature 2012;491:463-7
136. Steain M, Gowrishankar K, Rodriguez M, Slobedman B and Abendroth A. Upregulation of CXCL10 in human dorsal root ganglia during experimental and natural varicella-zoster virus infection. J Virol 2011;85:626-31
137. Ouwendijk WJ, Abendroth A, Traina-Dorge V, et al. T-cell infiltration correlates with CXCL10 expression in ganglia of cynomolgus macaques with reactivated simian varicella virus. J Virol 2013;87:2979-82
138. Gebhardt T, Wakim LM, Eidsmo L, Reading PC, Heath WR and Carbone FR. Memory T cells in nonlymphoid tissue that provide enhanced local immunity during infection with herpes simplex virus. Nat Immunol 2009;10:524-30
139. Wakim LM, Waithman J, van Rooijen N, Heath WR and Carbone FR. Dendritic cell-induced memory T cell activation in nonlymphoid tissues. Science 2008;319:198-202
140. van Lint AL, Kleinert L, Clarke SR, Stock A, Heath WR and Carbone FR. Latent infection with herpes simplex virus is associated with ongoing CD8+ T-cell stimulation by parenchymal cells within sensory ganglia. J Virol 2005;79:14843-51
141. Knickelbein JE, Khanna KM, Yee MB, Baty CJ, Kinchington PR and Hendricks RL. Noncytotoxic lytic granule-mediated CD8+ T cell inhibition of HSV-1 reactivation from neuronal latency. Science 2008;322:268-71
142. Liu T, Khanna KM, Chen X, Fink DJ and Hendricks RL. CD8(+) T cells can block herpes simplex virus type 1 (HSV-1) reactivation from latency in sensory neurons. J Exp Med 2000;191:1459-66
143. Ariotti S, Beltman JB, Chodaczek G, et al. Tissue-resident memory CD8+ T cells continuously patrol skin epithelia to quickly recognize local antigen. Proc Natl Acad Sci U S A 2012;109:19739-44
144. Gebhardt T, Whitney PG, Zaid A, et al. Different patterns of peripheral migration by memory CD4+ and CD8+ T cells. Nature 2011;477:216-9
145. Jiang X, Clark RA, Liu L, Wagers AJ, Fuhlbrigge RC and Kupper TS. Skin infection generates non-migratory memory CD8+ T(RM) cells providing global skin immunity. Nature 2012;483:227-31
146. Mackay LK, Stock AT, Ma JZ, et al. Long-lived epithelial immunity by tissue-resident memory T (TRM) cells in the absence of persisting local antigen presentation. Proc Natl Acad Sci U S A 2012;109:7037-42
147. Liesegang TJ. Varicella-zoster virus eye disease. Cornea 1999;18:511-31

148. Hillenkamp J, Nolle B, Bruns C, Rautenberg P, Fickenscher H and Roider J. Acute retinal necrosis: clinical features, early vitrectomy, and outcomes. Ophthalmology 2009;116:1971-5 e2
149. Ritterband DC, Friedberg DN. Virus infections of the eye. Rev Med Virol 1998;8:187-201
150. Zamir E. Herpetic posterior uveitis. Int Ophthalmol Clin 2005;45:89-97
151. Atherton SS, Streilein JW. Two waves of virus following anterior chamber inoculation of HSV-1. 1987. Ocul Immunol Inflamm 2007;15:195-204
152. Vandercam T, Hintzen RQ, de Boer JH and Van der Lelij A. Herpetic encephalitis is a risk factor for acute retinal necrosis. Neurology 2008;71:1268-74
153. Azumi A, Atherton SS. T cells in the uninjected eye after anterior chamber inoculation of herpes simplex virus type 1. Invest Ophthalmol Vis Sci 1998;39:78-83
154. Cousins SW, Gonzalez A and Atherton SS. Herpes simplex retinitis in the mouse. Clinicopathologic correlations. Invest Ophthalmol Vis Sci 1989;30:1485-94
155. Pettit TH, Kimura SJ, Uchida Y and Peters H. Herpes Simplex Uveitis: An Experimental Study with the Fluorescein-Labeled Antibody Technique. Invest Ophthalmol 1965;4:349-57
156. Milikan JC, Baarsma GS, Kuijpers RW, Osterhaus AD and Verjans GM. Human ocular-derived virus-specific CD4+ T cells control varicella zoster virus replication in human retinal pigment epithelial cells. Invest Ophthalmol Vis Sci 2009;50:743-51
157. Milikan JC, Kinchington PR, Baarsma GS, Kuijpers RW, Osterhaus AD and Verjans GM. Identification of viral antigens recognized by ocular infiltrating T cells from patients with varicella zoster virus-induced uveitis. Invest Ophthalmol Vis Sci 2007;48:3689-97
158. Milikan JC, Kuijpers RW, Baarsma GS, Osterhaus AD and Verjans GM. Characterization of the varicella zoster virus (VZV)-specific intra-ocular T-cell response in patients with VZV-induced uveitis. Exp Eye Res 2006;83:69-75
159. Verjans GM, Dings ME, McLauchlan J, et al. Intraocular T cells of patients with herpes simplex virus (HSV)-induced acute retinal necrosis recognize HSV tegument proteins VP11/12 and VP13/14. J Infect Dis 2000;182:923-7
160. Verjans GM, Feron EJ, Dings ME, et al. T cells specific for the triggering virus infiltrate the eye in patients with herpes simplex virus-mediated acute retinal necrosis. J Infect Dis 1998;178:27-34
161. Ouwendijk WJ, Laing KJ, Verjans GM and Koelle DM. T-cell immunity to human alphaherpesviruses. Curr Opin Virol 2013
162. Gershon AA, Chen J, Davis L, et al. Latency of varicella zoster virus in dorsal root, cranial, and enteric ganglia in vaccinated children. Trans Am Clin Climatol Assoc 2012;123:17-33; discussion 33-5
163. Gilden DH, Kleinschmidt-DeMasters BK, LaGuardia JJ, Mahalingam R and Cohrs RJ. Neurologic complications of the reactivation of varicella-zoster virus. N Engl J Med 2000;342:635-45
164. Kinchington PR. Latency of varicella zoster virus; a persistently perplexing state. Front Biosci 1999;4:D200-11
165. Oxman MN, Levin MJ, Johnson GR, et al. A vaccine to prevent herpes zoster and postherpetic neuralgia in older adults. N Engl J Med 2005;352:2271-84
166. Flatt A, Breuer J. Varicella vaccines. Br Med Bull 2012;103:115-27
167. Vazquez M, LaRussa PS, Gershon AA, Steinberg SP, Freudigman K and Shapiro ED. The effectiveness of the varicella vaccine in clinical practice. N Engl J Med 2001;344:955-60
168. Shapiro ED, Vazquez M, Esposito D, et al. Effectiveness of 2 doses of varicella vaccine in children. J Infect Dis 2011;203:312-5
169. Moffat JF, Stein MD, Kaneshima H and Arvin AM. Tropism of varicella-zoster virus for human CD4+ and CD8+ T lymphocytes and epidermal cells in SCID-hu mice. J Virol 1995;69:5236-42
170. Leung J, Siegel S, Jones JF, et al. Fatal varicella due to vaccine-strain varicella-zoster virus. Hum Vaccin Immunother 2013;10(1):Epub ahead of print

Chapter 10

Nederlandse Samenvatting

Nederlandse Samenvatting

Varicella-zoster virus (VZV) is een humaan alphaherpesvirus dat zowel varicella (waterpokken) als herpes zoster (HZ; gordelroos) veroorzaakt. De meeste mensen worden als kind geïnfecteerd met VZV wat, na een incubatieperiode van ongeveer twee weken, resulteert in varicella. Kenmerkend voor varicella zijn koorts en een verspreide jeukende rode huiduitslag. Normaliter is varicella een relatief onschuldige ziekte, maar vooral in immuungecompromitteerde personen en mensen die pas op latere leeftijd geïnfecteerd raken kunnen ernstige complicaties optreden (pneumonie, hepatitis en aandoeningen aan het centraal zenuwstelsel). Tijdens de primaire infectie bereikt het virus hoofdzakelijk sensorische, maar ook autonome ganglia, waar VZV een levenslange latente infectie van neuronen bewerkstelligt. Latente VZV infectie wordt gekenmerkt door beperkte productie van RNA en mogelijk ook eiwit, zonder dat nieuwe virus partikels aangemaakt worden. Als gevolg van een afname in de virus-specifieke cellulaire immuniteit kan het virus op latere leeftijd reactiveren en HZ veroorzaken. In tegenstelling tot varicella, wordt HZ gekenmerkt door een huiduitslag die zich beperkt tot één of meerdere aaneengrenzende dermatomen. HZ is een veelvoorkomende oorzaak van neurologische aandoeningen variërend in ernst van post-herpetische pijn tot levensbedreigende cerebrale vasculopathieën. Daarnaast leidt herpes zoster ophthalmicus vaak tot oogaandoeningen. Complicaties van HZ zijn meer frequent en ernstiger in de sterk groeiende populaties ouderen en immuungecompromitteerde individuen, zoals patiënten die een transplantatie hebben ondergaan of HIV-geïnfecteerde personen. Een levend-verzwakt VZV vaccin is beschikbaar en beschermt gevaccineerde kinderen tegen varicella. Toediening van het VZV vaccin aan ouderen voorkomt HZ in de helft van de gevaccineerde individuen. Echter, het vaccin virus infecteert en wordt latent in sensorische neuronen. Hierdoor kan het vaccin virus reactiveren en ziekte veroorzaken in gevaccineerde individuen. Daarom is het belangrijk om een veilig en meer efficiënt tweede generatie VZV vaccin te ontwikkelen. De ontwikkeling van nieuwe preventieve en therapeutische therapieën vereist inzicht in de pathogenese van VZV infecties.

De pathogenese van varicella en HZ, en de mechanismen die ten grondslag liggen aan latente VZV infectie zijn grotendeels onbekend. Dit komt hoofdzakelijk doordat VZV een uitsluitend humaan pathogeen is en geen ziekte veroorzaakt in proefdiermodellen. Het is onmogelijk het ziekteverloop van varicella of HZ in doelorganen van het virus zoals long, lymfeklieren en spinale ganglia in de mens te bestuderen. Ook de relatief lange incubatieperiode van 10 tot 21 dagen na primaire infectie bemoeilijkt studies naar de pathogenese van varicella. Simian varicella virus (SVV) lijkt genetisch zeer sterk of VZV en veroorzaakt een natuurlijke infectie van niet-humane primaten (NHP) die sterk lijkt op VZV infectie bij de mens. Primaire SVV infectie veroorzaakt varicella, waarna het virus latent wordt in neuronen van spinale en trigeminale ganglia (TG) en na stress of immuunsuppressie kan het virus reactiveren en herpes zoster veroorzaken. Daarom is in **hoofdstukken 2, 3 en 7** gebruik gemaakt van het SVV NHP model om de virus- en gastheerfactoren betrokken bij primaire infectie en reactivatie te bestuderen.

VZV wordt overgedragen van varicella of HZ patiënten op naïeve individuen via aerosolen. Waarschijnlijk infecteert het virus in eerste instantie de epitheelcellen van de bovenste luchtwegen, waarna VZV wordt overgedragen op lymfocyten die het virus naar doelorganen zoals de huid en ganglia transporteren. De celtypen en route betrokken bij de verspreiding van VZV door het lichaam tijdens primaire infectie zijn grotendeels onbekend, hoofdzakelijk door de lange incubatietijd en het beperkte gastheer tropisme. In **hoofdstukken 2 en 3** hebben wij de pathogenese van primaire SVV infectie in NHP bestudeerd als model voor varicella in de mens. De resultaten in **hoofdstuk 2** suggereren dat primaire SVV infectie van Chinese rhesus makaken asymptomatisch verloopt, terwijl beschreven is dat infectie van Indische rhesus makaken resulteert in de typische varicella huidlaesies. Waarschijnlijk liggen genetische verschillen in de twee subspecies ten grondslag aan het verschillende ziektebeeld na primaire SVV infectie. Ondanks het feit dat de dieren geen huiduitslag ontwikkelden was SVV in staat om sensorische ganglia te infecteren. Dit impliceert dat omvangrijke virus replicatie in de huid niet noodzakelijk is voor neuronale infectie en kan duiden op hematogene verspreiding van SVV naar de sensorische ganglia. Een goede antivirale adaptieve immuunrespons bevordert een relatief mild ziekteverloop tijdens primaire VZV en SVV infectie. Omgekeerd tonen de resultaten beschreven in **hoofdstuk 2** aan dat de omvang van de SVV-specifieke humorale en cellulaire immuniteit afhankelijk is van de hoeveelheid virus replicatie tijdens primaire infectie. Ook de adaptieve immuniteit geïnduceerd door het levend-verzwakte VZV vaccin virus lijkt minder robuust te zijn vergeleken met natuurlijke VZV infecties.

In **hoofdstuk 3** is gebruik gemaakt van een recombinant SVV dat groen fluorescerend eiwit (enhanced green fluorescent protein) tot expressie brengt (SVV-EGFP). SVV-EGFP geïnfecteerde cellen waren zichtbaar in weefselmonsters, waardoor de virus geïnfecteerde celtypen in bloed, longen, huid en ganglia geïdentificeerd konden worden. De resultaten tonen aan dat na intratracheale SVV infectie van groene meerkatten het virus respiratoire epitheelcellen en lokaal aanwezige antigeen presenterende cellen (APC), zoals alveolaire macrofagen en dendritische cellen (DC), infecteert. Waarschijnlijk wordt het virus in de luchtweg-drainerende lymfeklieren overgedragen op perifeer bloed mononucleaire cellen (PBMC) en dan vooral geheugen T-cellen. Mogelijk transporteren SVV geïnfecteerde APC het virus van de luchtwegen naar de lymfeklieren. Geïnfecteerde PBMC, waarschijnlijk hoofdzakelijk T-cellen, transporteren SVV naar de huid waar het virus wordt overgedragen op perivasculaire macrofagen, DC en dendrocyten. Het virus verspreidt zich vervolgens naar keratinocyten in de epidermis en haarfollikels via cel-op-cel transmissie. De resultaten in **hoofdstuk 3** ondersteunen twee verschillende, elkaar niet uitsluitende, hypotheses over de route waarmee SVV de neuronen van sensorische ganglia infecteert. De eerste hypothese stelt dat het virus de uiteinden van sensorische neuronen in de huid infecteert en vervolgens via transaxonaal transport het sensorisch ganglion bereikt. De tweede hypothese stelt dat SVV geïnfecteerde geheugen T-cellen het virus naar sensorische ganglia transporteren, waar het wordt overgedragen op neuronen. Toekomstige studies op vroege tijdstippen na infectie in het SVV-EGFP NHP model zullen de definitieve route van ganglionale infectie moeten aantonen.

De virus- en gastheerfactoren betrokken bij de totstandkoming en handhaving van latente VZV infectie zijn grotendeels onbekend. VZV latentie wordt hoofdzakelijk bestudeerd in humane ganglia die zijn verkregen bij autopsies. Voorafgaande studies hebben een aantal VZV transcripten en eiwitten gevonden in humane ganglia. Echter, verschillende studies rapporteren sterk uiteenlopende aantallen en expressieniveaus van VZV transcripten en eiwitten. De in **hoofdstuk 4** beschreven studie en een recent gepubliceerde studie van een andere onderzoeksgroep tonen aan dat de vermeende detectie van VZV IE62 en IE63 eiwitten in humane ganglia berust op non-specifieke neuronale kleuring. Muis monoclonale antistoffen (mAbs) afkomstig van ascites, zoals de gebruikte anti-VZV IE62 en IE63 mAbs, en polyclonale konijnen sera kunnen endogene anti-humaan bloedgroep A1 antistoffen bevatten die non-specifiek reageren met bloedgroep A1-geassocieerde antigenen in het Golgi-apparaat van een deelpopulatie sensorische neuronen. Ondanks het feit dat grote aantallen coupes van ganglia van verschillende donoren zijn onderzocht hebben wij nooit specifieke VZV eiwitten kunnen aantonen in humane ganglia. In voorafgaande studies is veelal gebruik gemaakt van ganglia die pas langere tijd na overlijden (vaak 24 uur of meer) verkregen zijn. De in **hoofdstuk 5** beschreven studie toont aan dat het postmortem interval (PMI; het interval tussen overlijden en het verkrijgen van ganglia voor wetenschappelijk onderzoek) van invloed is op het gedetecteerde VZV transcriptoom in humane TG. Zowel het gedetecteerde aantal verschillende VZV transcripten als de relatieve ORF63 expressie niveaus namen toe met een stijgend PMI. Over het geheel genomen tonen onze data aan dat VZV latentie wordt gekenmerkt door een zeer beperkte transcriptie, waarschijnlijk beperkt tot ORF63, en de afwezigheid van virale eiwitten

HZ is het gevolg van reactivatie van endogeen latent VZV, waarna het virus lokaal in het ganglion repliceert en zich via axonen verspreidt naar de huid die geïnnerveerd wordt door de betrokken sensorische zenuw (dermatoom). De meeste individuen ontwikkelen één episode van HZ in hun leven, maar de aanwezigheid van VZV DNA in PBMC en speeksel van gezonde individuen suggereert dat asymptomatische reactivatie vaker voorkomt. HSV-1 is nauw verwant aan VZV en is ook in staat om de sensorische neuronen van het TG latent te infecteren, waar beide virussen vaak gelijktijdig aanwezig zijn. Symptomatische en asymptomatische HSV-1 reactivatie komt vaak voor, maar de incidentie van subklinische VZV reactivatie en de relatie daarvan tot HSV-1 reactivatie in het zelfde individu is grotendeels onbekend. Omdat de incidentie van VZV en HSV-1 reactivatie hoger is in immuungecompromitteerde individuen zoals HIV patiënten, hebben wij in **hoofdstuk 6** de mate van subklinische VZV en HSV-1 reactivatie bestudeerd in speekselmonsters van individuen met HIV. De resultaten tonen aan dat VZV slechts zelden reactiveert, zelfs in immuungecompromitteerde individuen, terwijl HSV-1 frequent reactiveert. De frequentie van VZV reactivatie was helaas te laag om uitspraken te kunnen doen over een mogelijke relatie tussen VZV en HSV-1 reactivatie. Hoewel beide virussen sterk op elkaar lijken, suggereert deze data dat virus- en gastheerfactoren betrokken bij latentie sterk verschillen tussen beide virussen.

HZ gaat gepaard met een ganglionitis die tot maanden na VZV reactivatie kan

persisteren. Enkele maanden na HZ bestaan de immuuninfiltraten hoofdzakelijk uit niet-cytotoxische $CD8^+$ T-cellen. De oorzaak van de infiltratie en retentie van T-cellen in ganglia na HZ is onbekend, maar lokale productie van zowel virale antigenen als T-cel aantrekkende cytokines zoals CXCL10 kunnen een rol spelen. Waarschijnlijk dragen de ganglion-infiltrerende T-cellen bij aan lokale inhibitie van virus replicatie, zoals in de literatuur ook beschreven is voor HSV-1. Aangezien de meeste individuen slechts één episode van HZ ontwikkelen zijn ganglia van patiënten met HZ extreem schaars. Daarom hebben wij het SVV NHP model gebruikt om de T-cel respons in ganglia van cynomolgus makaken op verschillende tijdstippen na reactivatie te onderzoeken. Het onderzoek in **hoofdstuk 7** toont aan dat SVV reactivatie resulteert in een tijdelijke infiltratie en retentie van vooral $CD8^+$ T-cellen in sensorische ganglia. Lokale expressie van CXCL10, maar niet de aanwezigheid van viraal transcript of eiwit, correleerde met de hoeveelheid en locatie van infiltrerende T-cellen. De hoeveelheid CXCL10 expressie en T-cellen in ganglia overeenkomend met het HZ-aangedane dermatoom verschilden niet van de overige ganglia. Het is nog onduidelijk of CXCL10 primair verantwoordelijk is voor het rekruteren van T-cellen of een secundair gevolg van interferon-γ secretie door geactiveerde infiltrerende lymfocyten. Definitieve identificatie van de mechanismen achter de rekrutering van T-cellen en de specificiteit en functie van ganglion-infiltrerende T-cellen vereist bestudering van ganglia ten tijde van en direct na HZ in toekomstige studies.

Een goede T-cel immuniteit is essentieel voor de recuperatie van varicella en HZ zonder complicaties. Echter, weefselinfiltrerende virus-specifieke T-cellen kunnen ook ernstige immunopathologie veroorzaken in organen met een beperkte regeneratieve capaciteit, zoals het oog. Acute retina necrose (ARN) is inflammatoire oogaandoening, veelal veroorzaakt door VZV en HSV-1, waarbij de retina beschadigt raakt door een combinatie van virus-geïnduceerde cytopathologie en immunopathologie door infiltrerende virus-specificieke T-cellen. In voorafgaand onderzoek heeft onze groep aangetoond dat ooginfiltrerende T-cellen van herpetische ARN patiënten vaak kruisreagerend zijn met andere alphaherpesvirussen. In **hoofdstuk 8** hebben wij een humaan leukocytenantigen klasse II (HLA-II) promiscue $CD4^+$ T-cel epitoop in het VZV IE62 eiwit beschreven. Het VZV IE62 epitoop is compleet geconserveerd in de HSV homoloog, ICP4, en werd veelvuldig herkend door T-cellen van latent VZV/HSV-1 geïnfecteerde individuen. Opvallend was dat kruisreagerende $CD4^+$ T-cellen wel VZV maar niet HSV-1 geïnfecteerde retina pigment epitheel cellen herkenden, waarschijnlijk doordat HSV-1 immuun evasie strategieën toepast om herkenning door CD4+ T-cellen te voorkomen. De in hoofdstuk 8 beschreven studie is de eerste waarin een VZV/HSV-1 kruisreagerend T-cel epitoop wordt beschreven. Humaan alphaherpesvirus kruisreagerende T-cellen zijn potentieel interessant voor vaccinatiedoeleinden.

Samenvattend heeft het onderzoek beschreven in dit proefschrift geleid tot nieuwe inzichten in de pathogenese van varicella en HZ, en het beeld dat wij hadden van VZV latentie significant veranderd. Daarmee levert het onderzoek een bijdrage aan de ontwikkeling van nieuwe preventieve en therapeutische therapieën gericht op het beperken van VZV latentie en het voorkomen van reactivatie.

Chapter 11

About the Author

Curriculum Vitae

PhD Portfolio

List of Publications

Curriculum Vitae

The author of this Thesis, Werner J.D. Ouwendijk, was born on the 29th of October 1984 in Maassluis, the Netherlands. He graduated from high school at CSG Aquamarijn in Vlaardingen in 2003, after which he commenced the study of Biomedical Sciences at the Leiden University Medical Center (LUMC). During his bachelor's program he performed an internship at the department of Medical Pharmacology at the Leiden/Amsterdam Center for Drug Research (LACDR) in Leiden, focussed on glucocorticoid programming in early life and its impact on gene expression in the brain of adult marmosets. In 2006 he obtained his Bachelor of Science degree with honor (*cum laude*) and continued with the Master's Research specialization program. During his Master's program he performed two internships. The first was performed at the department of Endocrinology of the LUMC and involved characterization of signalling pathways antagonized by sclerostin and its DAN family members. This internship was rewarded with the LUMC Student Research Award 2008, an annual award presented by the executive board of the LUMC to students in Medicine or Biomedical Sciences who have performed extraordinary during their internship. He performed his second Master's internship at the department of Virology at the Erasmus MC in Rotterdam. This study aimed to characterize the varicella-zoster virus (VZV) proteins expressed during lytic and latent infection, and their role in MHC class I downregulation. He obtained his Master of Science degree with honor (*cum laude*) in 2008, after which he started his PhD study at the department of Viroscience of the Erasmus MC under supervision of Prof.dr. Albert D.M.E. Osterhaus and Dr. Georges M.G.M. Verjans. His PhD study focussed on the pathogenesis of primary, latent and reactivated VZV and simian varicella virus infections.

PhD Portfolio

Name: Werner Jan Dieter Ouwendijk
Research group: Erasmus MC, department of Viroscience
Research school: Post-graduate Molecular Medicine
PhD period: 2008-2013
Promotor: Prof.dr. Albert D.M.E. Osterhaus
Copromotor: Dr. Georges M.G.M. Verjans

In-depth courses:

• Course in Immunology (Leiden Institute for Immunology, LUMC)	2009
• Practical Introduction to Laser Scanning Microscopy (Erasmus MC)	2009
• Course in Virology (Molmed, Erasmus MC)	2010
• Course in Primate Biology (Biomedical Primate Research Center)	2010
• Course in Research Integrity (Molmed, Erasmus MC)	2012
• Course in Adobe Photoshop and Illustrator (Molmed, Erasmus MC)	2013
• Course in Adobe Indesign (Molmed, Erasmus MC)	2013

Poster presentations:

• 35th International Herpesvirus Workshop (Salt Lake City, USA)	2010
• 15th Molecular Medicine day (Rotterdam, the Netherlands)	2011
• 16th Molecular Medicine day (Rotterdam, the Netherlands)	2012
• 37th International Herpesvirus Workshop (Calgary, Canada)	2012
• 17th Molecular Medicine day (Rotterdam, the Netherlands)	2013

Oral presentations:

• Colorado Alphaherpesvirus Latency Symposium (Vail, USA)	2011
• Netherlands Brain Bank meeting (Rotterdam, the Netherlands)	2011
• 37th International Herpesvirus Workshop (Calgary, Canada)	2012
• Comparative Pathology meeting (Rotterdam, the Netherlands)	2012
• Colorado Alphaherpesvirus Latency Symposium (Vail, USA)	2013
• T-Cell Consortium meeting (Rotterdam, the Netherlands)	2013

Attended conferences, symposia and meetings:

• 13th Molecular Medicine day (Rotterdam, the Netherlands)	2009
• Virology symposium (Dakar, Senegal)	2009
• 14th Molecular Medicine day (Rotterdam, the Netherlands)	2010
• 35th International Herpesvirus Workshop (Salt Lake City, USA)	2010
• Advanced Immunology symposium (Amsterdam, the Netherlands)	2010

- 15th Molecular Medicine day (Rotterdam, the Netherlands) 2011
- Colorado Alphaherpesvirus Latency Symposium (Vail, USA) 2011
- Netherlands Brain Bank meeting (Rotterdam, the Netherlands) 2011
- 16th Molecular Medicine day (Rotterdam, the Netherlands) 2012
- 37th International Herpesvirus Workshop (Calgary, Canada) 2012
- Symposium: Multiple Sclerosis, Herpesviruses and Aging (Rotterdam, the Netherlands) 2012
- Comparative Pathology meeting (Rotterdam, the Netherlands) 2012
- 17th Molecular Medicine day (Rotterdam, the Netherlands) 2013
- Dutch Annual Virology Symposium (Amsterdam, the Netherlands) 2013
- Colorado Alphaherpesvirus Latency Symposium (Vail, USA) 2013
- T-Cell Consortium meeting (Rotterdam, the Netherlands) 2013

Supervision and teaching activities:

- Co-supervision MSc student (NT) 2011-2012
- Co-supervision MSc student (EH) 2012
- Lab Rotation MSc students “Infection and Immunity” 2012-2013

Awards:

- Travel Award 37th International Herpesvirus Workshop (Calgary, Canada) 2012

List of Publications

Functional characterization of ocular-derived human alphaherpesvirus cross-reactive CD4 T-cells
Werner J.D. Ouwendijk, Annemieke Geluk, Saskia L. Smits, Sarah Getu, Albert D.M.E. Osterhaus and Georges M.G.M. Verjans.
2013;Submitted.

Longitudinal study on oral shedding of herpes simplex virus 1 and varicella-zoster virus in individuals infected with HIV.
Monique van Velzen M, **Werner J.D. Ouwendijk**, Stacey Selke, Suzan D. Pas, Freek B. van Loenen, Albert D.M.E. Osterhaus, Anna Wald and Georges M.G.M. Verjans.
J Med Virol. 2013;85(9):1669-77

T-Cell tropism of simian varicella virus during primary infection.
Werner J.D. Ouwendijk, Ravi Mahalingam, Rik L. de Swart, Bart L. Haagmans, Geert van Amerongen, Sarah Getu, Don Gilden, Albert D.M.E. Osterhaus and Georges M.G.M. Verjans.
PLoS Pathog. 2013;9(5):e1003368

T-cell immunity to human alphaherpesviruses.
Werner J.D. Ouwendijk, Kerry J. Laing, Georges M.G.M. Verjans and David M. Koelle.
Curr Opin Virol. 2013;3(4):452-60

Comprehensive analysis of varicella-zoster virus proteins using a new monoclonal antibody collection.
Tihana Lenac Roviš, Susanne M. Bailer, Venkata R. Pothineni, **Werner J.D. Ouwendijk**, Hrvoje Šimić, Marina Babić, Karmela Miklić, Suzana Malić, Marieke C. Verweij, Armin Baiker, Orland Gonzalez, Albrecht von Brunn, Ralf Zimmer, Klaus Früh, Georges M.G.M. Verjans GM, Stipan Jonjić and Jürgen Haas.
J Virol. 2013;87(12):6943-54

T-cell infiltration correlates with CXCL10 expression in ganglia of cynomolgus macaques with reactivated simian varicella virus
Werner J.D. Ouwendijk, Allison Abendroth, Vicki Traina-Dorge, Sarah Getu, Megan Steain, Mary Wellish, Arno C. Andeweg, Albert D.M.E. Osterhaus, Don Gilden, Georges M.G.M. Verjans GM and Ravi Mahalingam.
J Virol. 2013;87(5):2979-82

Restricted varicella-zoster virus transcription in human trigeminal ganglia obtained soon after death.
Werner J.D. Ouwendijk, Alexander Choe, Maria A. Nagel, Don Gilden, Albert D.M.E. Osterhaus, Randall J. Cohrs and Georges M.G.M. Verjans.
J Virol. 2012;86(18):10203-6

Immunohistochemical detection of intra-neuronal VZV proteins in snap-frozen human ganglia is confounded by antibodies directed against blood group A1-associated antigens.
Werner J.D. Ouwendijk*, Sarah E. Flowerdew*, Desiree Wick, Anja K.E. Horn, Inga Sinicina, Michael Strupp, Albert D.M.E. Osterhaus, Georges M.G.M. Verjans and Katharina Hüfner.
J Neurovirol. 2012;18(3):172-80
* both authors contributed equally

Simian varicella virus infection of Chinese rhesus macaques produces ganglionic infection in the absence of rash.
Werner J.D. Ouwendijk, Ravi Mahalingam, Vicki Traina-Dorge, Geert van Amerongen, Mary Wellish, Albert D.M.E. Osterhaus, Don Gilden and Georges M.G.M. Verjans.
J Neurovirol. 2012;18(2):91-9

Chapter 12

Dankwoord

Dankwoord

Dit proefschrift vloeit voort uit samenwerkingen met vele mensen. Daarom wil ik graag mijn dank uitdragen aan iedereen die direct of indirect een bijdrage heeft geleverd aan de totstandkoming van dit proefschrift. Een aantal mensen wil ik in het bijzonder noemen.

Allereerst gaat mijn dank uit naar mijn promotor en copromotor. Beste Ab, bedankt voor de mogelijkheid om mijn promotieonderzoek of de afdeling Viroscience te kunnen uitvoeren. Jouw laboratorium vormde een inspirerende omgeving waar ik de afgelopen 5 jaar met veel enthousiasme heb gewerkt. Georges, bedankt voor de vele ideeën, suggesties, discussies en adviezen. Al met al heeft het vele “bomen” geleid tot mooie publicaties. Als onderzoeker met creatieve ideeën heb je mij veel bijgebracht over het uitdenken van experimenten, het belang van scherp formuleren in manuscripten en de rol van politiek in de wetenschap.

Dan mijn paranimfen, Sarah en Rory. Sarah, bedankt voor jouw tomeloze inzet op het lab. De afgelopen 2 jaar hebben we enorme hoeveelheden virus-stocks gemaakt, virus titraties ingezet, neuronen/T-cellen geteld, etc. Jouw enthousiasme maakte het plezierig samenwerken in het lab. Rory, bedankt voor het beantwoorden van mijn eindeloze stroom vragen over procedures bij het promoveren. Ook bedankt voor jouw advies en hulp bij experimenten en de gezelligheid op het lab.

Graag wil ik ook de overige (ex-)leden van de Herpesgroep bedanken, allen hebben jullie geholpen bij het uitvoeren van experimenten. Monique, vier jaar lang kamergenoten en altijd vrolijk en in voor een discussie. Geduldig heb je mij al tijdens mijn Masterstage veel geleerd en ook daarna kon ik altijd bij je terecht voor advies, een mening of ideeën voor de laatste zin van een manuscript (“iets met puppies” of “de wereld redden”). Gijs, bedankt voor de ideeën en hulp bij al het VMT-werk, maar vooral ook voor de gezelligheid op het lab en als kamergenoot het laatste jaar. Ook kon ik altijd bij je terecht voor een kritische mening over resultaten of de lay-out van mijn proefschrift. Succes met het afronden van je promotie! Freek, jouw enthousiasme voor massa-experimenten blijft bijzonder. Bedankt voor de hulp en gezelligheid op het lab en bij de analyse van de vele ABO sequenties.

Geert, bedankt voor de hulp bij onze experimenten en ook voor het meedenken wanneer de experimenten niet volgens plan verliepen!

I would like to express my gratitude to the VZV/SVV laboratory of Prof.dr. Gilden at the University of Colorado Denver Medical School (Aurora, Colorado, USA), with whom we have collaborated extensively. Dear Don, thank you for the opportunity to collaborate with your lab and your important contributions to manuscripts. Ravi, thank you for the close collaboration and the materials, protocols and advise that you have so generously provided. Dear Randy, it was a pleasure to work together with you on the detection of VZV transcripts in human ganglia and thank you for the wonderful meetings in Vail.

I am looking forward to continue collaborating with all of you during the next five years. Further I would like to thank Mary for her assistance with culturing SVV and Stephanie for the generous hospitality during my stay in Denver.

Also, I would like to express my gratitude to Anna Wald and Stacy Selke from the University of Washington in Seattle (Washington, USA) for sharing materials and contributing to the manuscript. I would like to thank David Koelle and Kerry Laing for our collaborative paper. In addition, I would like to thank Sarah Flowerdew and Katharina Hüfner from the Ludwig-Maximilians University in Munich (Germany) for our collaboration on VZV protein expression in human ganglia.

Uiteraard wil ik ook de collega's van het 1710-lab en (ex-)kamergenoten bedanken voor samenwerkingen, hulp, adviezen, materialen en gezelligheid: Tien, Joyce, Selma, Fatiha, Leon, Rik, Bart, Stalin, Lisette, Claudia, Rui, Saskia, Anna, Marleen en Rachel. Tien, van arts tot wetenschapper: succes met het afronden van je promotie! Rik, bedankt voor jouw hulp bij onze experimenten en bijdrage aan het manuscript. Bart, jouw suggesties voor de structuur van het gezamenlijke manuscript worden zeer gewaardeerd. Maarten en Stella: koekjesmiddag, altijd gezellig. Peter, Debby en Lonneke: bedankt voor de coupes, adviezen, materialen en gezelligheid op het histologie lab. Petra, bedankt voor het delen van jouw VMT kwaliteiten. Dames van het secretariaat (Simone, Loubna, Anouk en Maria): bedankt voor al het regelwerk! Wim, bedankt voor de financiële aspecten. Robert, bedankt voor alles (van PBS tot goodie-goodie box).

Tenslotte wil ik graag mijn familie bedanken voor jullie betrokkenheid en interesse in mijn onderzoek. Bovenal wil ik Annette bedanken voor de continue steun tijdens mijn promotietraject, waarbij zij de zin "het wordt vanavond iets later" te vaak heeft moeten horen.